

SEA LEVEL VARIATIONS IN
GULF OF THAILAND

Vichai Punpuk

NAVAL POSTGRADUATE SCHOOL

Monterey, California



THESIS

SEA LEVELS VARIATION IN
GULF OF THAILAND

by

Vichai Punpuk

March 1981

Thesis Advisors:

J. B. Wickham
W. C. Thompson

Approved for public release; distribution unlimited

T200662

REPORT DOCUMENTATION PAGE		READ INSTRUCTIONS BEFORE COMPLETING FORM
1. REPORT NUMBER	2. GOVT ACCESSION NO.	3. RECIPIENT'S CATALOG NUMBER
4. TITLE (and Subtitle) Sea Level Variations in Gulf of Thailand		5. TYPE OF REPORT & PERIOD COVERED Master's Thesis March 1981
		6. PERFORMING ORG. REPORT NUMBER
7. AUTHOR(s) Vichai Punpuk		8. CONTRACT OR GRANT NUMBER(s)
9. PERFORMING ORGANIZATION NAME AND ADDRESS Naval Postgraduate School Monterey, California 93940		10. PROGRAM ELEMENT, PROJECT, TASK AREA & WORK UNIT NUMBERS
11. CONTROLLING OFFICE NAME AND ADDRESS Naval Postgraduate School Monterey, California 93940		12. REPORT DATE March 1981
		13. NUMBER OF PAGES 149
14. MONITORING AGENCY NAME & ADDRESS (if different from Controlling Office)		15. SECURITY CLASS. (of this report) Unclassified
		15a. DECLASSIFICATION/DOWNGRADING SCHEDULE
16. DISTRIBUTION STATEMENT (of this Report) Approved for public release; distribution unlimited		
17. DISTRIBUTION STATEMENT (of the abstract entered in Block 20, if different from Report)		
18. SUPPLEMENTARY NOTES		
19. KEY WORDS (Continue on reverse side if necessary and identify by block number) Sea levels, seasonal variation, mean annual variation, meteorological effects.		
20. ABSTRACT (Continue on reverse side if necessary and identify by block number) From a study of low-pass filtered hourly sea levels for Sattahip and Ko-Lak in the northern Gulf of Thailand during the period 1960 through 1966, the sea level variations due to meteorological effects are found. The mean annual variation of the filtered sea level, which averages 0.5 meters, is consistent with the climatological mean annual wind variations. This sea level change appears to be a response to the Ekman transport which would be expected from the seasonal		

monsoon wind regimes. Sea level response to atmospheric pressure is negligible compared with response to wind. Analyses performed to find relations between the filtered sea level and the gulf-wide geostrophic wind and local surface wind show that the sea level slopes upward across the gulf in the same direction as the local wind blows, the response being coherent in the frequency band 0.083-0.117 cycles per day (period 8 to 12 days). This wind set-up effect is clearly secondary to the Ekman transport in inducing the seasonal sea level variations observed in the gulf.

Approved for public release; distribution unlimited

Sea Level Variations in
Gulf of Thailand

by

Vichai Punpuk
LTJG., Royal Thai Navy
B.S., Royal Thai Navy Academy, 1974

Submitted in partial fulfillment of the
requirements for the degree of

MASTER OF SCIENCE IN OCEANOGRAPHY

from the

NAVAL POSTGRADUATE SCHOOL
March 1981

ABSTRACT

From a study of low-pass filtered hourly sea levels for Sattahip and Ko-Lak in the northern Gulf of Thailand during the period 1960 through 1966, the sea level variations due to meteorological effects are found. The mean annual variation of the filtered sea level, which averages 0.5 meters, is consistent with the climatological mean annual wind variations. This sea level change appears to be a response to the Ekman transport which would be expected from the seasonal monsoon wind regimes. Sea level response to atmospheric pressure is negligible compared with response to wind. Analyses performed to find relations between the filtered sea level and the gulf-wide geostrophic wind and local surface wind show that the sea level slopes upward across the gulf in the same direction as the local wind blows, the response being coherent in the frequency band 0.083-0.117 cycles per day (period 8 to 12 days). This wind set-up effect is clearly secondary to the Ekman transport in inducing the seasonal sea level variations observed in the gulf.

TABLE OF CONTENTS

I.	INTRODUCTION -----	10
II.	NON-ASTRONOMICAL FLUCTUATION IN SEA LEVEL -----	13
III.	DATA -----	15
IV.	ANALYSIS OF SEA LEVEL HEIGHTS -----	18
	A. ALIASING -----	19
	B. LEAKAGE -----	21
V.	RESULTS OF THE ANALYSIS -----	24
	A. SEASONAL VARIATION OF SEA LEVEL -----	24
	B. MEAN ANNUAL VARIATION OF SEA LEVEL -----	24
	C. SPECTRUM OF SEA LEVEL -----	26
	D. METEOROLOGICAL EFFECTS -----	36
	1. Response of sea level to atmospheric pressure ----	39
	2. Sea level and the geostrophic wind -----	40
	3. Sea level slope and the local wind -----	41
VI.	SUMMARY AND CONCLUSIONS -----	57
APPENDIX A: RAW AND FILTERED HOURLY SEA LEVEL DATA -----		59
APPENDIX B: HOURLY SEA LEVEL DATA FILTERED WITH GODIN AND 28-DAY FILTERS -----		74
APPENDIX C: SPECTRA, CROSS-SPECTRA, COHERENCE, AND PHASE OF RAW SEA LEVEL DATA -----		89
APPENDIX D: SPECTRA, CROSS-SPECTRA, COHERENCE, AND PHASE OF LOW-PASS FILTERED SEA LEVEL -----		118
LIST OF REFERENCES -----		147
INITIAL DISTRIBUTION LIST -----		148

LIST OF TABLES

TABLE		PAGE
1.	Gaps in sea level records -----	17
2.	Mean monthly sea level, pressure, and wind -----	27

LIST OF FIGURES

FIGURE	PAGE
1. The study area -----	12
2. Spectra of filtered sea level -----	23
3. Mean monthly sea level and climatological elements -----	28
4. Seven years of filtered sea level spectra for three-month periods at Sattahip -----	32
5. Seven years of filtered sea level spectra for three-month periods at Ko-Lak -----	33
6. Seven-year ensemble averaged filtered sea level spectra for three-month periods at Sattahip -----	34
7. Seven-year ensemble averaged filtered sea level spectra for three-month periods at Ko-Lak -----	35
8. Seven-year ensemble averaged filtered sea level spectra over the whole year -----	37
9. Seven-year ensemble averaged filtered sea level spectra according to season -----	38
10. Daily filtered sea level data (1962) -----	44
11. Daily sea surface pressure at Singapore and Bangkok (1962) -----	45
12. Daily sea surface pressure at Saigon (1962) -----	46
13. The spectra, cross-spectra, coherences, and phases for filtered sea level (Sattahip) and pressure difference (Bangkok-Saigon) -----	47
14. The spectra, cross-spectra, coherence, and phases for filtered sea level (Ko-Lak) and pressure difference (Bangkok-Saigon) -----	48
15. The spectra, cross-spectra, coherence, and phases for filtered sea level (Sattahip) and pressure difference (Bangkok-Singapore) -----	49

16.	The spectra, cross-spectra, coherence, and phases for filtered sea level (Ko-Lak) and pressure difference (Bangkok-Singapore) -----	50
17.	Daily wind components (N-S, and E-W) -----	51
18.	Daily wind components (X and Y) -----	52
19.	The spectra, cross-spectra, coherences, and phases of sea level slope (Ko-Lak-Sattahip) and N-S wind component -----	53
20.	The spectra, cross-spectra, coherence, and phases of sea level slope (Ko-Lak-Sattahip) and E-W wind component -----	54
21.	The spectra, cross-spectra, coherence, and phases of sea level slope (Ko-Lak-Sattahip) and Y wind component -----	55
22.	The spectra, cross-spectra, coherence, and phases of sea level slope (Ko-Lak-Sattahip) and X wind component -----	56

ACKNOWLEDGMENTS

The author wishes to express his sincere appreciation to Professors Jacob B. Wickham and Warren C. Thompson for their assistance and guidance in the preparation of this thesis and making useful comments.

In addition, the author is indebted to Captain Banchong Subsandee and the officers of the Hydrographic Department, Royal Thai Navy and to Commander T. G. Fitzpatrick, NAVOCEANCOMDET, Asheville, N.C., for timely procurement and transmission of data. The author also wishes to thank the Commanding officer, JUSMAGTHAI, and Commander R. A. McGonical, International Education Coordinator, Naval Post-graduate Schools, for assistance in the transmission of data.

Special appreciation is given to my loving wife, Wunwipar whose work in key-punching of sea level data, and whose understanding and patience enabled me to complete the necessary research.

I. INTRODUCTION

In 1934 the Hydrographic Department of the Royal Thai Navy installed a tide gauge to record sea level at the mouth of the Chao-Phaya river in the Gulf of Thailand and sent the data to the U.S. Coast and Geodetic Survey (U.S.A.) for analysis and prediction. In 1959, the Royal Thai Navy bought the Doodson-Lé'gé prediction machine from England and used it to predict tides in 1960. It also set up tide gauges at many stations along the coast of the gulf until today it is possible to predict tides at about 29 stations. Since 1972, tide prediction has been done with the computing machine (I.B.M.360) at the Supreme Command, Ministry of Defence, but still the Doodson tide prediction machine is used also for comparison. For the analysis by the Doodson harmonic method (Doodson, 1941) about 30 constituents are calculated.

Tide in the Gulf of Thailand is the shallow tide; the coast and continental shelf are irregular. This gulf is bordered by Thailand on the north, Cambodia and Vietnam on the east, and Malaysia on the west, and its mouth opens to the South China Sea (Figure 1). It has a width of about 200 nm., length about 400 nm., and average depth about 80 meters. At the northern end, the head of the gulf narrows. This region is about 60 nm. wide and about 80 nm. long, with average depth about 20-30 meters. The gulf is affected by monsoon winds and by tropical storms. There are 3 seasons: 1) southwest monsoon, April-September (about 6 months); 2) northeast monsoon, October-January (about 4 months); 3) southeast season, February-March (about 2 months) with the wind from the South China Sea which has high humidity.

The analysis and prediction done by the Royal Thai Navy treats only the forcing with periods of the astronomical tides. This thesis will be concerned with seasonal variation and other largely non-astronomical effects on sea level, and their causal relationship to meteorological conditions. It will be shown that non-astronomical events contribute substantially to the water level variations in the gulf and are therefore important in prediction of sea level.

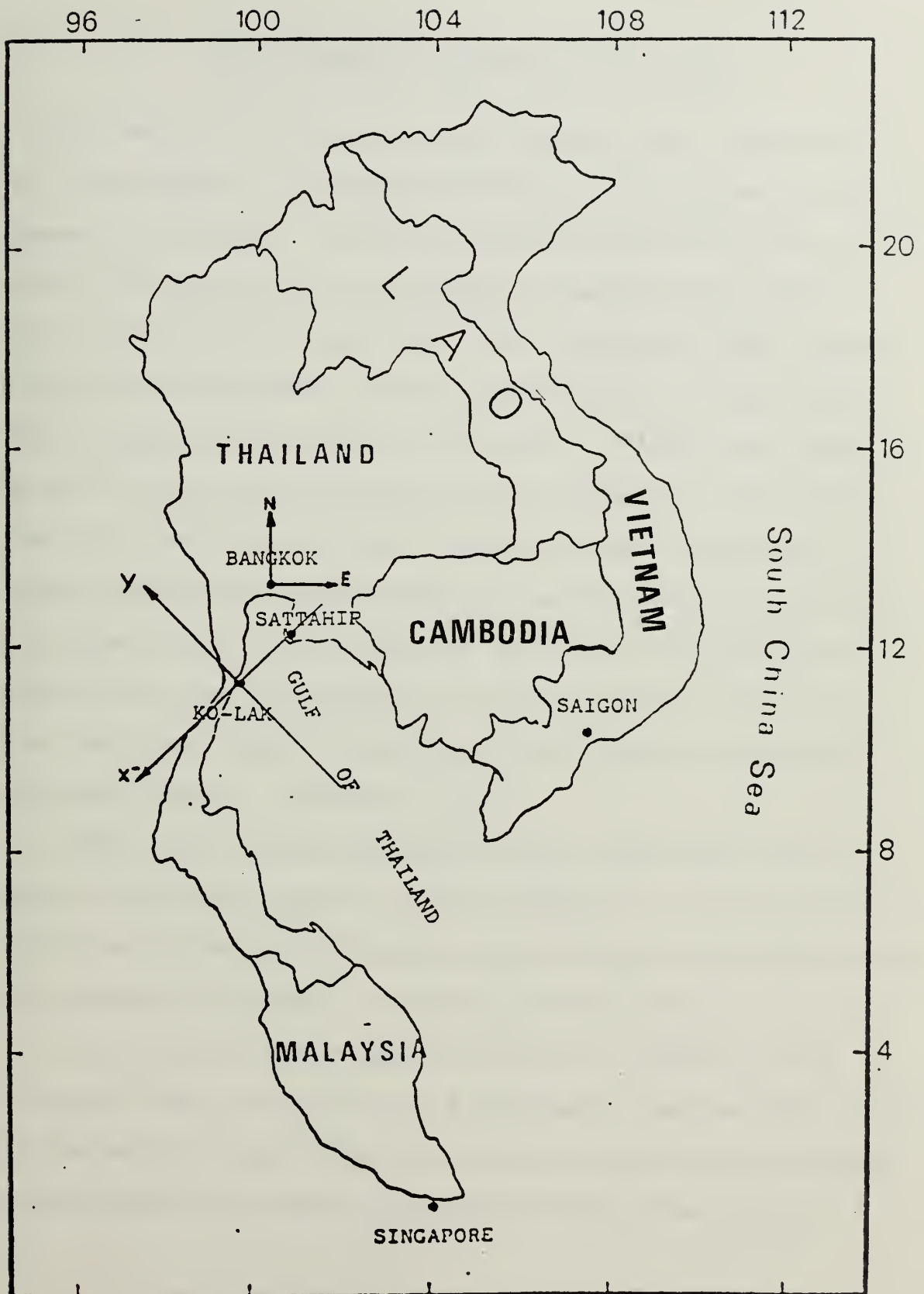


Figure 1. Study area.

II. NON-ASTRONOMICAL FLUCTUATION IN SEA LEVEL

The observed elevation of the ocean's surface at any location and time is influenced by a combination of factors, including the large scale atmospheric circulation. Generally, the 12.4- and 24.8-hour tide-raising forces of the earth-moon-sun system generate the most conspicuous and easily recognized of all ocean tides. The observed sea level, however, is modified by combinations of other less predictable and quantifiable factors, operating individually or in concert. "These include atmospherically driven on-and offshore Ekman mass transport, direct set-up or set-down of water due to winds, spatial and temporal variations in atmospheric pressure, wind generated waves and swell, density variations in the water column, crustal subsidence or uplift, eustatic sea level variations resulting from changes in the mass of the polar ice packs, surge from distant storms or tsunamis, and low frequency astronomical tide-raising forces". (Chelton, 1980).

In 1969, the Fleet Numerical Weather Central (now called "Fleet Numerical Oceanography Center" or "FNOCC"), Monterey, California (U.S.A.) studied tides in the Gulf of Thailand, and pointed out some of the features of the atmospheric overtides. According to FNOCC (1969):

"a) Any wind can cause changes of sea level in addition to the astronomical tides. Thus, there is a difference in mean sea level during different monsoon winds, the difference varying from location to location and being greatly influenced by the bathymetry at a given location.

b) There is a considerable mass transport of water by waves in shallow water. This mass transport can cause strong alongshore currents, which might also, during storms, cause a considerable shift of the sand bank. If there are sand bars or coral reefs off the coast, a considerable amount of water is carried over them by waves. This wave "set-up" can account, occasionally, for as much as three-foot changes of water level.

c) The sea level also acts as an inverted barometer. A 1-mb decrease in atmospheric pressure will cause a 1-cm. rise in the sea level.

d) If the atmospheric pressure disturbance moves with a speed comparable to the speed of a shallow water wave, $v = \sqrt{gd}$; g = acceleration of gravity, and d = depth in meters; the atmospheric pressure effects are overamplified.

e) Twelve inches or more of rainfall during a 24-hour period can be caused by typhoons. This river run-off can cause water level changes in addition to those due to wind and atmospheric factors.

f) There are relatively great differences in the storm surge characteristics between geographical points only 10 miles or so apart.

g) There are "overshooting" or "resurge" effects, especially in bays and estuaries in connection with storm surges.

h) In extensive shallow water areas the local wind effects on the water and movement of the water within the bay are as important as the external surges entering the area".

It is obvious that improved sea level prediction can be the result of applying the non-astronomical variation to that given by the astronomical tides alone. One purpose of this thesis is to assess the importance of some of the non-astronomical factors in the Gulf of Thailand.

III. DATA

Sea level data and mean annual climatological elements from Sattahip and Ko-Lak, and daily atmospheric pressure and wind from Bangkok, Sattahip, Singapore, and Saigon were used in this study.

The hourly tide heights from Sattahip and Ko-Lak were provided by the Hydrographic Department of the Royal Thai Navy. Sattahip station is on the east coast and Ko-Lak station is on the west coast in the northern part of the gulf. They are 80 nm. apart and situated as shown in Figure 1. Station Sattahip is in Sattahip Bay, which has dimensions 4 nm. in width, 1 nm. in length, and average depth about 6 meters.

About 20 years of hourly readings were available for both stations and these have been tabulated in the standard table form (Form 362, U.S. Coast and Geodetic Survey) for the period 1 January 1960 through 31 December 1979. Some of these data were punched on computer cards for use in later analyses. Because it takes a lot of time to punch the cards and because a shorter time is enough for the present analysis, only 7 years of data, for the period 1 January 1960 through 31 December 1966, were used. The hourly heights had numerous short gaps and some long gaps (Table 1), the longest being 14 days in 1960 at Sattahip station. These gaps were filled by conventional harmonic prediction.

The mean monthly climatological data presented herein from Sattahip and Ko-Lak were monthly averages from the years 1951 through 1975. These data were provided by the Meteorological Department, Ministry of communications, Bangkok, Thailand.

Daily atmospheric pressure and surface wind data were obtained from the NAVOCEANCOMDET, Asheville, N.C. These data were available for Bangkok, Sattahip, Singapore, and Saigon during January 1960-December 1965. The data were recorded usually for the hours 00, 03, 06, 09, 12, and 18 GCT. These records, however, are not regularly available for the same hour for every day, except for the time 0600 hours in 1962 which has continuous values. Sattahip has a lot of missing data, so it was not considered in this analysis. Accordingly, meteorological data at 0600 hours in 1962 for Bangkok, Saigon, and Singapore were used.

TABLE 1

Gaps in Sea Level Records

Station Ko-Lak

0000	8 Mar.	to	1100	10 Mar.	1960	(2 days)
1600	26 Oct.	to	0600	29 Oct.	1960	(4 days)
2000	10 Dec.	to	0600	13 Dec.	1960	(3 days)
1200	6 Jul.	to	1000	14 Jul.	1961	(9 days)
0000	15 Jul.	to	1500	16 Jul.	1962	(2 days)
0900	16 Jun.	to	1500	19 Jun.	1963	(4 days)
1800	29 Aug.	to	2300	31 Aug.	1963	(2 days)
1600	12 Dec.	to	2300	21 Dec.	1964	(9 days)
0900	25 Nov.	to	2300	30 Nov.	1965	(5 days)
0000	1 Dec.	to	0700	6 Dec.	1965	(5 days)
0000	1 Nov.	to	1600	4 Nov.	1966	(3 days)
0000	1 Dec.	to	0800	1 Dec.	1966	(8 hours)

Station Sattahip

2000	5 Sep.	to	1600	20 Sep.	1960	(14 days)
0400	16 Nov.	to	0800	23 Nov.	1960	(8 days)
1800	6 Dec.	to	1600	10 Dec.	1960	(4 days)
1100	31 May	to	2300	31 May	1965	(13 hours)
0000	20 Mar.	to	1000	22 Mar.	1966	(3 days)
1100	24 Apr.	to	1000	27 Apr.	1966	(3 days)
0000	6 Jun.	to	0900	8 Jun.	1966	(3 days)
1800	20 Jun.	to	2300	20 Jun.	1966	(6 hours)
1400	30 Oct.	to	2300	31 Oct.	1966	(2 days)
0000	1 Nov.	to	1000	2 Nov.	1966	(2 days)
1100	11 Dec.	to	1000	14 Dec.	1966	(3 days)

IV. ANALYSIS OF SEA LEVEL HEIGHTS

The hourly heights for both stations, Ko-Lak and Sattahip, can be reduced to approximately the level of the non-astronomical water level by separating the prominent semi-diurnal and diurnal tide components from the non-harmonic components of the hourly height. Then the non-astronomical part of the height change can be seen clearly. This process, a low-pass filtering, was done by computing running means of the hourly heights using averaging intervals determined by the period of harmonic components to be suppressed. Godin's (1966) filter accomplished this effectively. The filter performs an unweighted arithmetic running mean of the data set, passing over the data three times. It averages sequences of 24 values on the first and second passes, and 25 values on the third-pass. Appendix A shows the unfiltered hourly heights, the filtered semi-diurnal and diurnal tides ($\eta(o)-\eta(f)$), and the filtered residual hourly heights, with each figure containing one year of data.

The filtered heights from both tide stations show a lot of noise throughout the year, much of which is at clearly non-astronomical frequencies. The maximum difference between high and low water is 8-10 dm. in all the years. Large and rapid changes at each station occur at almost the same times and are of similar height. The spikes (both maxima and minima) are about 5-6 dm. in height over intervals of 12-30 days. These spikes usually are largest during the period January through March. These kinds of variations might be expected as the result of meteorological disturbances, which have similar time scales.

To study the sea level and its relation to meteorological forcing more closely, spectrum and cross-spectrum analyses of data were made. Two problems that arise in spectrum analysis are aliasing from high frequencies and leakage, usually from low frequency spectral peaks. These problems are discussed below.

A. ALIASING

If energy is present at frequencies higher than the highest analyzable (or Nyquist) frequency ($1/2\Delta$), this energy will appear at an apparent frequency lower than the actual frequency, where Δ is the sampling interval. This energy is said to be "aliased" into the lower frequency which is also lower than $1/2\Delta$.

The phenomenon of aliasing is important in practical data analysis. The sampling interval (Δ) must be short enough to cover the full frequency range of the continuous time series. Otherwise the spectrum derived from equally spaced samples will differ from the true spectrum because of aliasing. In some cases the only way to be certain that this condition is met may be to filter the time series to remove intentionally all frequency components higher than $1/2\Delta$ before beginning the analysis (Newland, 1974). This procedure is of course impossible if the data set is available only at the sampling interval (Δ).

One source of aliasing in sea level data in the present analysis may be a resonant frequency in the Gulf of Thailand, a frequency which is estimated to be close to the Nyquist frequency ($f = 0.5$ cpd) for the once daily sea-level heights left after the use of Godin's filter. This frequency can be estimated as follows.

Since the Gulf of Thailand is shallow, the resonant period can be estimated from the Sverdrup wave phase speed,

$$c = \frac{\sigma \sqrt{gh}}{\sqrt{\sigma^2 - f^2}}$$

where

g = gravity acceleration

h = the mean depth

σ = radian frequency

f = coriolis parameter

Resonant fundamental frequency for an open rectangular basin of constant depth, f_r , is

$$f_r = c/4l$$

where l is the length of the gulf. Assuming the gulf is rectangular with a mean depth (h) of 60 meters, length (l) of 400 nm., and mean latitude of 10 degrees, the estimated resonant frequency is 0.6 cycles per day (cpd).

For most spectra and cross-spectra involving the meteorological data used here, the sampling interval is $\Delta = 1$ day. So the Nyquist frequency (f_n) = $1/2\Delta = 0.5$ cpd. This means that, if the estimated free (resonant) frequency is correct,

$$f_n < f_r$$

Thus an important frequency may be aliased into the frequency

$$f = 2f_n - f_r.$$

In fact, the estimate of resonant frequency is crude. So one can say that the resonant frequency is either barely resolved or not quite

resolved. As a result, energy at the resonant frequency may account for spectral peaks seen near the Nyquist frequency or at the Nyquist frequency itself.

B. LEAKAGE

Another problem in spectrum analysis is "leakage" from a low frequency or other spectral peak. This can be suppressed by prewhitening.

According to Newland (1974), "The process of 'prewhitening' involves operating on raw data before spectral analysis in such a way that the processed data has an approximately flat spectrum. Normalizing to zero mean and correcting for slow trends are two examples of this. Such initial processing of data before analysis is carried out for two reasons. One is that, because large peaks in the spectrum are reduced, spectral 'leakage' due to the imperfect shape of the spectral window is reduced. The other arises because the standard error of a measurement is proportional to the mean value of this measurement. The variance of a large spectral estimate is therefore proportionally more than the variance of a small estimate. By whitening the spectrum before analysis, the estimated spectrum can be given uniform accuracy at all frequencies".

In order to test the spectrum analysis procedure as to the need for prewhitening of the low-pass filtered sea levels at Sattahip and Koolak, spectra from the 1962 data were calculated both with and without prewhitening by the program FTFREQ (IMSL, 1980). These spectra are shown in Figure 2. The spectra with prewhitening were obtained by replacing the i th term of each series X_i was replaced by $X_i - X_{i-1}$ before analysis. The two processes (with and without prewhitening) covered the 6-month periods (October-March and April-September).

The maximum number of lags in cross-and autocorrelation was $m = 30$, the number of terms was $n = 180$, and the number of degrees of freedom for the estimation of confidence limit was $d.f. = 2n/m = 12$.

The spectra from both analyses are very nearly the same. This means that leakage is not a problem and that one can analyze similar data without prewhitening.

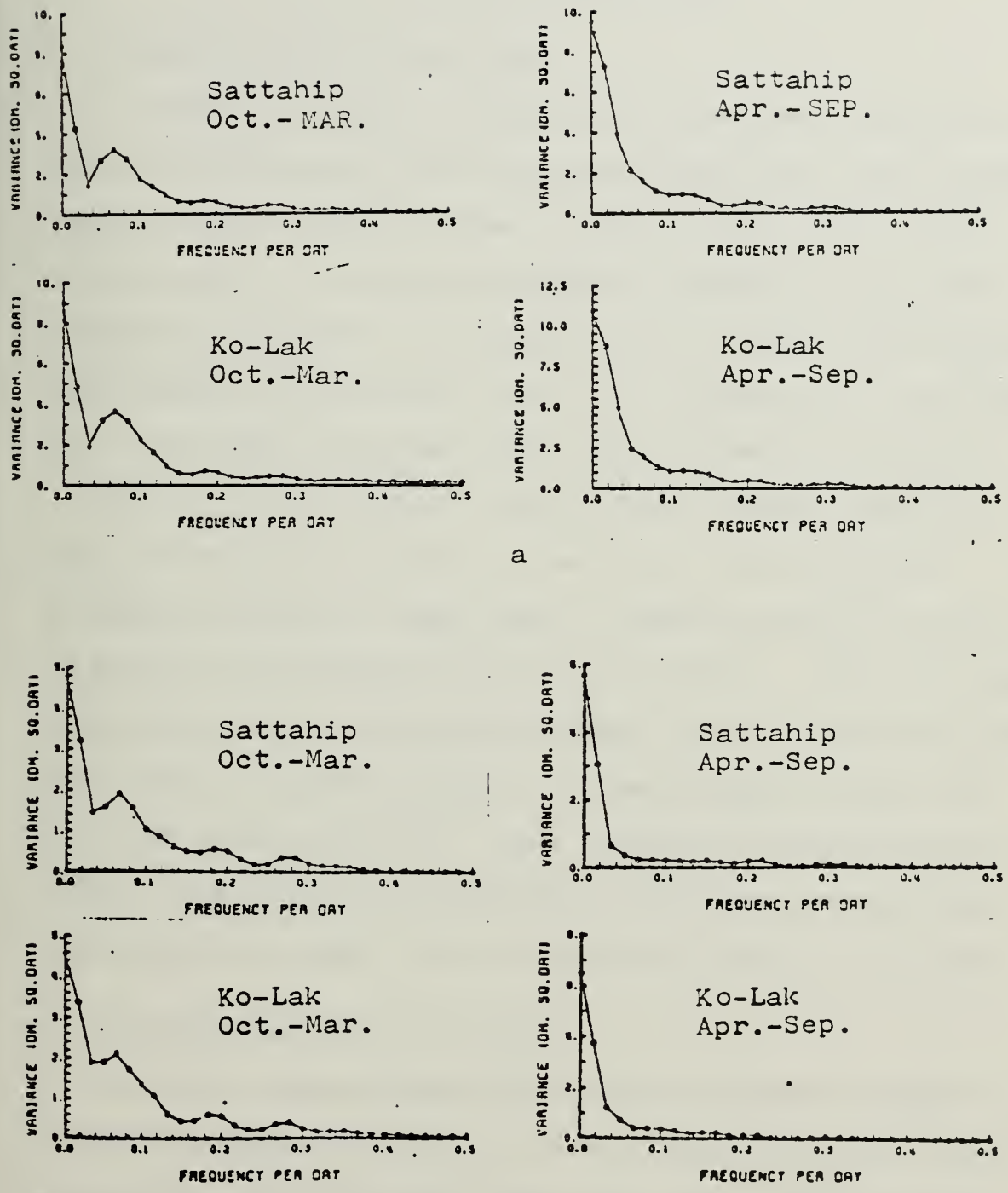


Figure 2. Spectra of Filtered Sea Level (1962)
 (a) with prewhitening (b) without prewhitening

V. RESULTS OF THE ANALYSIS

A. SEASONAL VARIATION OF SEA LEVEL

To examine the seasonal variation free of the short period variation, additional smoothing was done of the residual hourly sea levels obtained from application of Godin's filter. A 28-day period (672 hours) was selected because it minimizes the prominent fortnightly cycle and the bi-fortnightly variation of spring/neap tides, it suppress the relatively high-frequency non-astronomical noise, it is the length of a lunar month, and it approximates the commonly used comparison period of one month.

The time series of Appendix B show the hourly heights treated by Godin's filter (24-24-25 hours) and the 28-day filter (672 hours). The figures show that sea level usually increases from July to January and decreases from February to June at both stations. This corresponds to increasing sea level during the northeast monsoon, and decreasing sea level during the southwest monsoon. In these figures the sea level still shows great variability. These long-period fluctuations may be caused by meteorological and oceanographic effects and perhaps also by local bathymetric changes, such as formation and removal of sand bars.

B. MEAN ANNUAL VARIATION OF SEA LEVEL

The relation between seasonal sea level and atmospheric changes can be studied by comparing the annual sea level change with annual atmospheric pressure changes and variations in the local wind. The mean annual variation of meteorological elements is given in Table 2. The mean monthly sea levels were computed by averaging monthly levels from 1960

to 1966. The monthly pressure and wind data are averages from 1951 to 1975. These values are plotted in Figure 3. It is seen that sea level decreases from February to June and increases from June to February, which is in general agreement with the seasonal tendency of the mean monthly atmospheric pressure. The effect of atmospheric pressure on sea level can be estimated by applying the inverted barometer (hydrostatic) relationship, i.e., sea level is depressed by approximately 1 centimeter for every millibar of pressure increase. The mean annual variation of sea level, however, is seen in Figure 3 to be about 8 times the inverse barometer effect, and in addition the observed relationship is direct rather than inverse. This shows that the annual variation of atmospheric pressure accounts for very little of the annual sea level variation in this region.

Now consider the relations between the annual wind variation and the annual variation of sea levels at Sattahip and Ko-Lak, these variations being shown in Table 2. and graphically in Figure 3. These variations can be viewed as having two components, one representing the mean rise in level at the northern end of the gulf, the other representing the cross-gulf slope between the Ko-Lak and Sattahip. It is obvious from the similarity between the annual regimes at the two stations (Figure 3c) that the variations in mean level are much greater than those associated with cross-gulf slopes. The variation in mean sea level is consistent, qualitatively, with a tendency for water to leave the gulf by Ekman transport associated with winds from the south (as in February through June) and to return to the gulf when the winds are from the north (as in October through January). The cross-shelf slopes are small, but there

is a tendency for Sattahip to be relatively high during the period of west or southwest winds (June through September). This is consistent with a shallow water set-up response in phase with those winds.

C. SPECTRUM OF SEA LEVEL

To examine the sea level and its relation to forcing processes more closely, spectrum analysis of the data was used. The spectrum of sea level represents the distribution of "energy", or mean-square oscillation, over a range of frequencies. The frequency components present in a particular time series can be found and their significance evaluated. The method can also be applied to studying the relation between two time series, for example, the sea level at two neighboring stations for the same period of time. According to Hamon (1962), "In such cases the degree of association ('coherence') is obtained as a function of frequency; and the time displacement of one series relative to the other is found in terms of the 'phase difference', also as a function of frequency. The coherence and phase difference can give useful information even when the spectrums of the separate time series are relatively featureless".

Characteristic features of the sea level spectrum can be considered in three frequency regions according to Godin (1966):

"1) The low frequency band, defined over an interval extending from 0 to 1 cycle per day;

2) The central band, limited to 1 to 6 cycles per day;

3) Finally, the high frequency band containing all the frequencies above 6 cycles per day".

Table 2. Mean monthly sea level, pressure, and wind

	Month												AVE
	J	F	M	A	M	J	J	A	S	O	N	D	
Sattahip													
Z dm.	28.9	26.0	25.0	24.3	23.2	22.3	22.4	25.6	23.2	24.8	25.5	28.2	24.3
P mb.	12.8	11.8	10.9	9.6	8.0	7.7	7.7	7.8	8.5	10.2	11.6	12.6	9.9
V knots	6.0	6.8	7.4	7.2	7.2	9.8	9.4	9.1	7.4	5.8	6.8	7.1	7.5
V(dir)	N	S	S	S	SW	SW	SW	WSW	WSW	N	N	N	N
Ko-Lak													
Z dm	26.9	26.9	25.9	25.2	24.1	22.9	23.0	23.2	23.8	25.8	26.8	26.9	25.2
P mb.	12.7	11.5	10.7	9.3	7.8	7.6	7.7	7.7	8.3	10.0	11.3	12.3	9.7
V knots	6.7	5.6	6.0	6.2	6.0	6.8	6.7	6.9	6.2	6.1	8.3	8.7	6.7
V(dir)	N	S	S	S	W	W	W	W	W	N	N	N	N

Z = Monthly sea level (1960-1966) relate to arbitrary datum at both stations

P = Sea level atmospheric pressure (1951-1975) above 1000 mb.

V = Surface velocity (1951-1975).

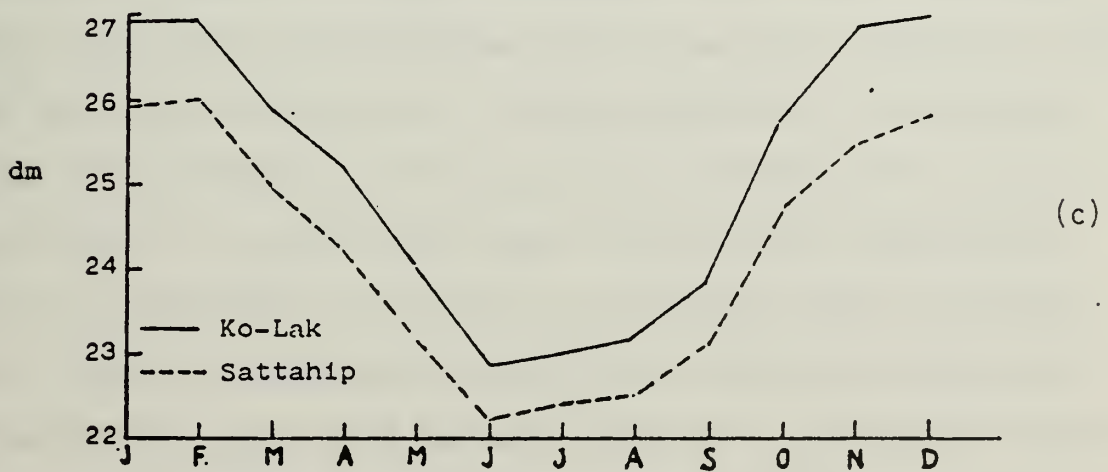
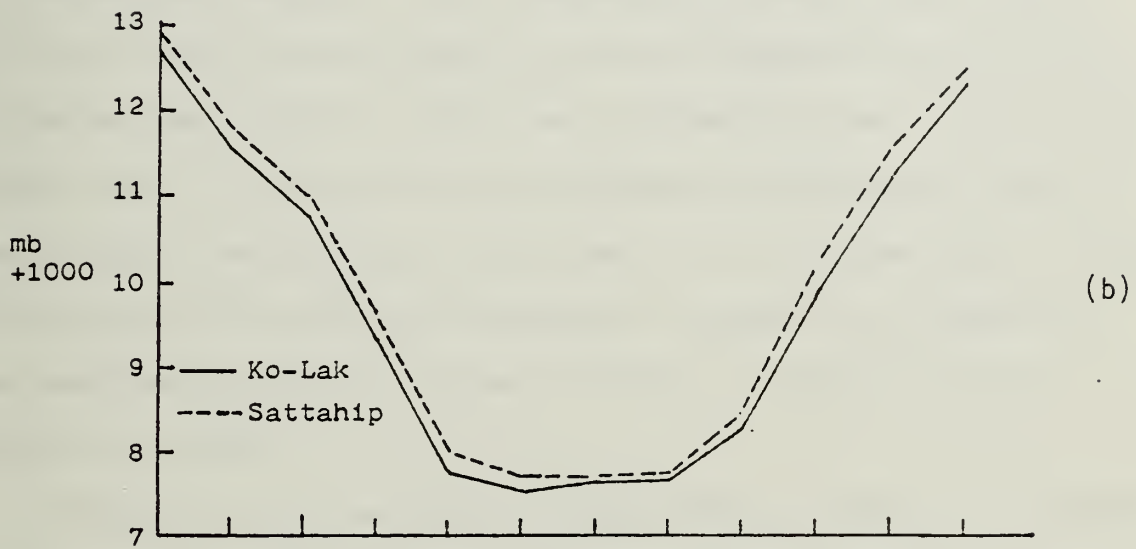
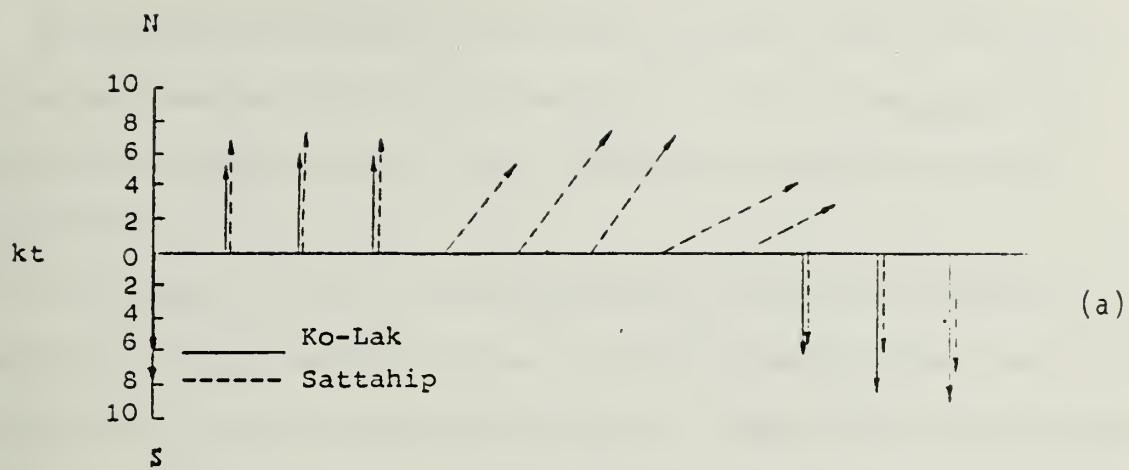


Figure 3. Mean monthly sea level and climatological elements: a) wind (1951-1975), b) atmospheric pressure (1951-1975), c) sea level (1960-1966).

The central band contains the diurnal and semi-diurnal periods and is the most energetic part of the spectrum. The low-frequency band contains the seasonal cycle, yearly variations, and meteorological disturbances.

In this analysis, the variance densities of the hourly heights at Sattahip and Ko-Lak were calculated, and the coherence, phase, and cross-spectra of the two data sets were obtained. These spectra are examined in two frequency regions; first, including the central band (0.04 to 0.25 cycles per hour) and second, in the low frequency band (0 to 0.04 cycles per hour) with the central band eliminated by the low pass filter (Godin, 1966). Both analyses were performed on three-month blocks of hourly height (January-March, April-June, etc.,) for seven years of data. These analyses are graphically presented in Appendix C and Appendix D. The spectrum for each data set has resolution $f = 1/512 \text{ hr}^{-1}$ and 8 degrees of freedom.

The spectra of the raw hourly heights, shown in Appendix C, which are dominated by frequencies lying in the central band, show the prominent peaks of the diurnal and semidiurnal tidal components at frequencies about 0.041 and 0.08 cycles per hour. At these frequencies, the coherence between the two stations tends toward unity, which means that they are fully related. The phase graph shows that these tidal components at Ko-Lak lag behind those at Sattahip by 3-20 degrees, which corresponds 0.2-1.7 hours. The amplitude of the diurnal tide is much higher than the semi-diurnal tide, which indicates that usually the tide has diurnal form.

To consider the seasonal variation and others of low frequency, it is useful to eliminate the effect of the prominent semi-diurnal and diurnal astronomical tides. The spectra are made free of these astronomical tides by low pass filtering (Godin, 1966). This essentially filters out high-frequency fluctuations. In addition, the linear trend was removed from the records to make the time series as stationary as possible (Roden, 1966). The results are graphically presented in Appendix D and summarized for each three-month period for seven years in Figures 4 and 5. These spectra show a large interannual (year-to-year) variation, especially in the January-March period. The years 1962 and 1964 have 8 or 10 times the energy of 1960 and 1965. This means that the non-astronomical sea level variations can not be predicted well from a mean annual variation. It is important to know the variation from year-to-year.

To increase stability of the spectral estimates and to show the mean spectral form, the spectra for each three-month period in Figures 4 and 5, were ensemble averaged over the seven-year period. These averaged spectra are presented in Figures 6 and 7; they have resolution $f = 1/512 \text{ hr}^{-1}$ and 56 degrees of freedom. The energy in frequencies above 0.021 cycles per hour quickly tends toward zero, and consequently these frequencies are omitted. This cut-off held true for both raw and filtered hourly data, with the exception of the extremely strong energy peaks at the 12.4 and 24.8 hr. lunar-solar tidal periods in the hourly data. The spectra show the highest energy in the period January-March at both stations. This shows that the large variations in the sea level occur in the period of the northeast monsoon season.

To study the interannual variation for the entire year, the spectra for each three-month block are ensemble averaged over each whole year (as in Figures 6 and 7; resolution $f = 1/512 \text{ hr}^{-1}$ and 56 degrees of freedom). These spectra are shown in Figure 8; they have the same resolution and 224 degrees of freedom. The spectra show high peaks at frequency 0.00195 cycles per hour (period 21.4 days) and rapid decrease to frequency 0.0058 cycles per hour (period 7.1 days). For these spectra the energy at frequency $1/512 \text{ hr}^{-1}$ has contributions from the annual frequency and other low frequencies. Their energy all appears at that (first resolvable) frequency. This is the characteristic feature of a "red spectrum", which defines the increase in energy density with decreasing frequency. The spectra of non-periodic sea level fluctuations are decidedly red, showing a concentration of spectral energy at low frequencies (Roden, 1960).

In Figure 8, the spectra are seen to be very similar at the two stations (Ko-Lak and Sattahip). This suggests that the low-frequency non-astronomical components of sea level at both stations may be responding to the same driving mechanisms, perhaps variations in the monsoon wind.

For the analysis of seasonal differences the spectra from each station were ensemble averaged over each monsoon season, and are shown in Figure 9. The spectra in each three-month period in Figures 6 and 7, (with resolution $f = 1/512 \text{ hr}^{-1}$ and 56 degrees of freedom) were then ensemble averaged in 6-month periods in order to include the northeast monsoon (October-March) and southwest monsoon (April-September) seasons. The resulting spectra have the same resolution and 112 degrees of freedom. Due to the constraints imposed by the three-month analysis process, the

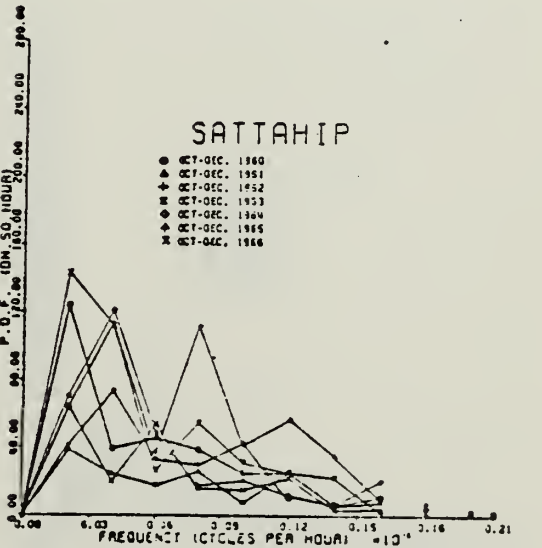
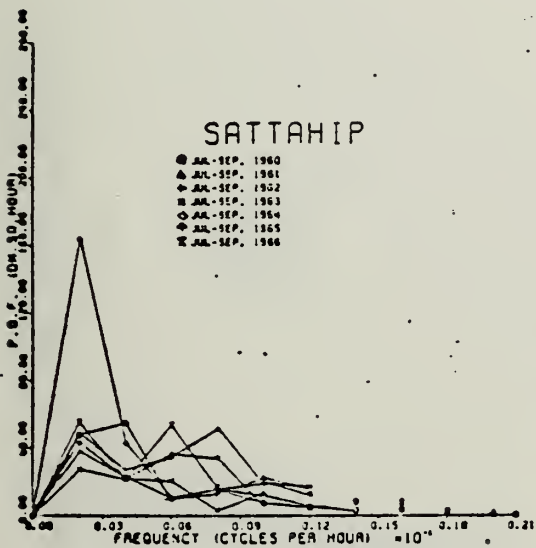
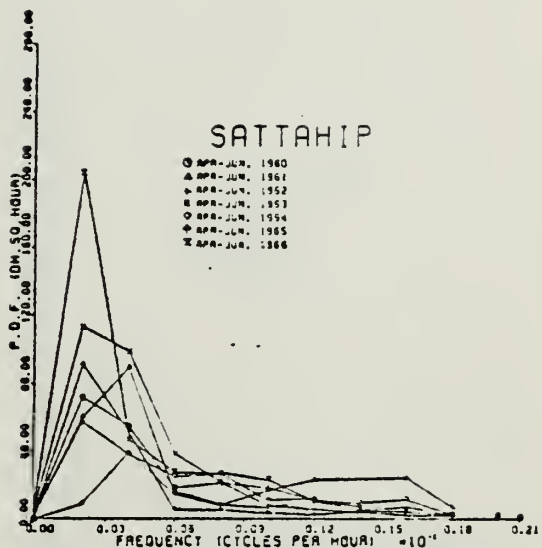
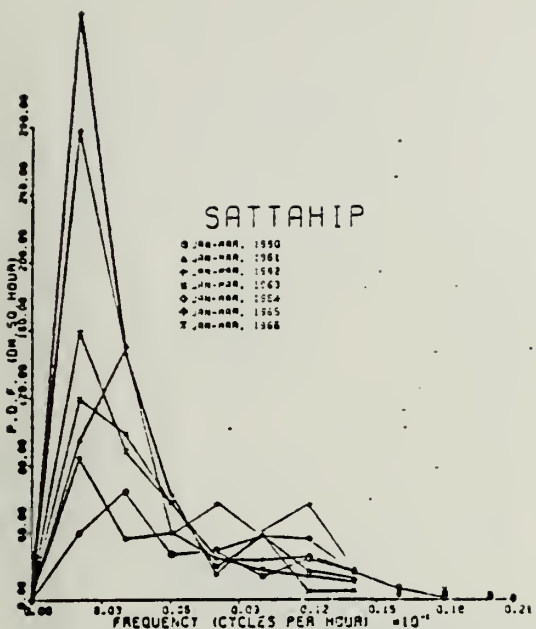


Figure 4. Seven years of filtered sea-level spectra for three-month periods at Sattahip (8 degrees of freedom).

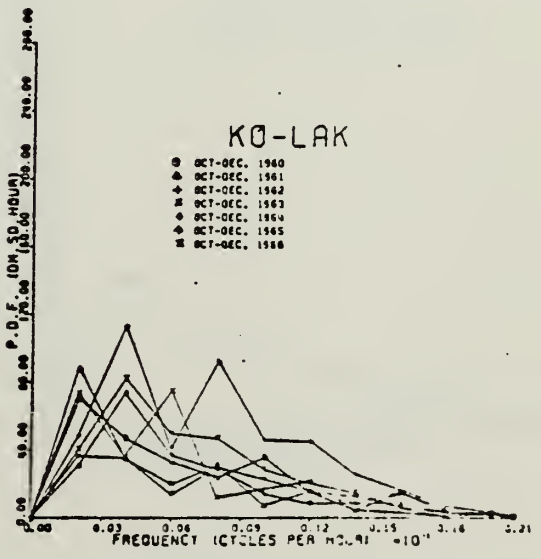
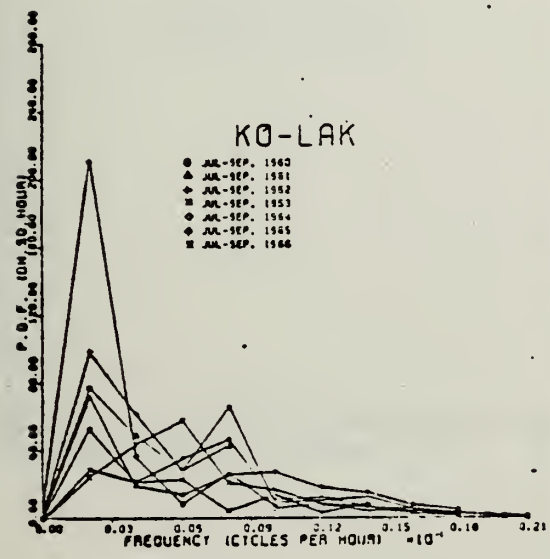
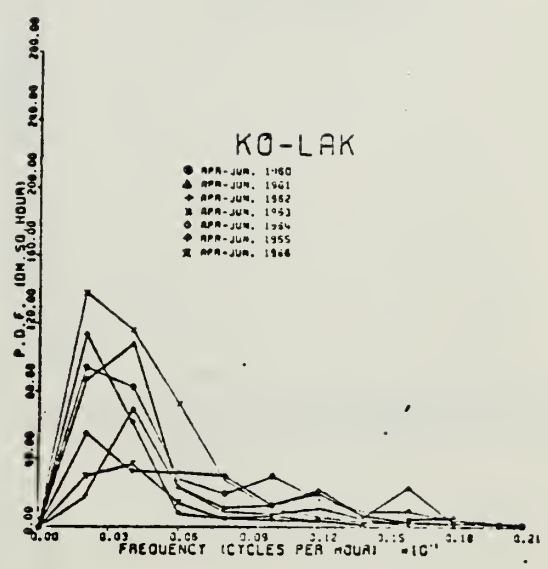
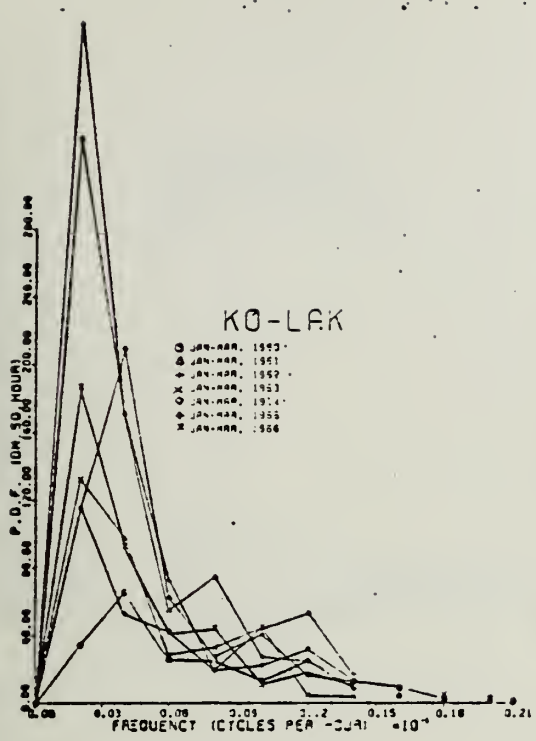


Figure 5. Seven years of filtered sea-level spectra for three-month periods at Ko-Lak (8 degrees of freedom).

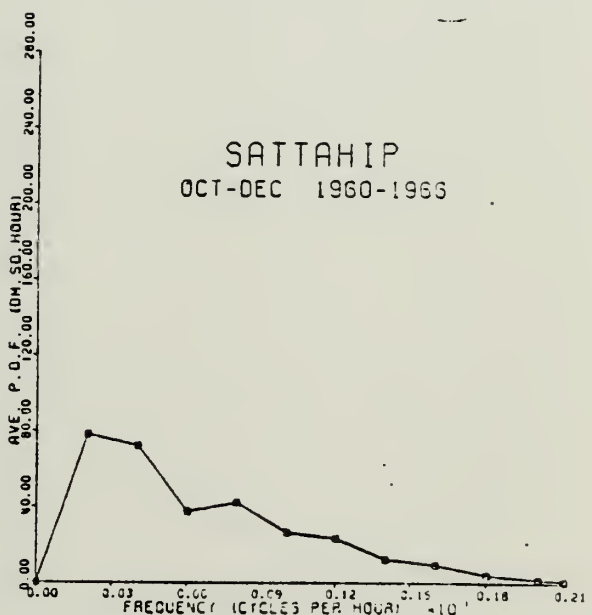
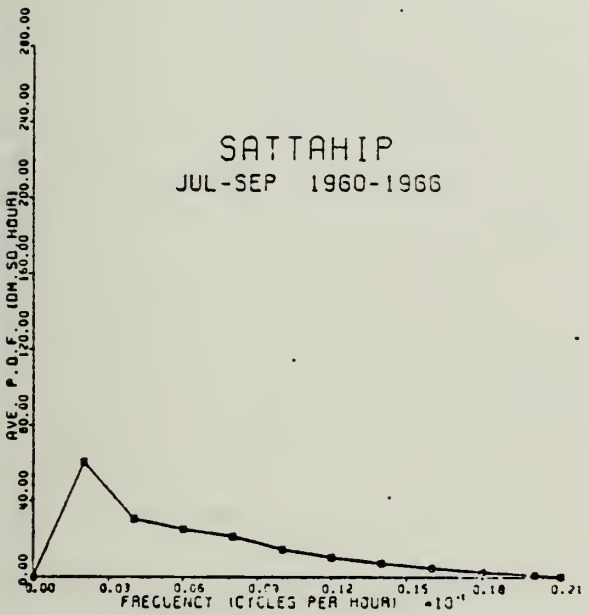
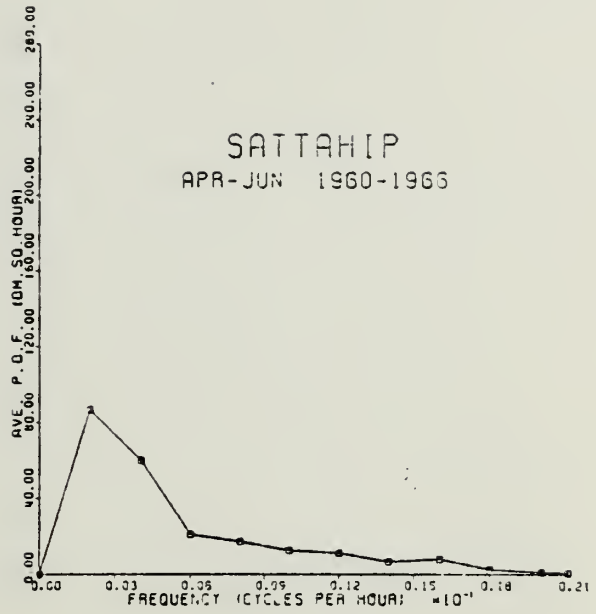
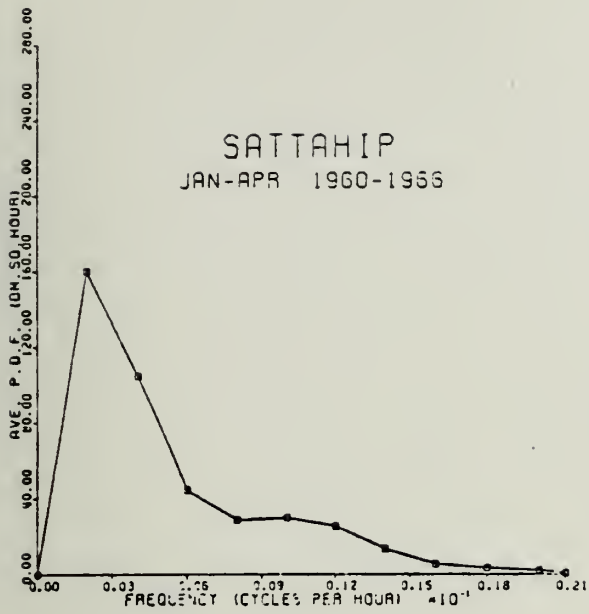


Figure 6. Seven-year ensemble averaged filtered sea-level spectra for three-month periods at Sattahip (56 degrees of freedom).

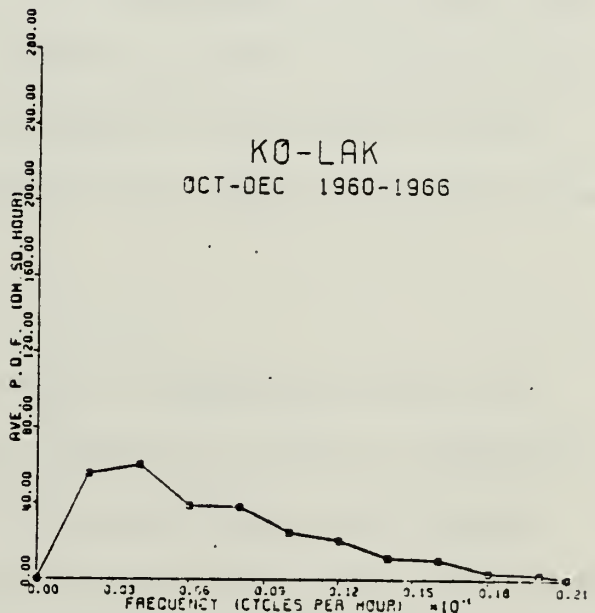
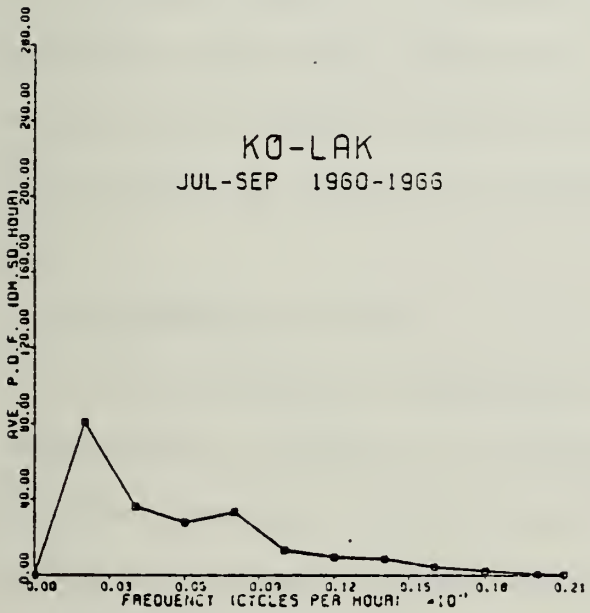
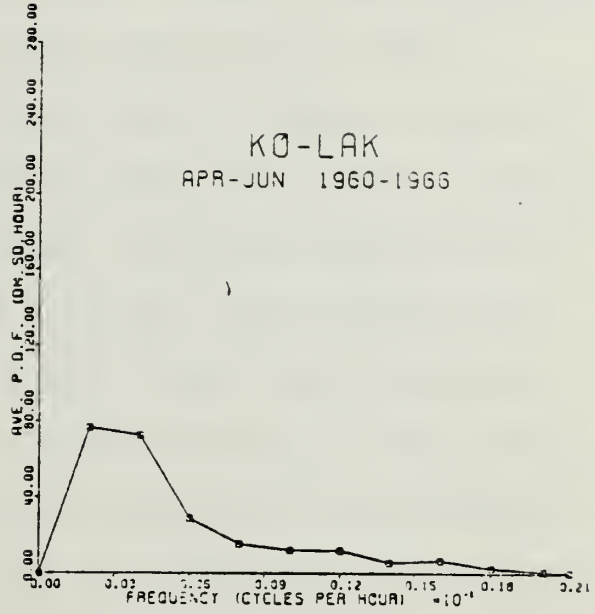
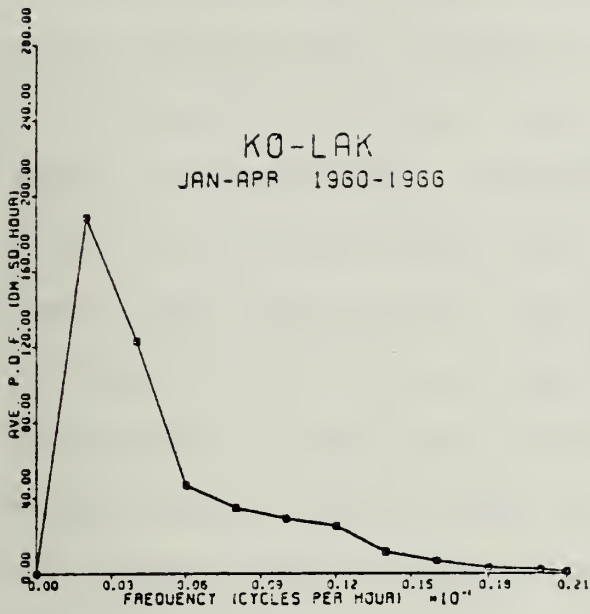


Figure 7. Seven-year ensemble averaged filtered sea-level spectra for three-month periods at Ko-Lak (56 degrees of freedom).

seasonal periods each contain an even number of months, with the southeast season (February-March) included in the northeast monsoon season.

The spectra from the two stations are similar in shape, as shown in Figure 9, for each season. Both monsoon seasons show maxima at frequency 0.00195 cycles per hour (period 512 hours) and decrease rapidly to frequency 0.0058 cycles per hour (period 171 hours), then decrease slowly to frequency 0.014 cycles per hour (period 73 hours) where the energy tends to zero. These spectra differ in that the energy in the northeast monsoon season is clearly higher than that during the southwest monsoon. This suggests that the northeast monsoon wind has greater variation than the southwest monsoon. Obviously, this is the season in which sea level prediction most needs consideration of forcing by wind. A question which arises later is whether the sea level response is due to local forcing over the Gulf of Thailand or to remote forcing, perhaps in the South China Sea.

D. METEOROLOGICAL EFFECTS

To find connections between sea levels at Sattahip and Ko-Lak and meteorological processes, the relations between sea level and atmospheric pressure (Sattahip), sea level and the mean geostrophic wind (Bangkok-Saigon and Bangkok-Singapore), and sea level and local surface wind (Bangkok) were examined. The spectrum, cross-spectrum, coherence, and phase were calculated by program FTFREQ (IMSL, 1980), which covered a 6-month period (October-March and April-September); the maximum number of lags was 30 and spectral estimates have 12 degrees of freedom.

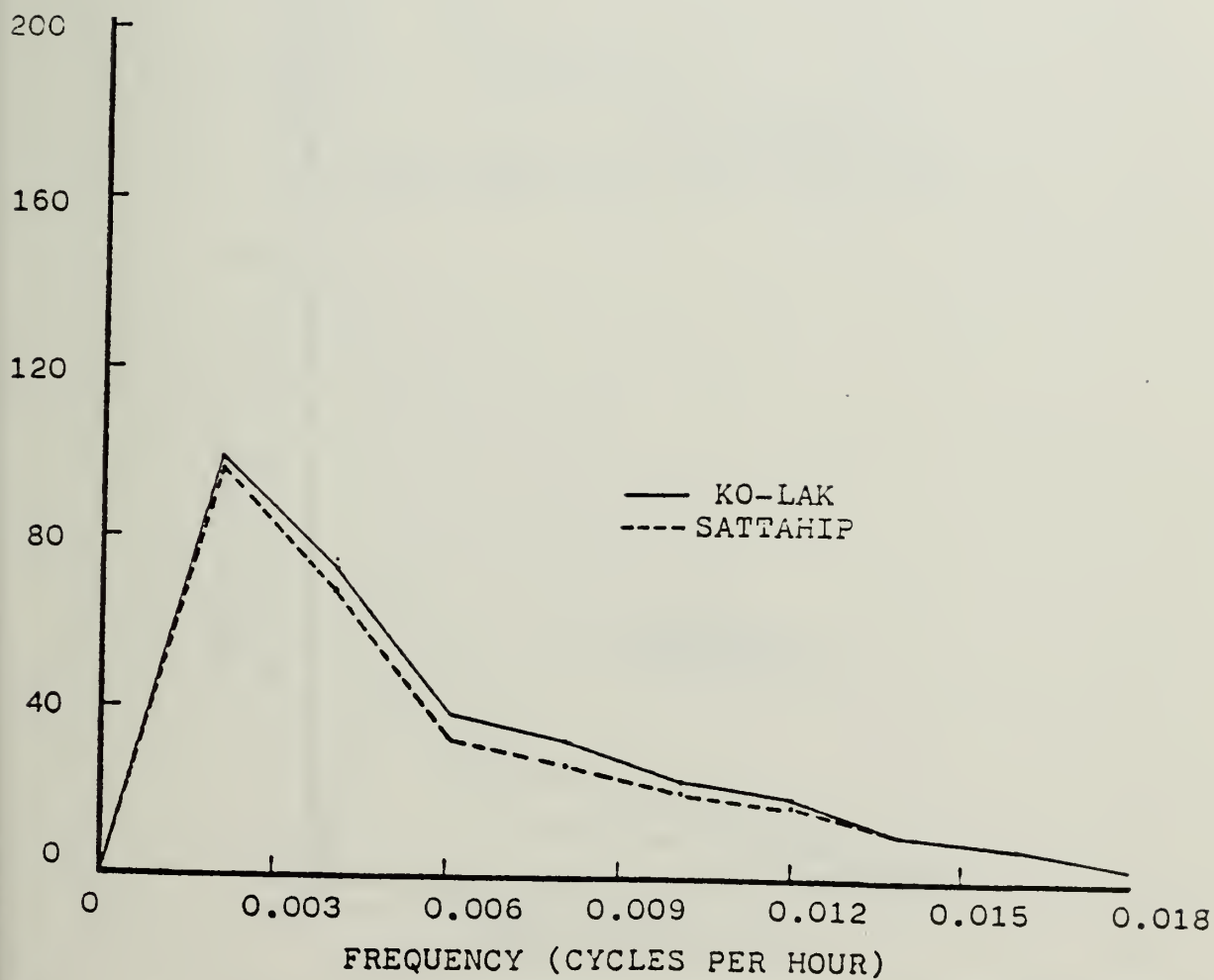


Figure 8. Seven-year ensemble averaged nontidal sea-level spectra over the whole year (224 degrees of freedom).

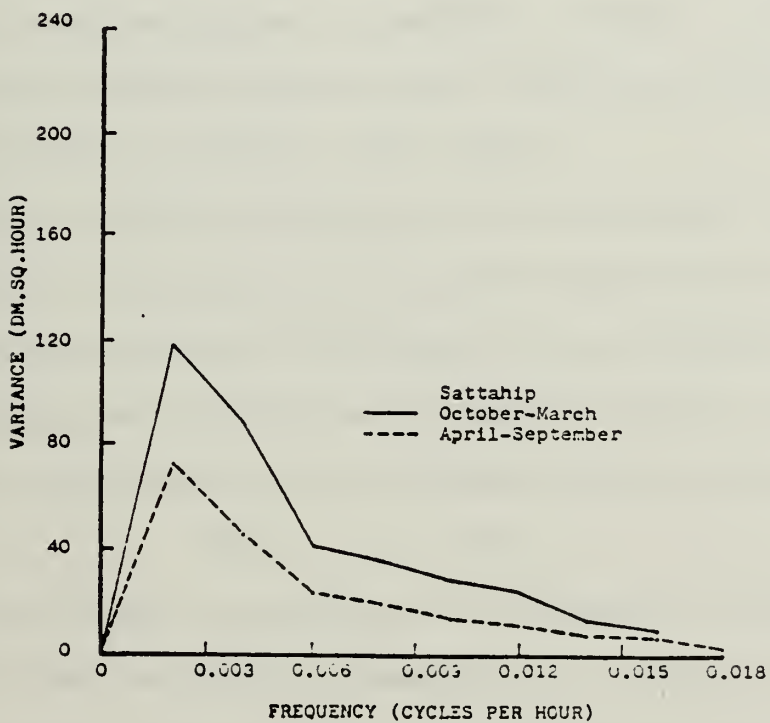
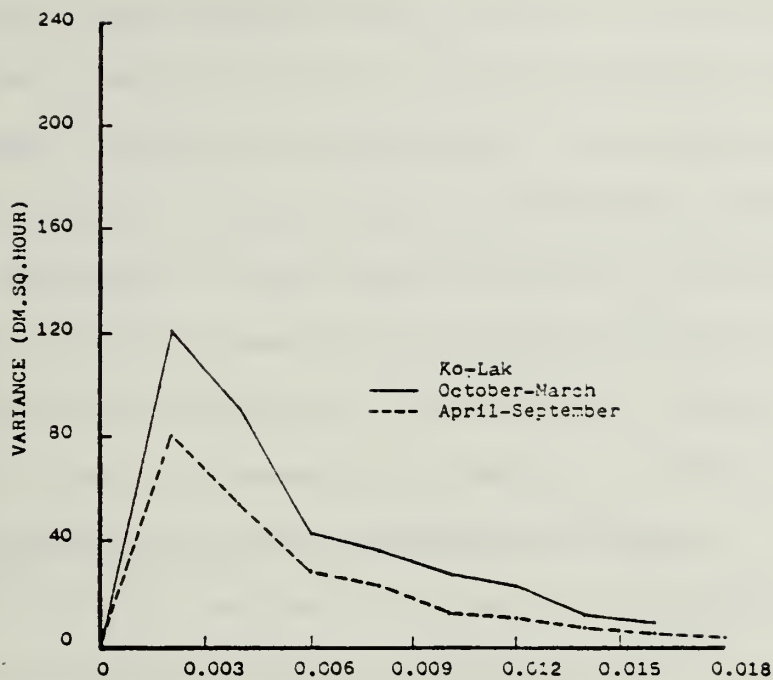


Figure 9. Seven-year ensemble averaged filtered sea-level spectra according to season (112 degrees of freedom).

The term, "meteorological effect", generally includes the effects of (1) atmospheric pressure, (2) the transient wind that accompanies rapidly moving storms, and (3) the steadier winds on sea level (Miller, 1956).

In this analysis, the sea level, the atmospheric pressure, and the wind are represented by daily values at 06 hours in the year 1962. The sea levels with the astronomical tide removed by low pass filter (24-24-25 hr.) are shown in Figure 10. The atmospheric pressures from which geostrophic winds were computed are presented in Figures 11 and 12.

1. Response of Sea Level to Atmospheric Pressure

The change of sea-level in response to atmospheric pressure variation in time equals the height of a column of water having the same weight per unit area as the change in atmospheric pressure. A pressure increase of 1 mb. would decrease the sea surface elevation by approximately 1 cm. under quasi-static conditions (Roden, 1966).

Since the filtered sea levels and local atmospheric pressures are available only at Sattahip, and because of many missing values in the atmospheric pressure data, the response of the filtered sea levels to the variable atmospheric pressure were calculated from their statistics.

The ratio of the response can be estimated formally from the ratio

$$\text{Resp} = E_p/E_z$$

where E_p and E_z are the variances of the atmospheric pressure fluctuations and the filtered sea levels, respectively. A value of 1.0 would indicate total response. The result for this response at Sattahip is 0.0003.

This suggests that the atmospheric pressure does not influence sea level to an important extent.

2. Sea Level and the Geostrophic Wind

Geostrophic wind from daily weather records was used to infer the strength and direction of wind stress on the sea surface. The procedure is not completely satisfactory, since the relationship between surface and geostrophic wind is not always consistent; but within reasonable limits, it is useful to assume that surface wind varies linearly with the geostrophic wind (Petterson, 1940).

The geostrophic winds were investigated by use of surface pressures at three stations (Bangkok, Saigon, and Singapore). The geostrophic winds found from these pressures were related to the sea levels at Sattahip and Ko-Lak. For example, the Bangkok-Saigon pressure difference (Figure 1) can be viewed as representing the mean cross-gulf geostrophic wind, a positive pressure difference implying wind from the east.

The spectra, cross-spectra, coherences, and phases between the Bangkok-Saigon pressure differences and the filtered sea levels at Sattahip and Ko-Lak are shown in Figures 13 and 14. The relationships for each monsoon season (October-March and April-September) at the two tide stations are similar. For the northeast monsoon season (October-March), high coherence occurs at frequency 0.117 cycles per day (period 8.6 days), and the phase difference is about 0-10 degrees indicating that the geostrophic wind leads sea level. For the southwest monsoon, high coherence occurs at frequency 0.083 cycles per day (period 12.1 days), with phase about 40 degrees. This seems to indicate that the northeast anomaly of winds produces a rise in sea level and the southwest anomaly leads to low sea level in the northern end of the gulf, as can be expected from Ekman transport.

For the filtered sea levels at Ko-Lak or Sattahip and the atmospheric pressure difference between Bangkok and Singapore, shown in Figures 15 and 16, there is high coherence at frequency 0.117 cycles per day, with a phase difference of about 220 degrees at Ko-Lak and 0 degrees at Sattahip, during the northeast monsoon. For the southwest monsoon, the high coherence occurs at frequency 0.083 cycles per day, phase about 10 degrees at Ko-Lak and 50 degrees at Sattahip. This shows a less consistent relation between sea level and the mean geostrophic wind between Bangkok and Singapore than for the Bangkok-Saigon mean. The implication is that Bangkok-Saigon pressure differences are better representative of the cross-gulf wind.

3. Sea Level Slope and the Local Wind

The wind is one of the primary agencies that drives ocean currents and influences the redistribution of density within the ocean. This also is one of the major factors in producing sea level variations.

The effect of local wind is most pronounced according to Groves (1956) as follows:

- "1) Where (or when) there are strong winds
- 2) On the edge of continents; this follows from the fact that divergence of the horizontal wind-stress is one of the most effective agencies in bringing about surface slopes. A coast line will act as a line of divergence if the wind is blowing across it.
- 3) At stations where there is an extensive shoal region adjacent to the tide gauge, which follows from the fact that the total horizontal force on a vertical column of water is independent of the water depth in the case of surface wind stress, although it is proportional to the depth in the case of the pressure gradient associated with a given surface slope".

The slope ($\Delta\eta$) across the northern gulf may be measured by the difference in sea level between Ko-Lak and Sattahip ($\eta_k - \eta_s$). The observed local wind at Bangkok was examined for its relation to the slope ($\Delta\eta$). The wind was analyzed into north-south (V_{NS}), east-west (V_{EW}), components and also X(V_x), Y(V_y) components, where X is the axis along the line connecting Ko-Lak and Sattahip, as shown in Figure 1. Time series of the wind components are shown in Figures 17 and 18.

The spectra, cross-spectra, coherences and phases between $\Delta\eta$ and each of the four components of the local wind have been calculated and are shown in Figures 19-22 for each season. The cross-spectra for ($\Delta\eta, V_{NS}$) and ($\Delta\eta, V_y$) show high coherence at frequency 0.2 cycles per day and phase difference about 20 degrees (V_{NS} and V_y lead $\Delta\eta$) during the northeast monsoon. They also show high coherence at frequencies 0.1-0.133 cycles per day, phase about 10 degrees, during the southwest monsoon. This means that at those frequencies the water of the upper gulf tends to slope downward to the east when the anomalous wind is from the south and vice versa, which is contrary to expectation from the Ekman relationship. The spectra for ($\Delta\eta, V_{EW}$) and ($\Delta\eta, V_x$) show high coherence at frequency 0.117 cycles per day, phase about 200 degrees (V_{EW} and V_x lead $\Delta\eta$), during the northeast monsoon. They also show high coherence at frequency 0.083 cycles per day, phase about 180 degrees. This is consistent with wind set-up in response to east-west and X components of the local wind, although this effect is secondary to the Ekman effect over the gulf as a whole as was concluded in Section V B.

It may be concluded that the most important relation between local wind and response of cross-gulf sea level slope between Sattahip and Koolak is that in which the wind blows across the gulf and the response is in frequency band 0.083-0.117 cycles per day (period 8-12 days), is increased sea surface slope upward in the direction toward which the wind blows.

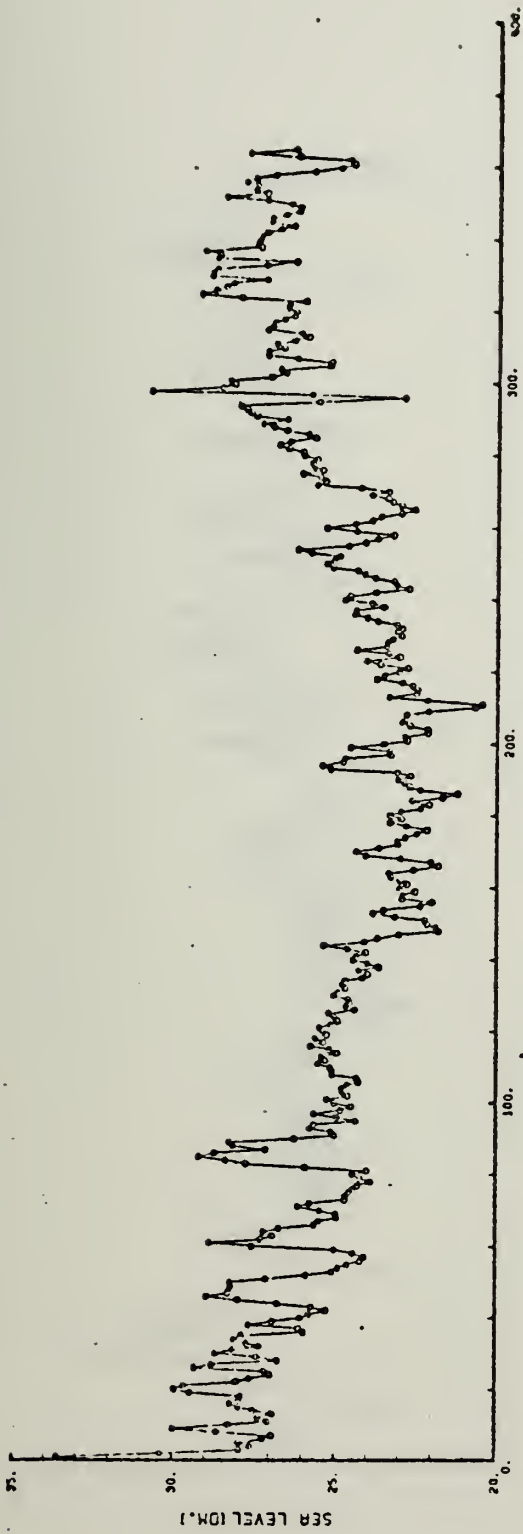
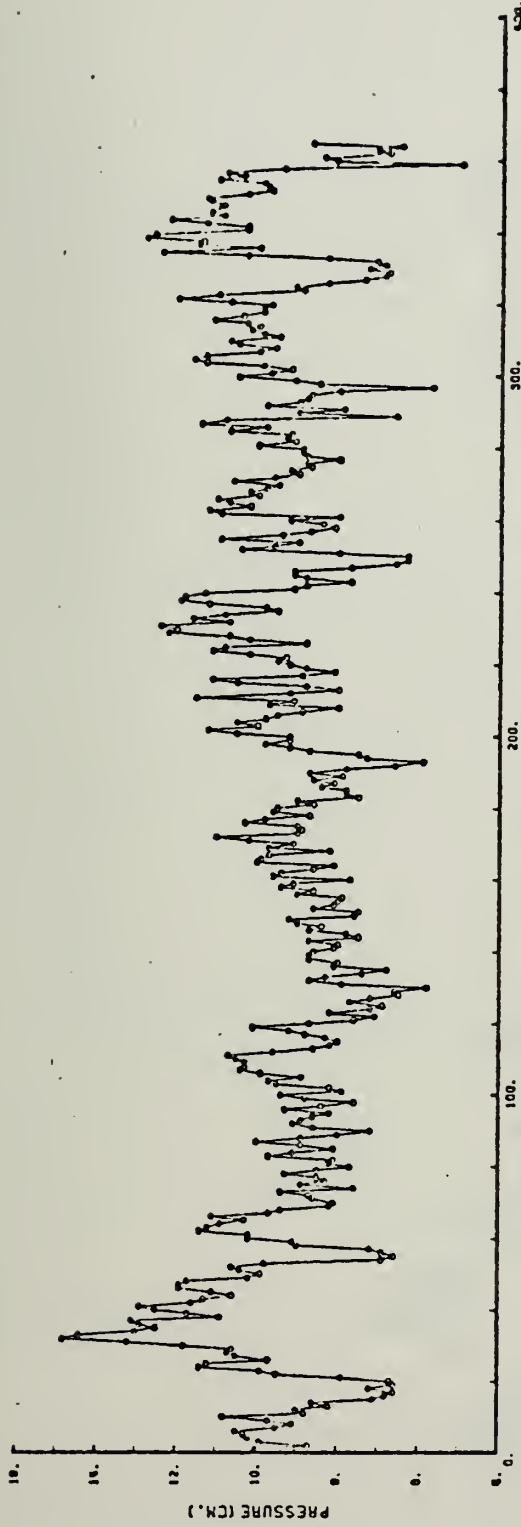
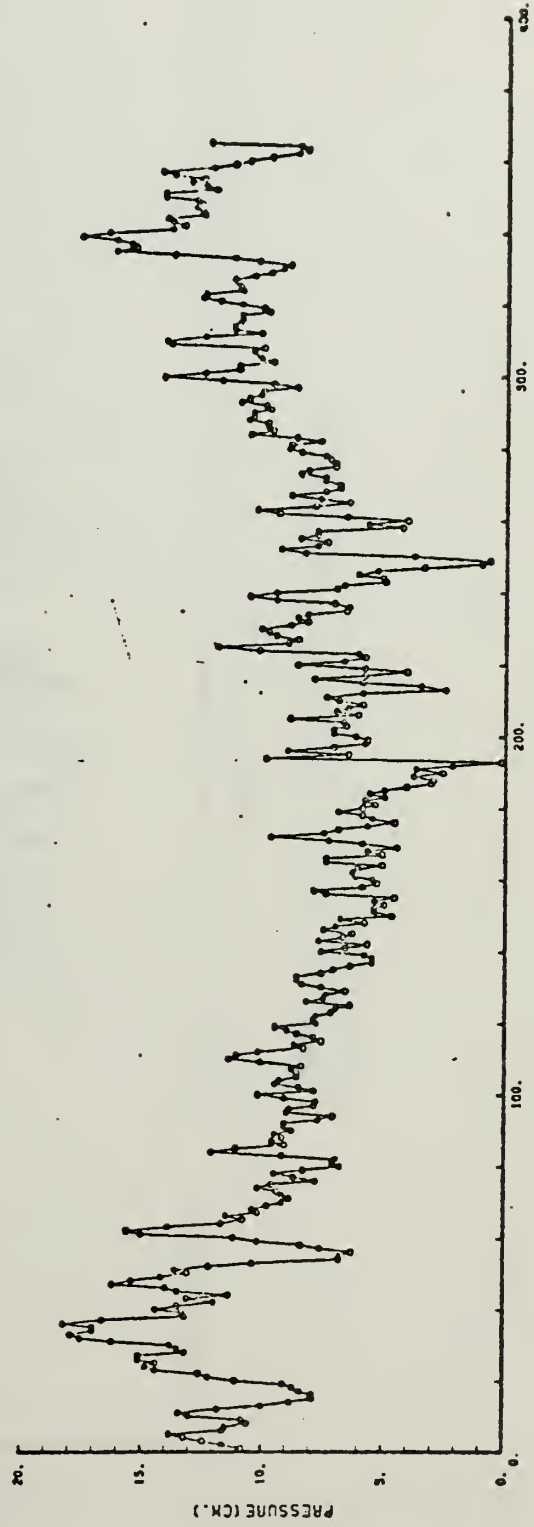


Figure 10. Daily filtered sea level at Ko-Lak and Sattahip (1962)



SINGAPORE 6TH DAILY



BANGKOK 6TH DAILY

Figure 11. Daily sea surface pressure at Singapore and Bangkok (1962)

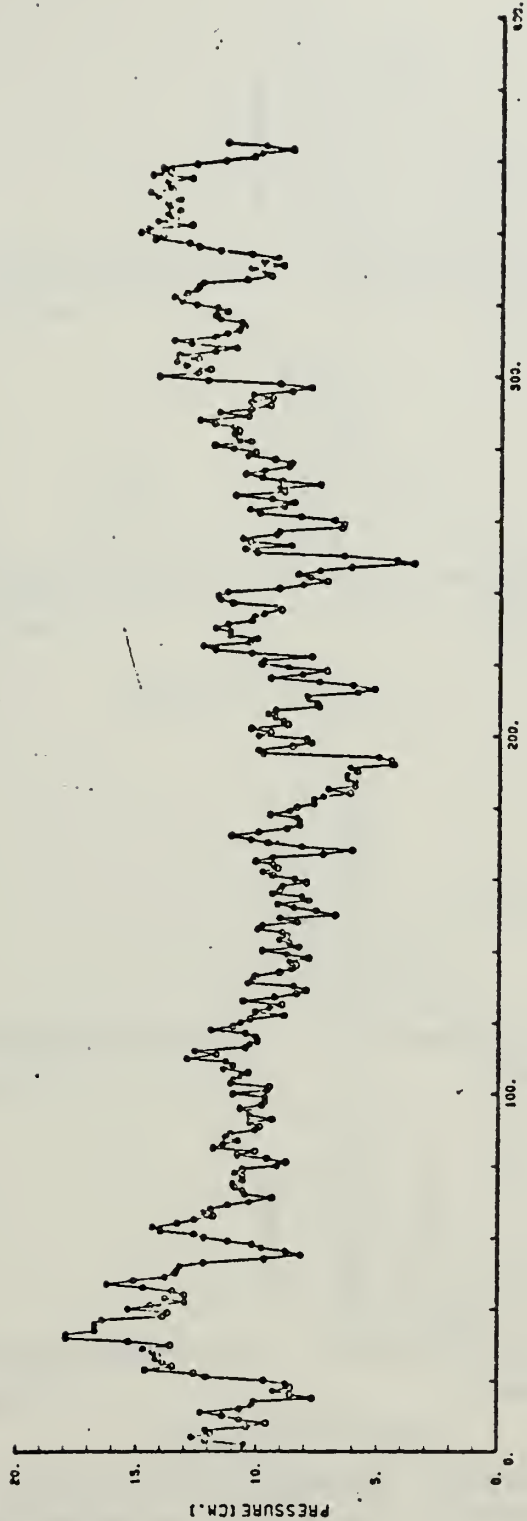
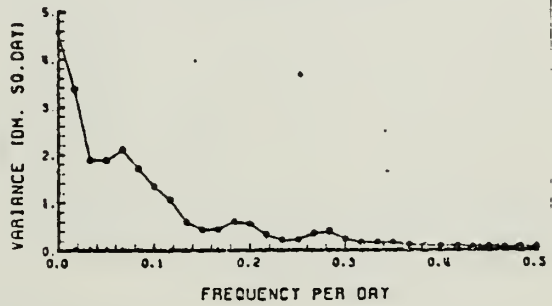
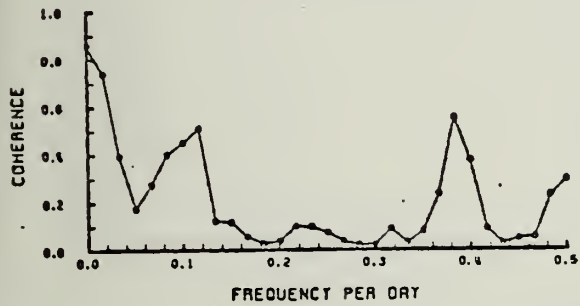
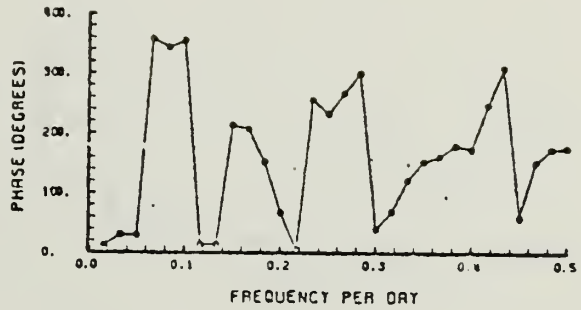
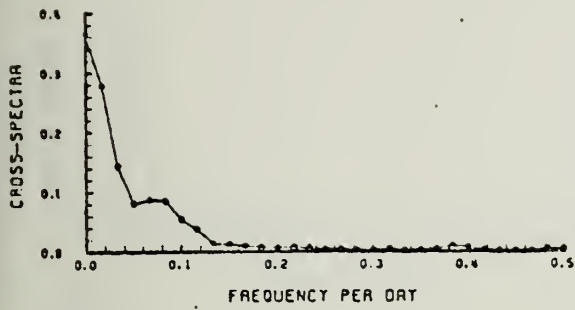
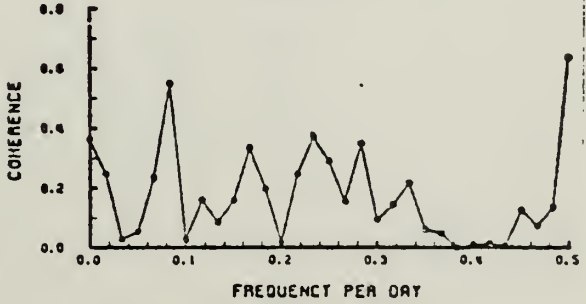
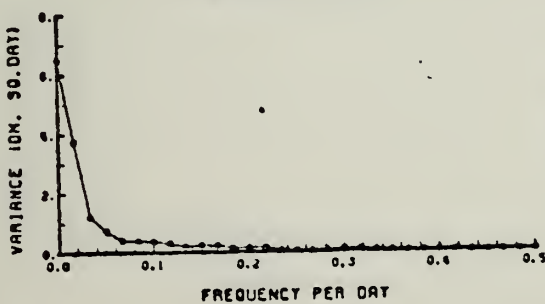
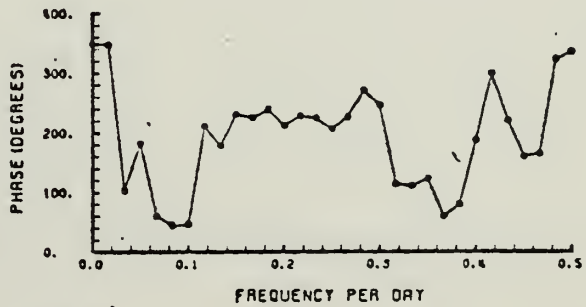
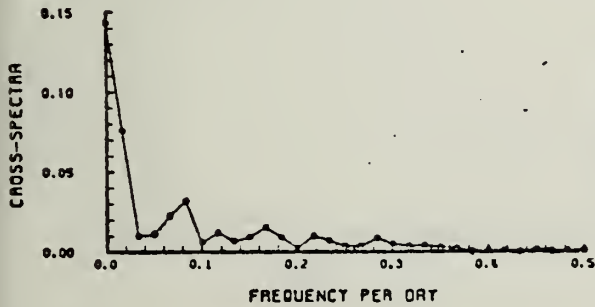


Figure 12. Daily sea surface pressure at Saigon (1962).

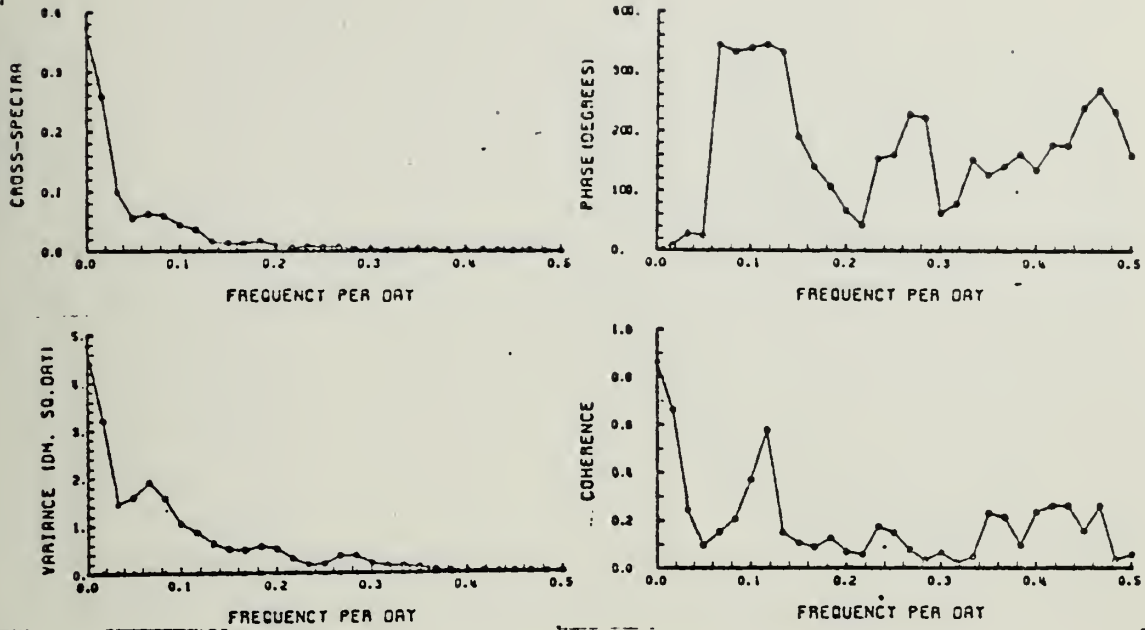


October-March

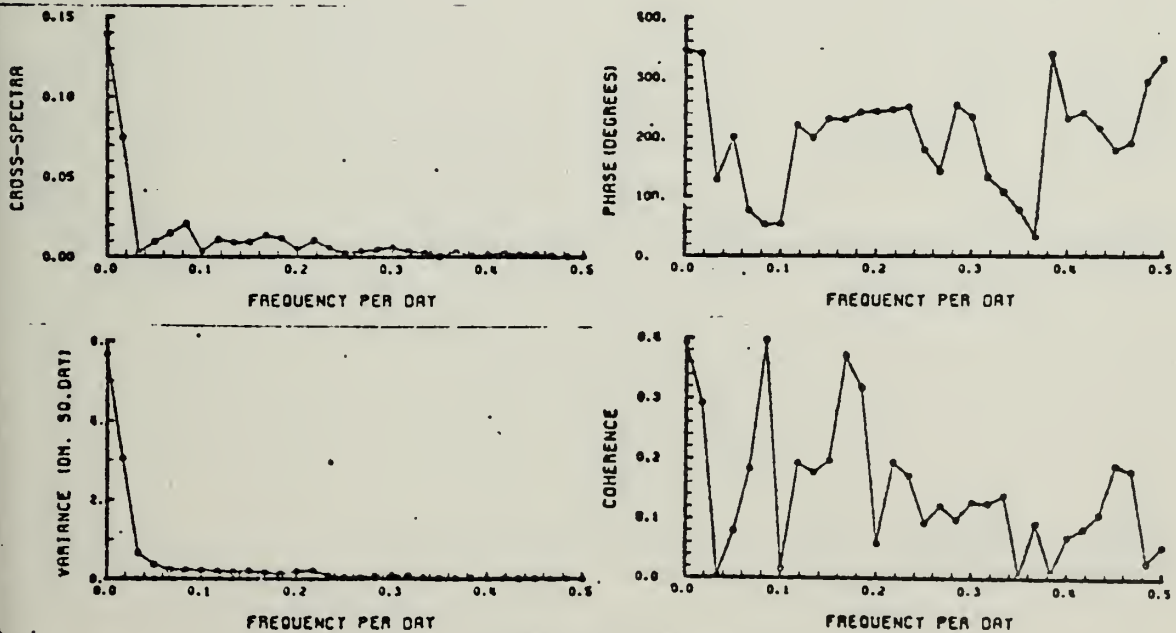


April-September

Figure 13. The spectrum, cross-spectrum, coherence, and phase for filtered sea level (Sattahip) and pressure difference (Bangkok-Saigon), (12 degrees of freedom).

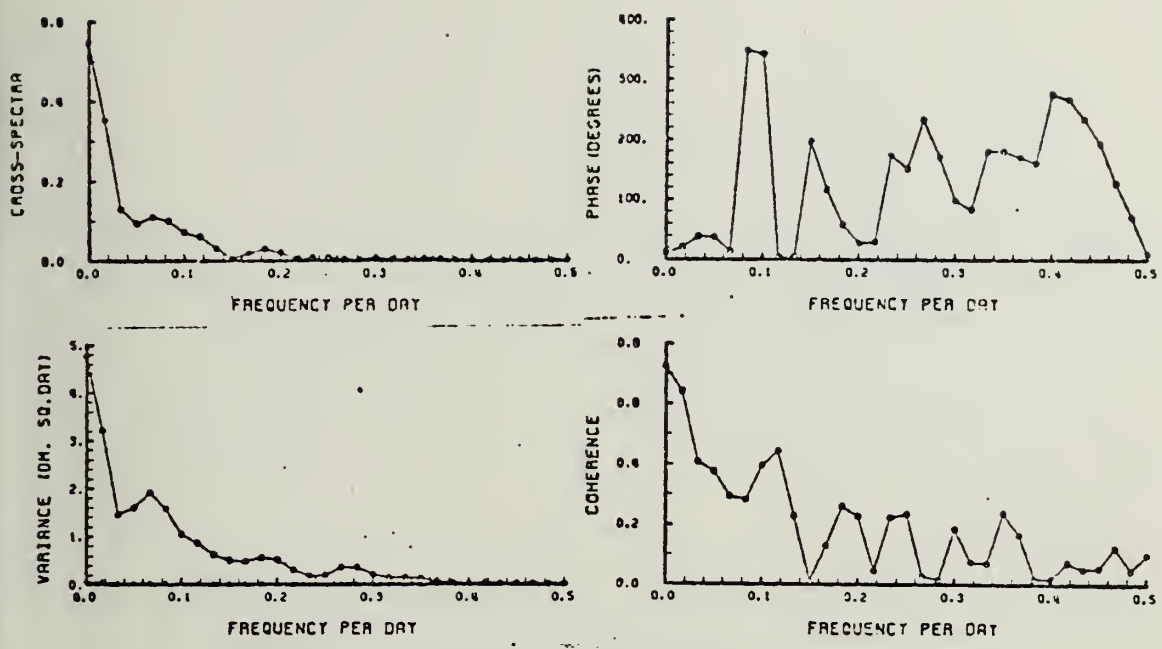


October-March

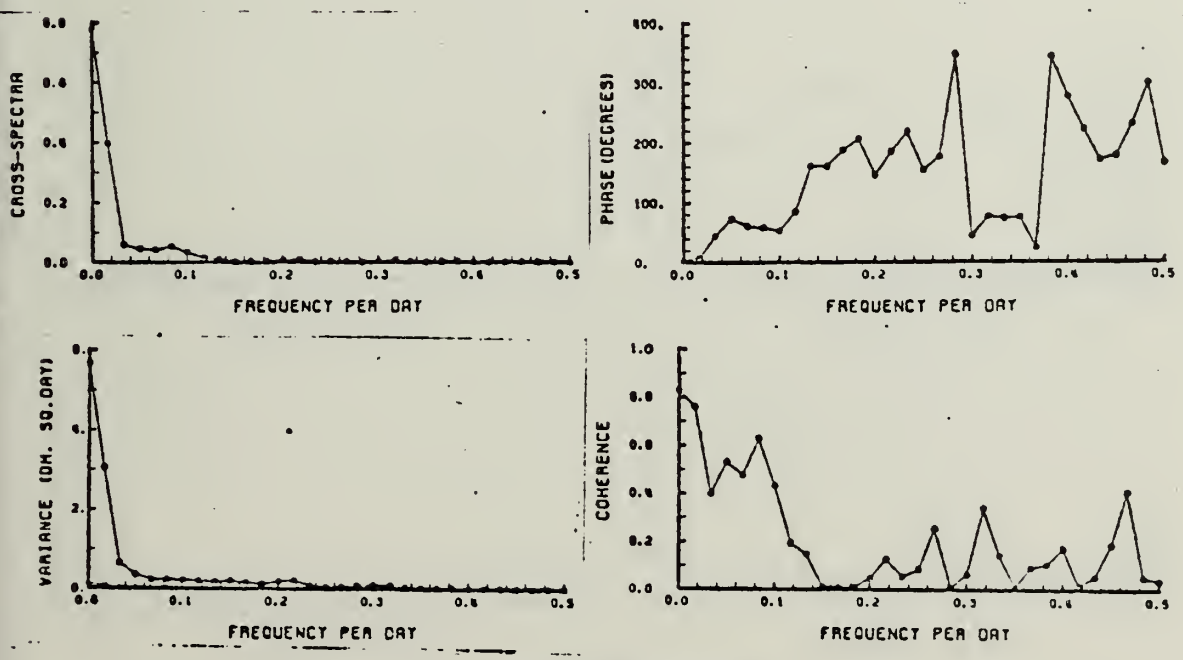


April-September

Figure 14. The spectrum, cross-spectrum, coherence, and phase for filtered sea level (Sattahip) and pressure difference (Bangkok-Saigon), (12 degrees of freedom).

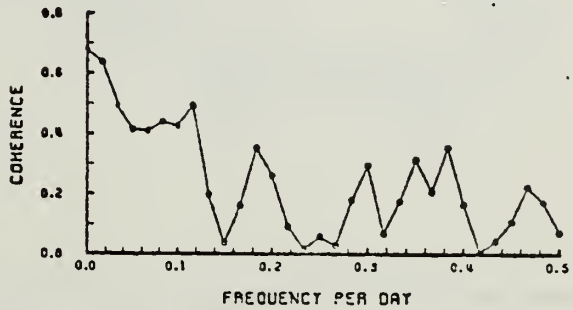
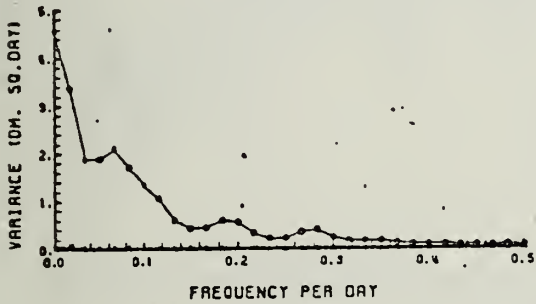
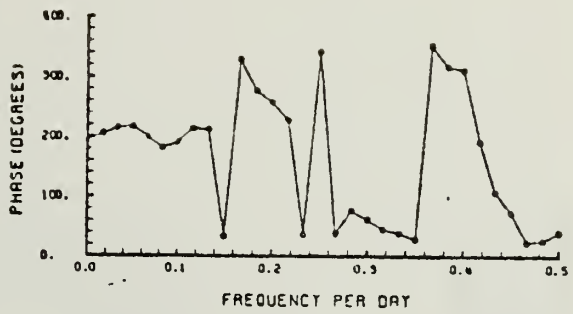
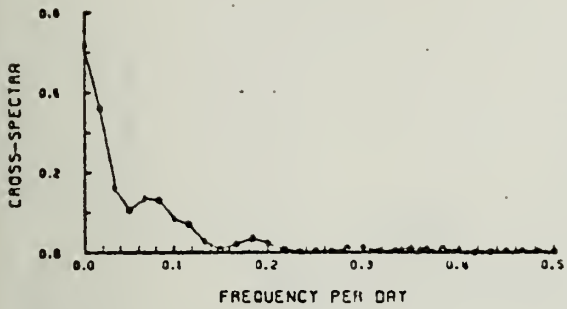


October-March

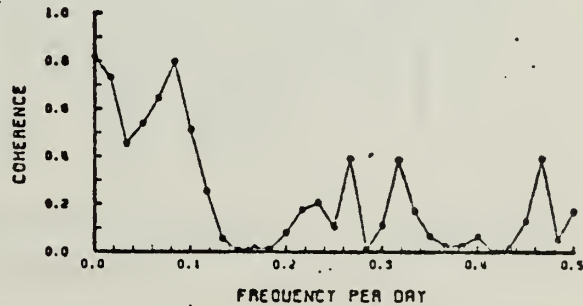
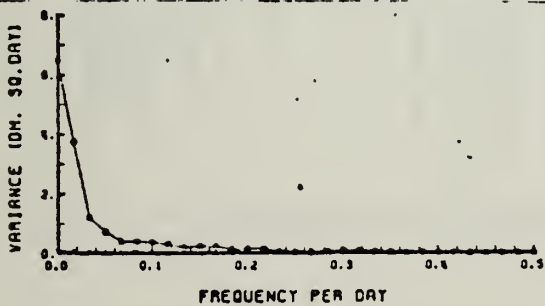
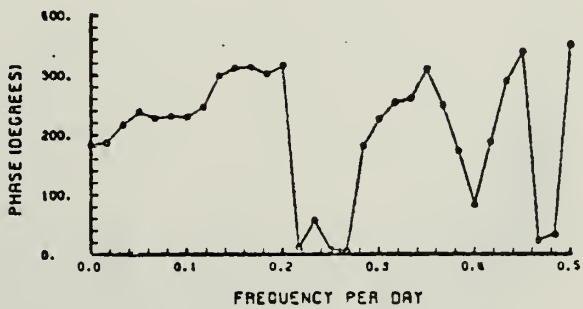
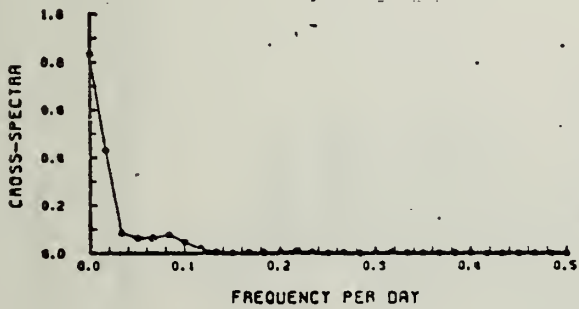


April-September

Figure 15. The spectrum, cross-spectrum, coherence, and phase for filtered sea level (Sattahip) and pressure difference (Bangkok-Singapore), (12 degrees of freedom).



October-March



April-September

Figure 16. The spectrum, cross-spectrum, coherence, and phase for filtered sea level (Ko-Lak) and pressure difference (Bangkok-Singapore), (12 degrees of freedom).

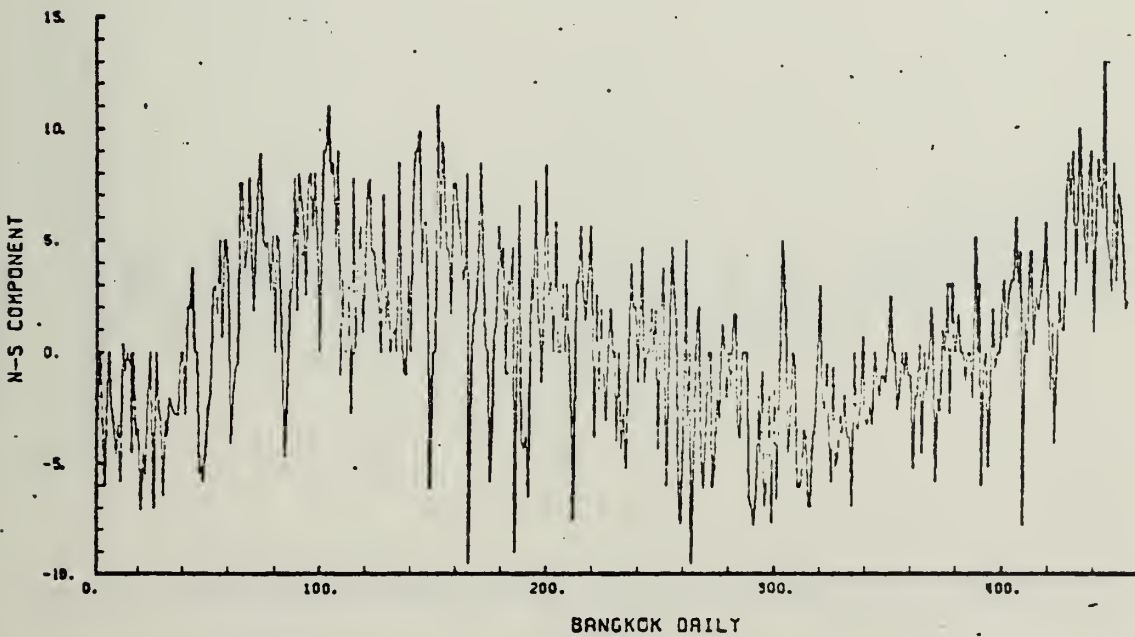
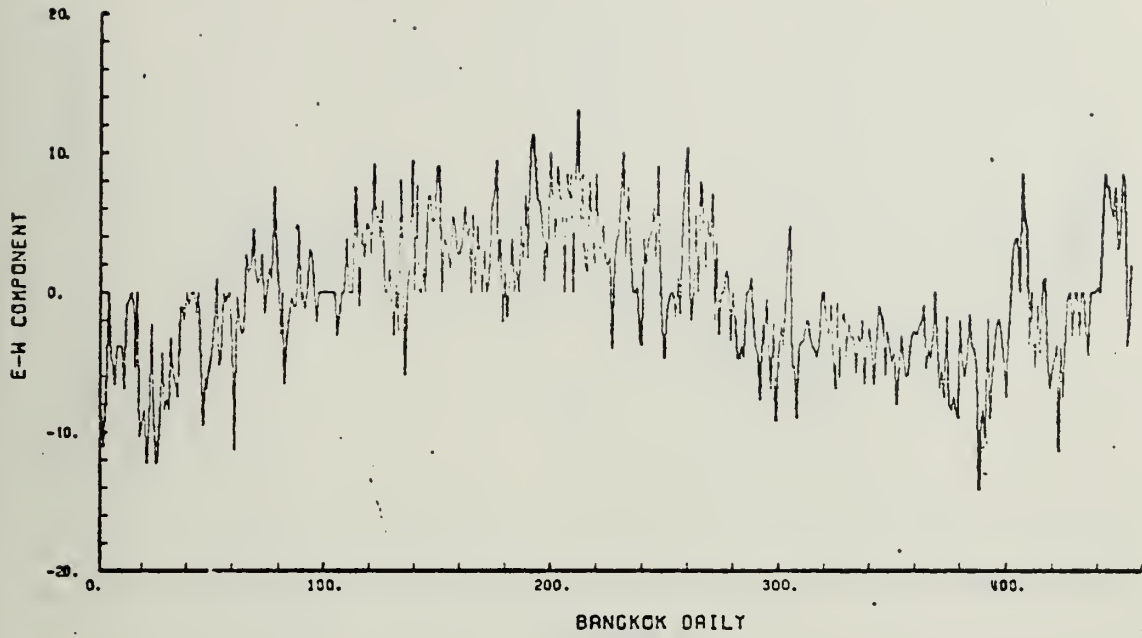


Figure 17. Daily wind components (N-S, and E-W), wind speed in knots.

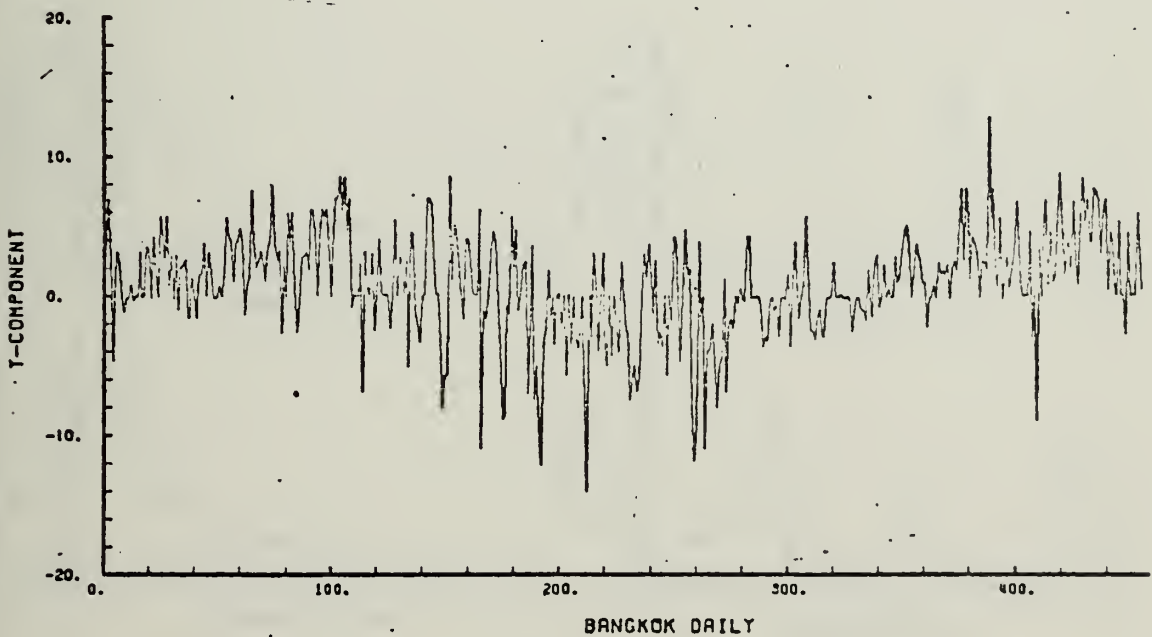
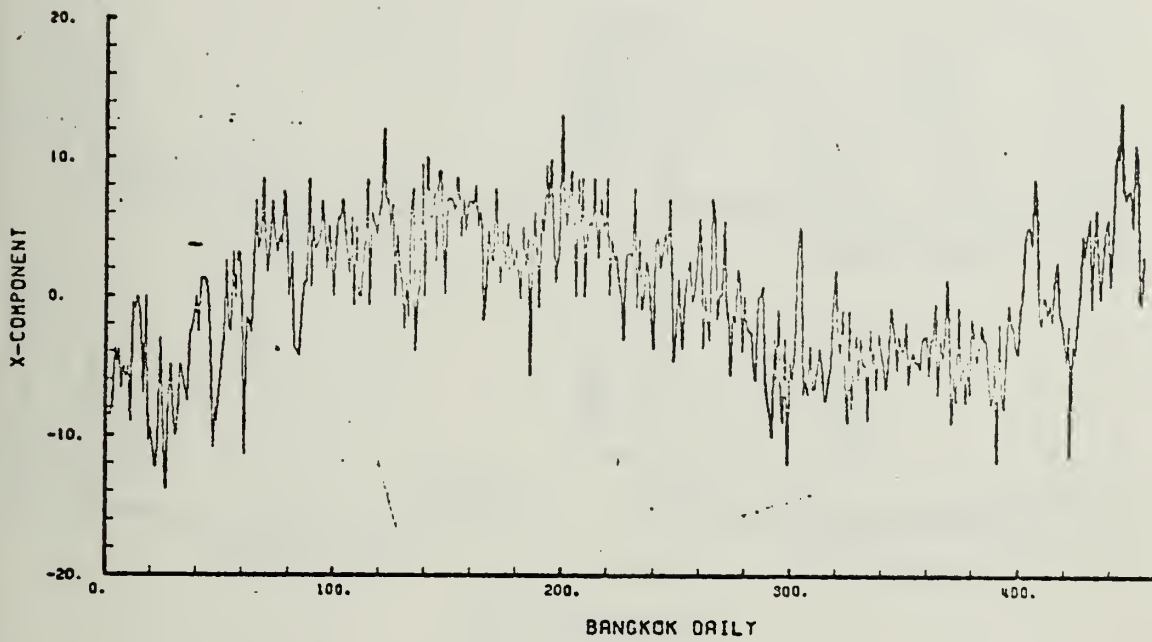
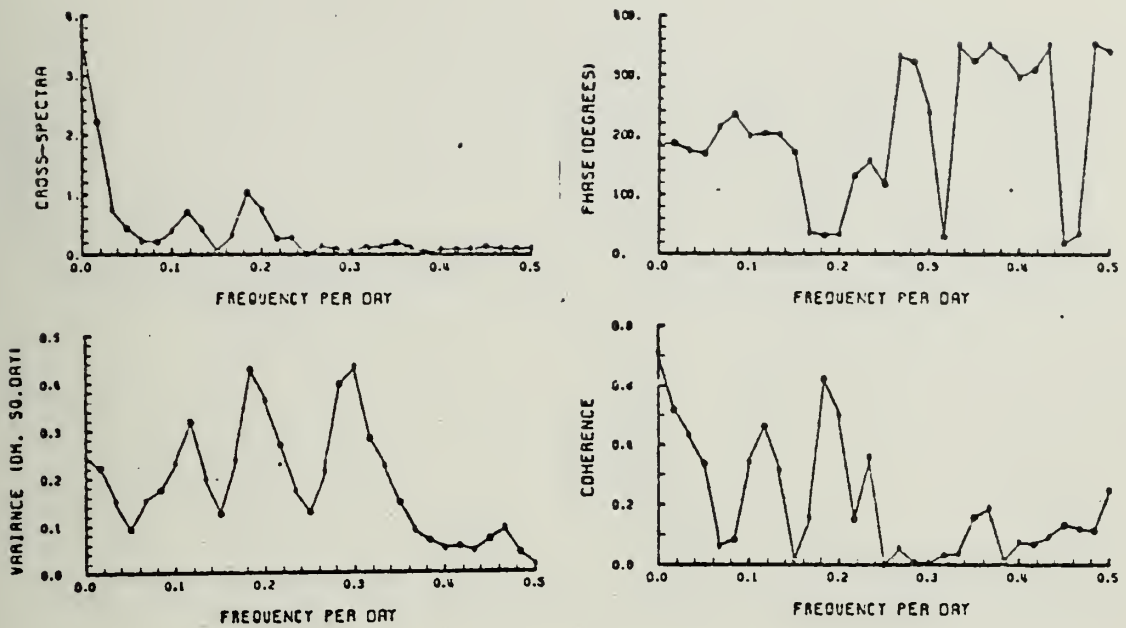
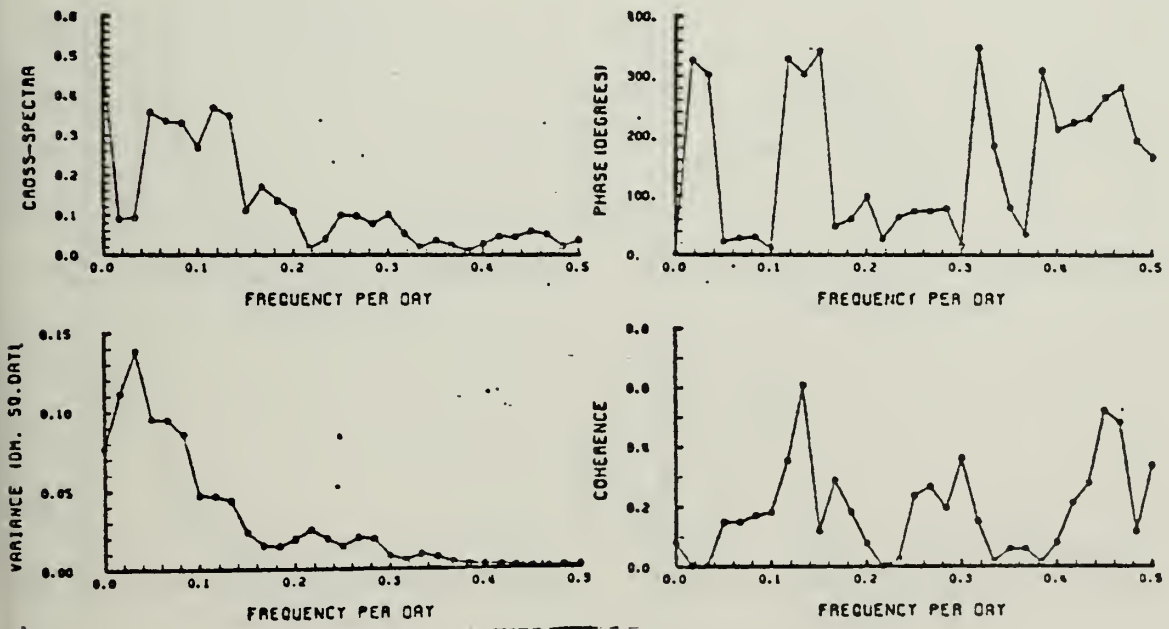


Figure 18. Daily wind components (X and Y), (See Figure 1), wind speed in knots.

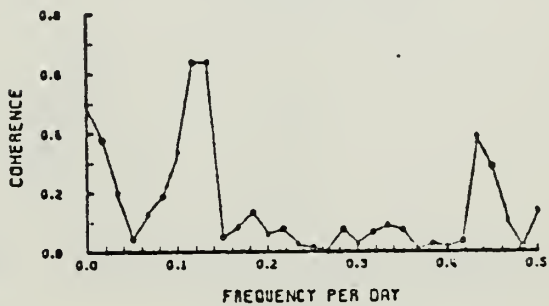
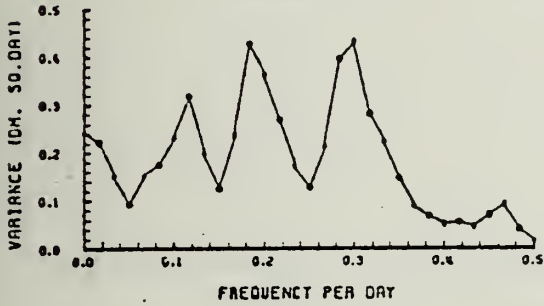
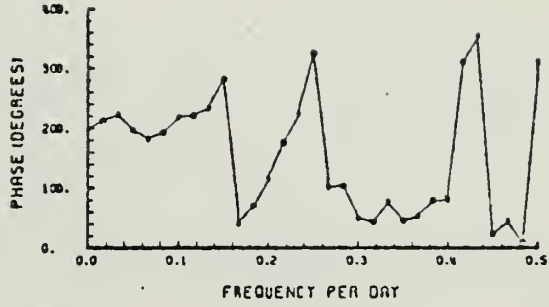
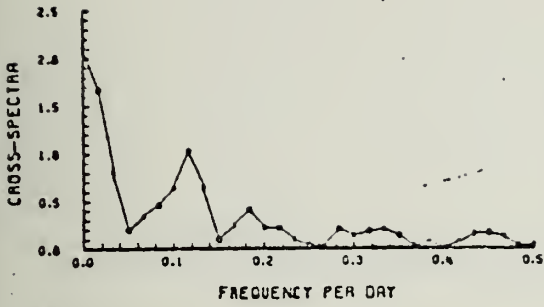


October-March

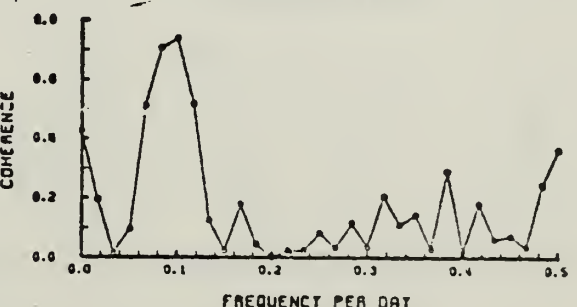
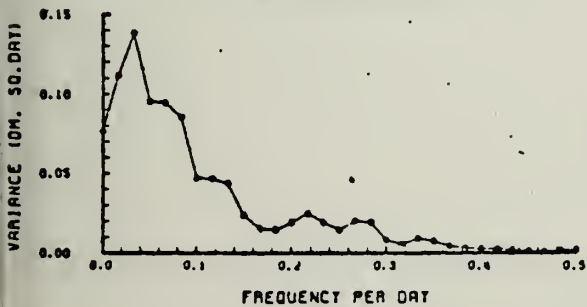
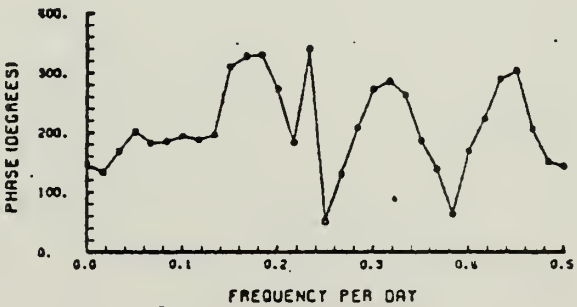
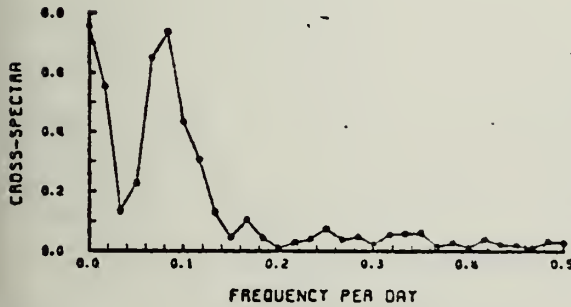


April-September

Figure 19. The spectrum, cross-spectrum, coherence, and phase of sea-level slope (Ko-Lak - Sattahip) and north-south wind component (12 degrees of freedom).

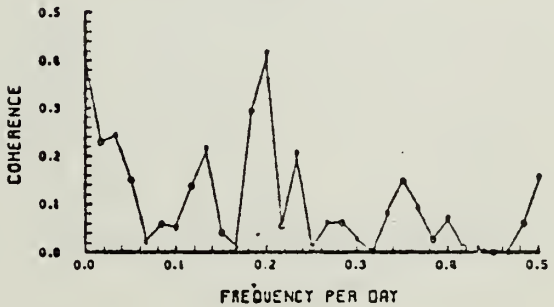
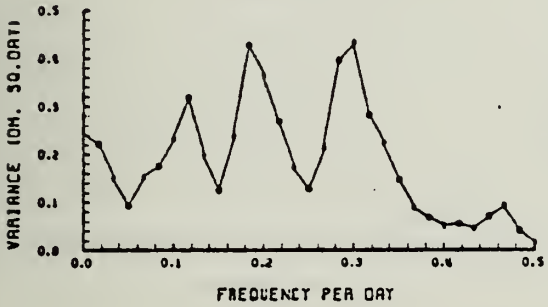
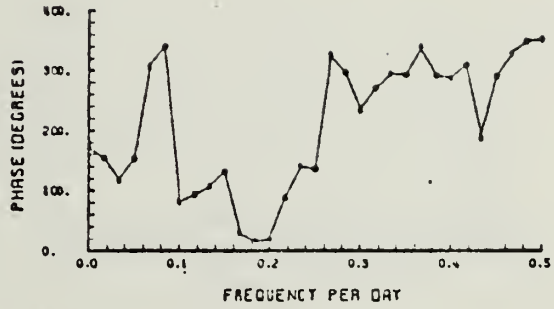
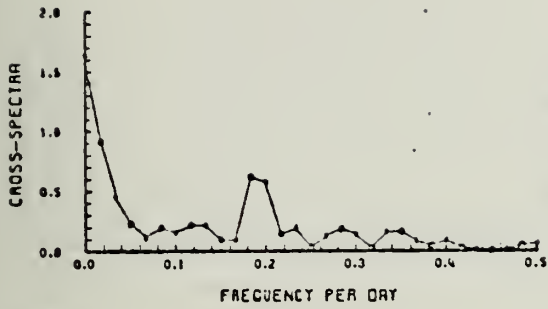


October-March

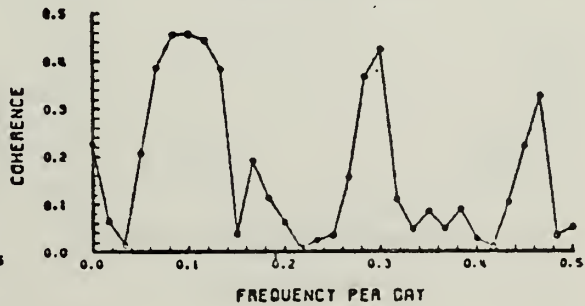
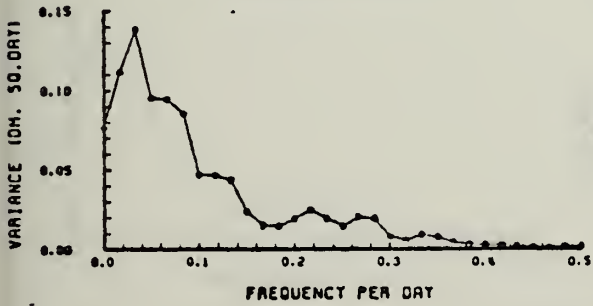
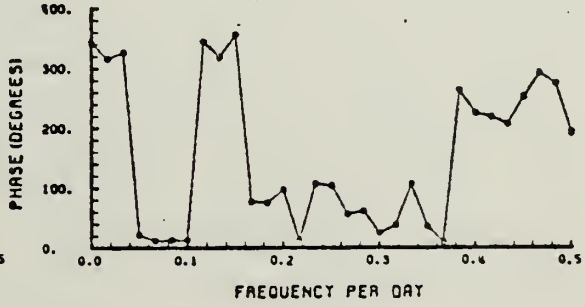
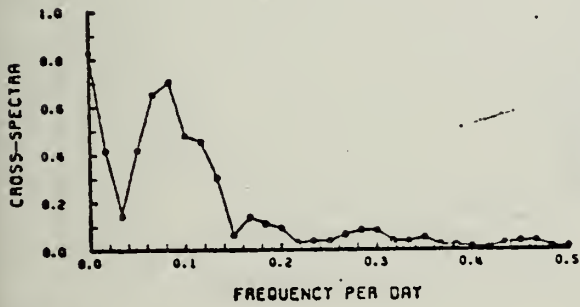


April-September

Figure 20. The spectrum, cross-spectrum, coherence, and phase of sea-level slope (Ko-Lak - Sattahip) and east - west wind component (12 degrees of freedom).

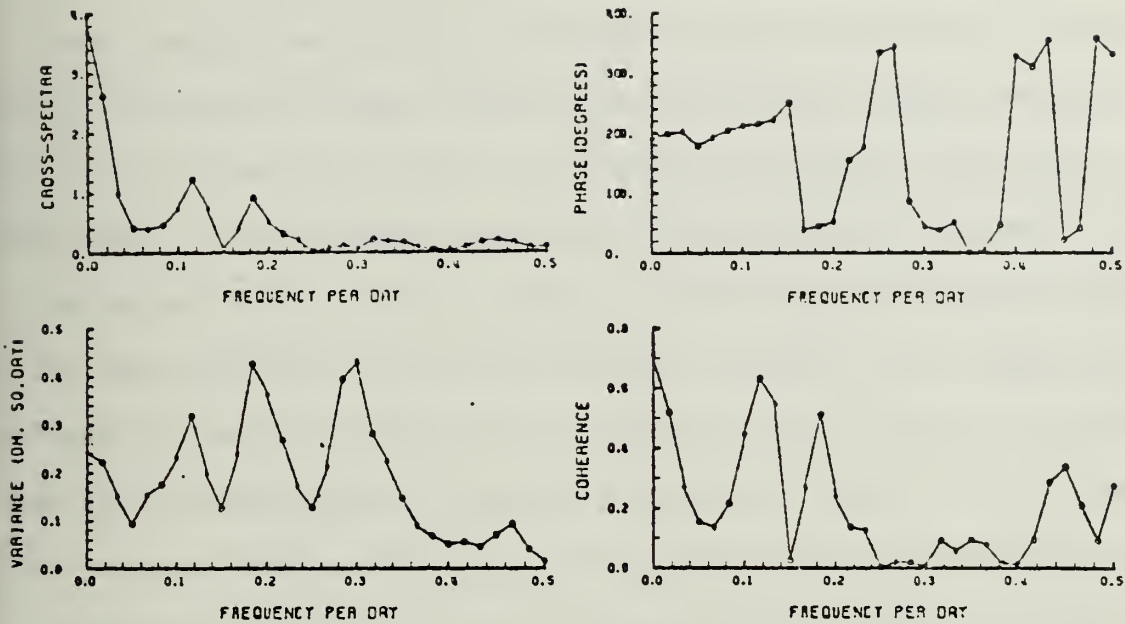


October-March

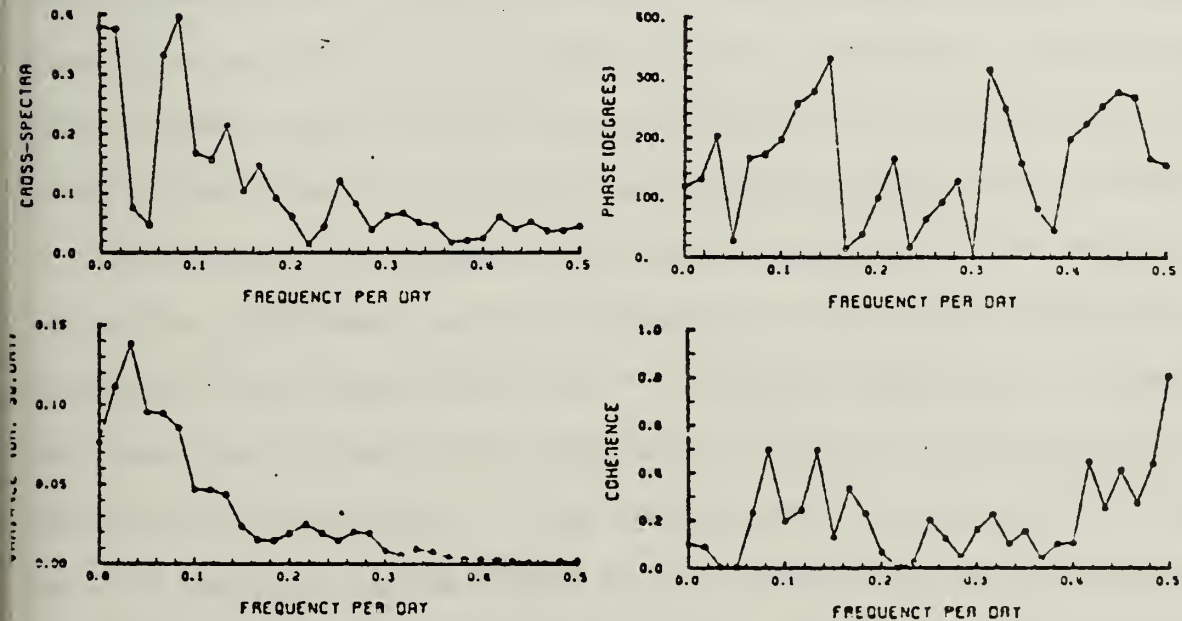


April-September

Figure 21. The spectrum, cross-spectrum, coherence, and phase of sea-level slope (Ko-Lak - Sattahip) and Y wind component (12 degrees of freedom).



October-March



April-September

Figure 22. The spectrum, cross-spectrum, coherence, and phase of sea-level slope (Ko-Lak - Sattahip) and X wind component (12 degrees of freedom).

VI. SUMMARY AND CONCLUSIONS

Seven years of hourly sea level data from two tide stations in the northern Gulf of Thailand have been treated by low pass filter (using averages of 24, 24, and 25 hours) to remove the prominent semi-diurnal and diurnal tidal components. Further smoothing minimized the prominent fortnightly cycle of spring/neap tides. It was found that the seasonal sea level variation is of the same magnitude as the semi-diurnal and diurnal tides (range about 5 decimeters), and that the larger short-term sea level variations superimposed range up to 4 decimeters with durations of about 8 days. It was determined that these sea level variations are due principally to meteorological effects.

The annual variations of sea level were studied by comparing them with the annual variations of atmospheric pressure and wind. The atmospheric pressure was found to vary directly with the sea level, and accordingly can account for very little of the annual sea level variation. For the comparison with the annual wind, sea level varies seasonally as if controlled by the Ekman transport which would be expected from the monsoon wind regime over the Gulf.

The spectra, cross-spectra, coherences, and phases for the hourly sea levels show significant peaks at frequencies of the diurnal and semi-diurnal astronomical tide forces, the diurnal component dominating. The spectra were made free of these tidal components by low-pass filtering (24-24-25 hours) of the hourly tide heights. These spectra were, in turn, ensemble averaged over the seven-year period (Figure 8). The spectra are seen to be very similar for both tide stations. This implies that residual sea levels at both stations change in response to the same driving mechanisms.

For the purpose of examining seasonal variation, the spectra of the filtered heights were ensemble averaged for each monsoon season (Figure 9).

The spectra show higher energy in the northeast monsoon than during the southwest monsoon. This is interpreted to mean that the northeast monsoon winds have greater variation than the southwest monsoon winds.

The spectra, cross-spectra, coherences, and phases between the low-passed sea level and the geostrophic wind were also computed (Figures 13-16). These show that the sea levels are in phase with the geostrophic winds computed from pressure measurements at Bangkok and Saigon. This suggests that sea levels relate to fluctuations in the monsoon winds in a way consistent with piling up of water at the northern boundary of the gulf by northward Ekman transport and vice versa for southward transport.

The relationship of the low-pass filtered sea level slopes between the two tide stations, located on opposite sides of the northern gulf, and the local wind was also studied. The cross-spectra (Figures 19-22) show high coherence in the frequency band 0.083-0.117 cycles per day for the east-west and X-components of the wind. This indicates that in this frequency band the sea level slopes upward across the gulf in the same direction as that toward which the anomalous wind blows, the response being most coherent for periods of 8-12 days. This effect is clearly secondary to the effect of Ekman transport in producing the seasonal sea level variations observed in the northern Gulf of Thailand.

It is clear that the sea level variations studied here are affected by the monsoon wind and its variations. The observed sea level variations are not totally explained by wind-forcing over the gulf. They are possibly, in part, responses to forcing over the South China Sea. Future studies should examine: (1) correlation between gulf sea levels and wind forcing in the South China Sea and (2) dynamical/numerical models for responses to local forcing and to forcing over and from the South China Sea.

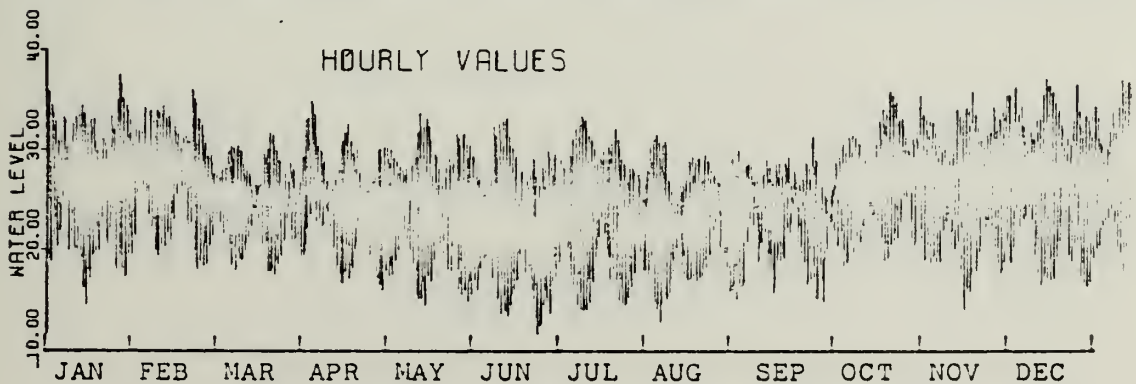
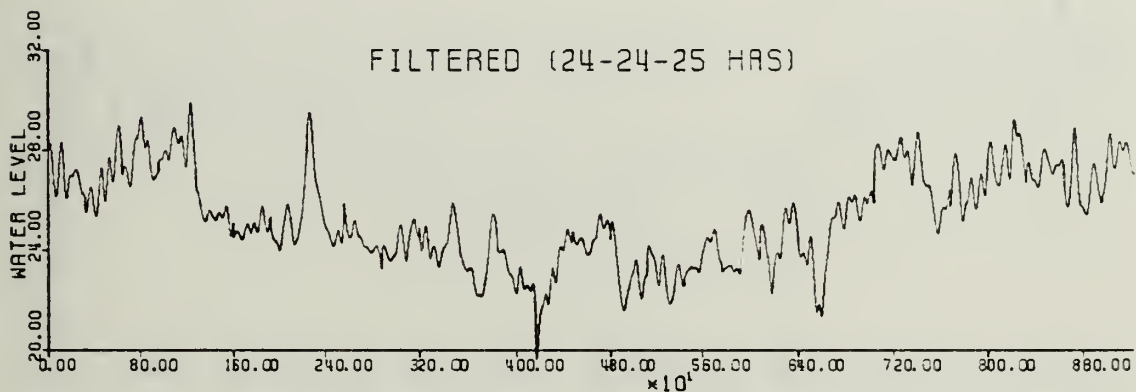
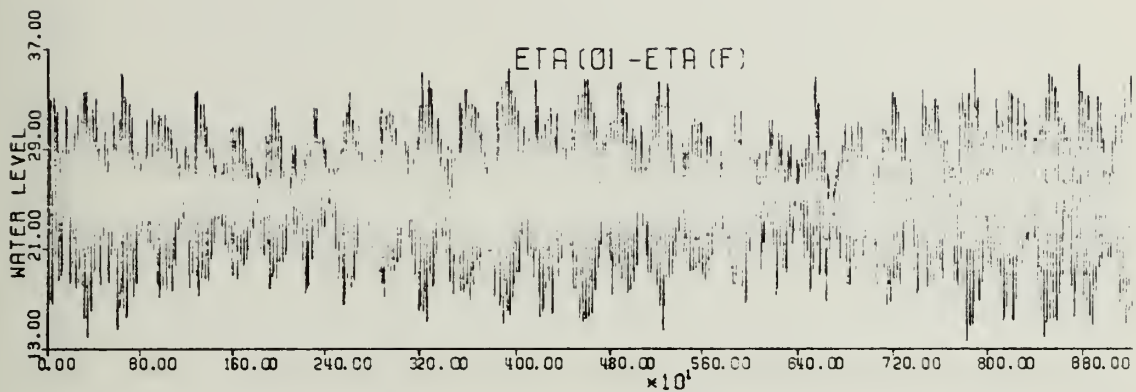
APPENDIX A

RAW AND FILTERED HOURLY SEA LEVEL DATA

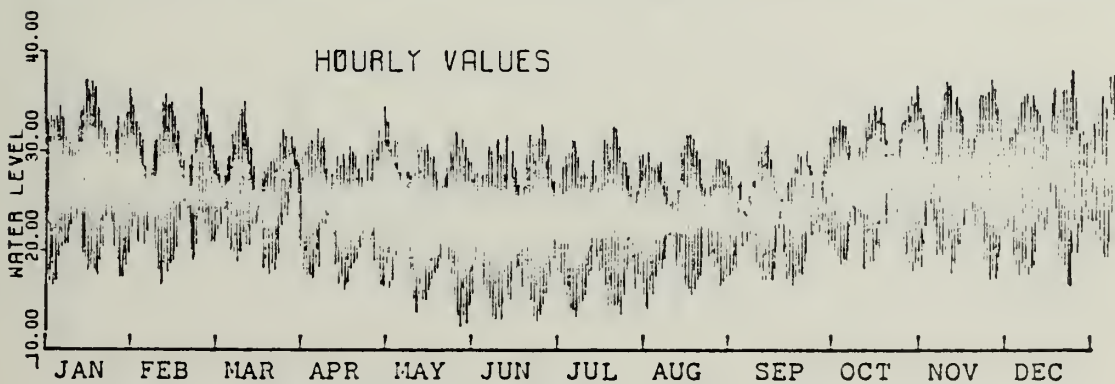
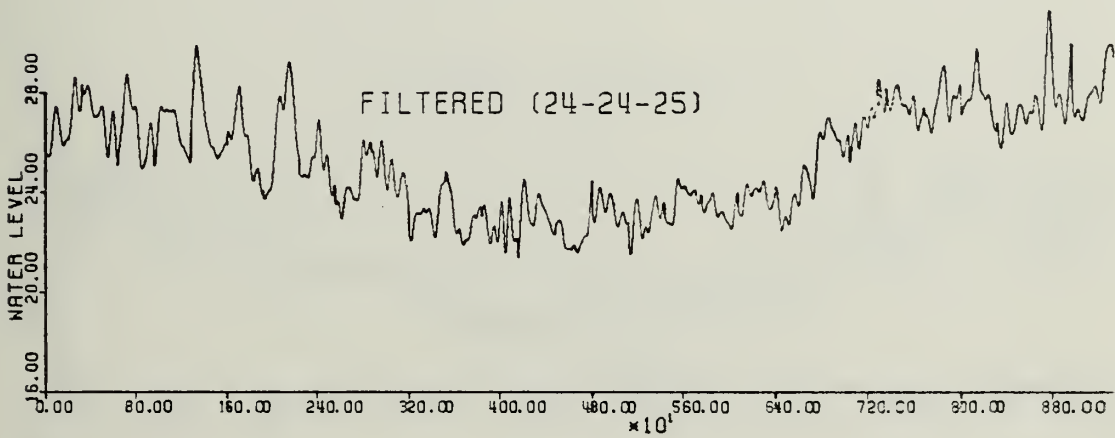
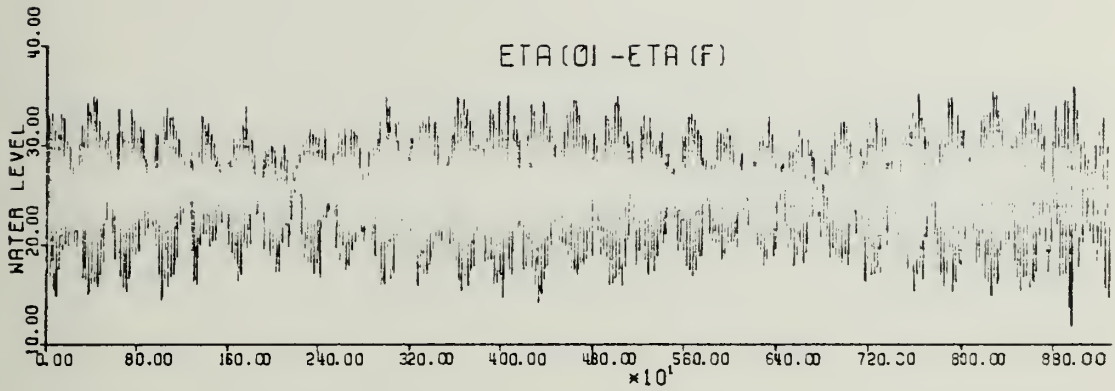
The following time-series graphs for Sattahip and Ko-Lak show:

(1) raw or unfiltered hourly sea levels (lower), (2) semi-diurnal and diurnal hourly water levels extracted using a 24-24-25 hour filter (upper), and (3) the residual hourly water levels remaining (middle). The water levels are in decimeters and measured from 0000Z on 1 January. Each graph covers one year of data.

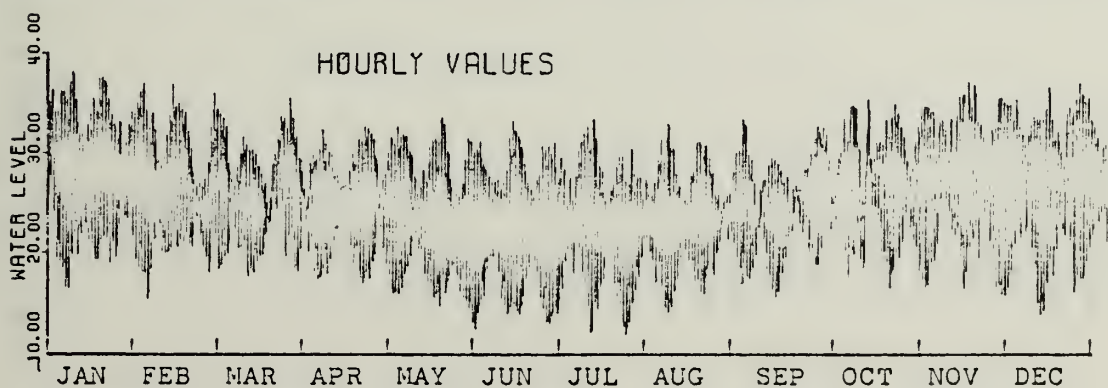
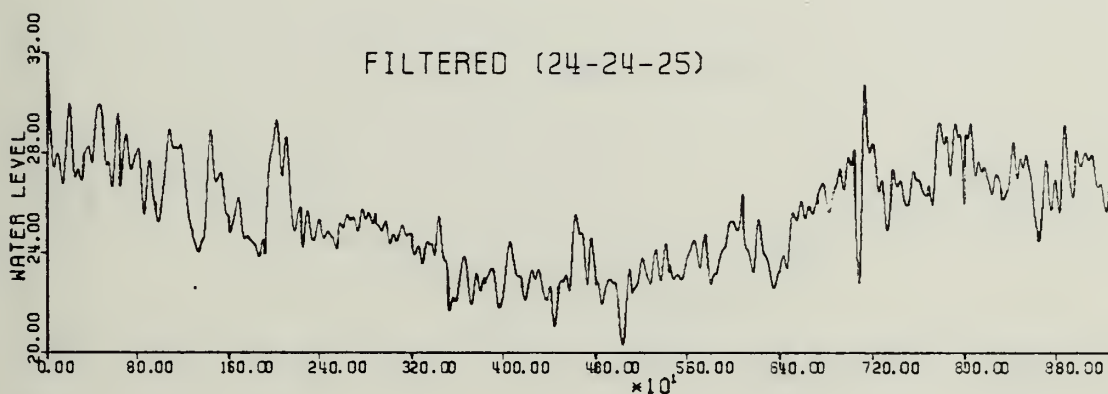
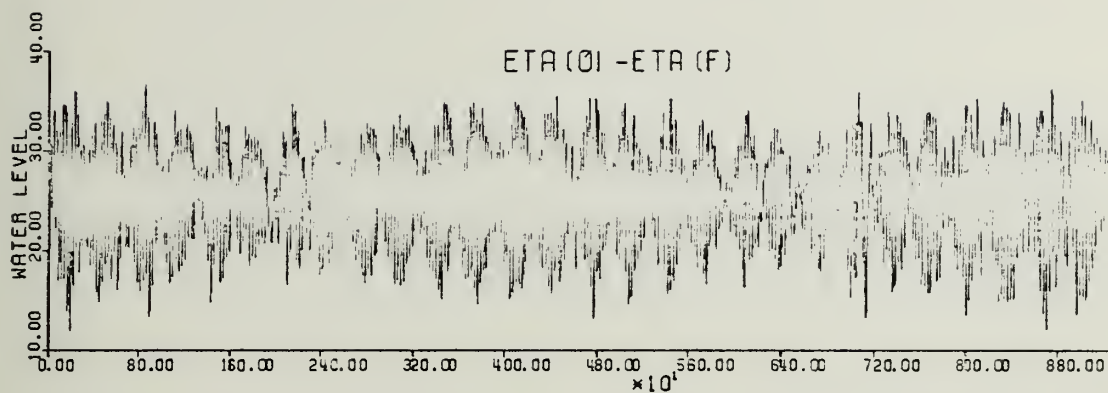
KØ-LAK 1960



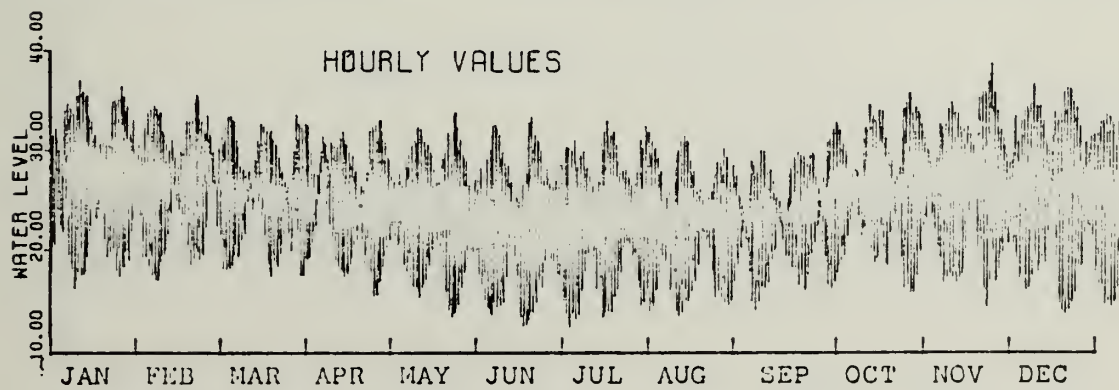
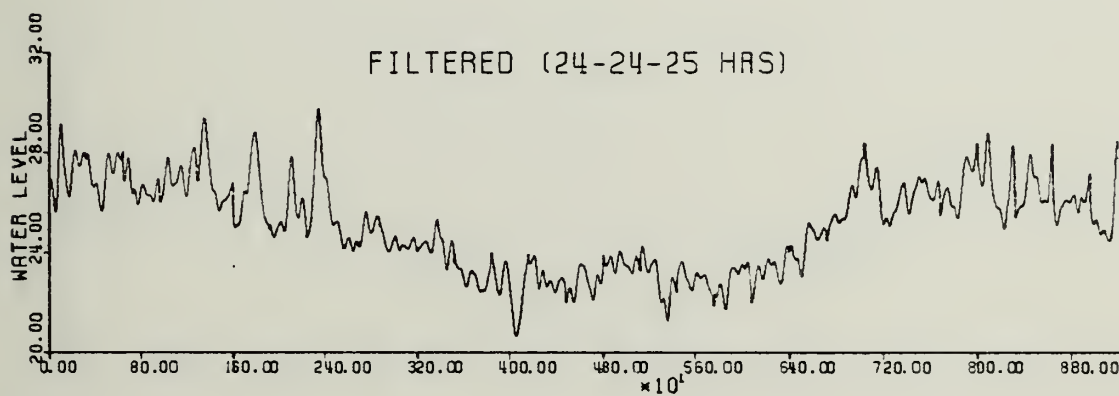
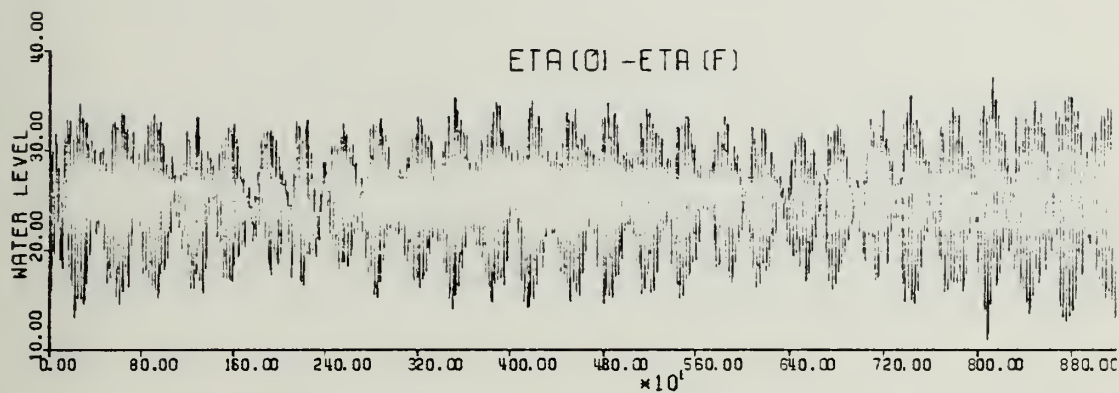
KO-LAK 1961



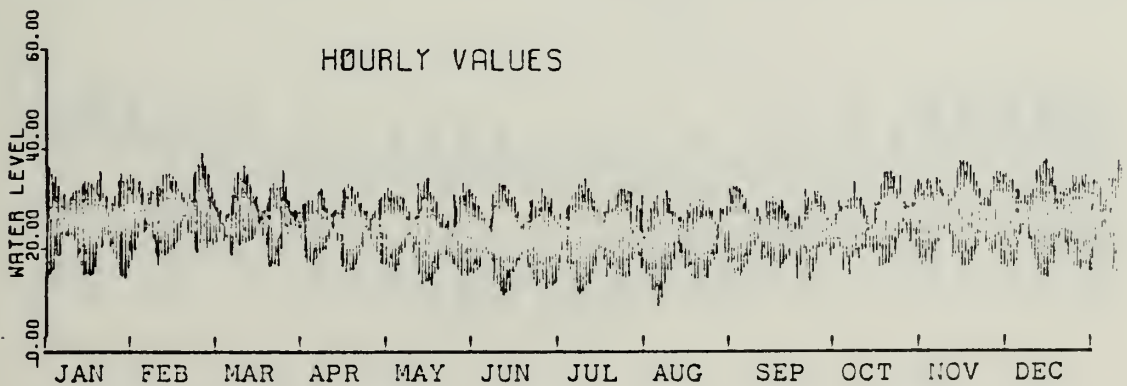
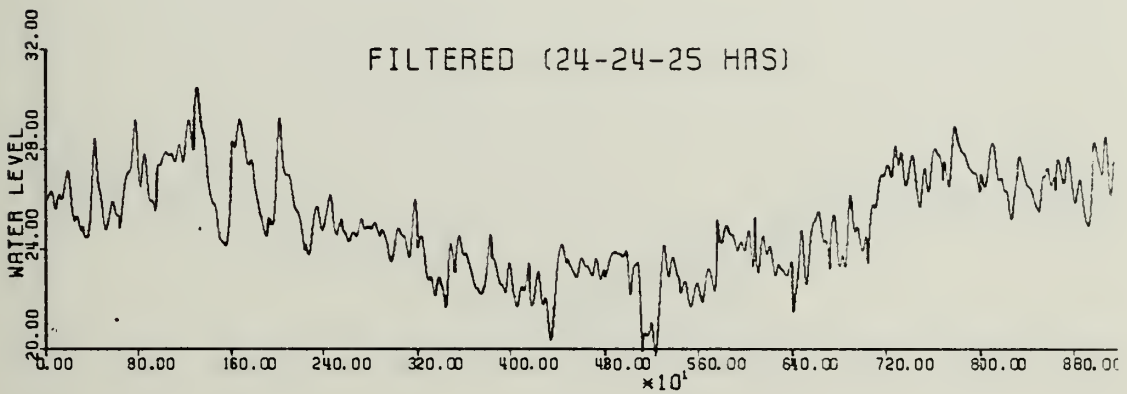
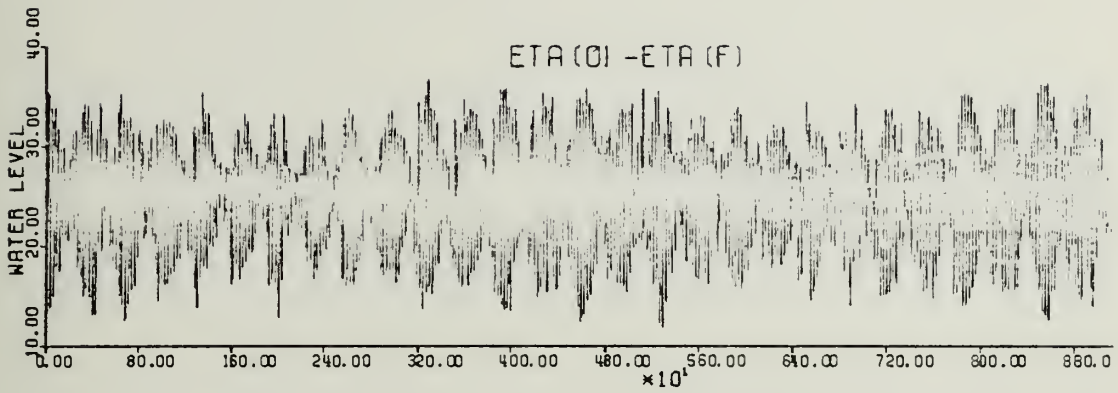
KO-LAK 1962



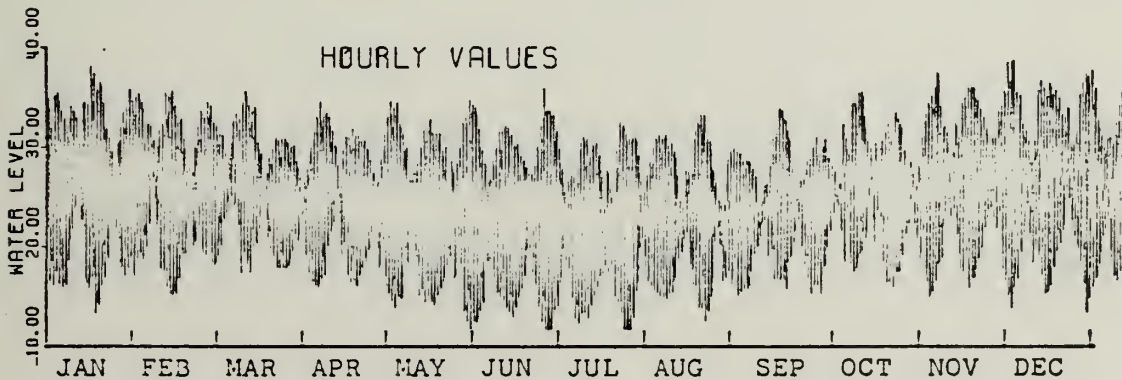
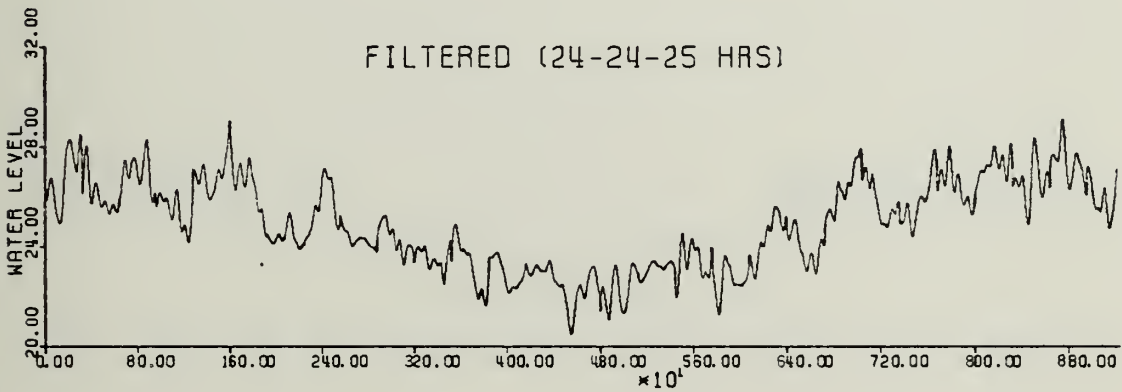
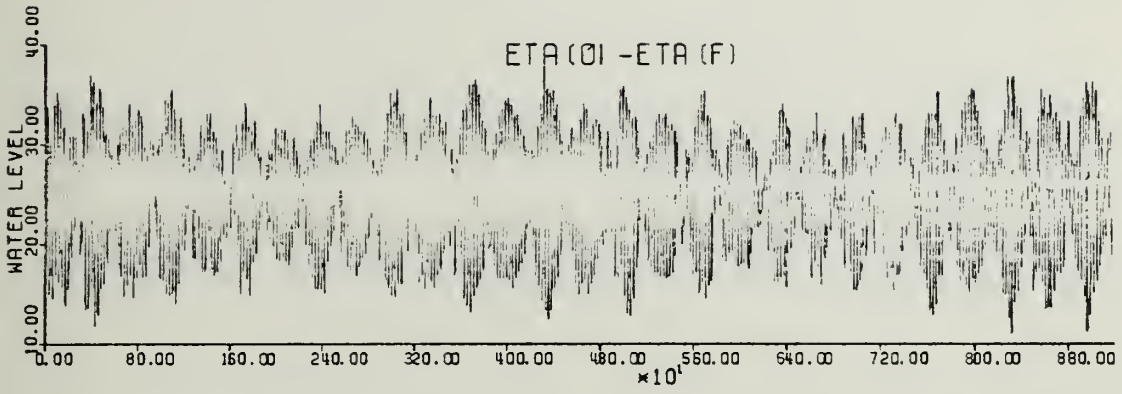
KO-LAK 1963



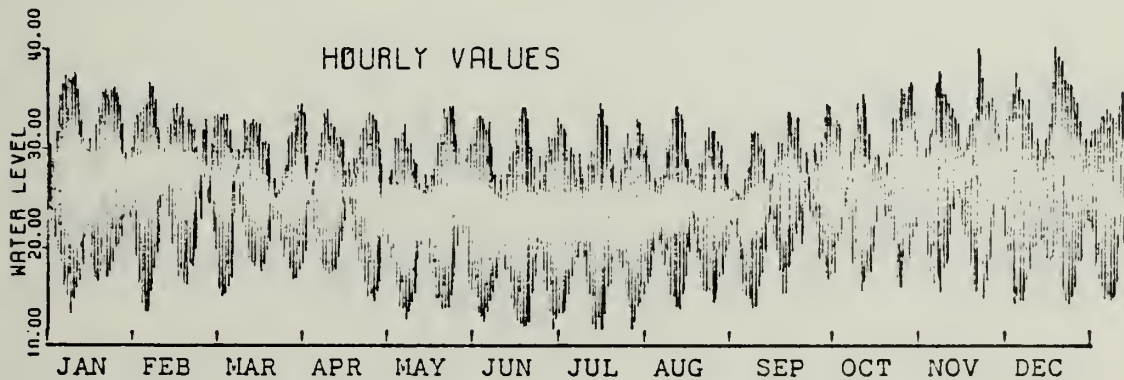
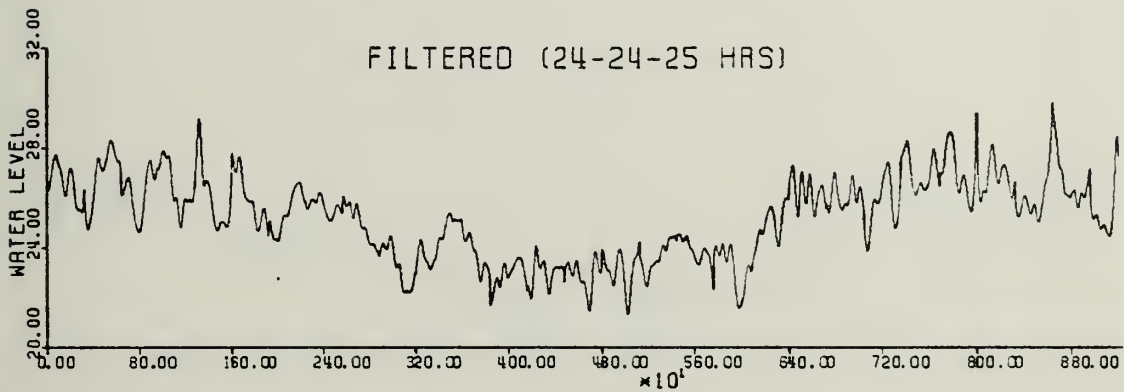
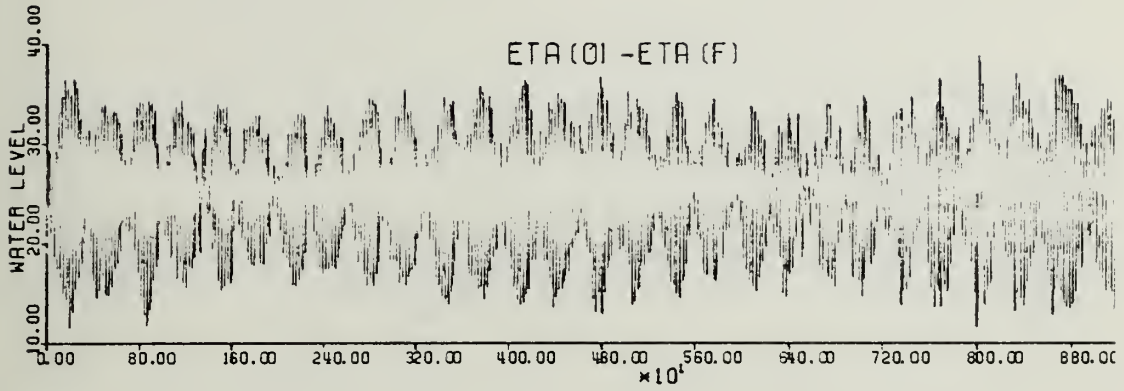
KO-LAK 1964



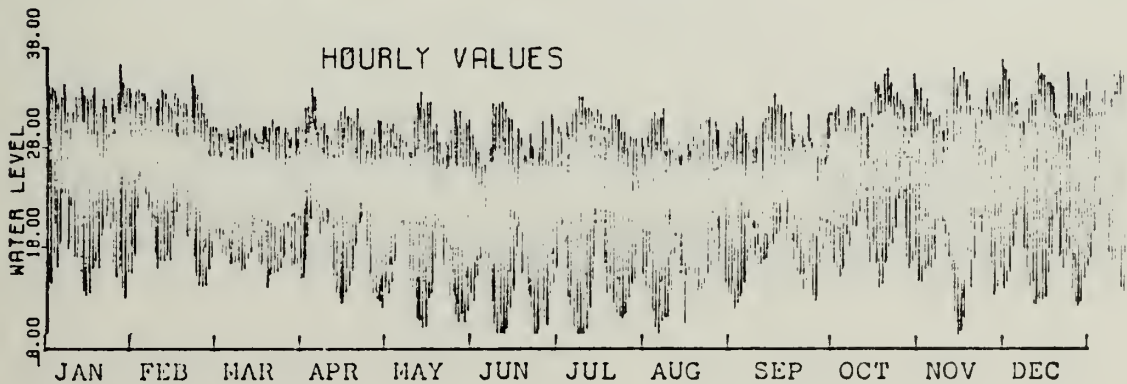
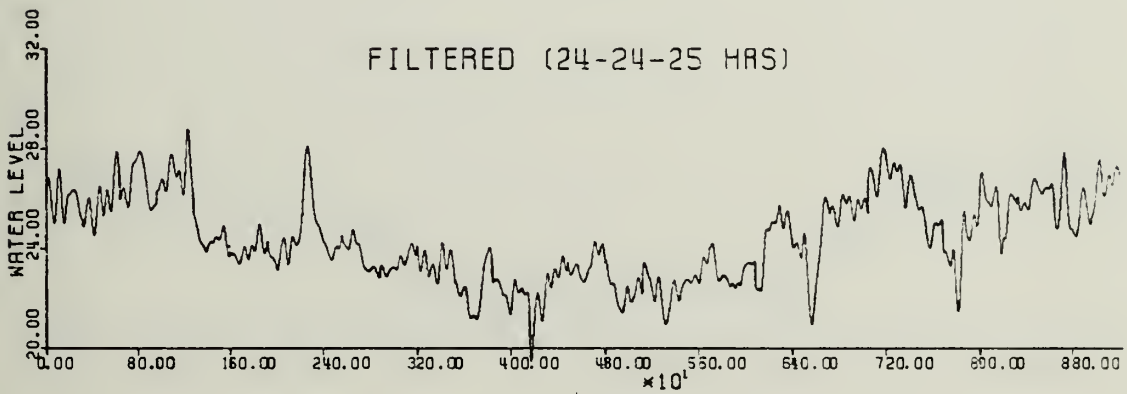
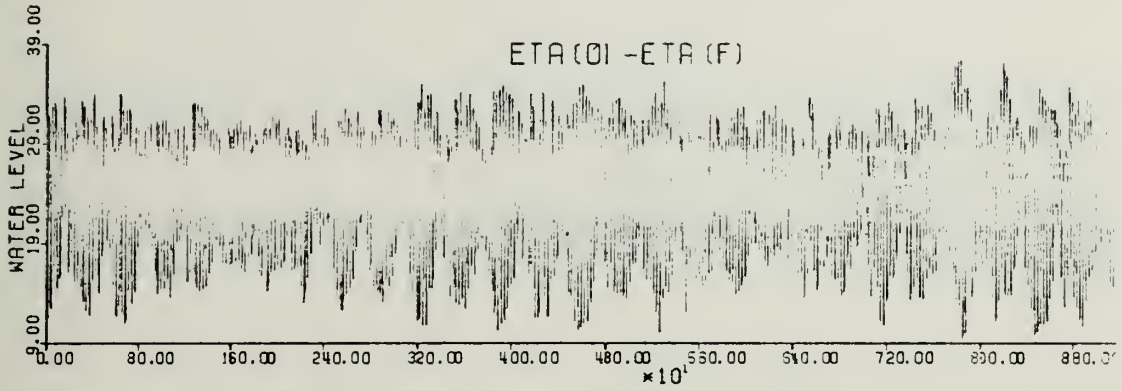
KO-LAK 1965



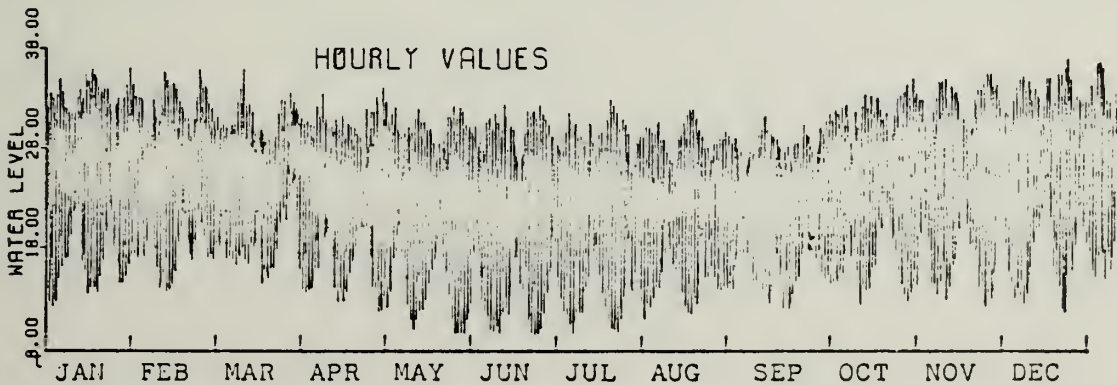
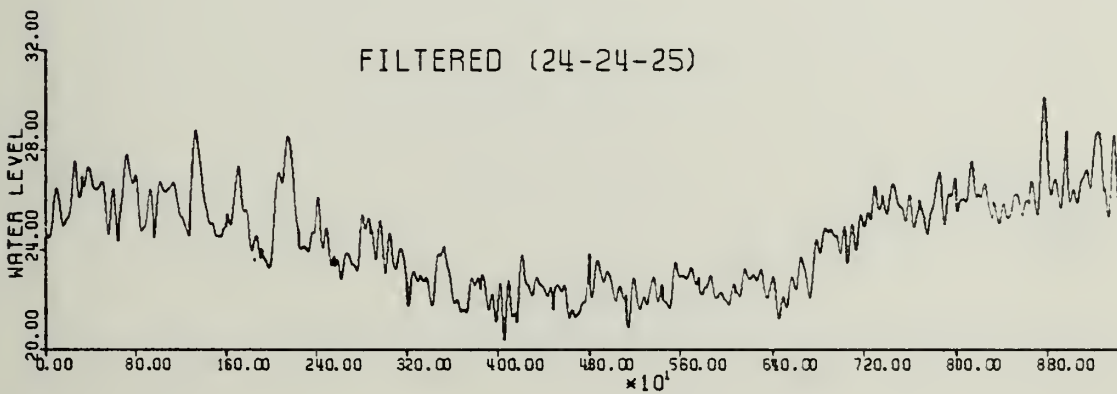
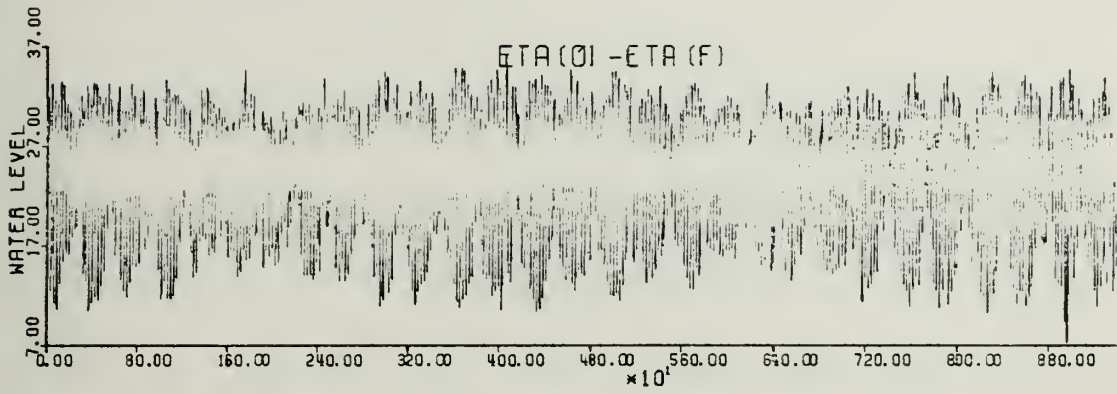
KO-LAK 1966



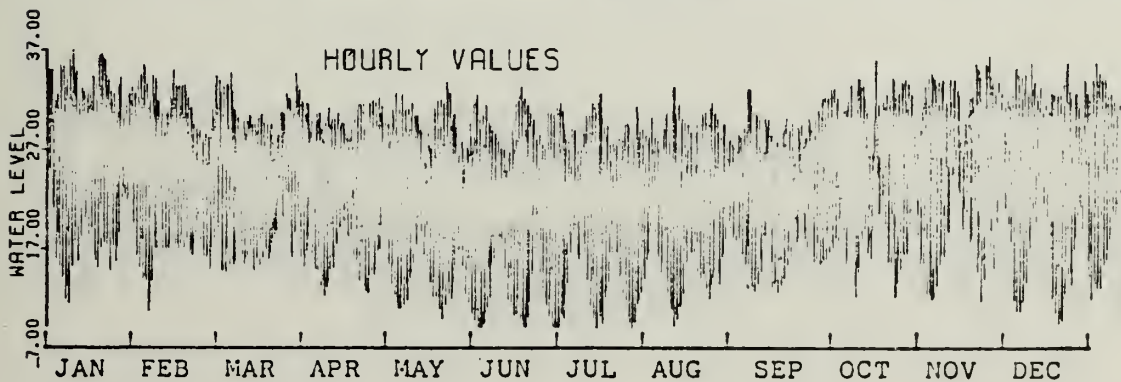
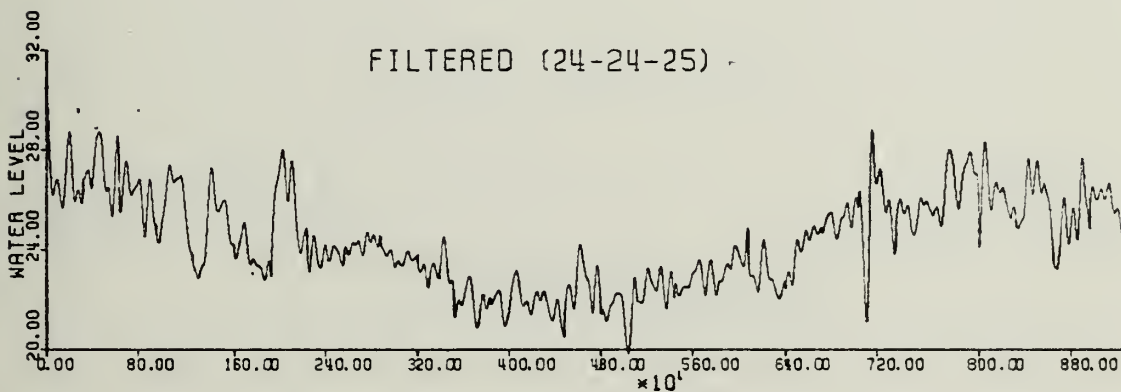
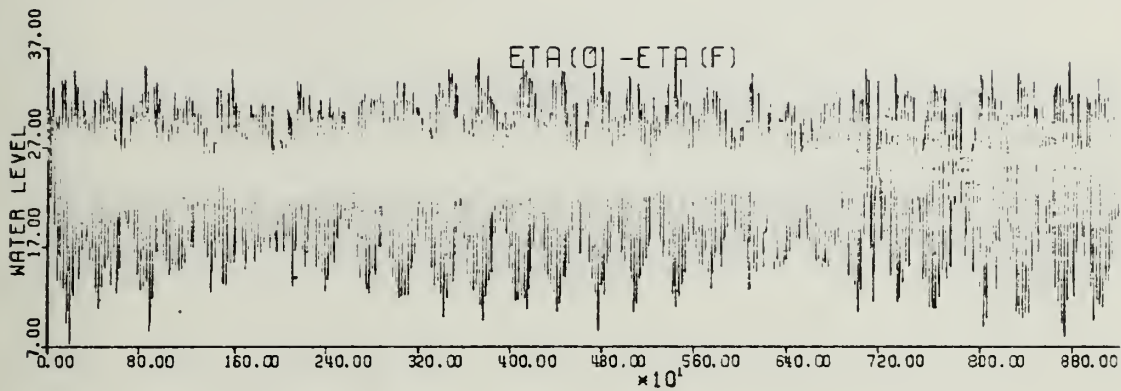
SATTAHIP 1960



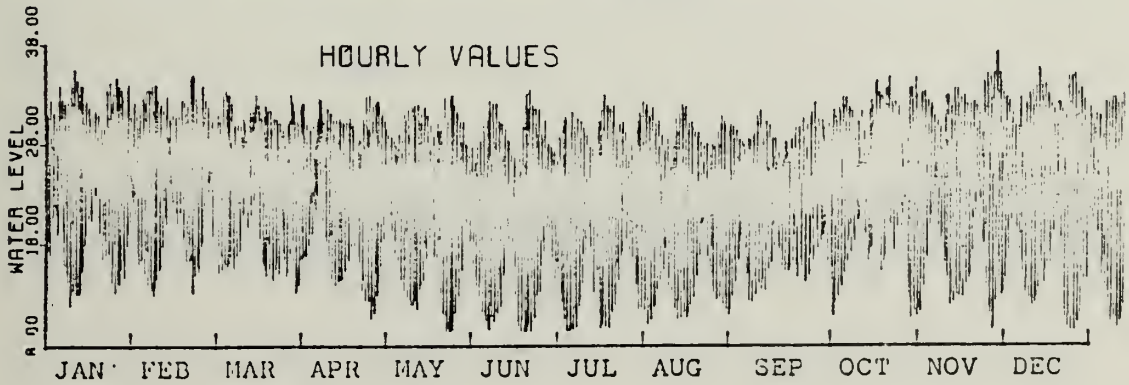
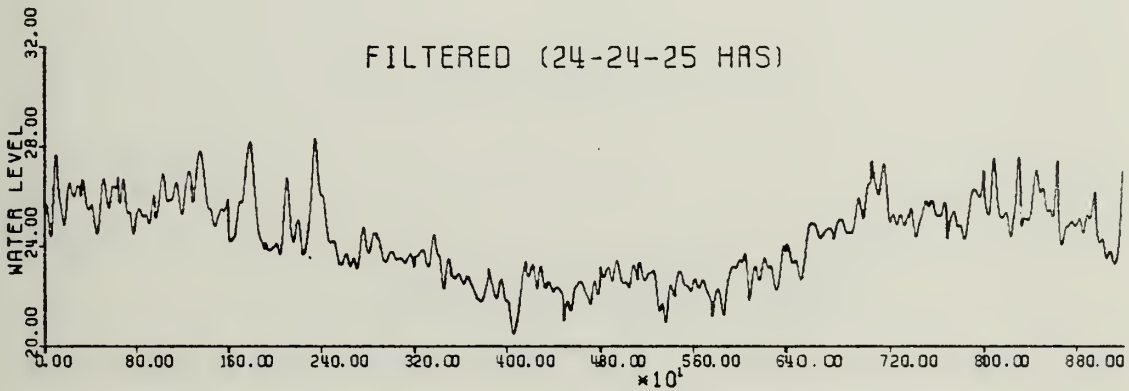
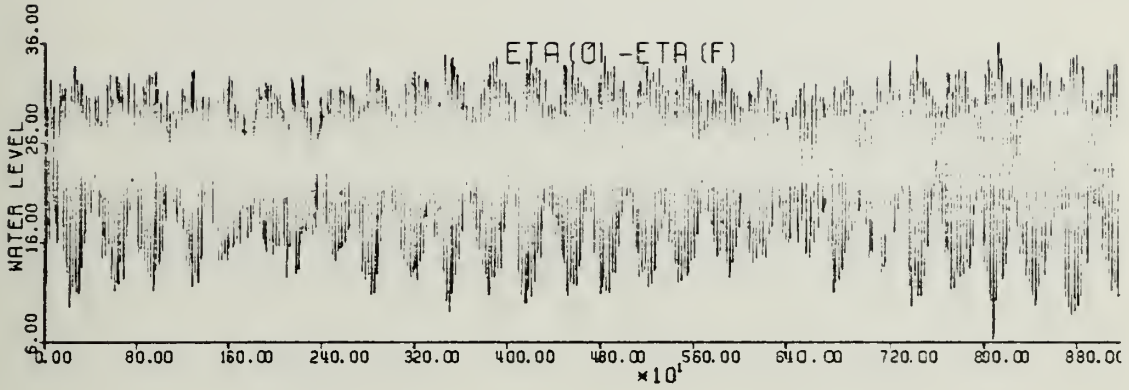
SATTAHIP 1961



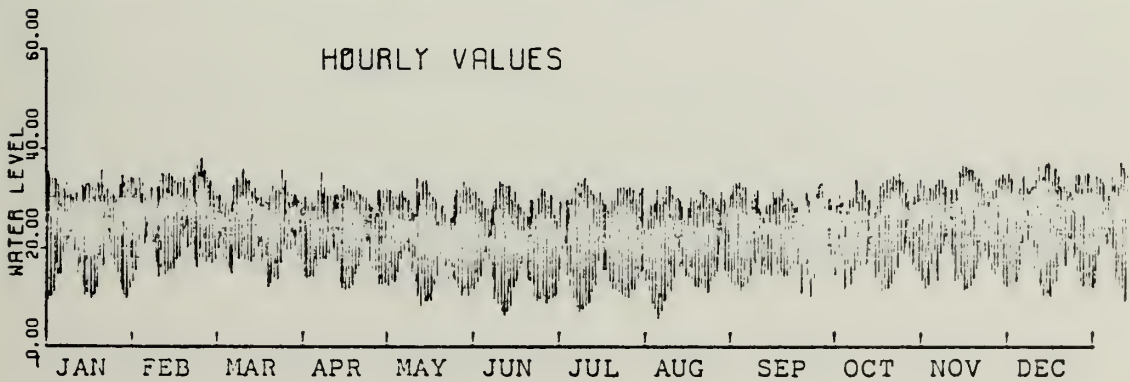
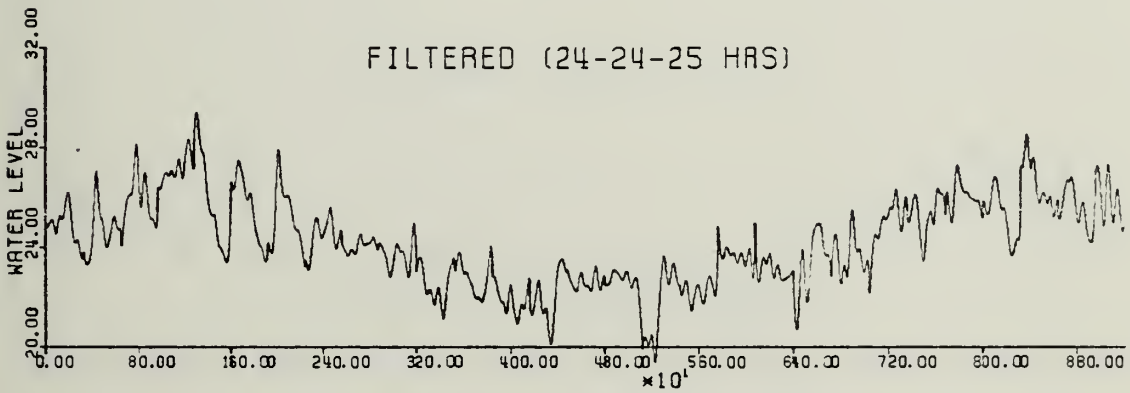
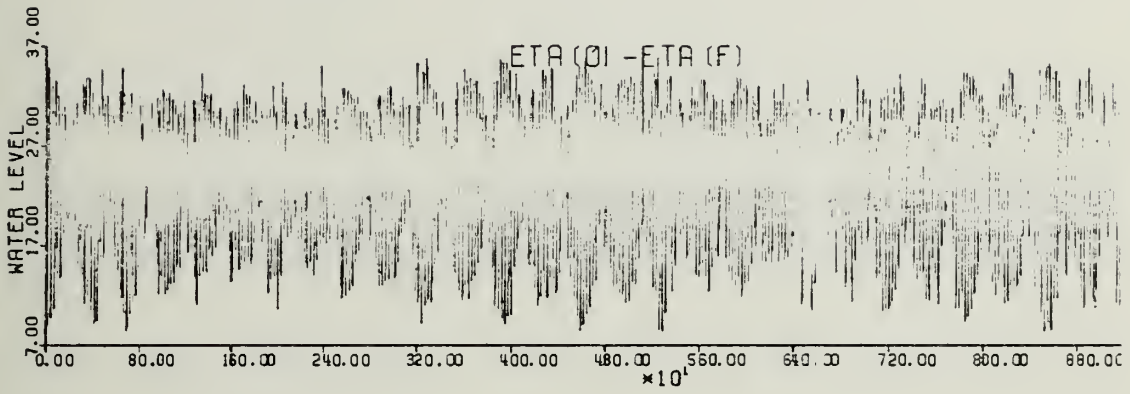
SATTAHIP 1962



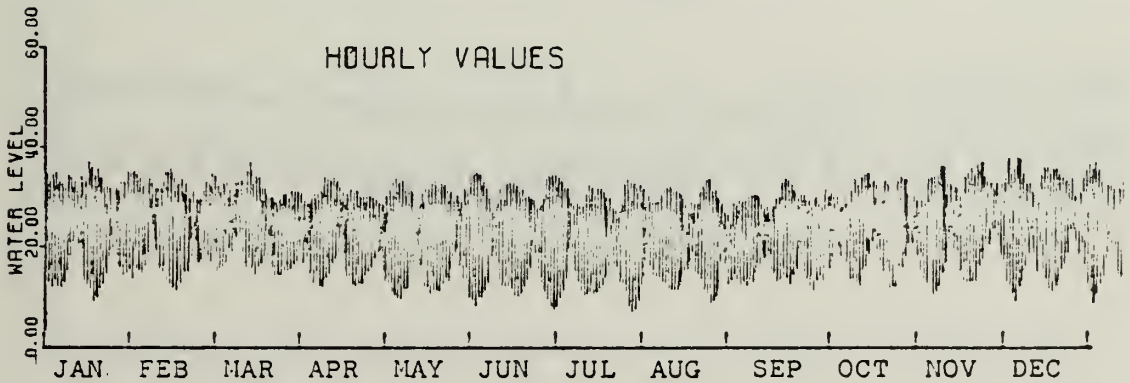
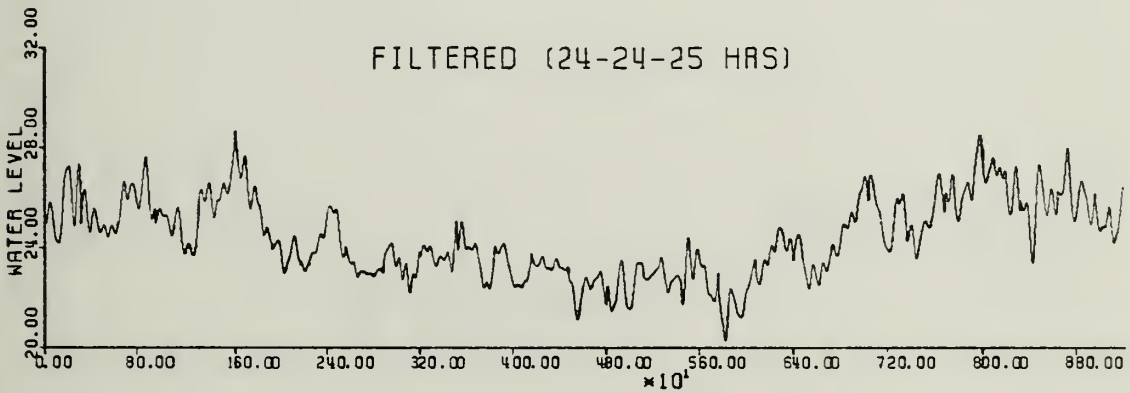
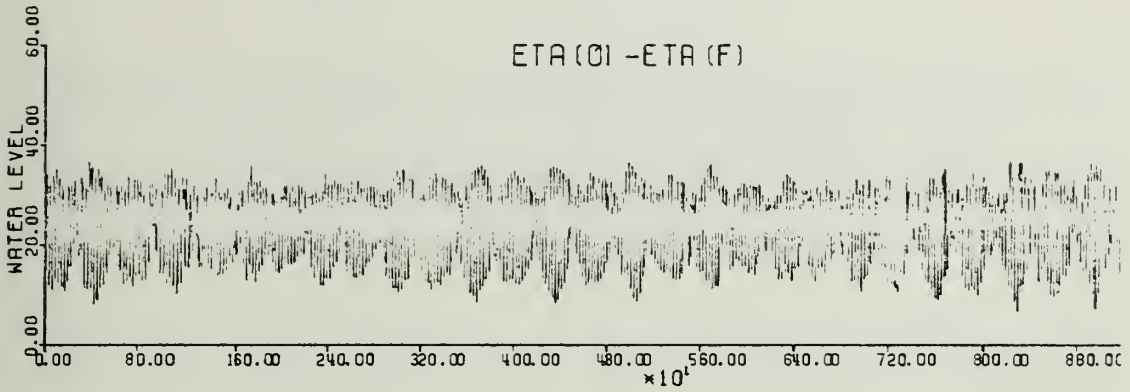
SATTAHIP 1963



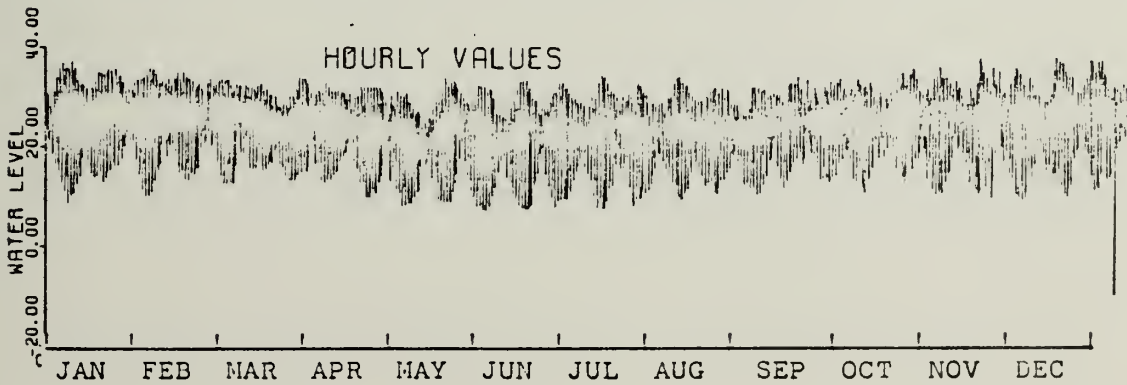
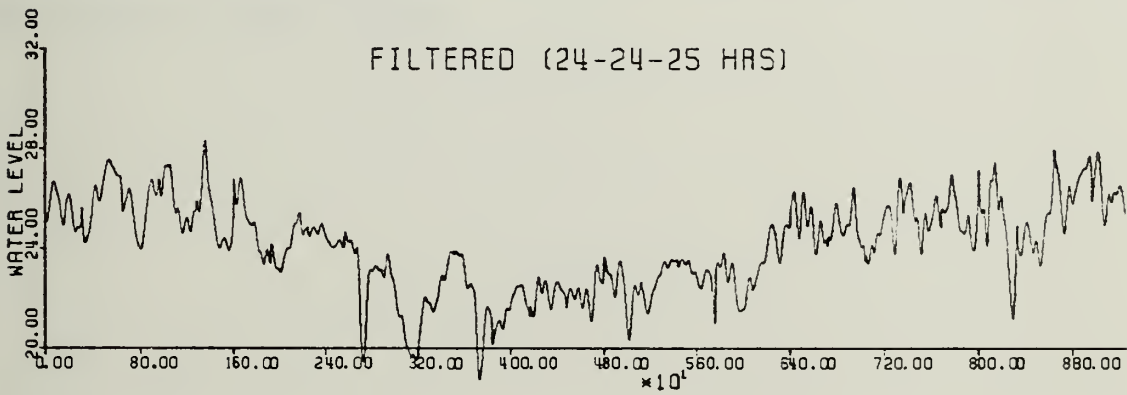
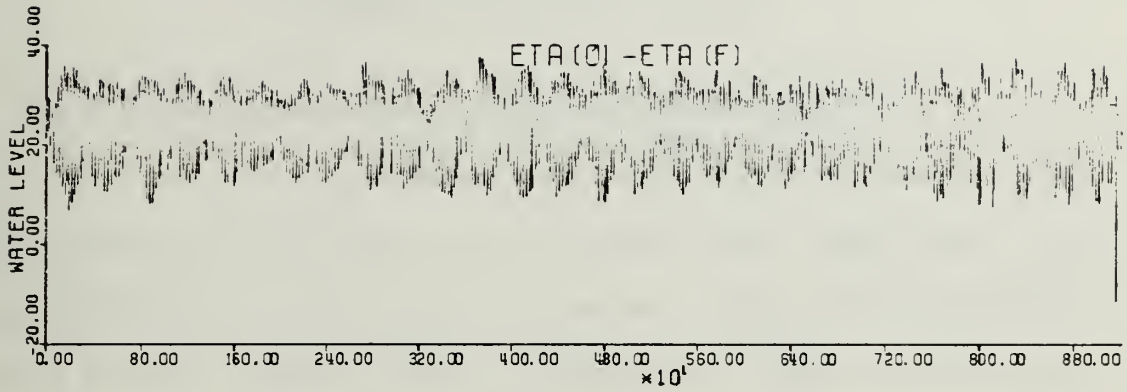
SATTAHIP 1964



SATTAHIP 1965



SATTAHIP 1966

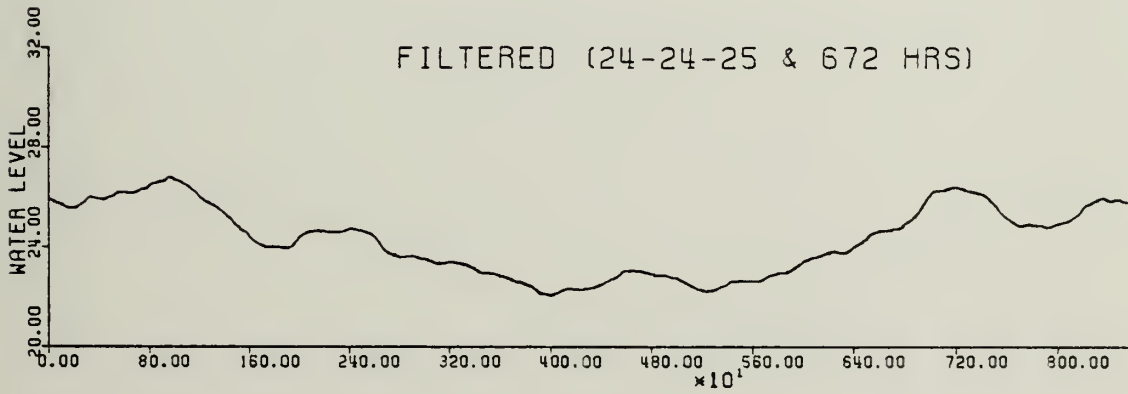
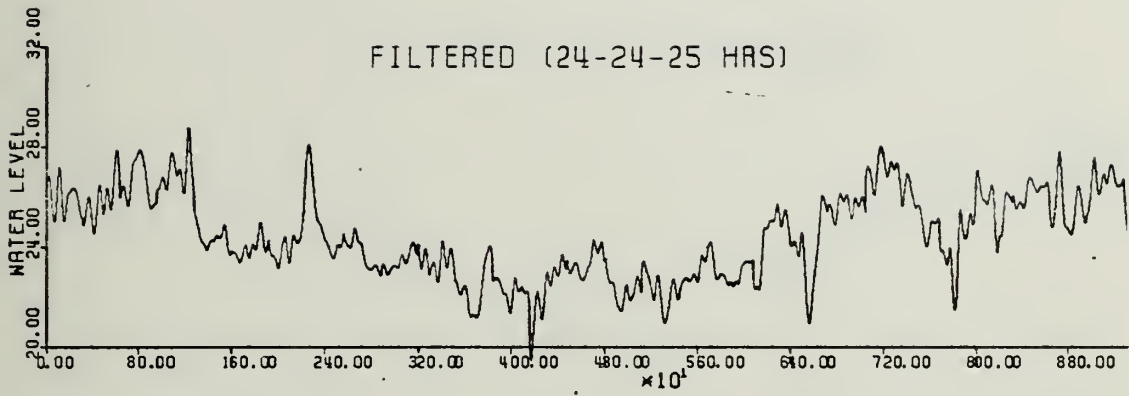


APPENDIX B

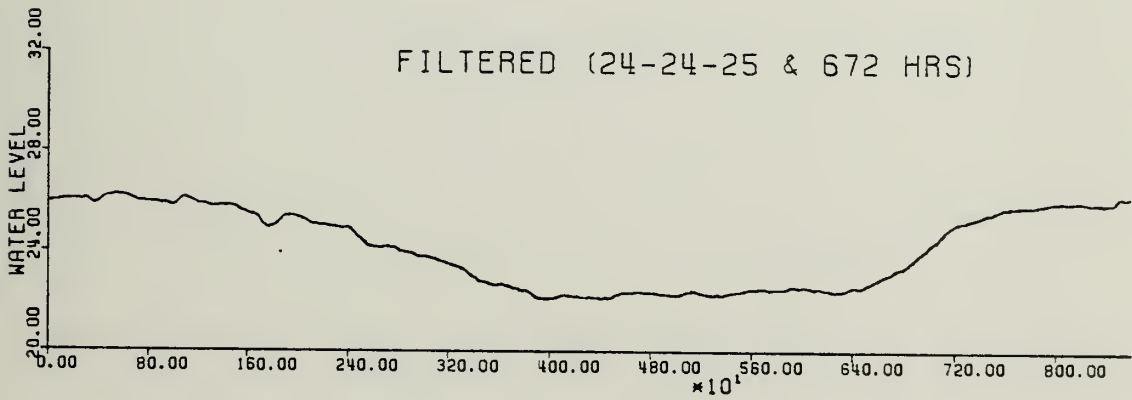
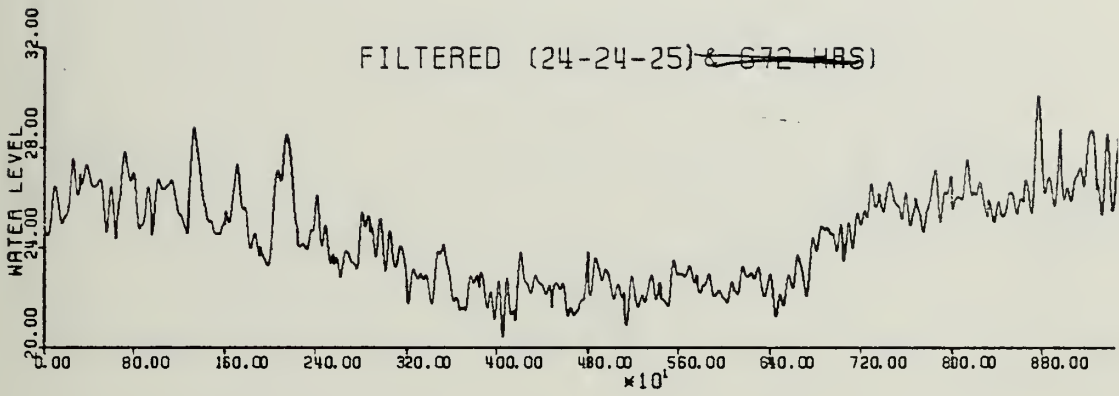
HOURLY SEA LEVEL DATA FILTERED WITH GODIN AND 28-DAYS FILTER

The following time-series graphs for Sattahip and Ko-Lak show: (1) residual hourly water levels remaining after application of Godin (24-24-25 hour) filter to the raw hourly data (upper graph; also shown in Appendix A), and (2) the same data after further smoothing using a 672-hour (28-day) filter. Water levels are in decimeters and the time scale is in hours measured from 0000Z on 1 January. Each graph covers one year of data.

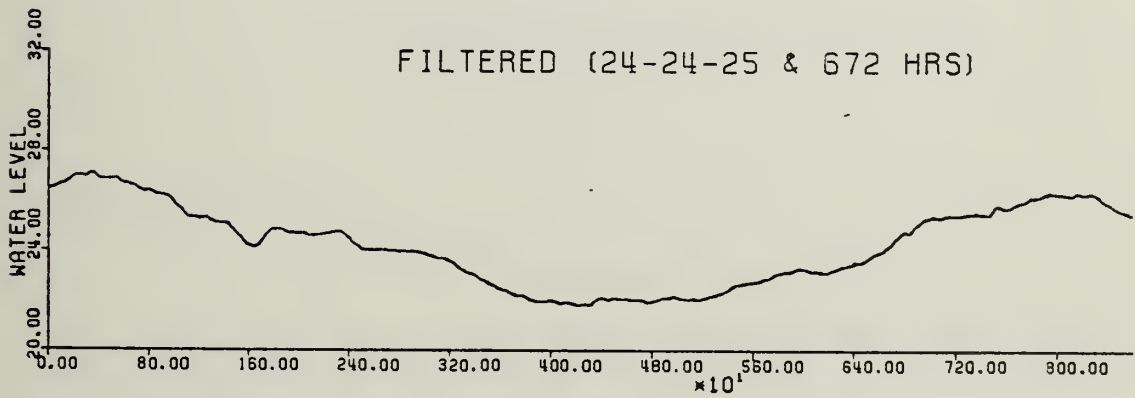
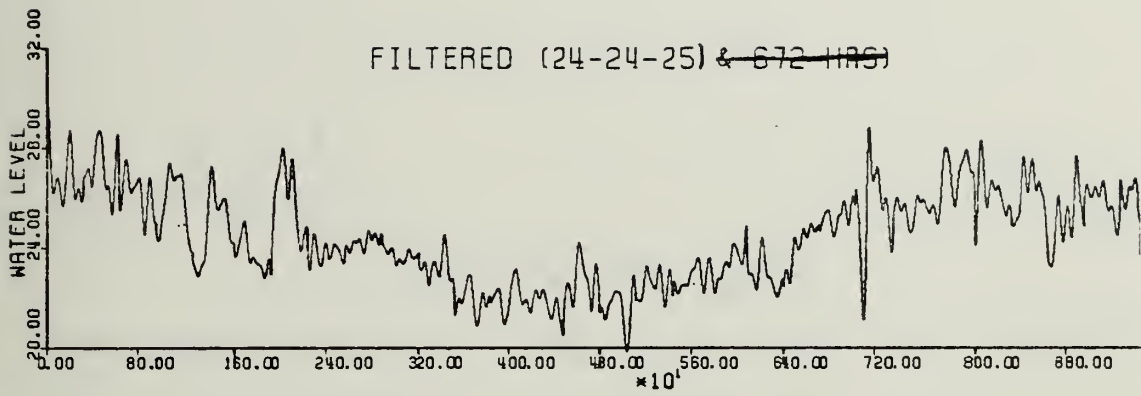
SATTAHIP 1960



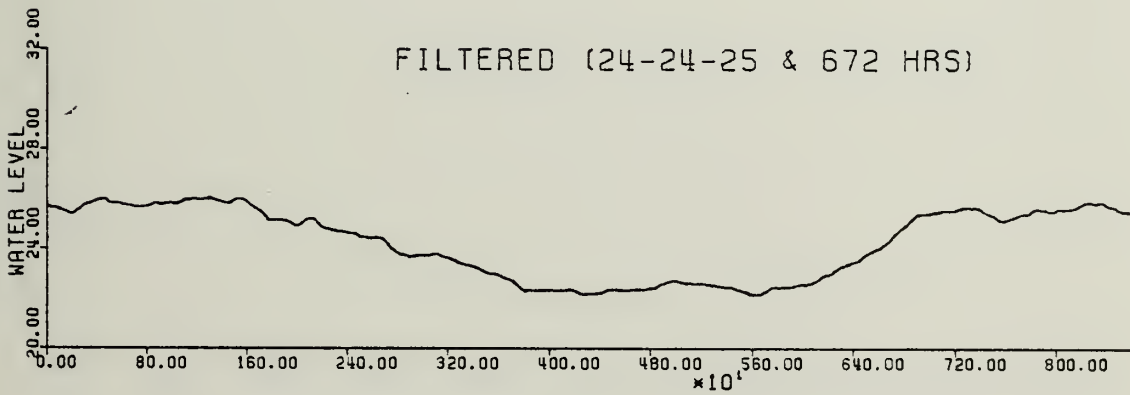
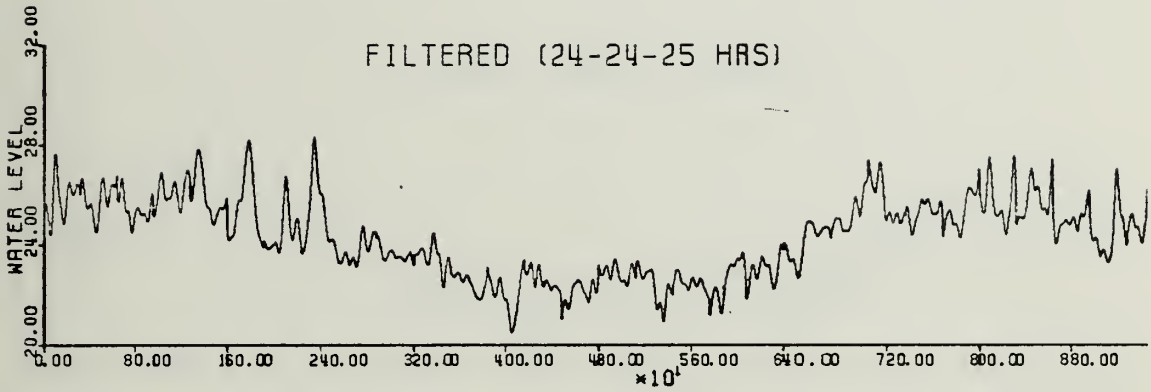
SATTAHIP 1961



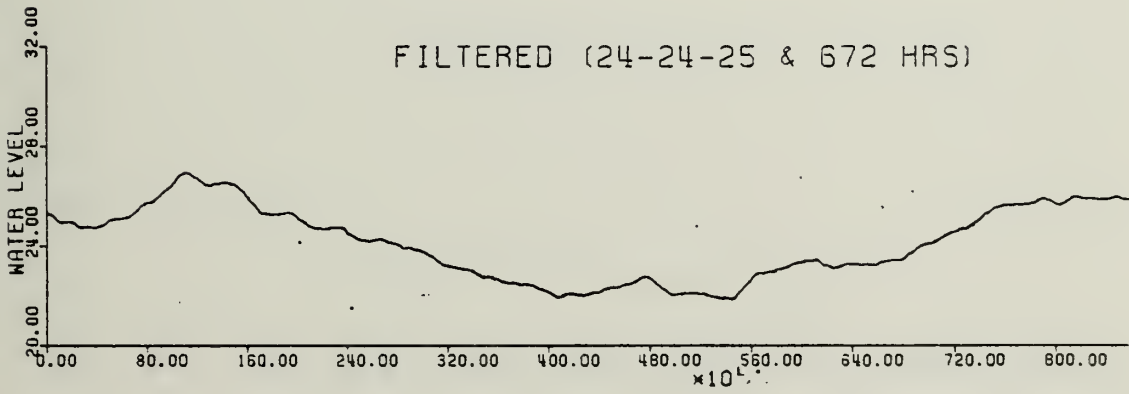
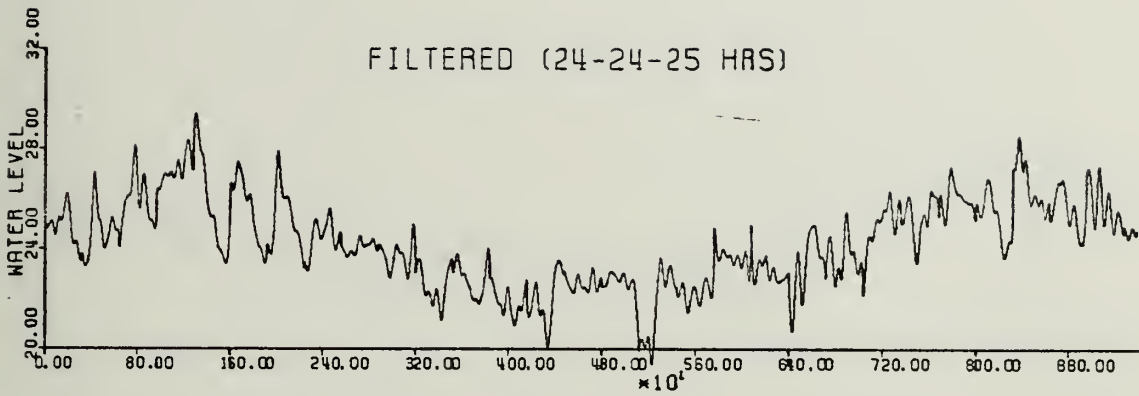
SATTAHIP 1962



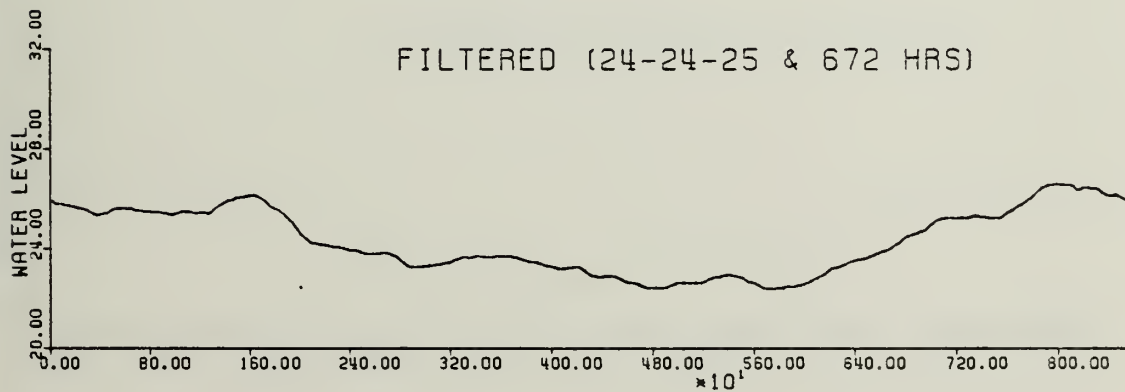
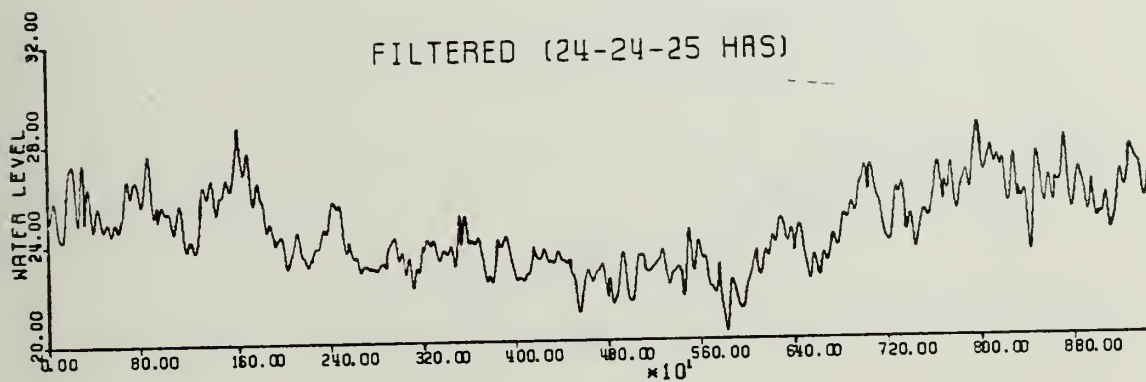
SATTAHIP 1963



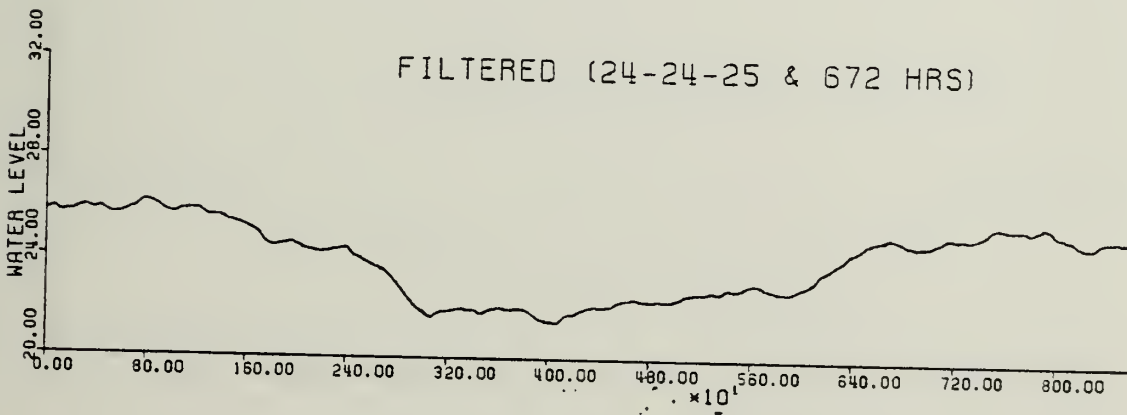
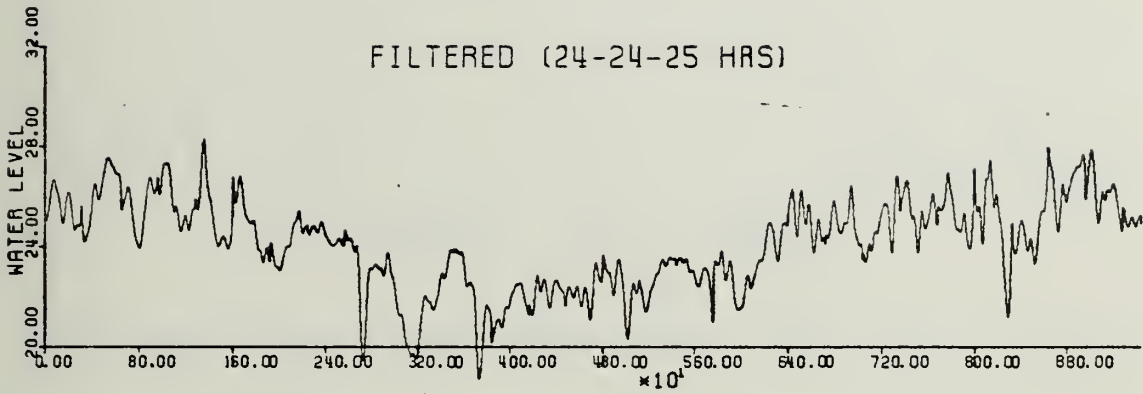
SATTAHIP 1964



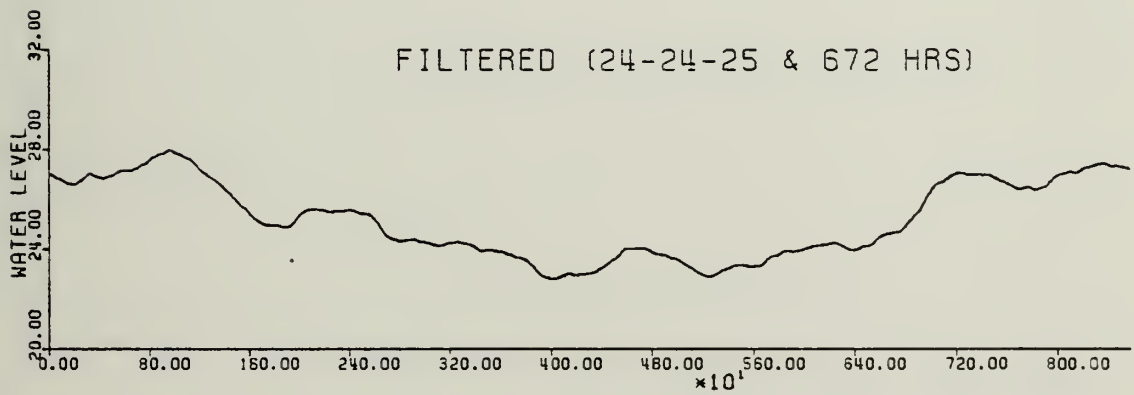
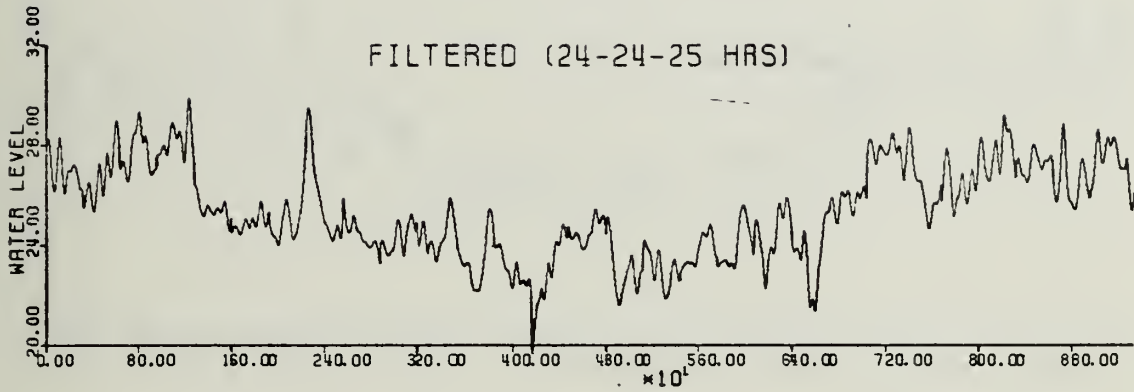
SATTAHIP 1965



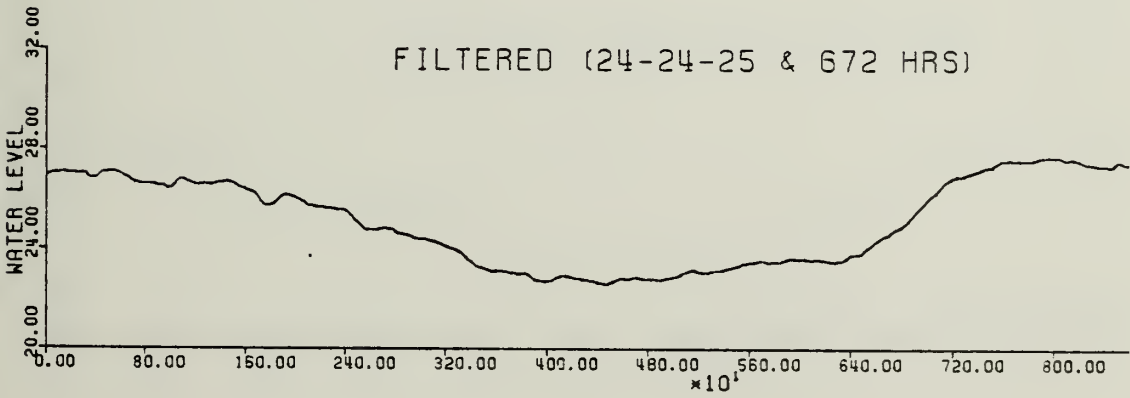
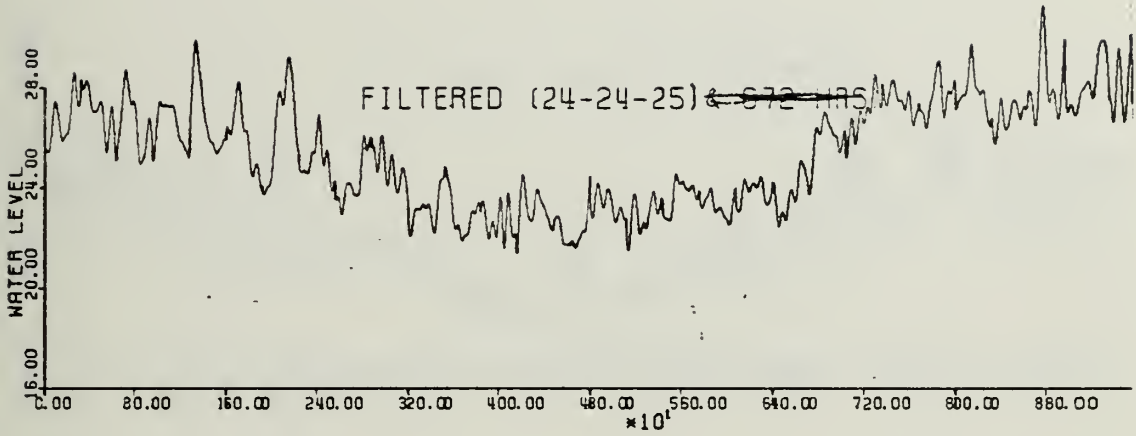
SATTAHIP 1966



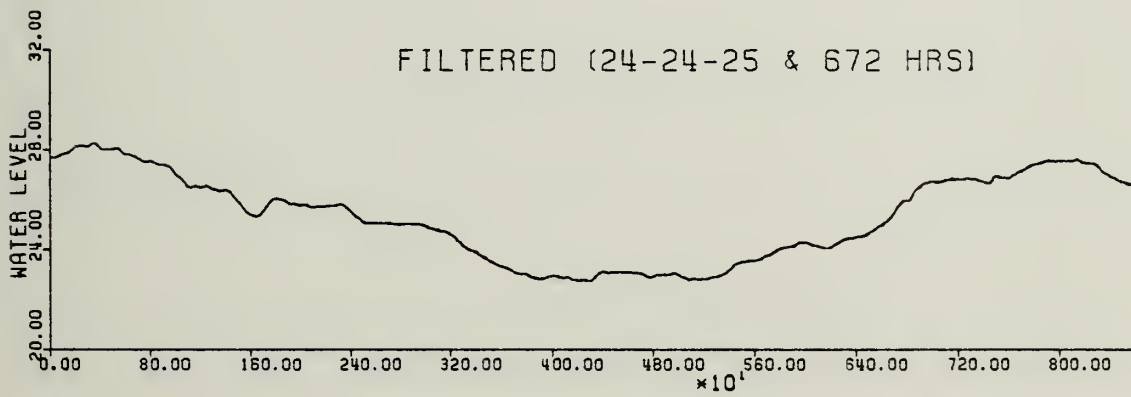
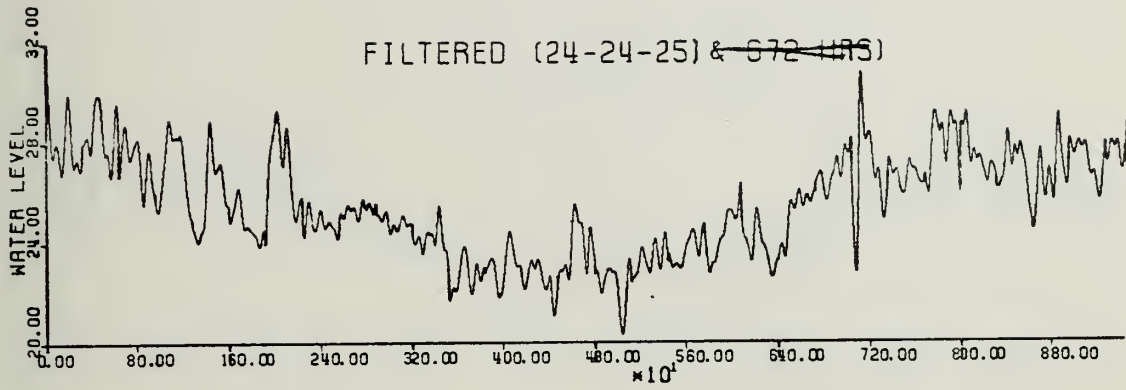
KO-LAK 1960



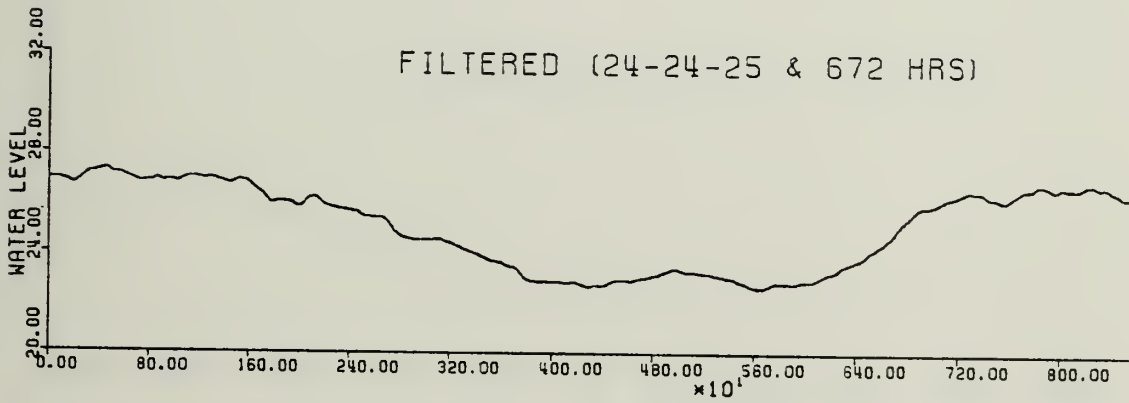
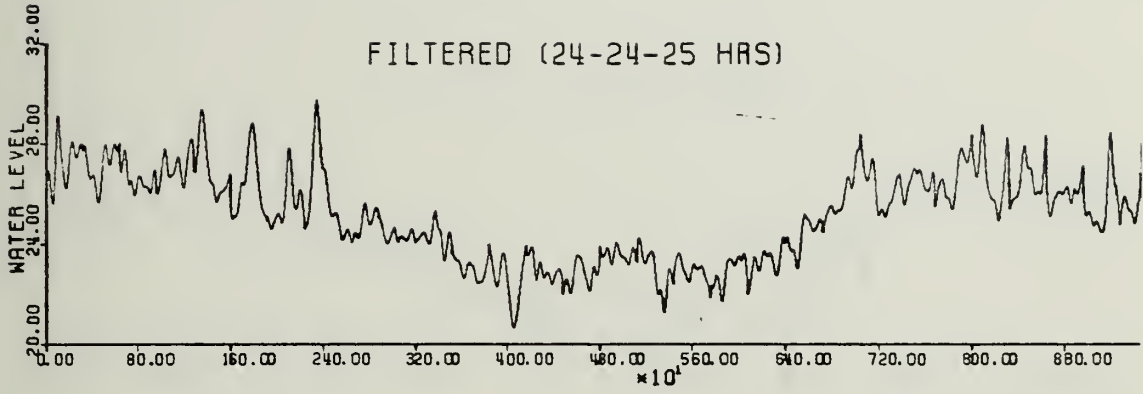
KO-LAK 1961



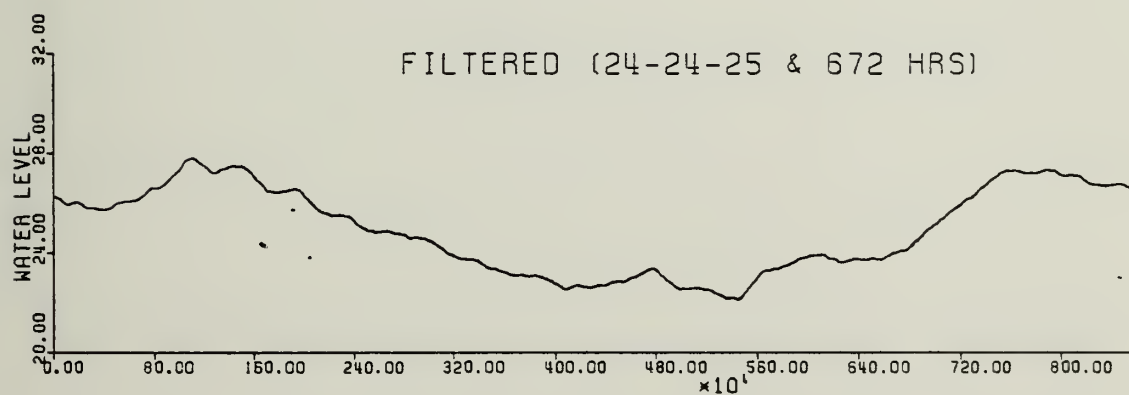
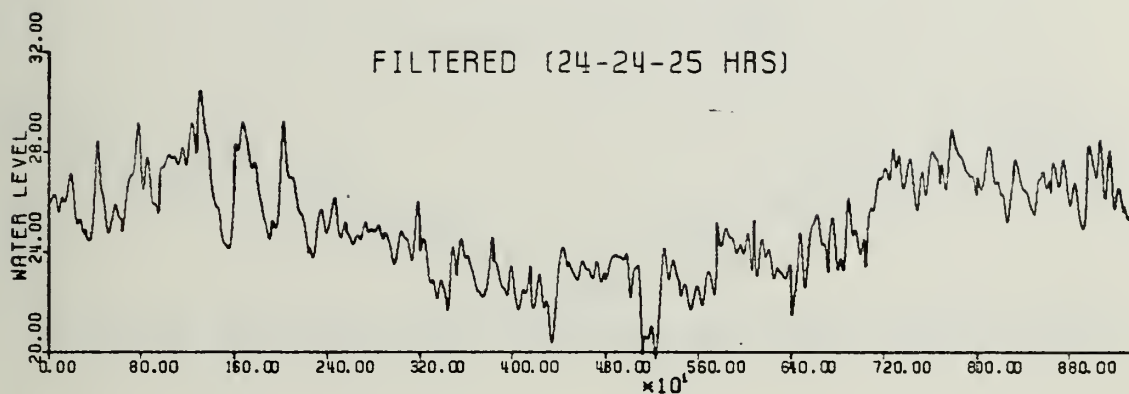
KO-LAK 1962



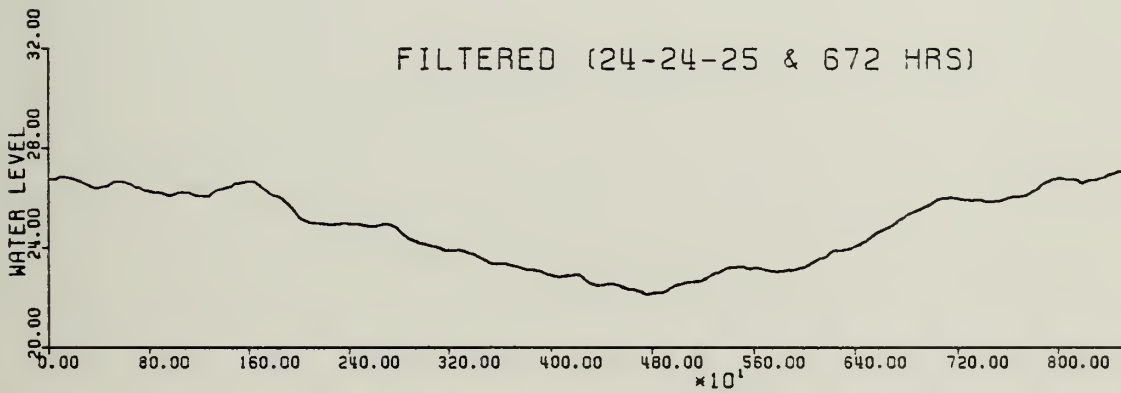
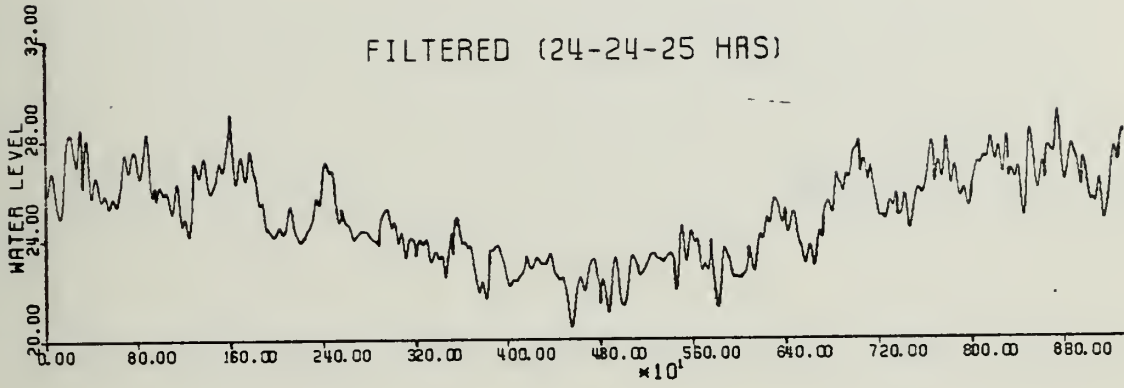
KO-LAK 1963



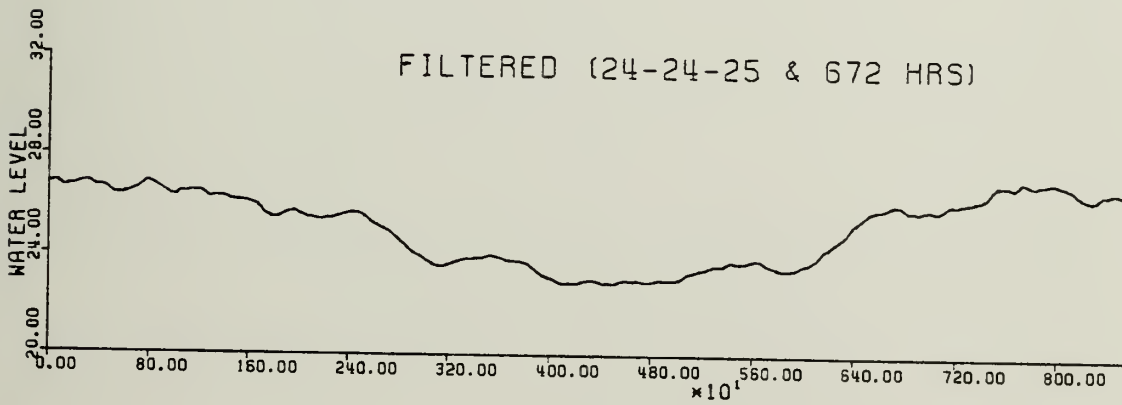
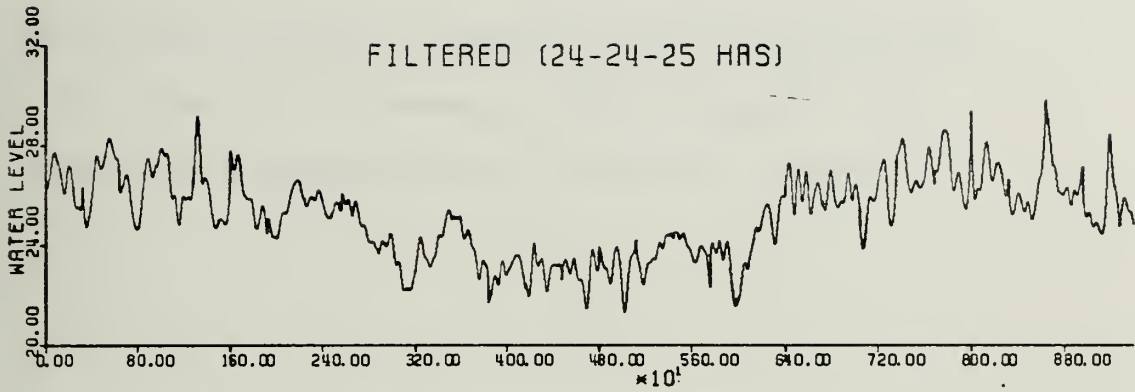
KO-LAK 1964



KO-LAK 1965



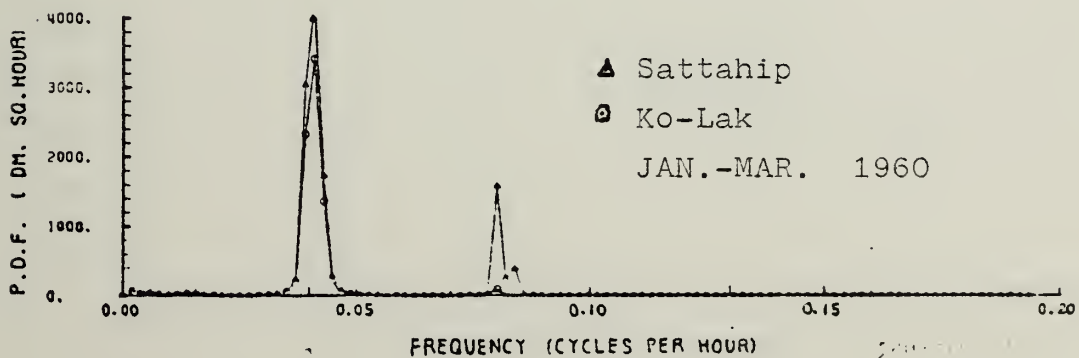
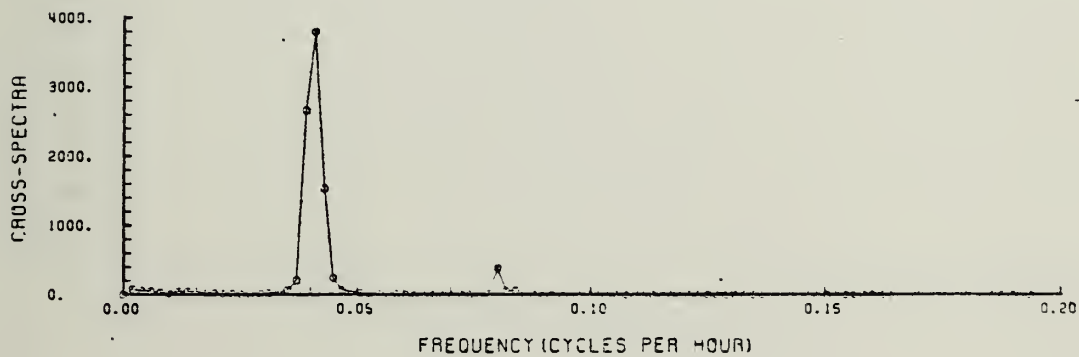
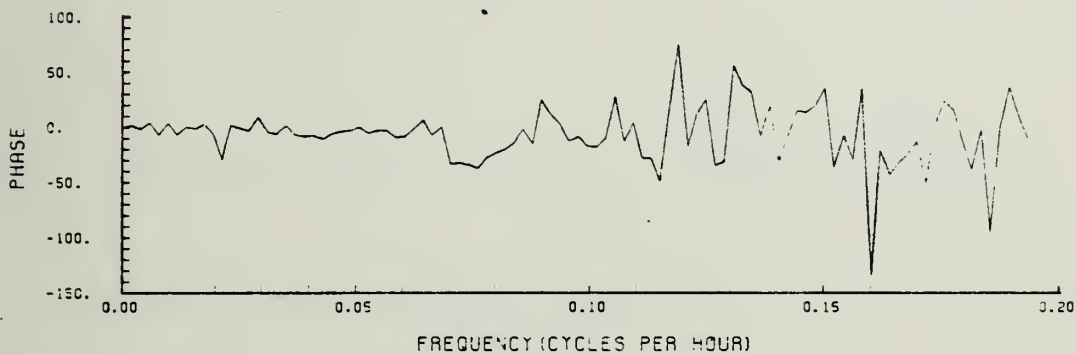
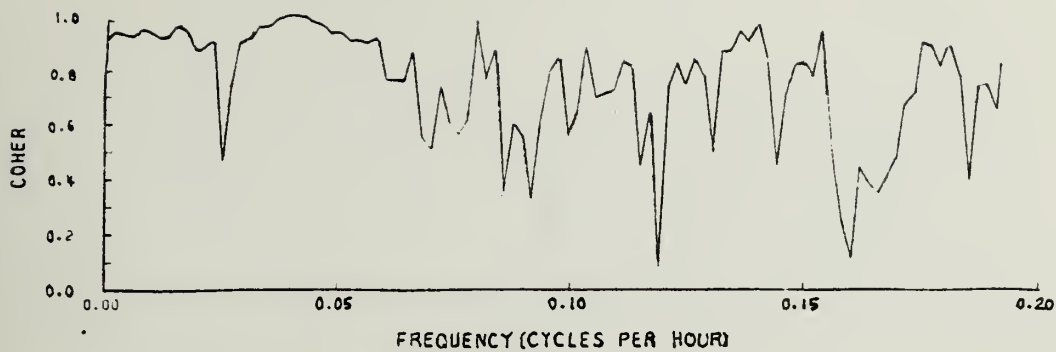
KO-LAK 1966

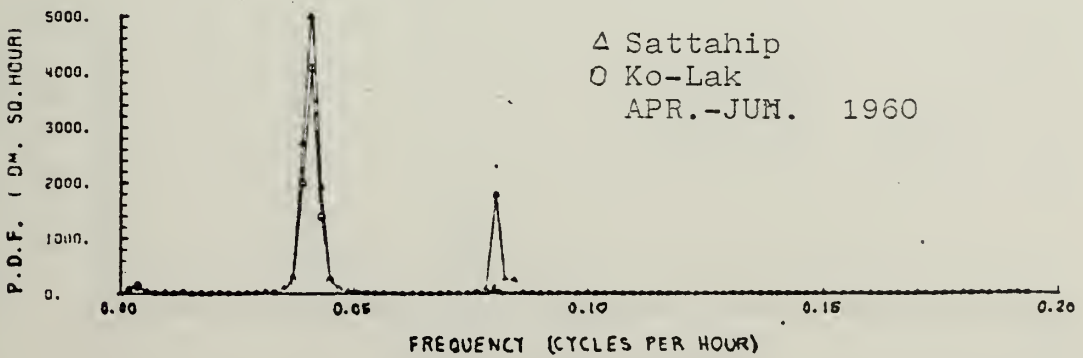
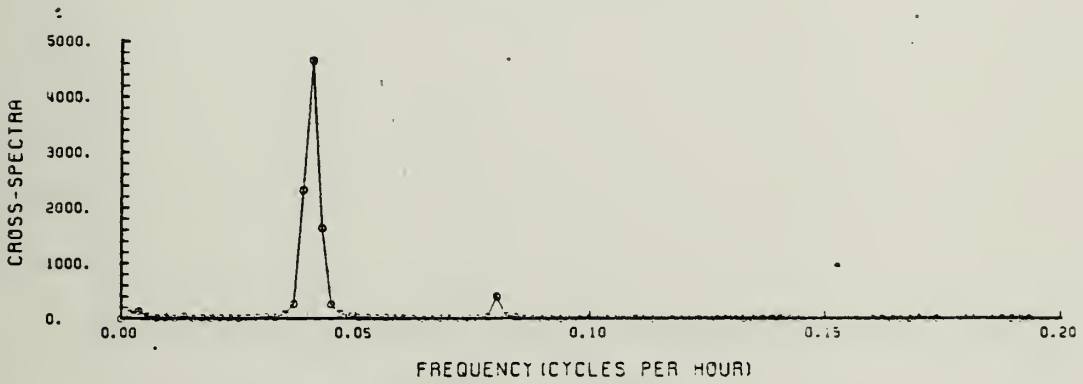
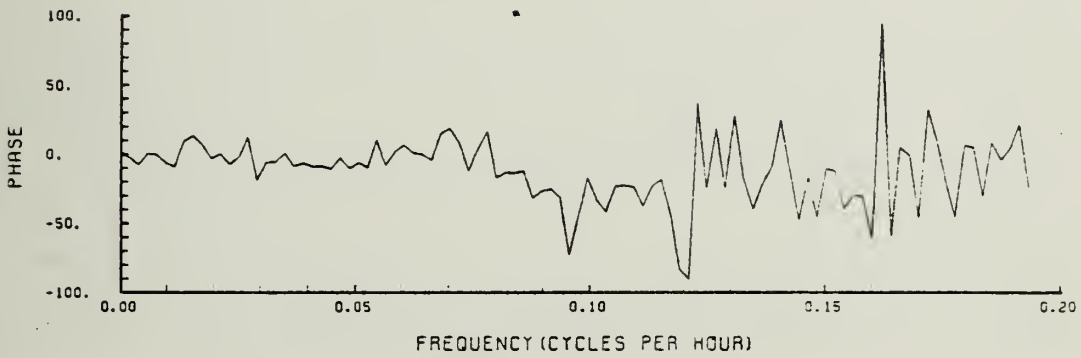
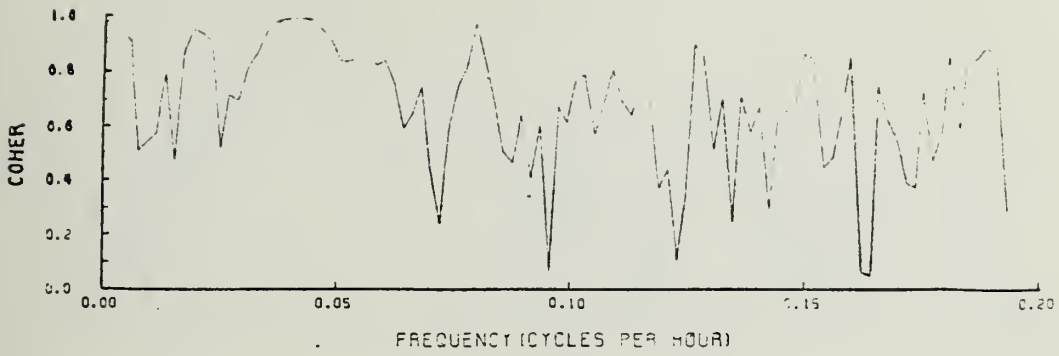


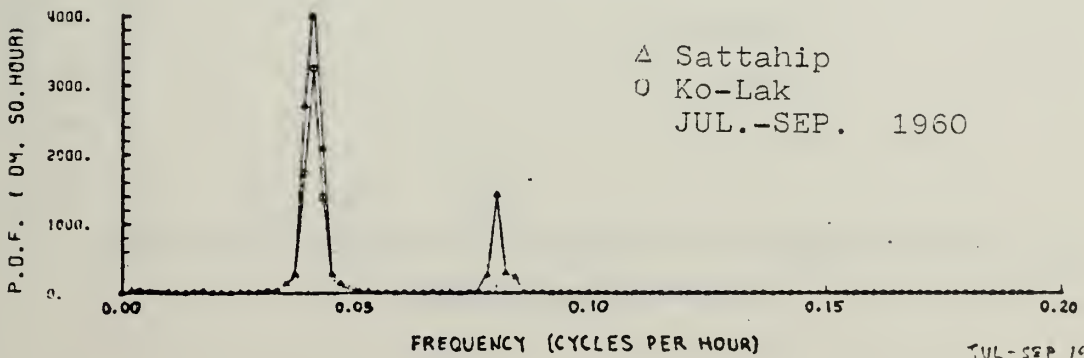
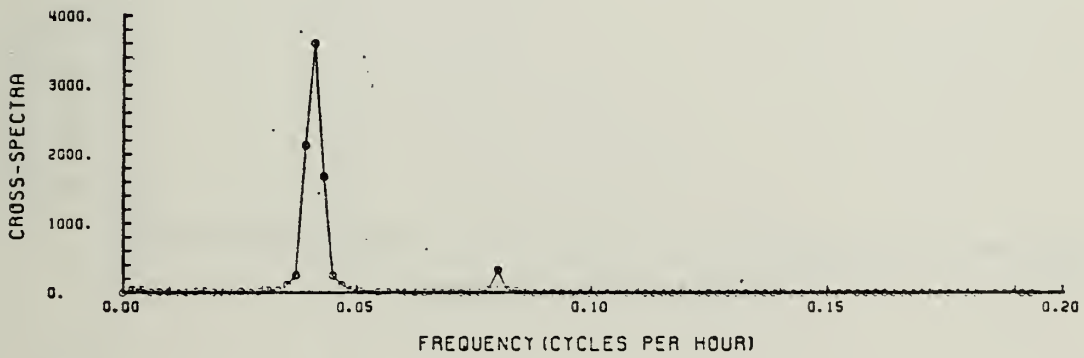
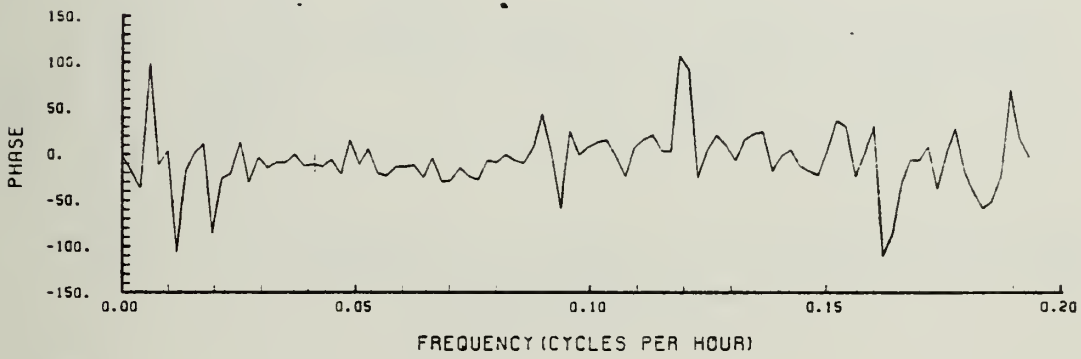
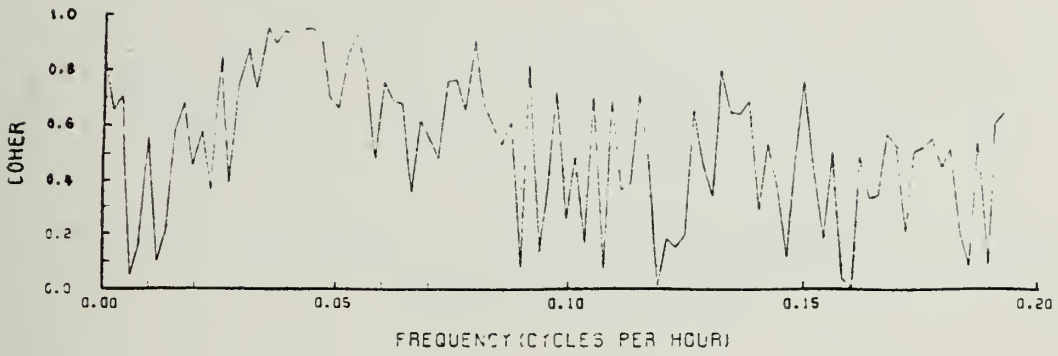
APPENDIX C

SPECTRA, CROSS-SPECTRA, COHERENCE, AND PHASE OF RAW SEA LEVEL DATA

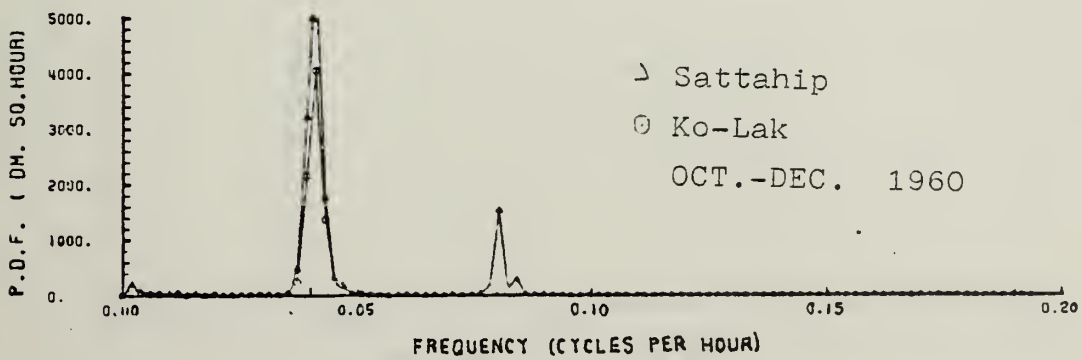
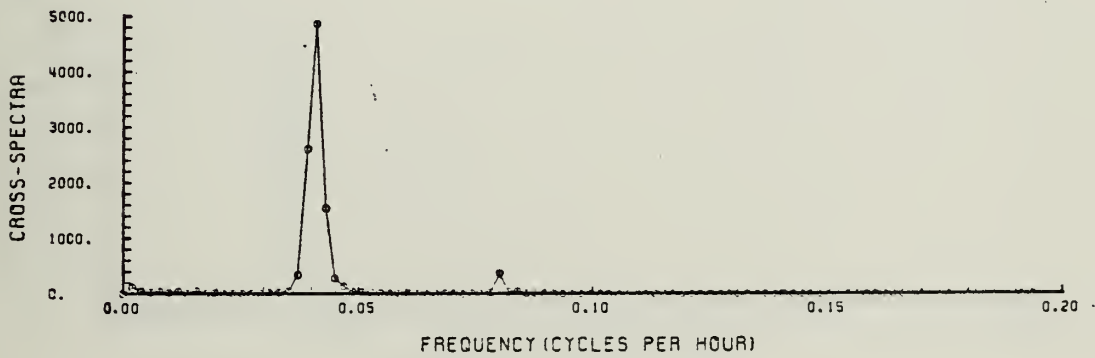
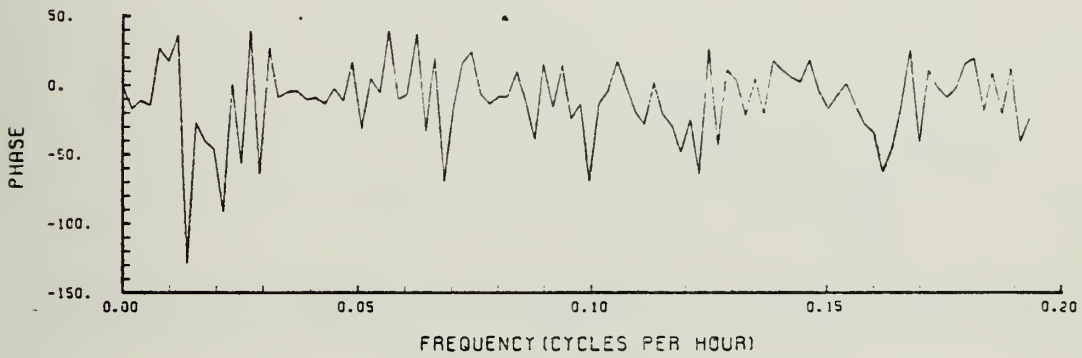
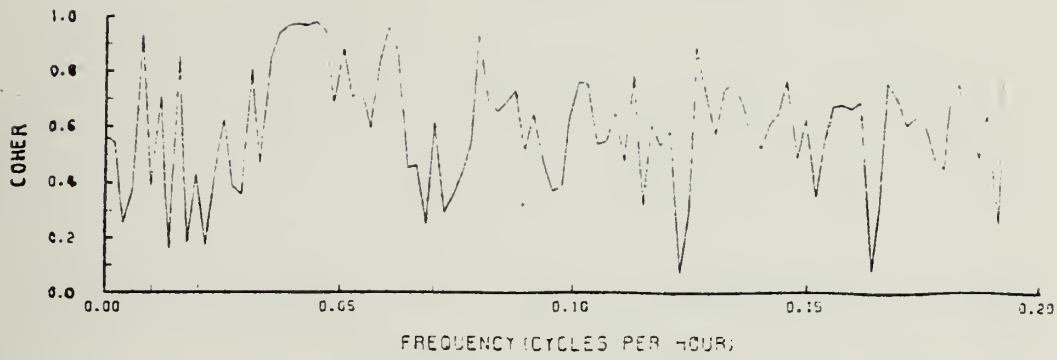
The following graphs for Sattahip and Ko-Lak show (from the top): (1) phase, (2) coherence, (3) cross-spectra, and (4) spectra for three-month period (8 degrees of freedom).

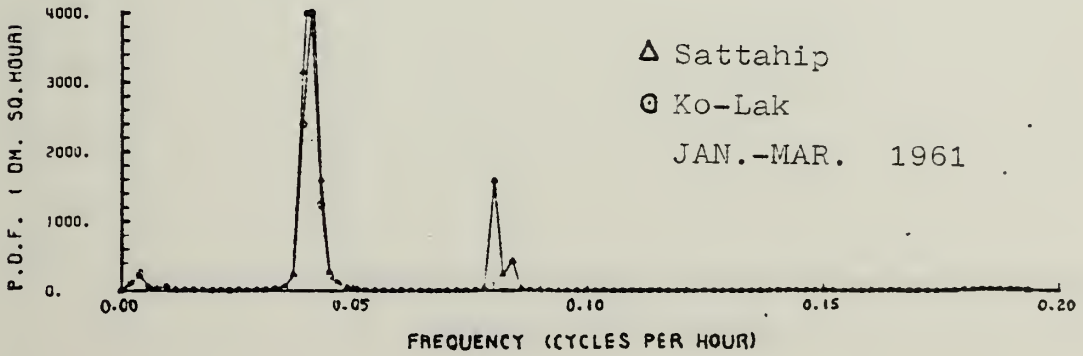
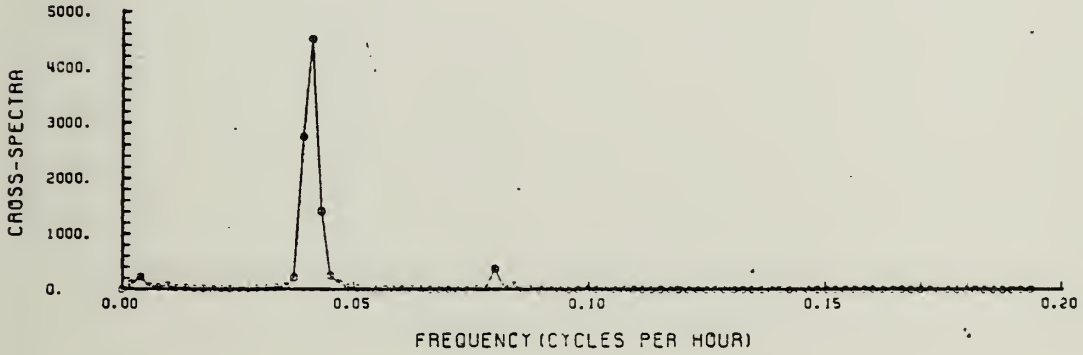
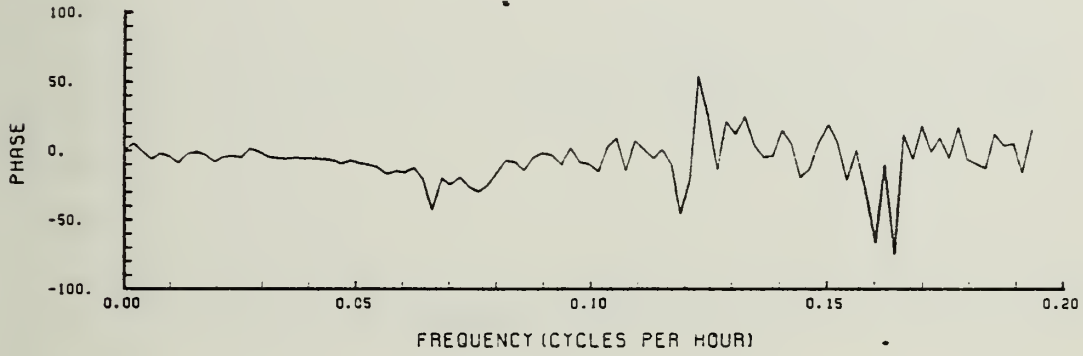
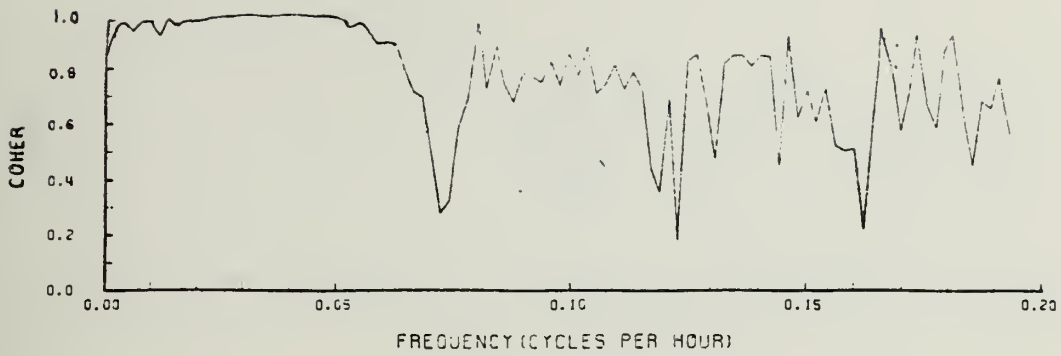


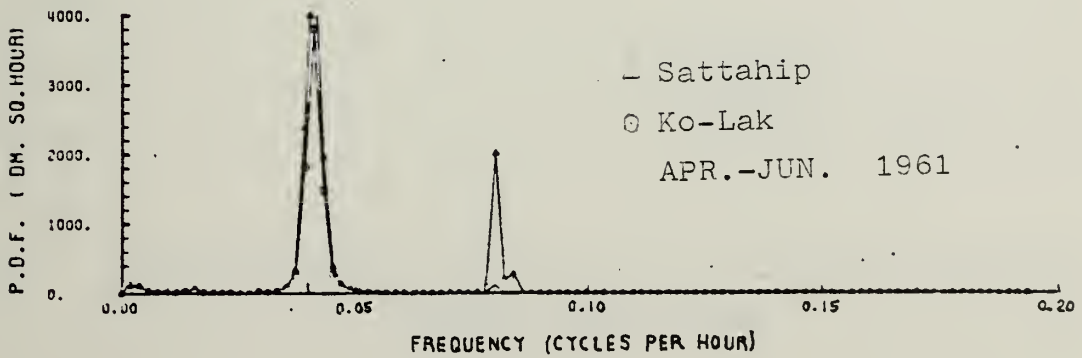
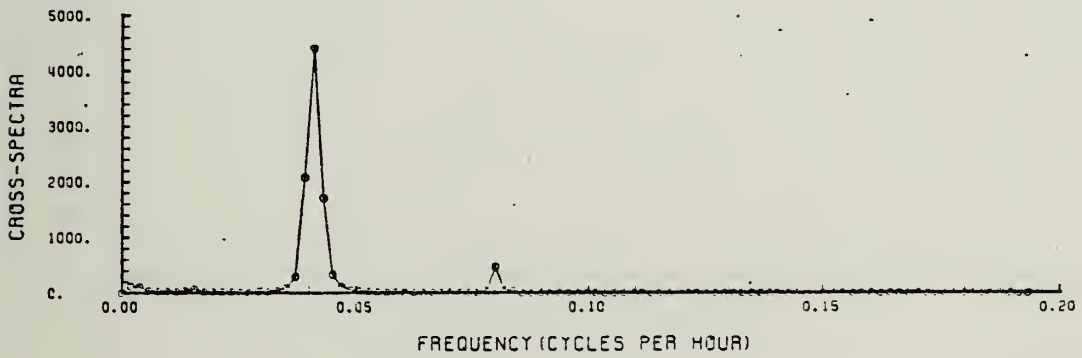
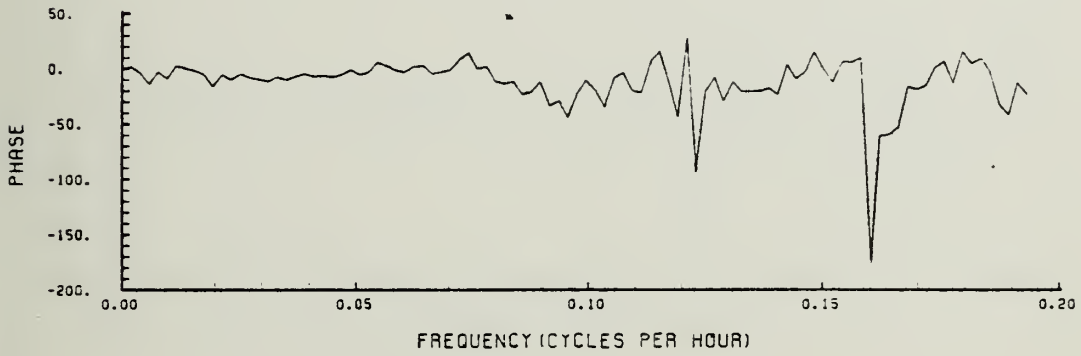
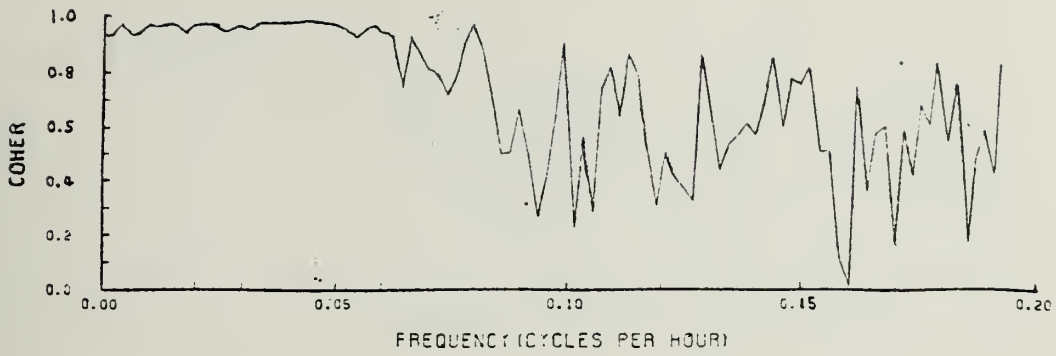


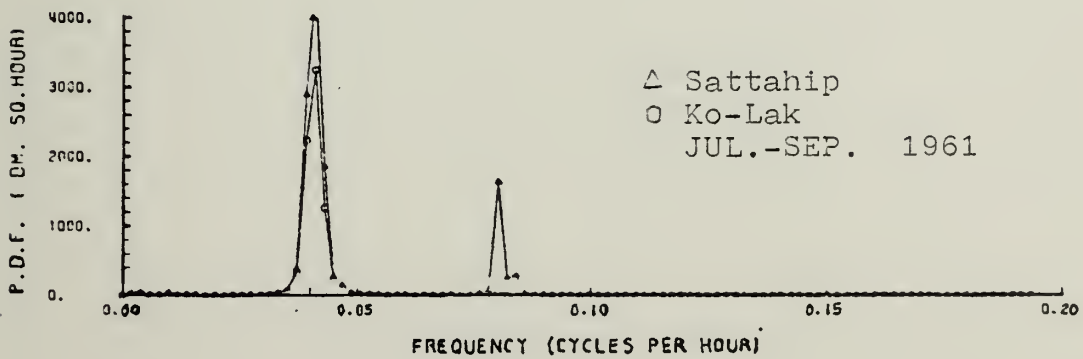
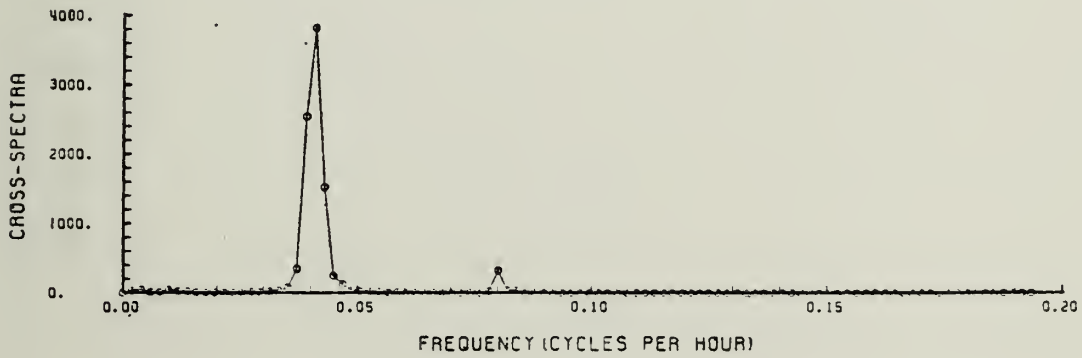
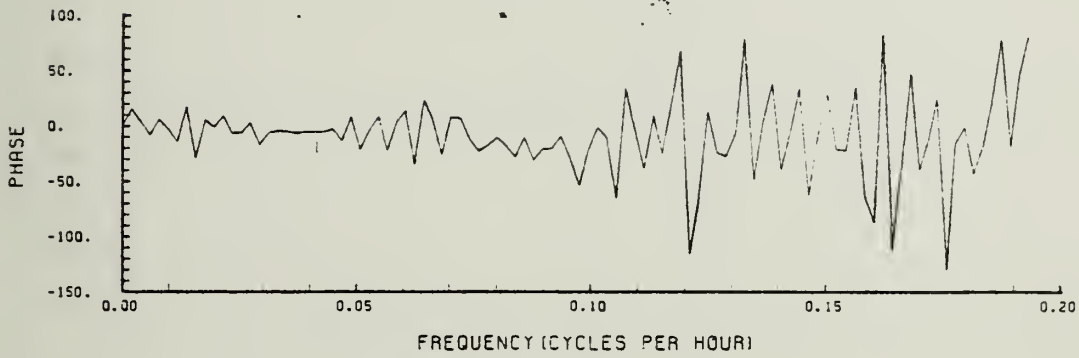
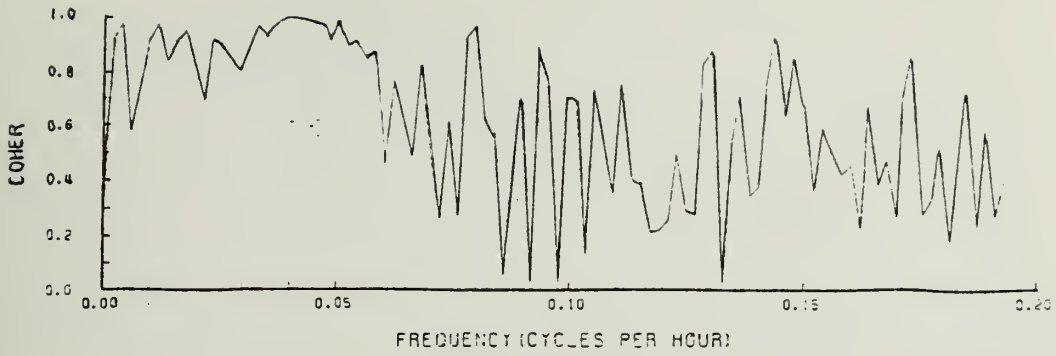


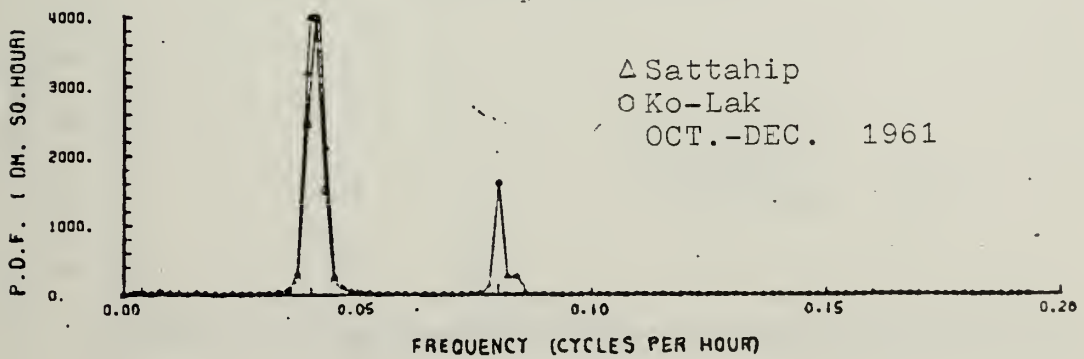
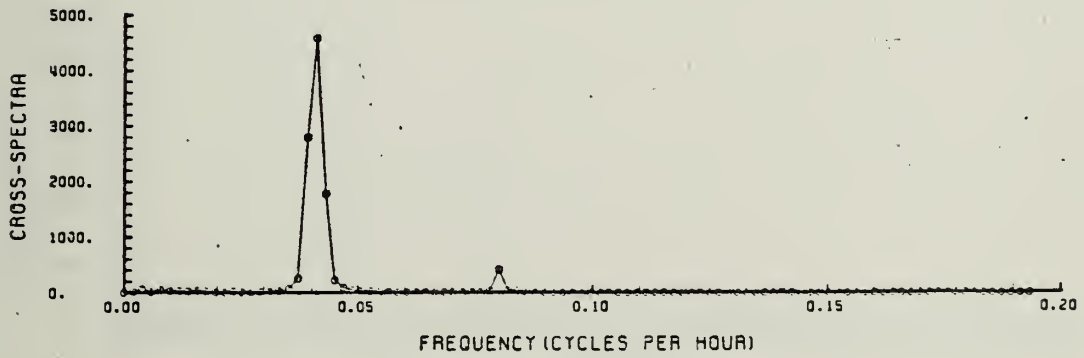
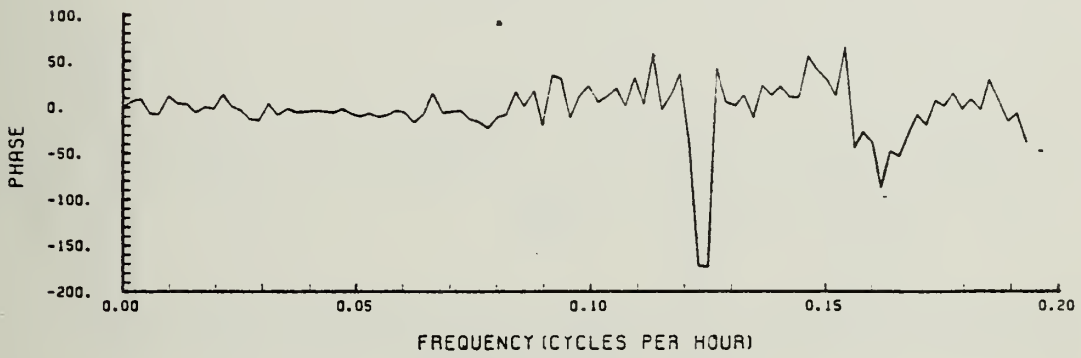
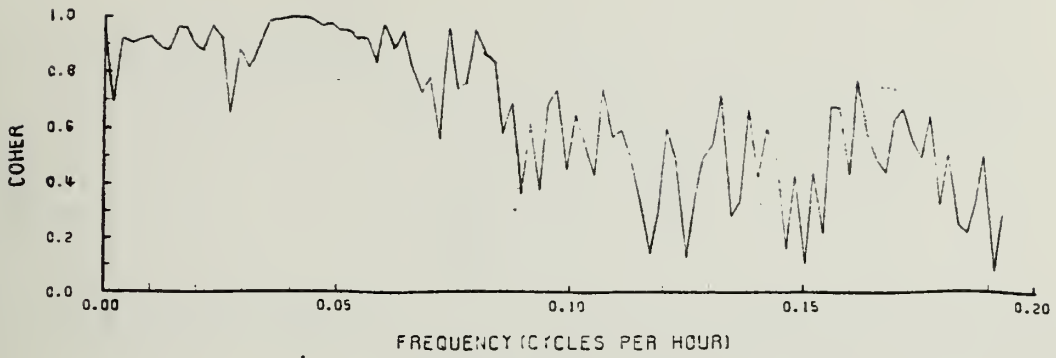
JUL-SEP 1960

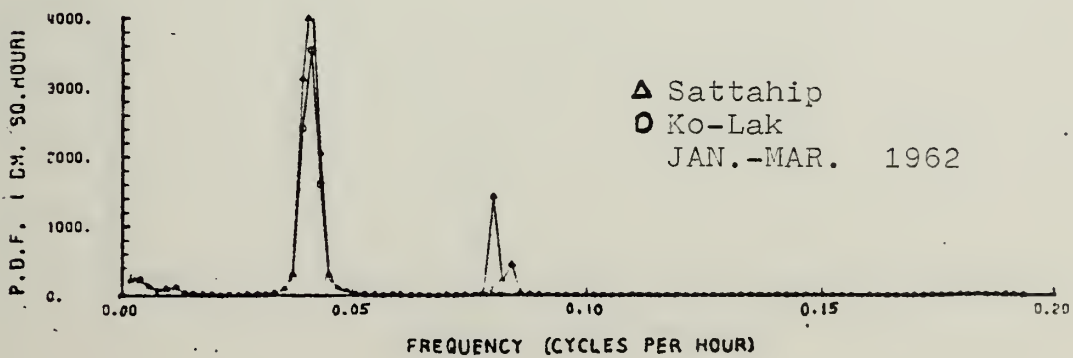
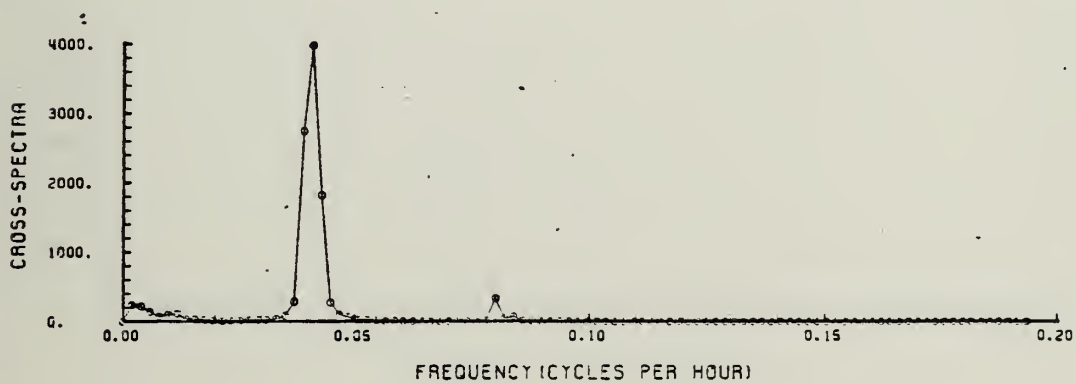
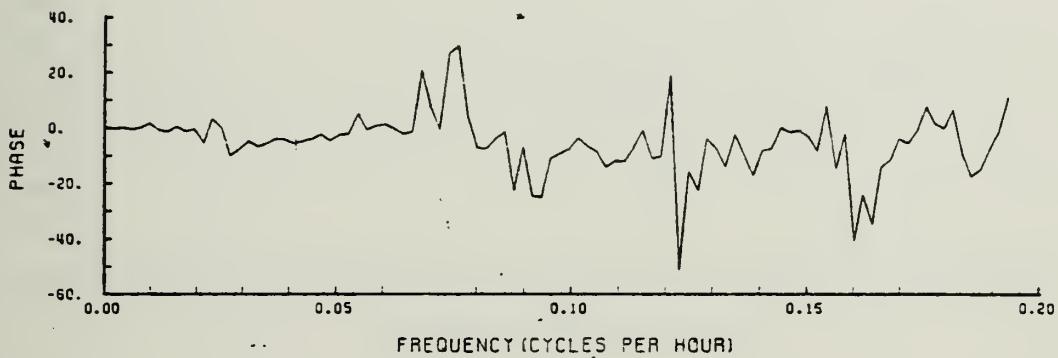
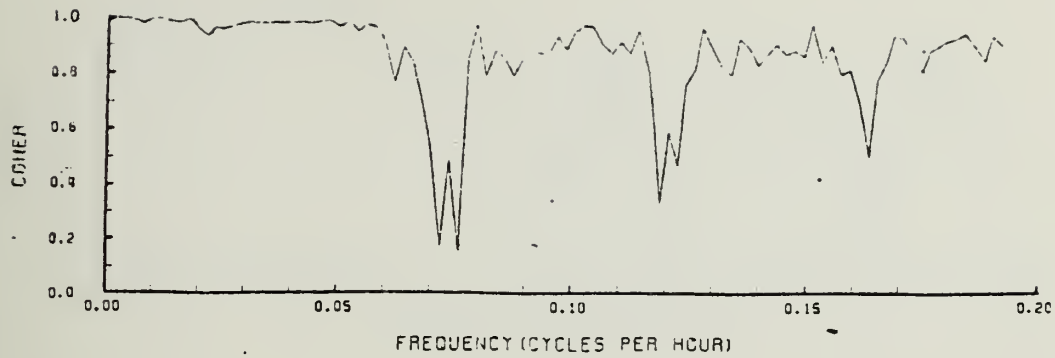


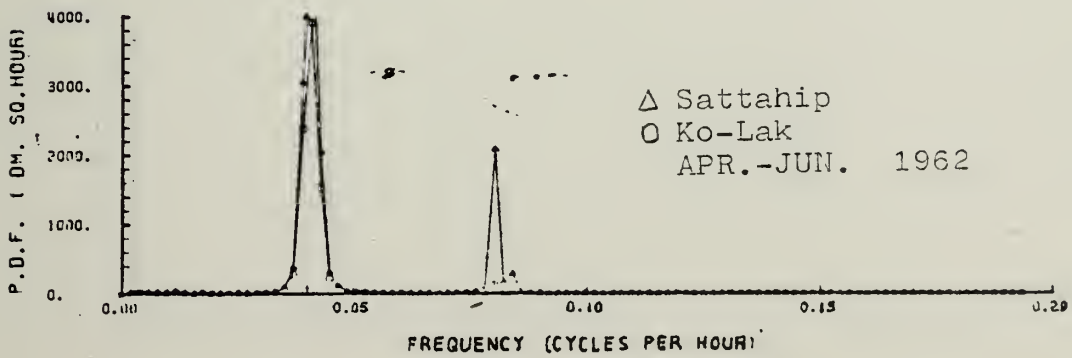
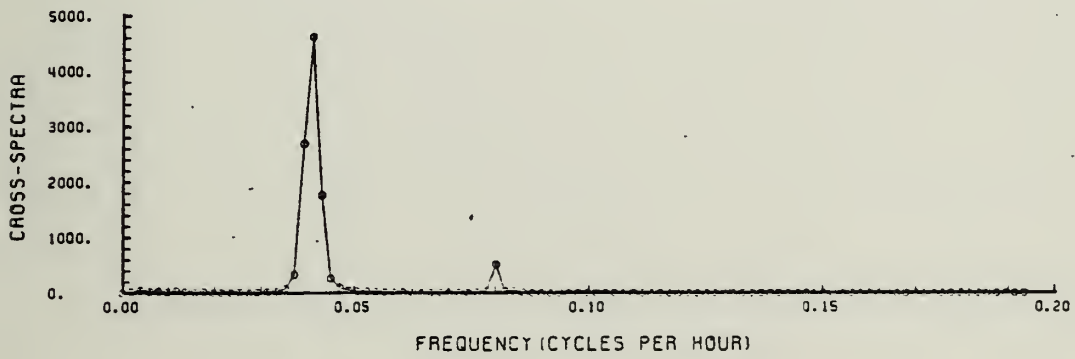
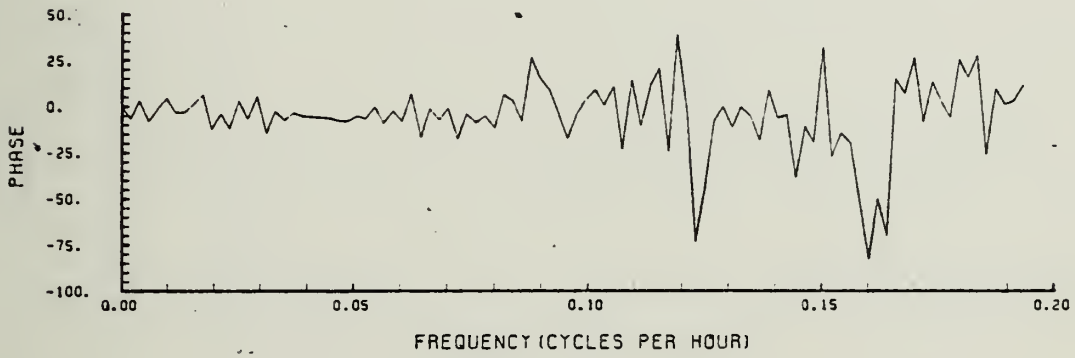
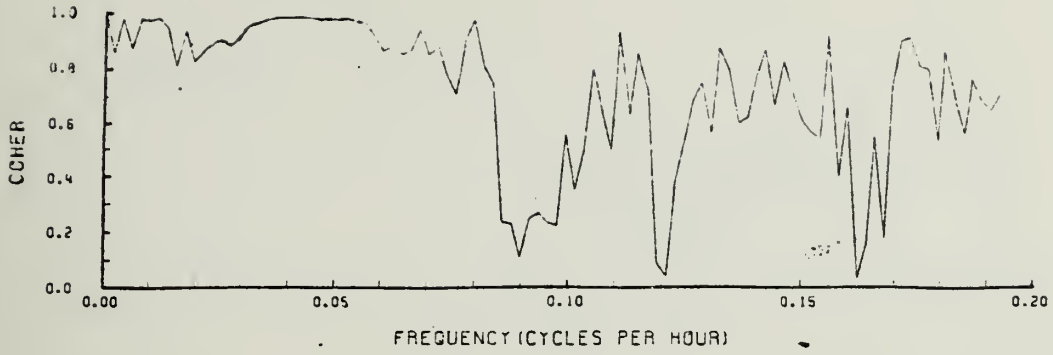


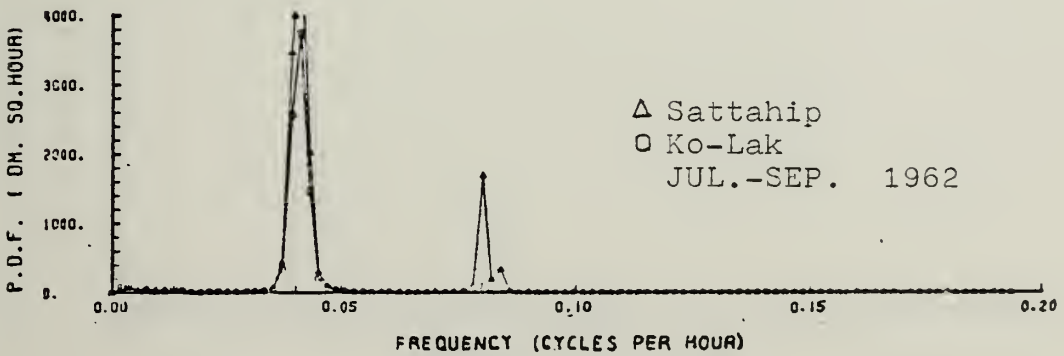
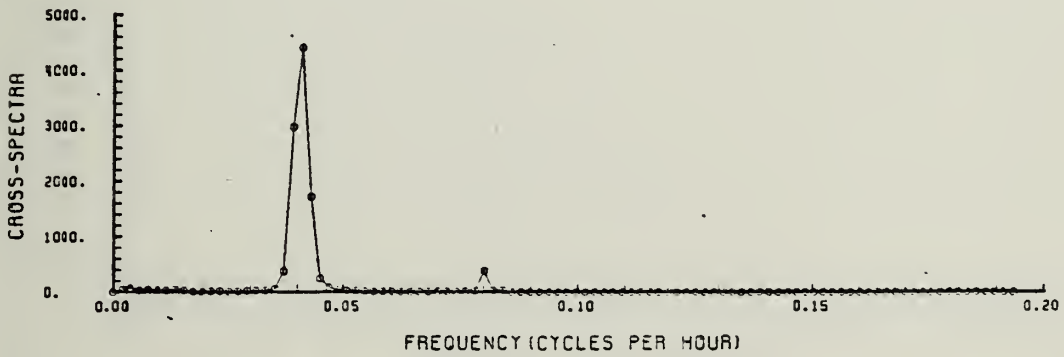
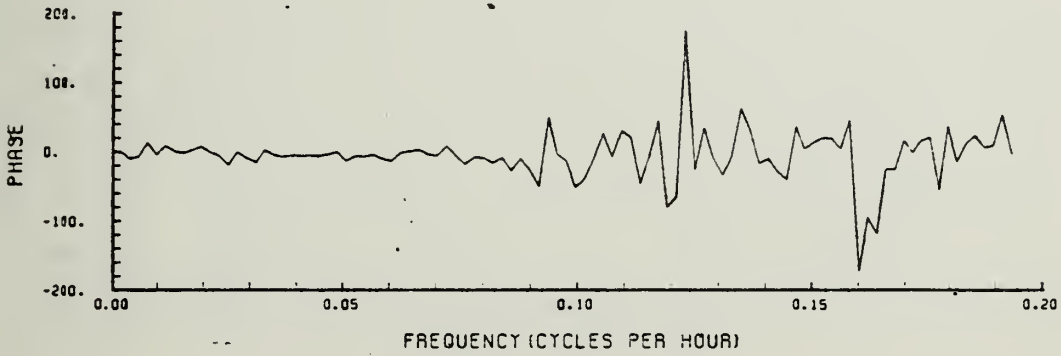
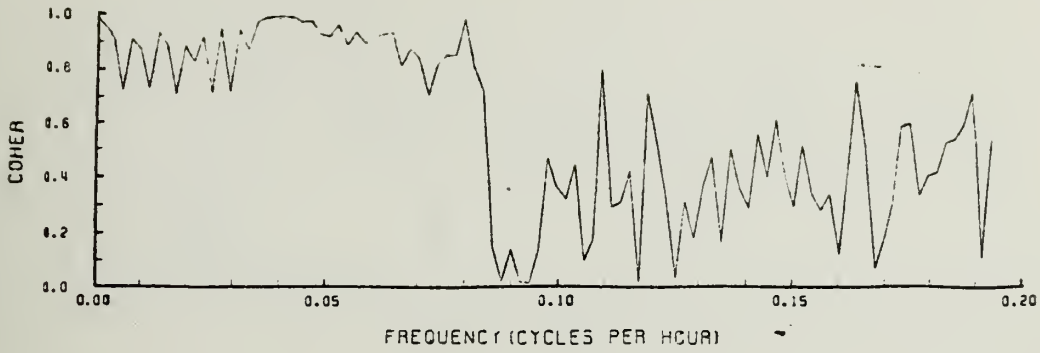


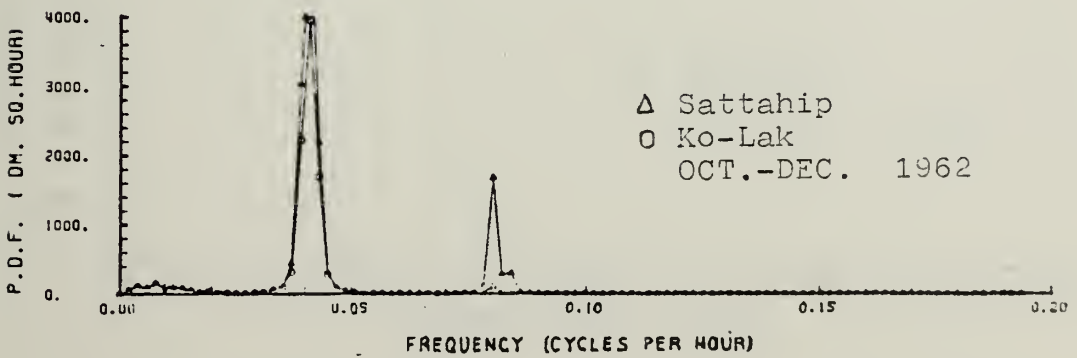
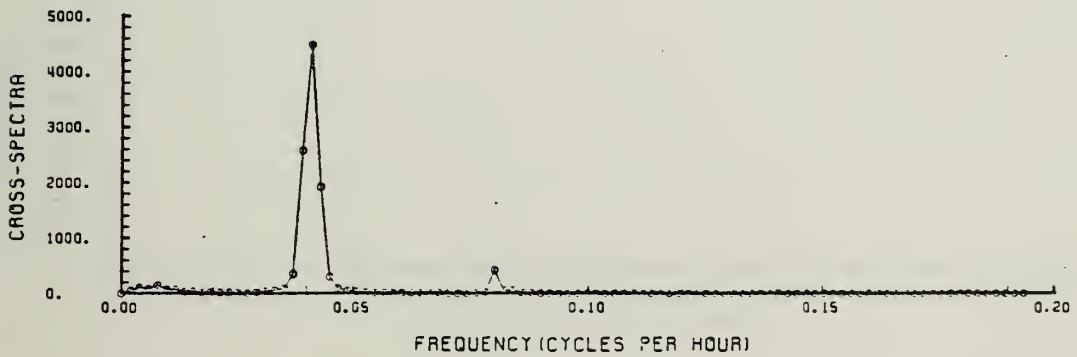
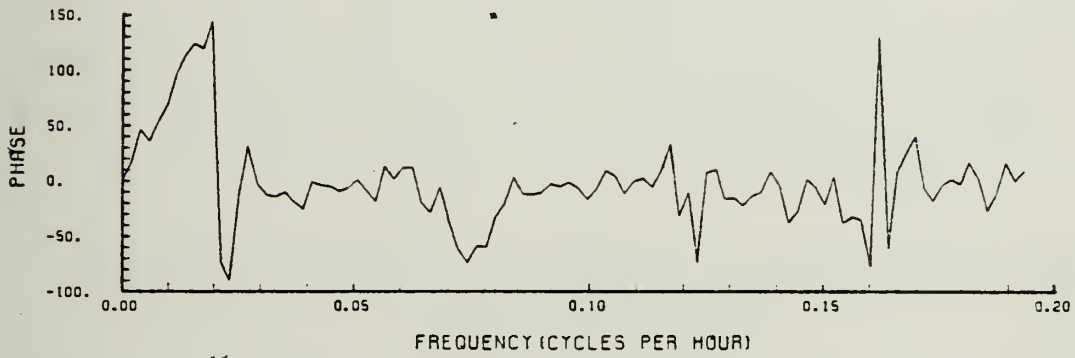
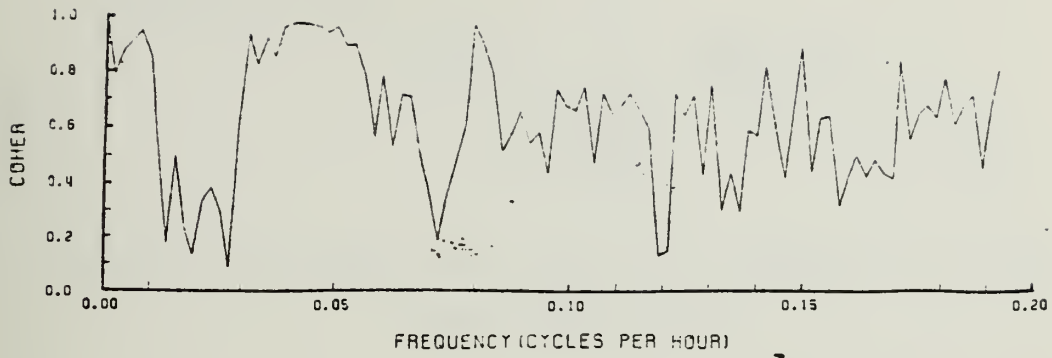


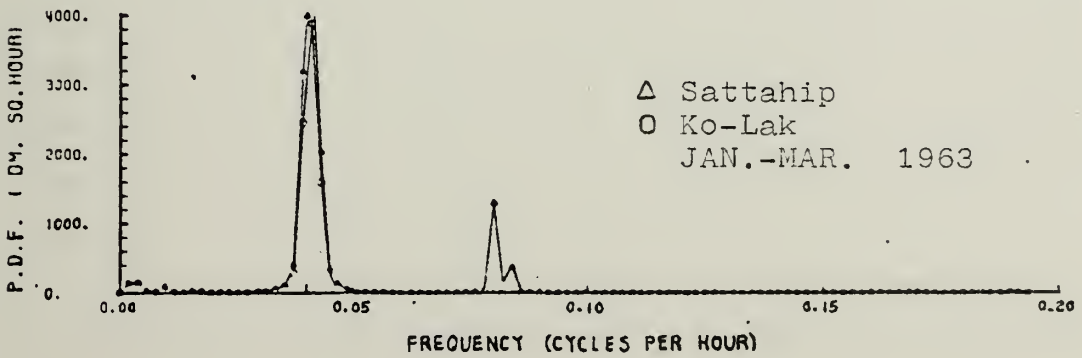
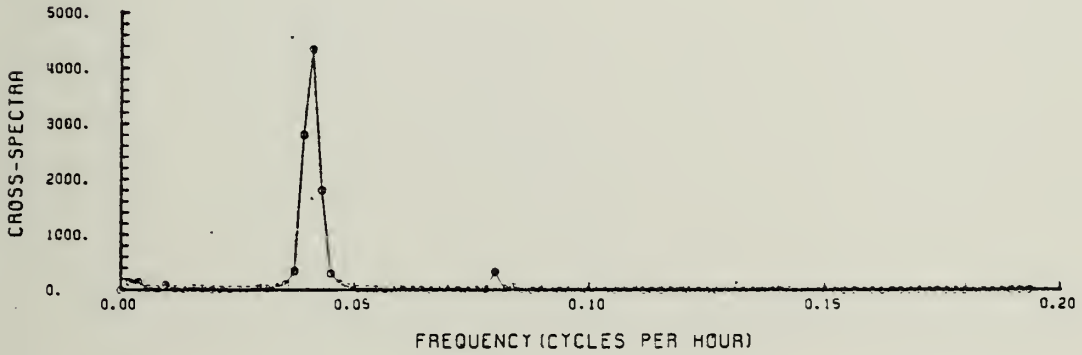
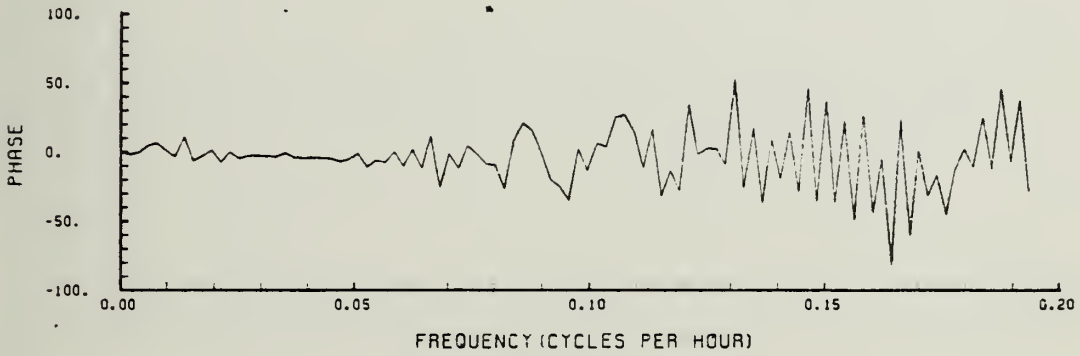
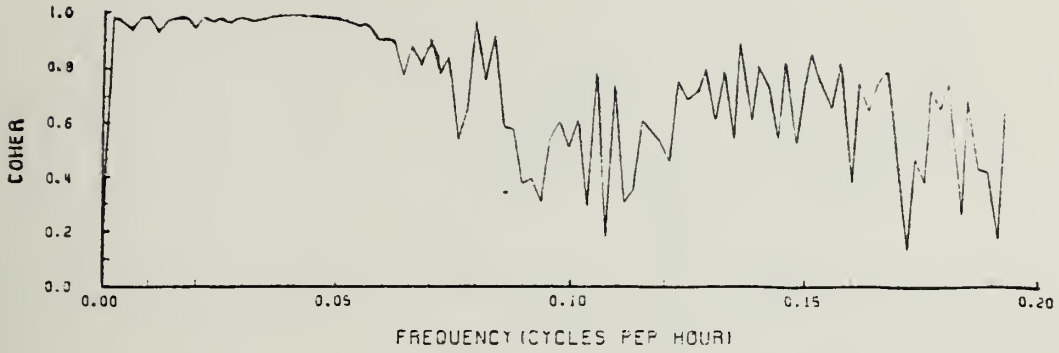


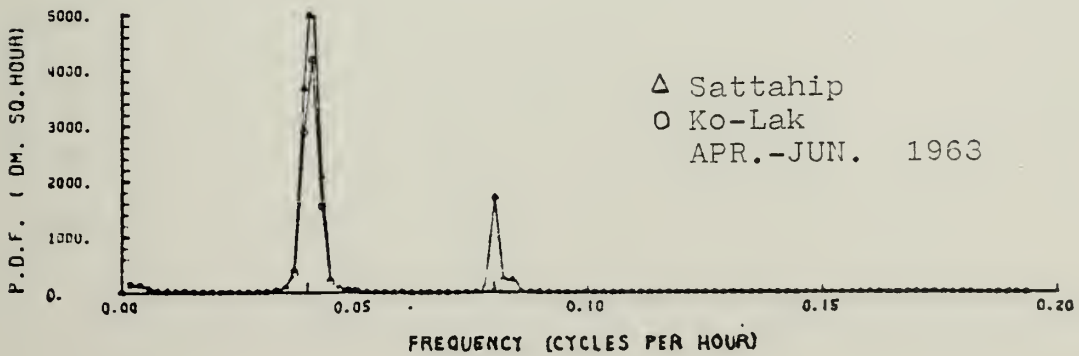
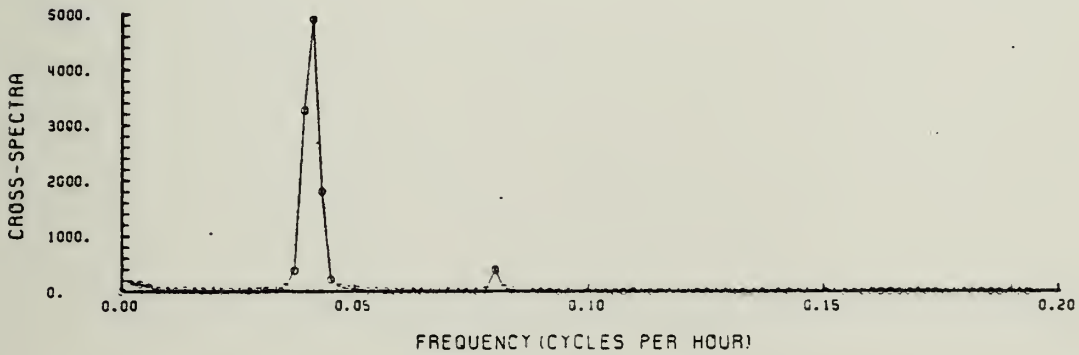
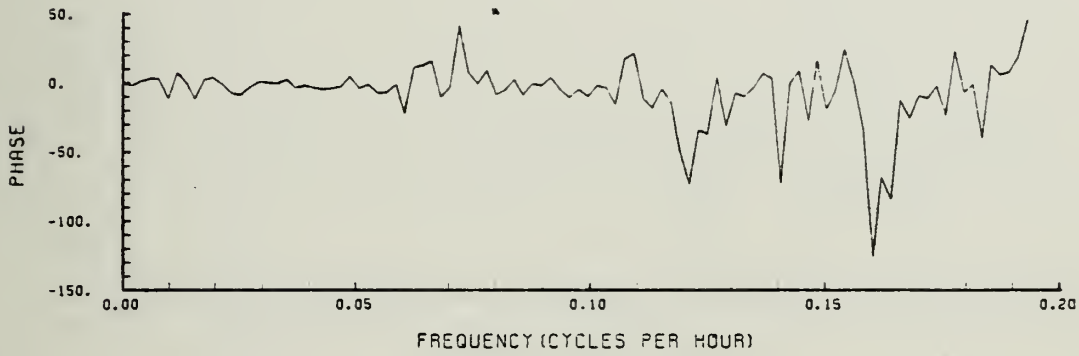
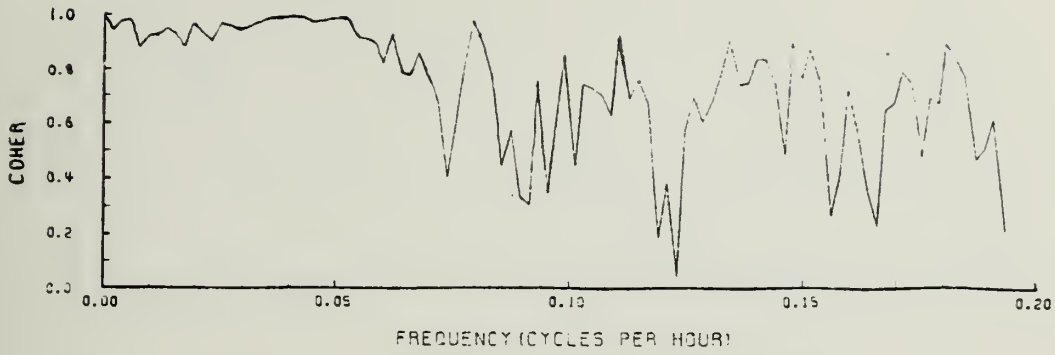


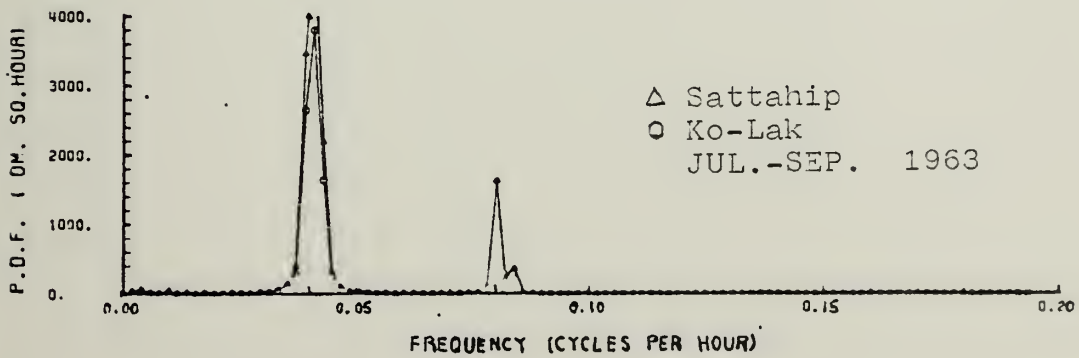
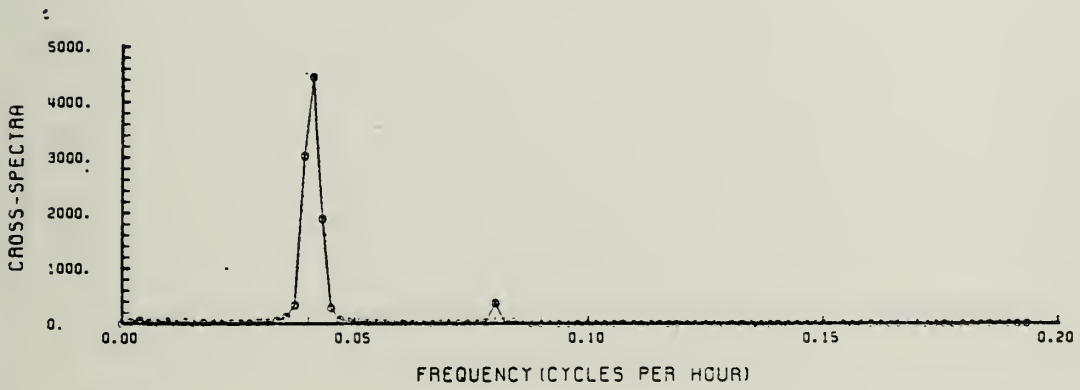
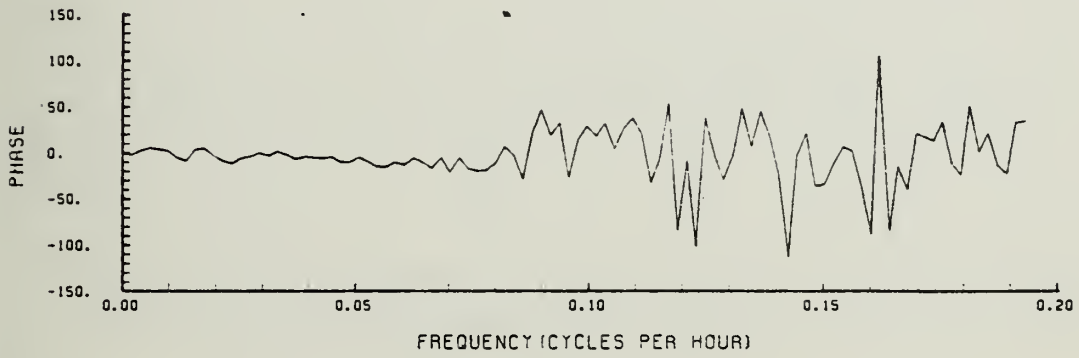
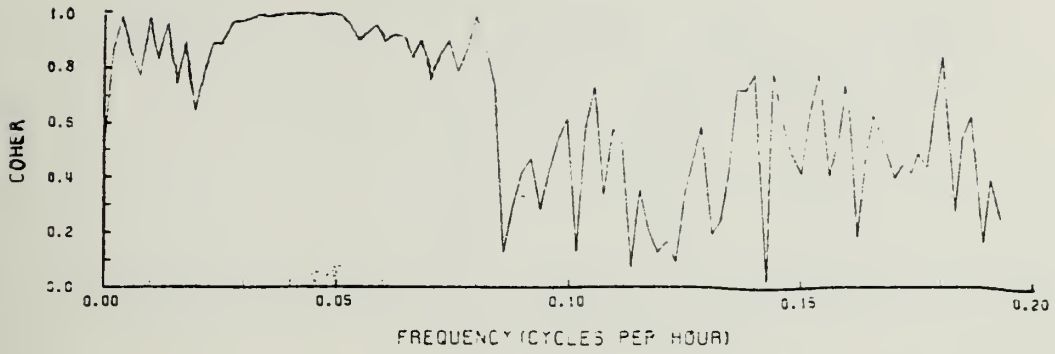


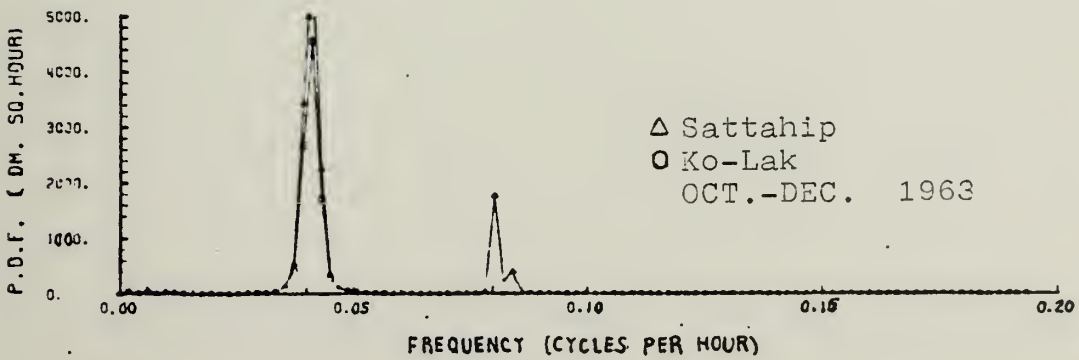
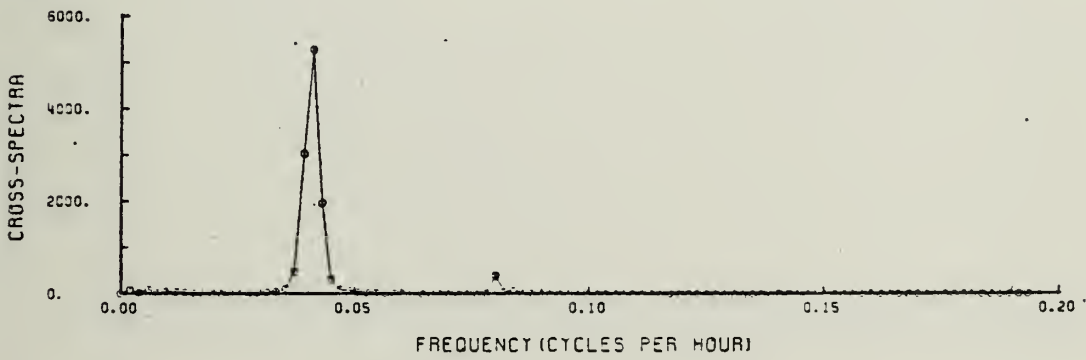
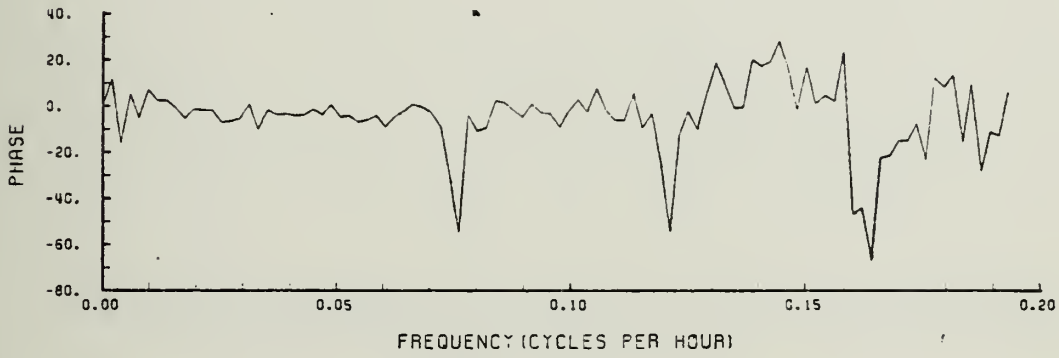
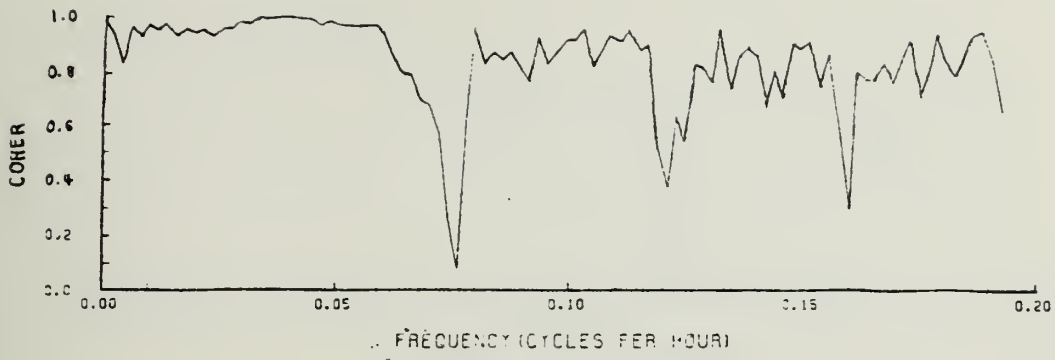


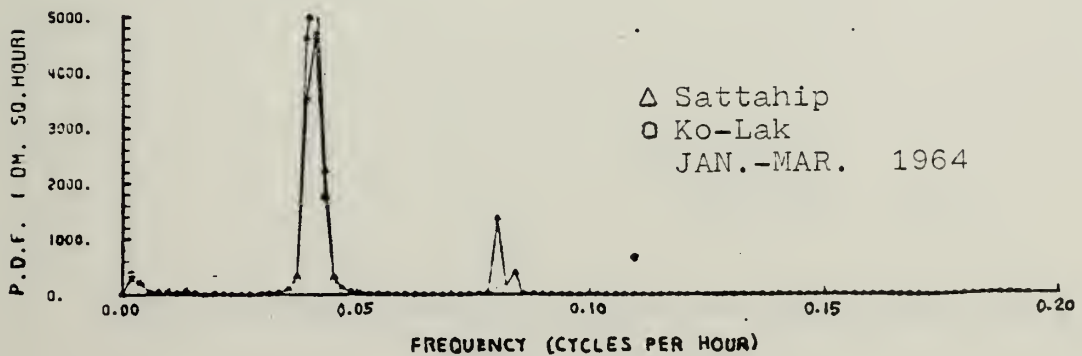
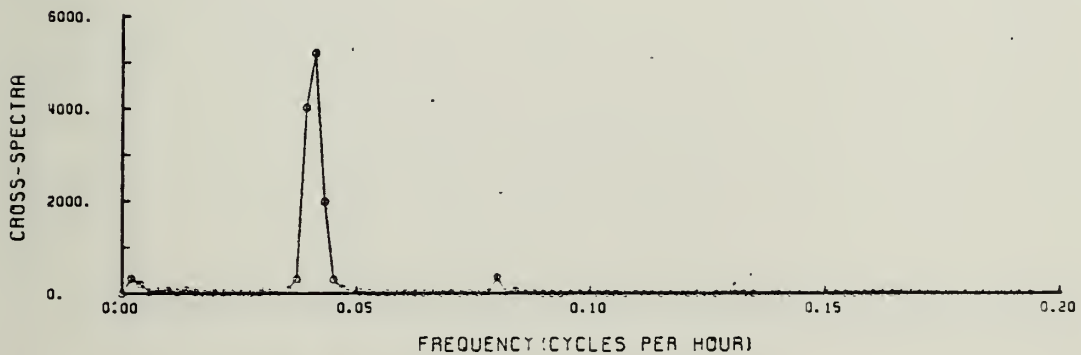
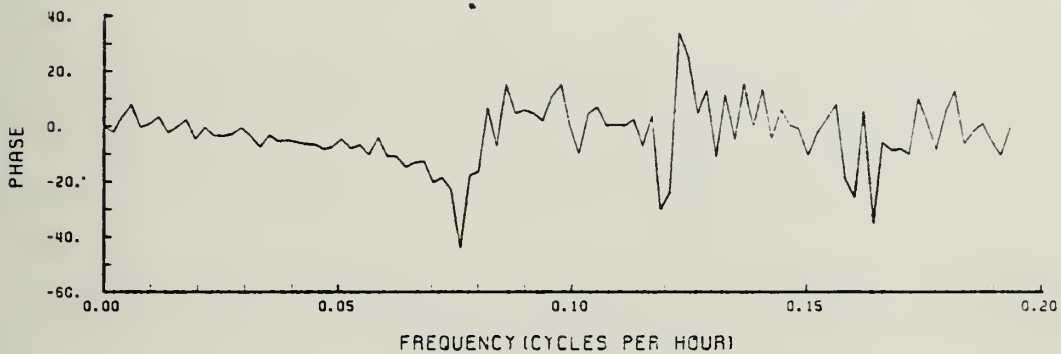
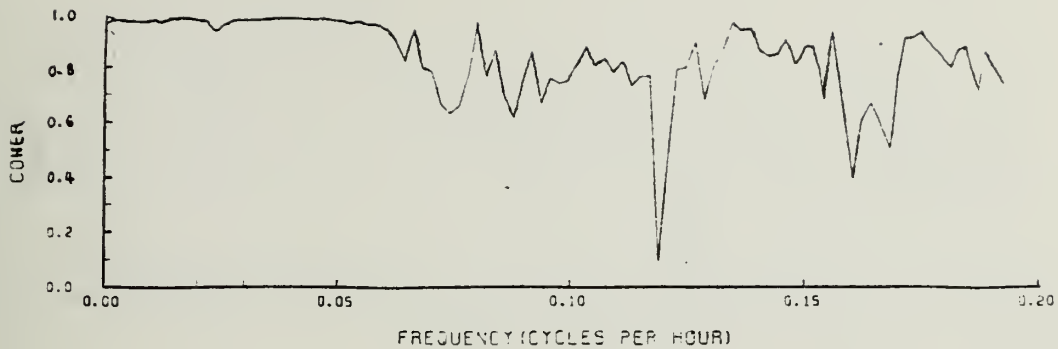


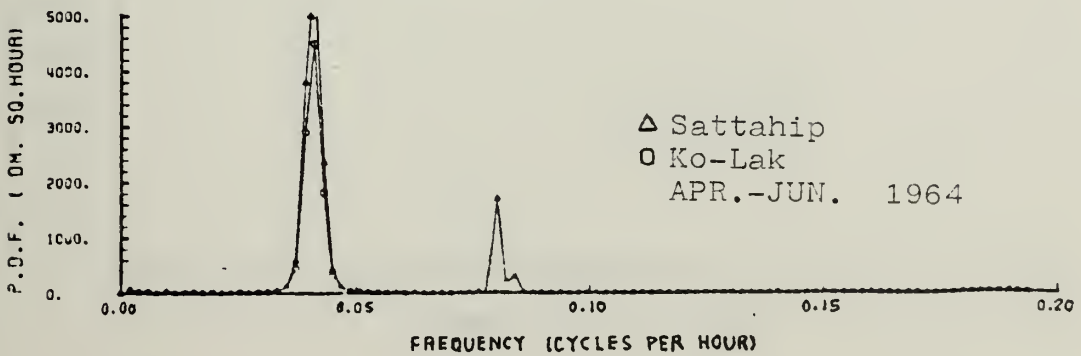
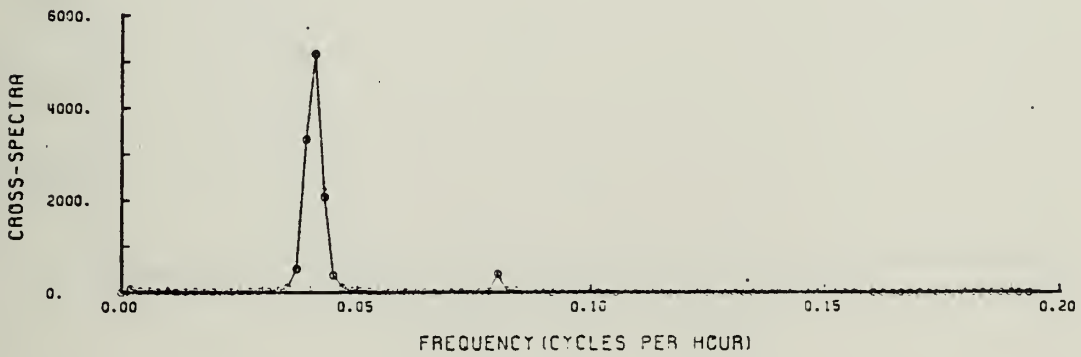
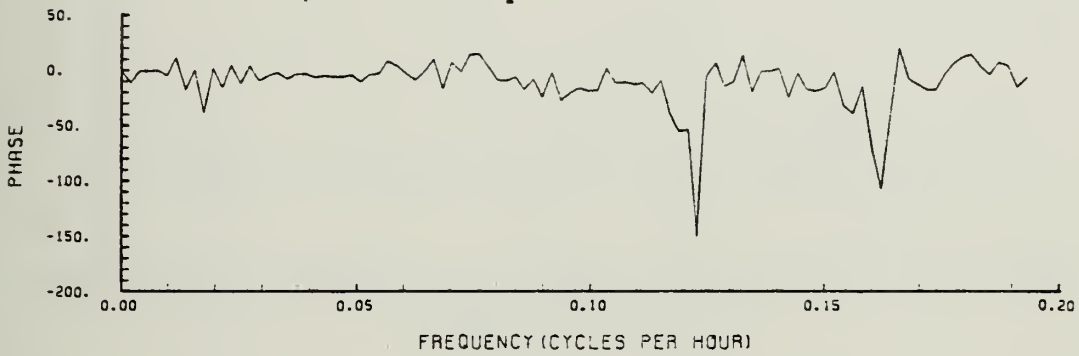
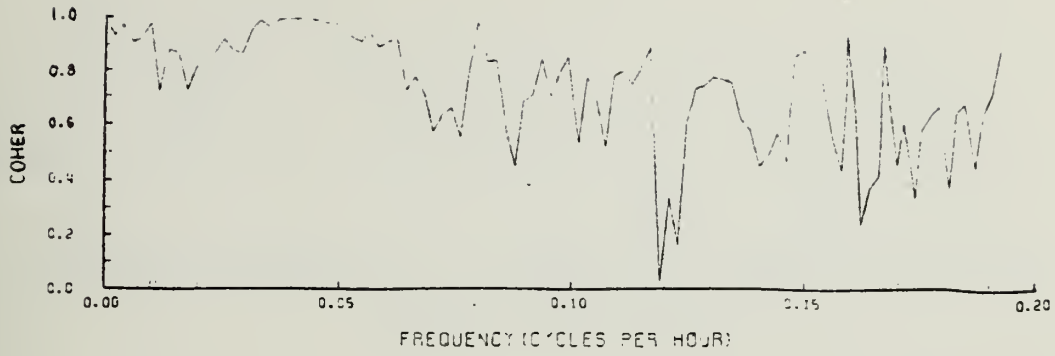


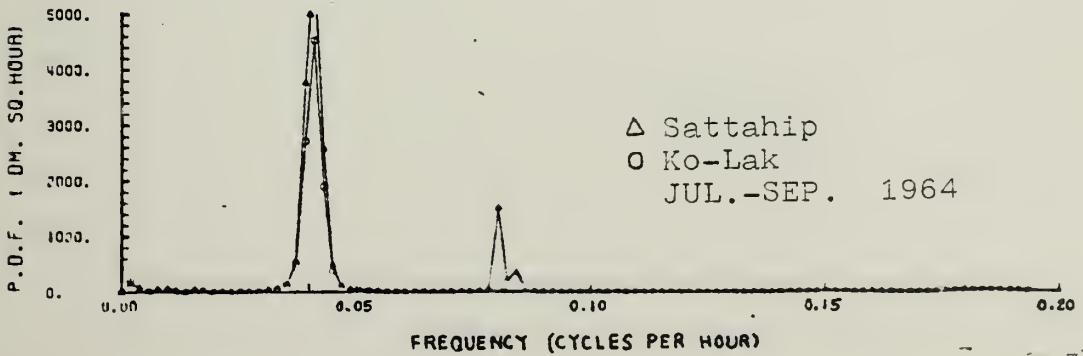
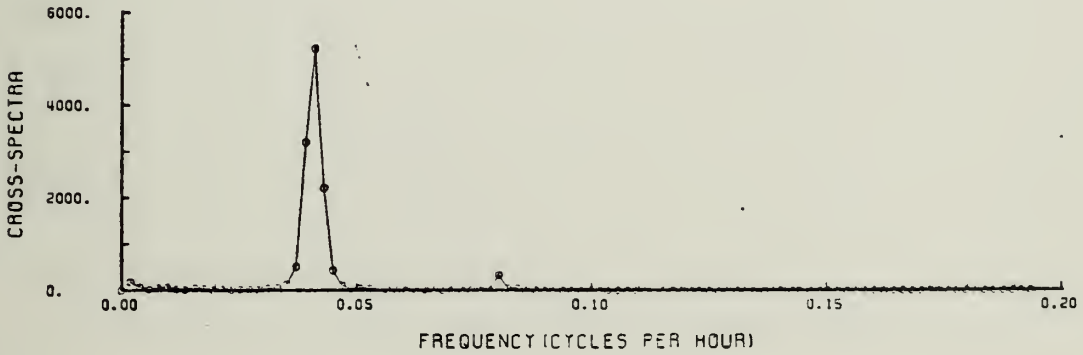
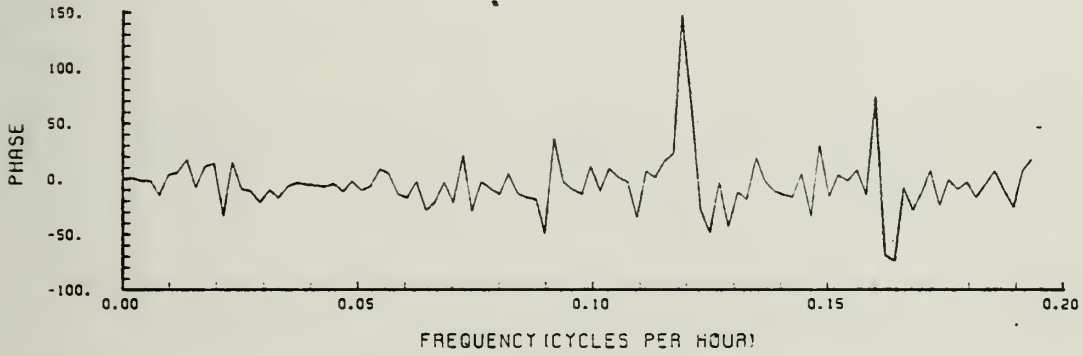
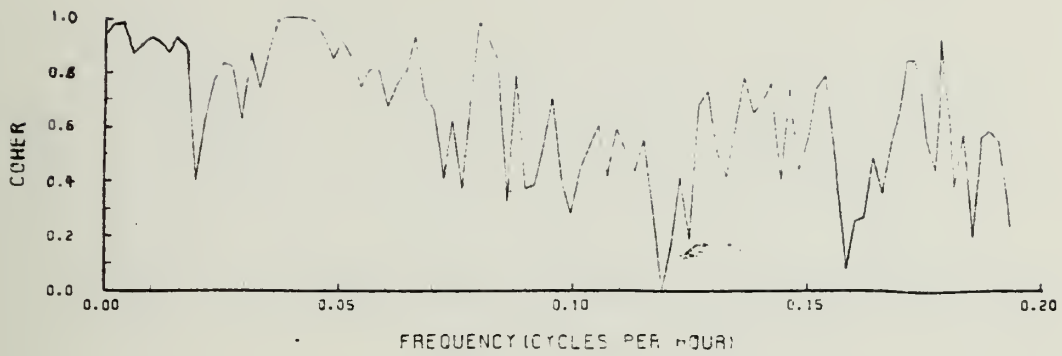


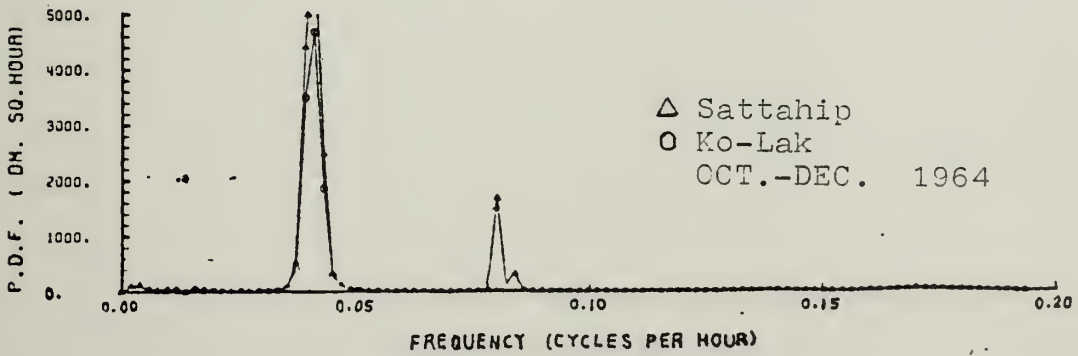
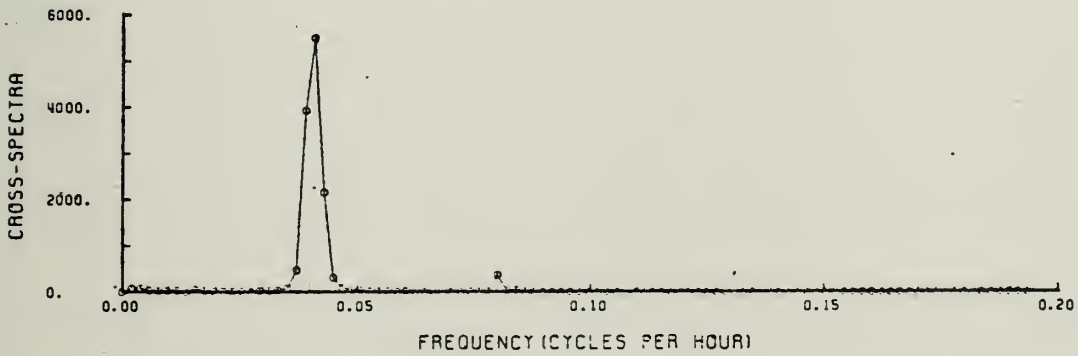
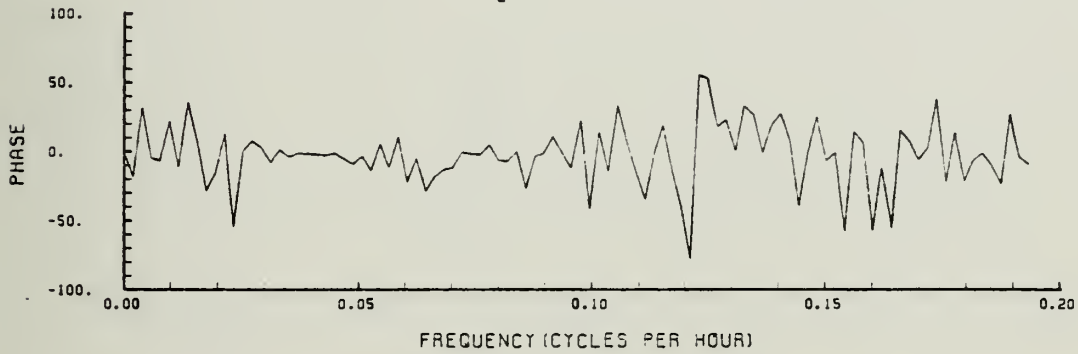
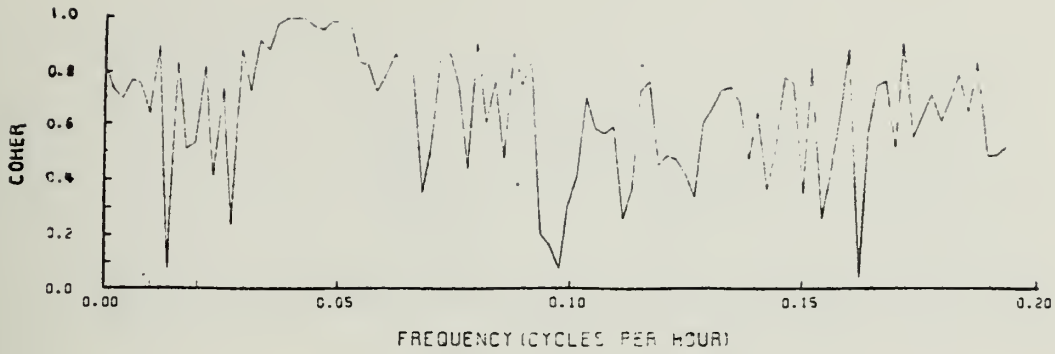


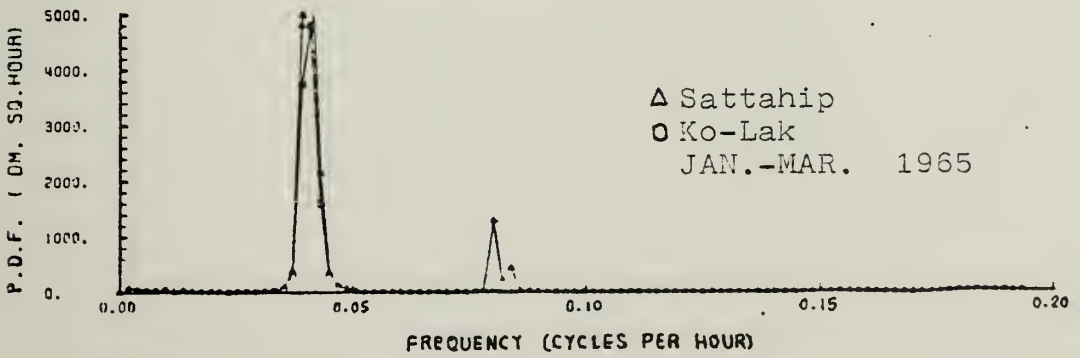
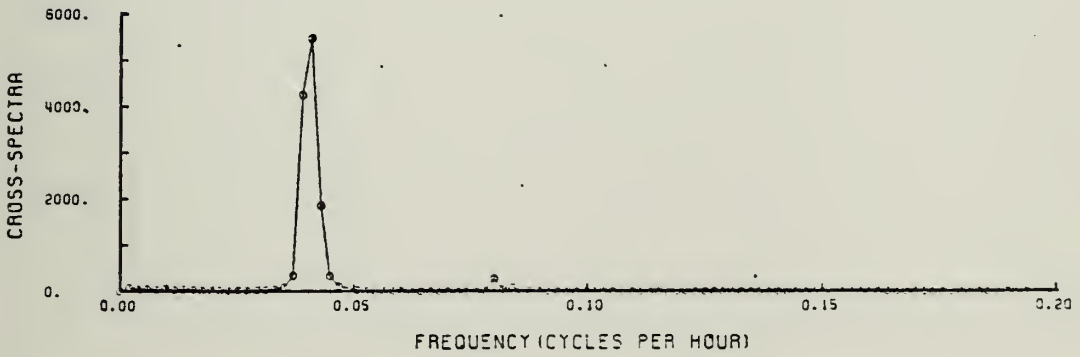
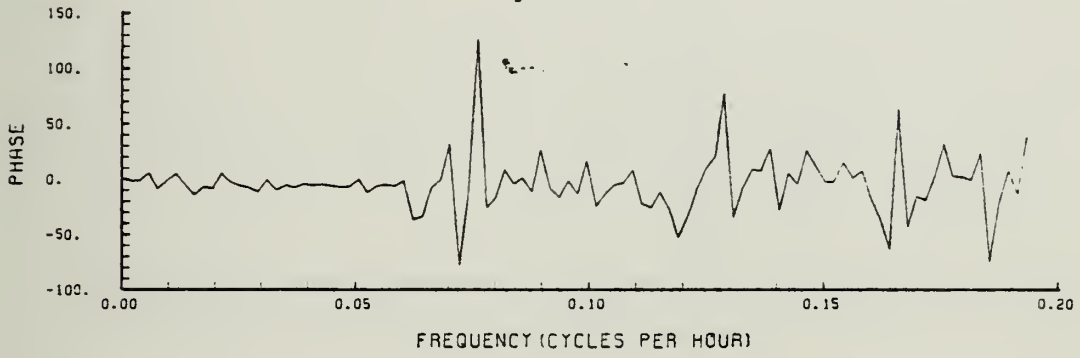
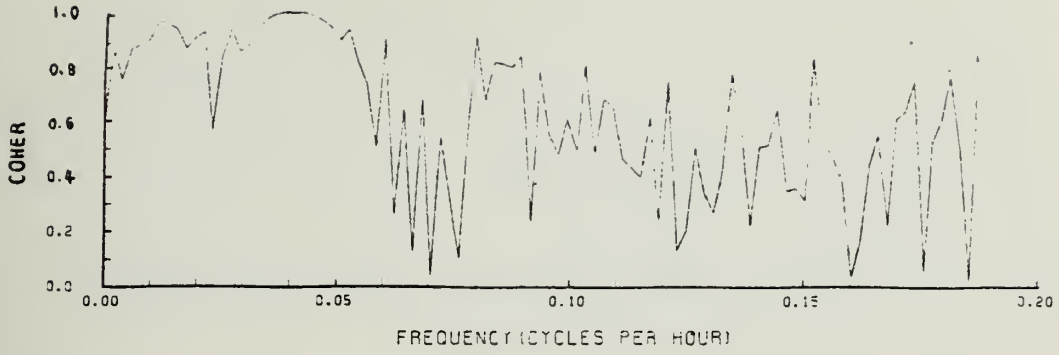


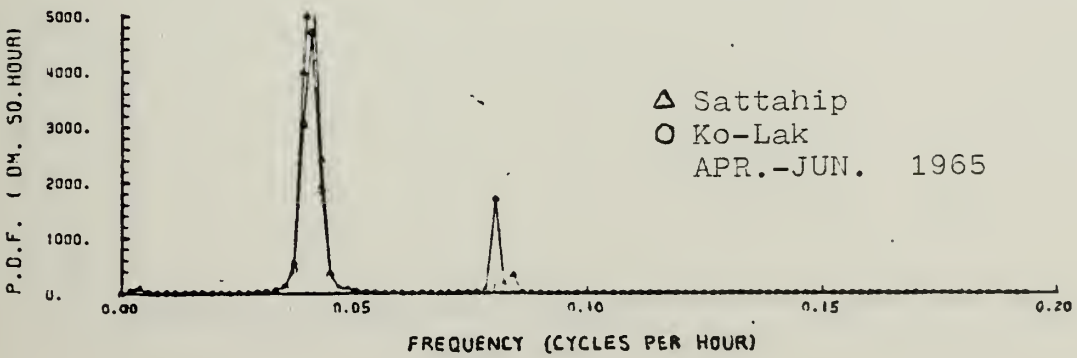
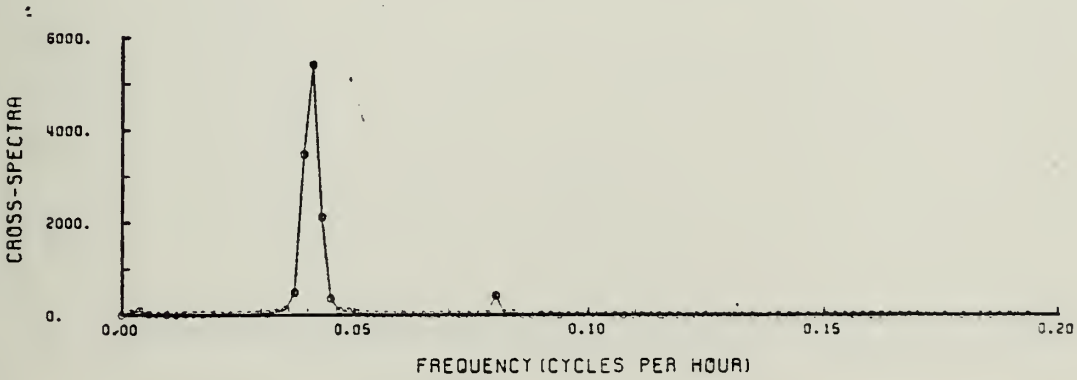
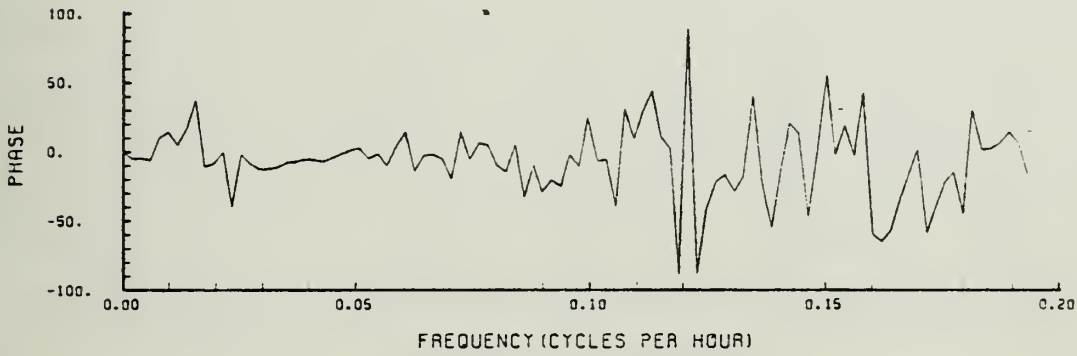
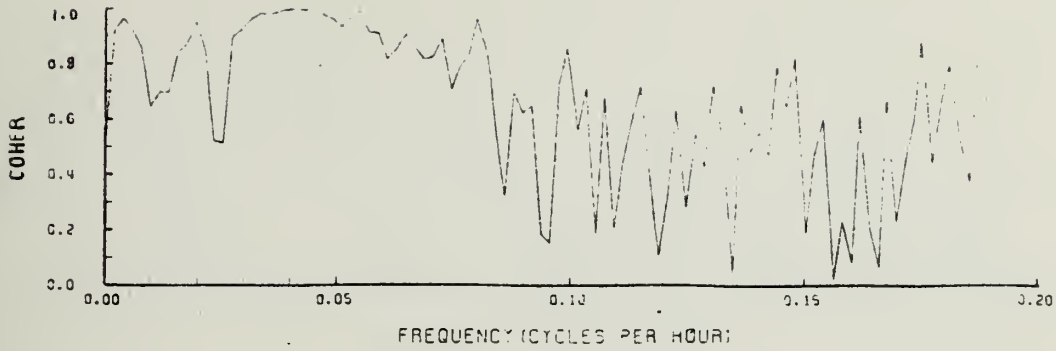


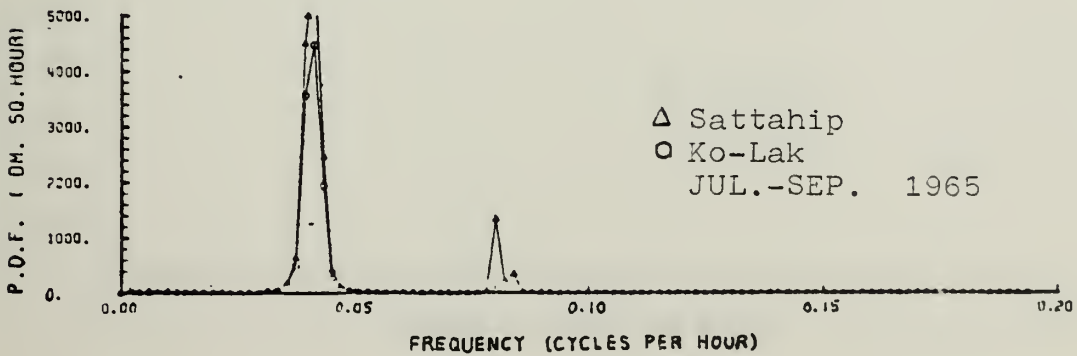
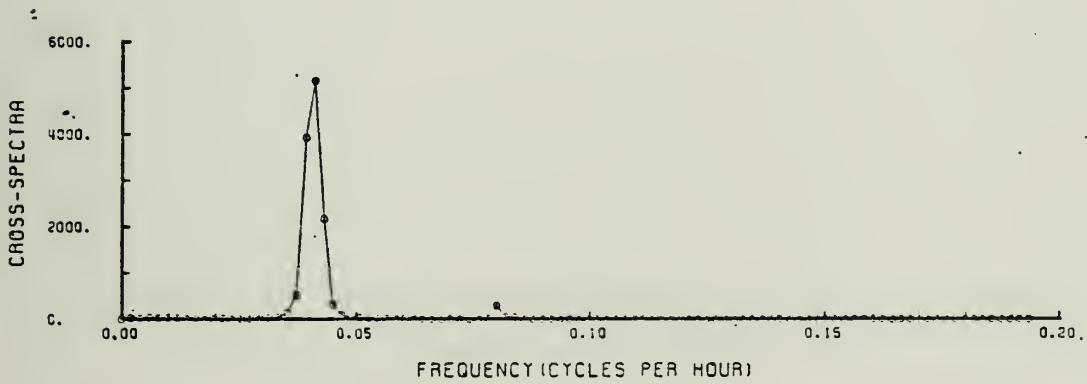
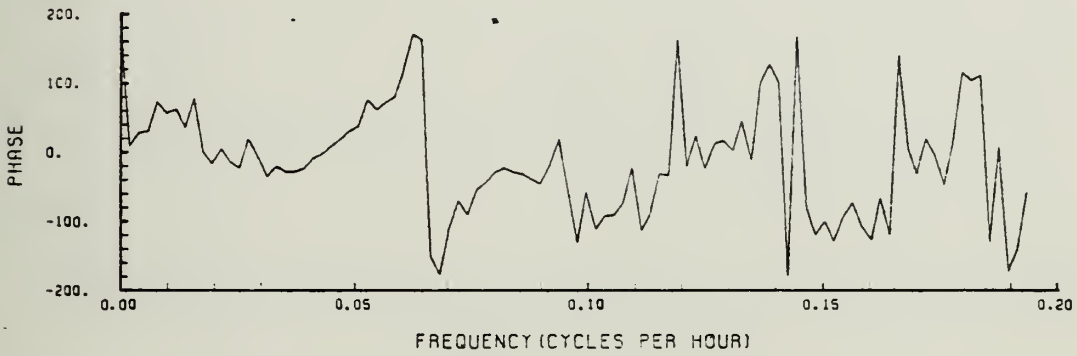
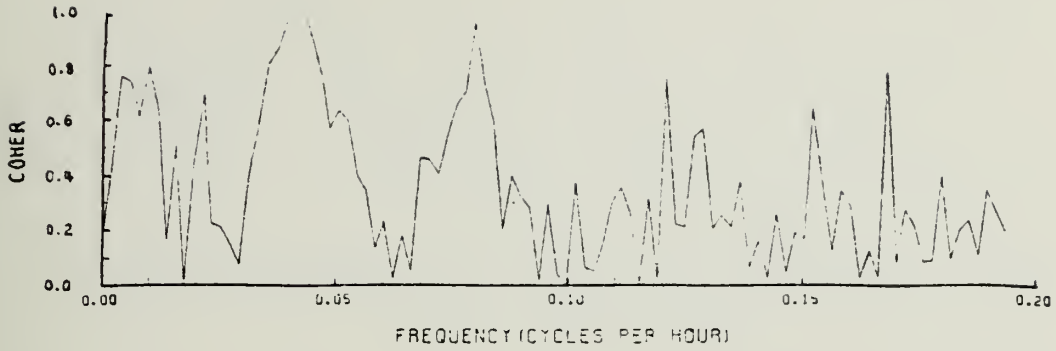


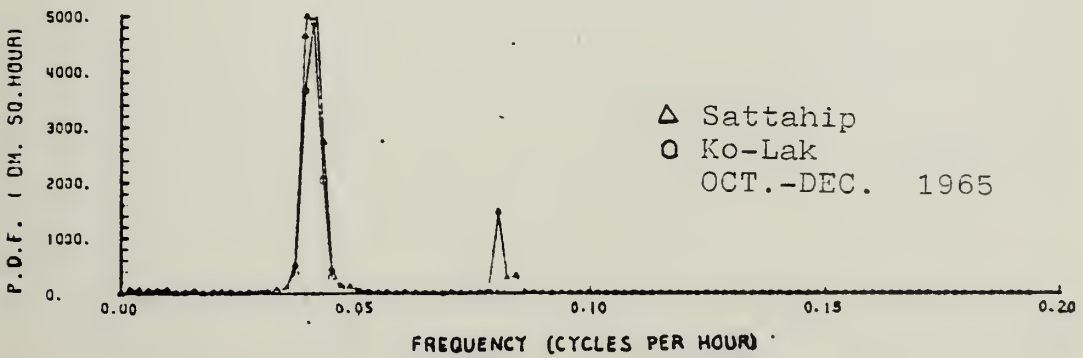
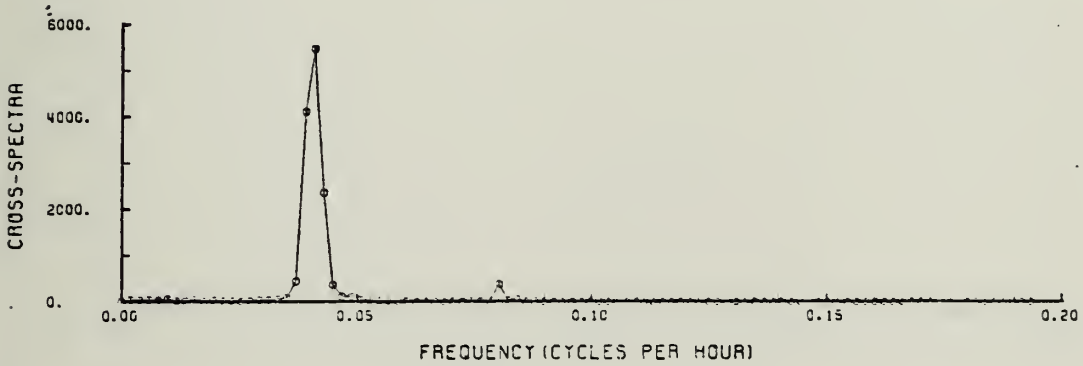
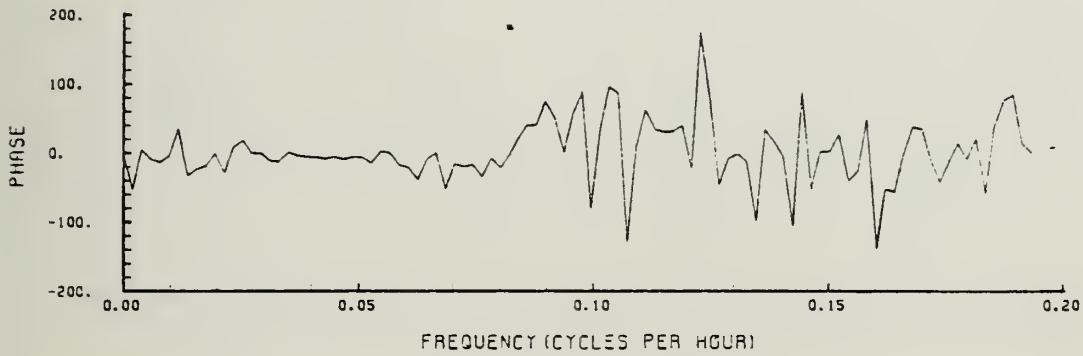
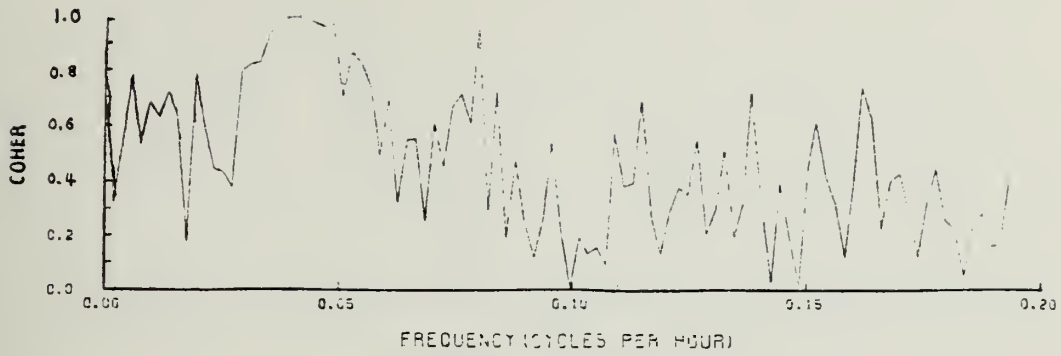


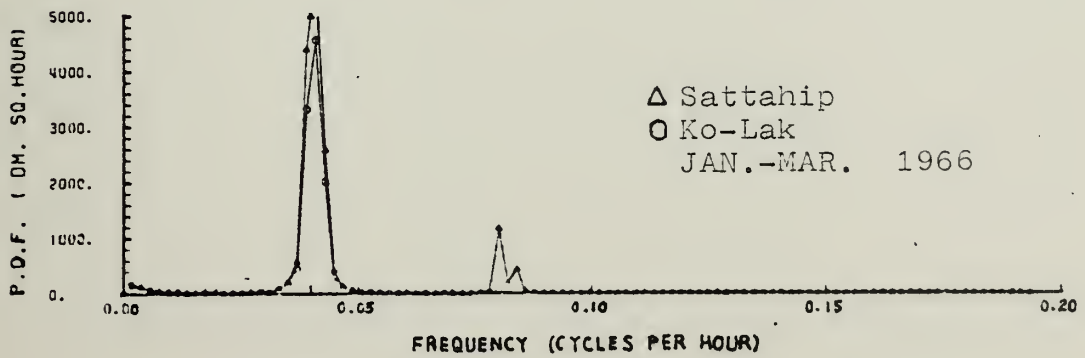
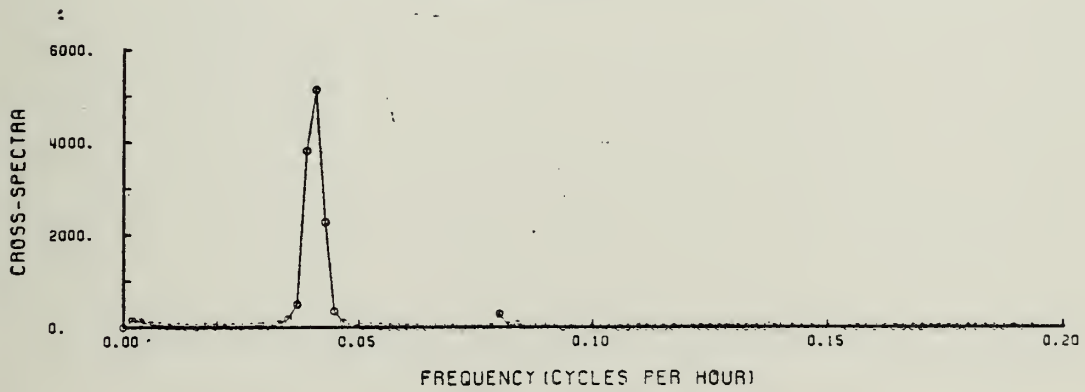
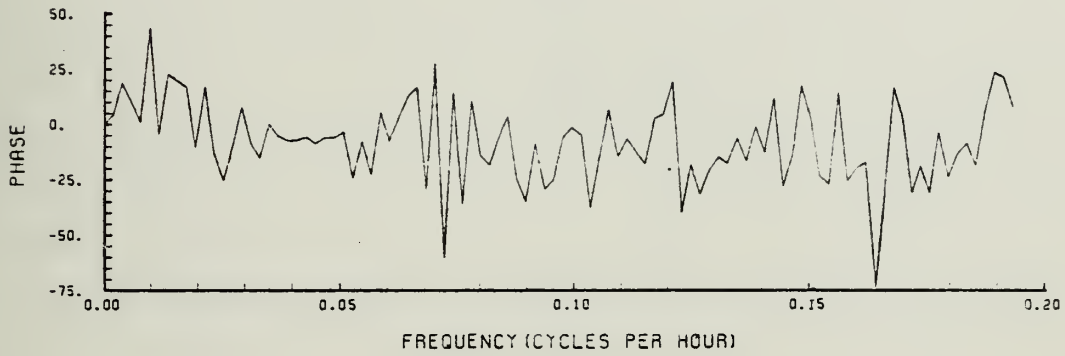
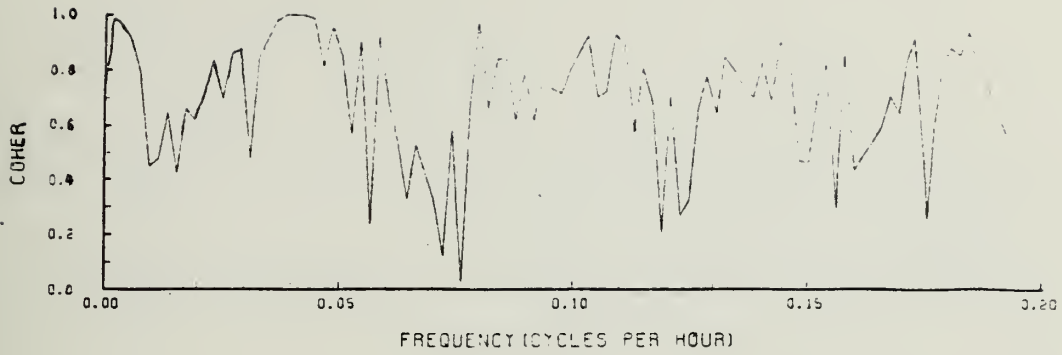


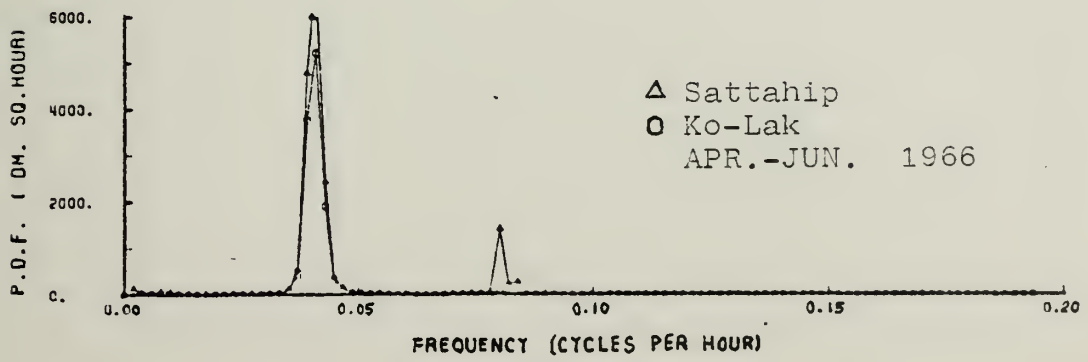
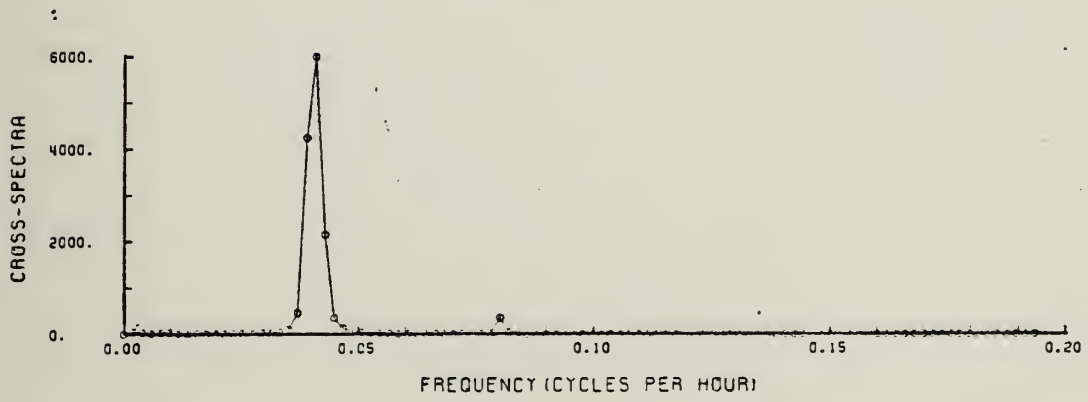
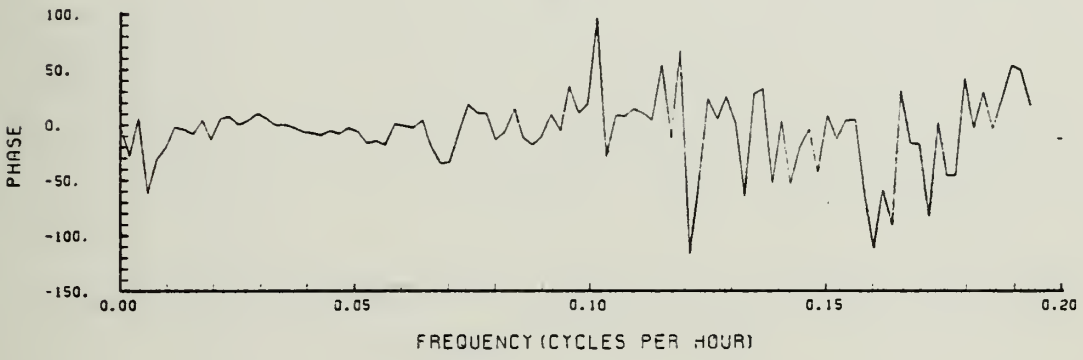
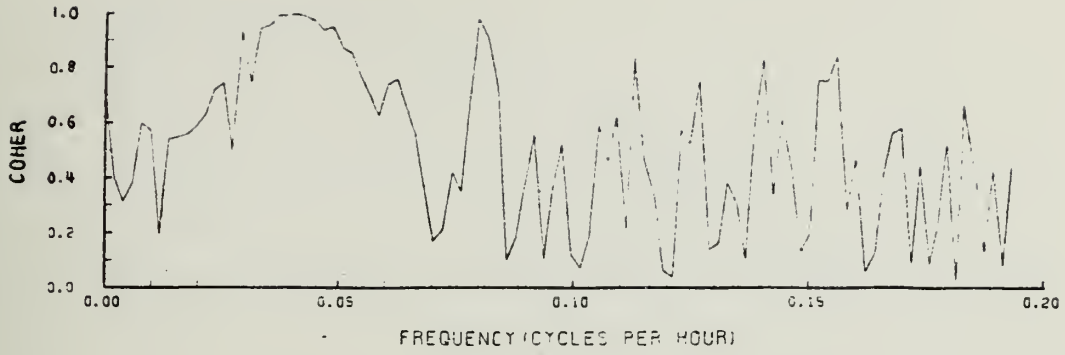


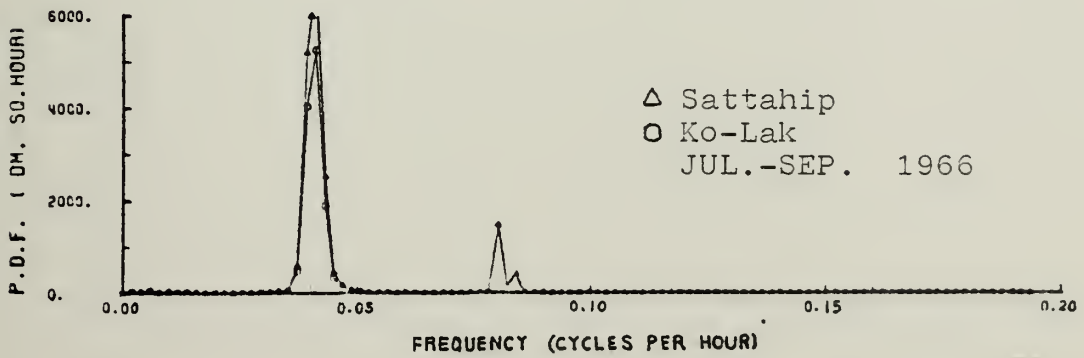
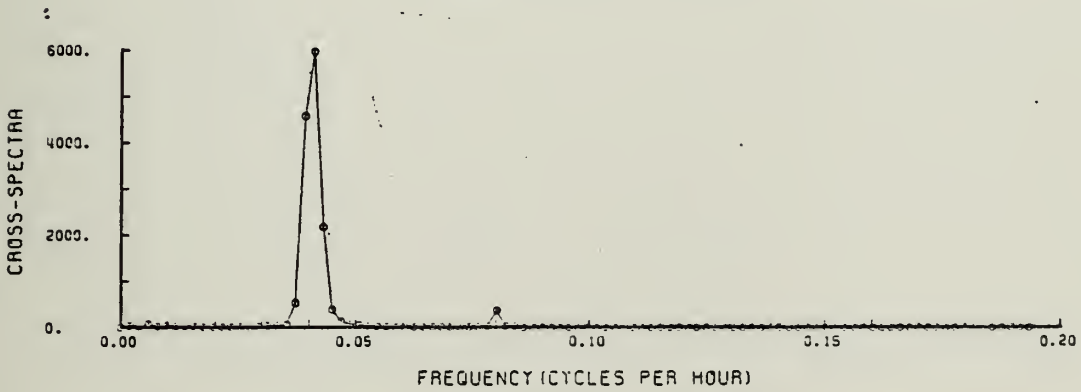
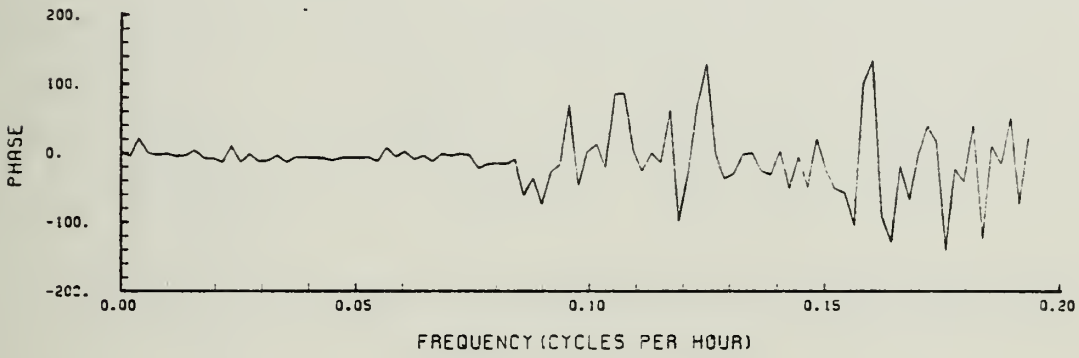
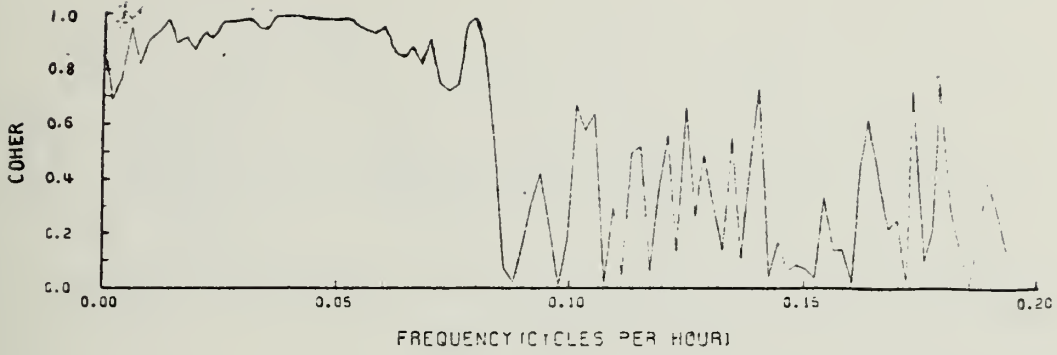


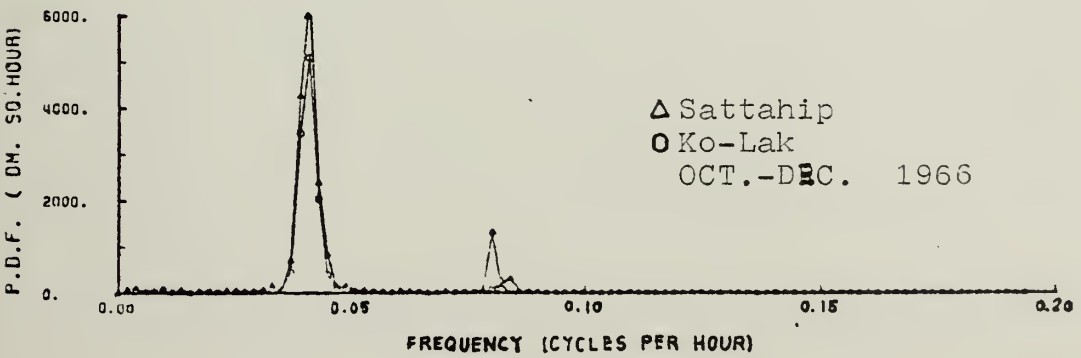
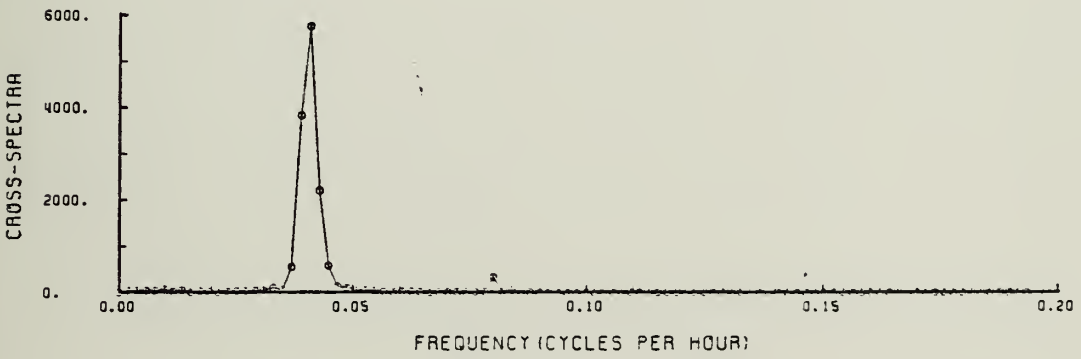
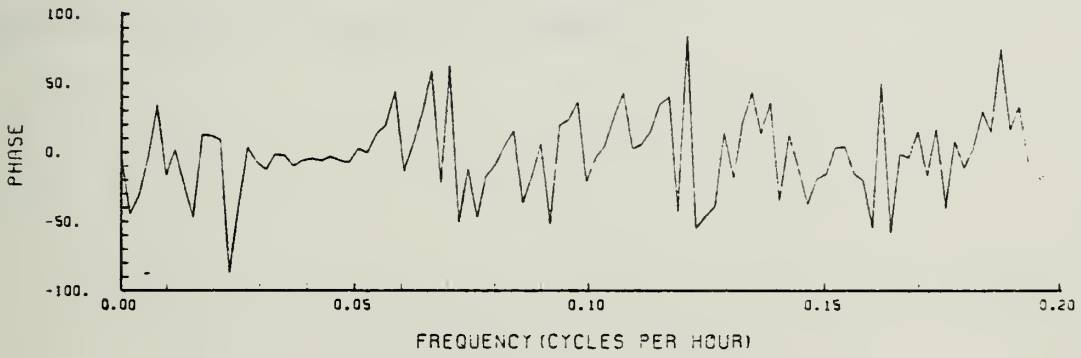
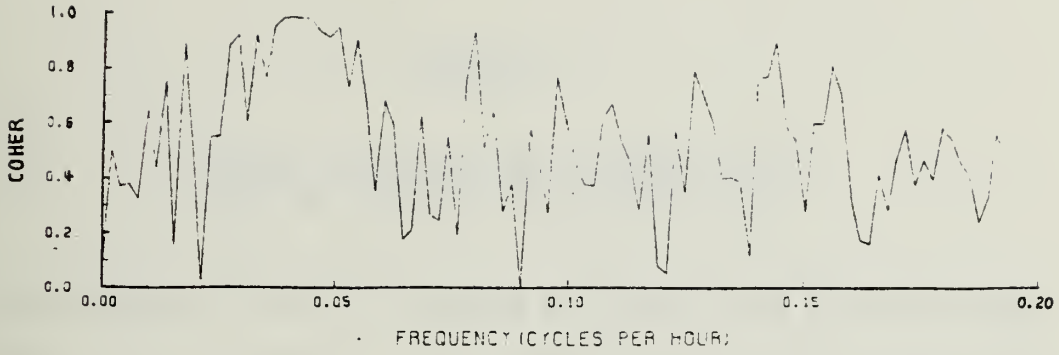








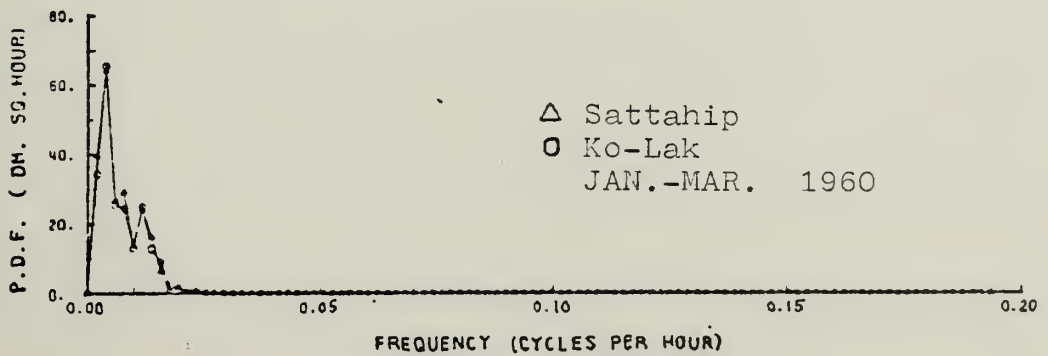
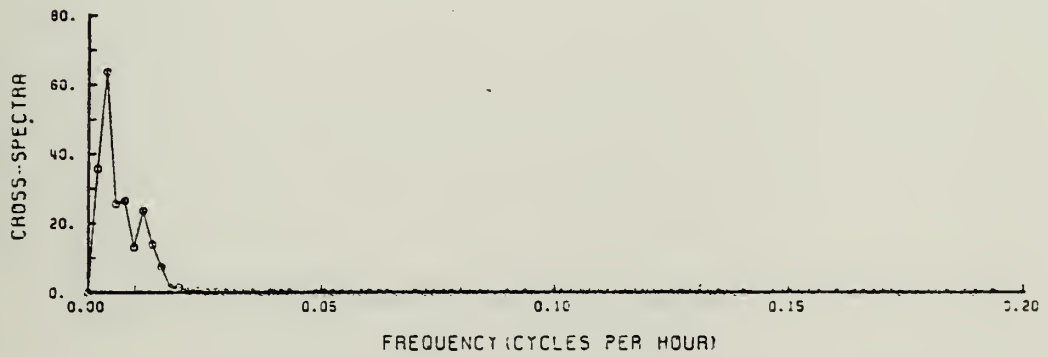
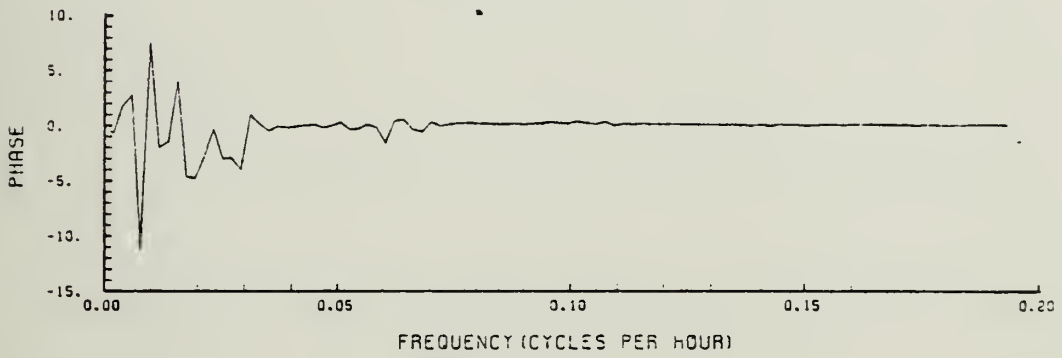
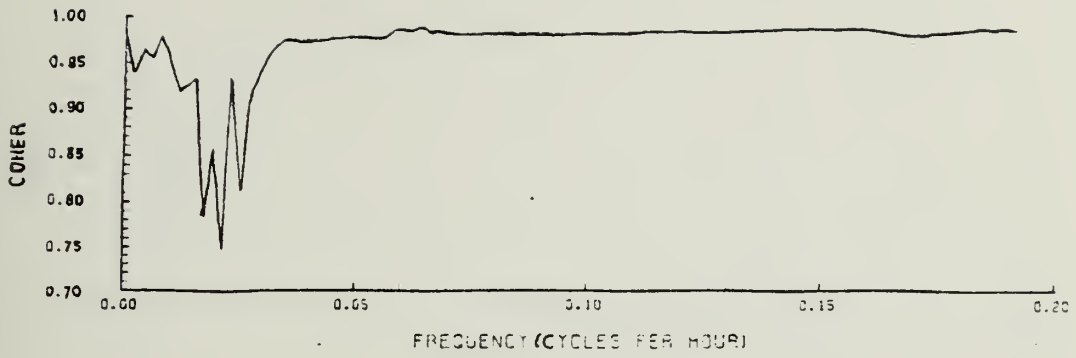


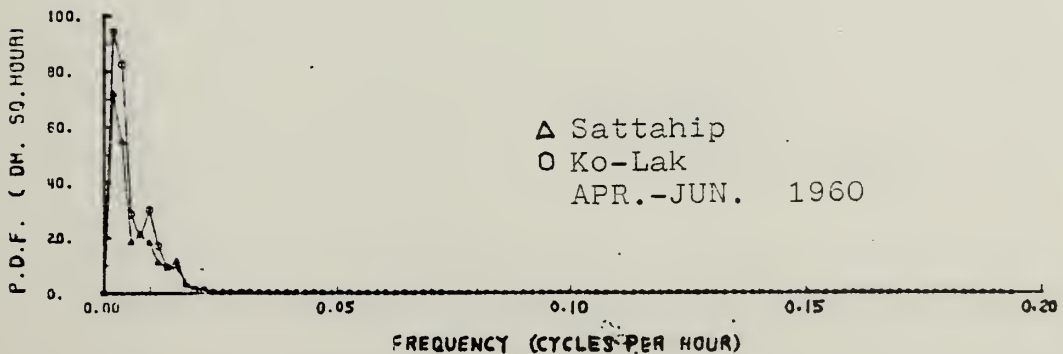
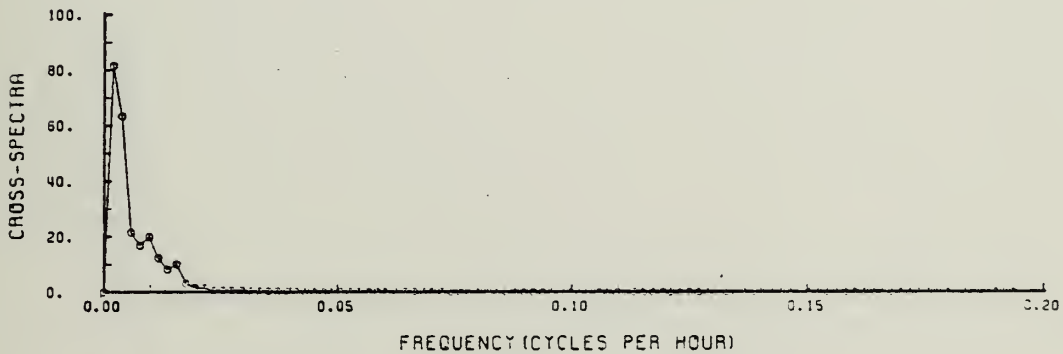
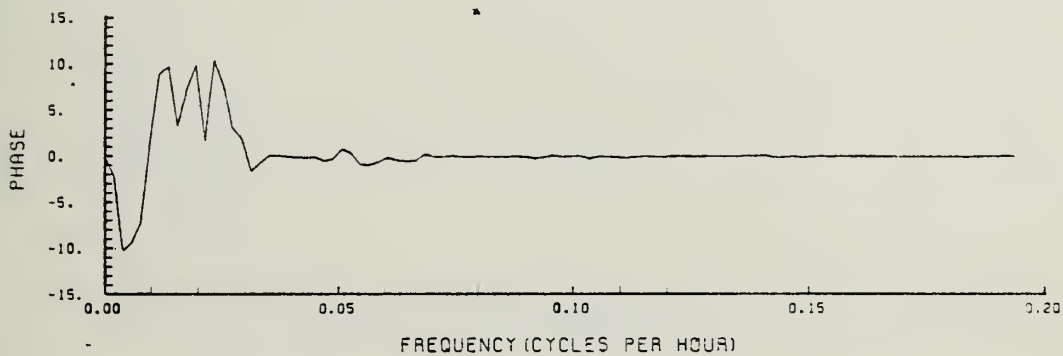
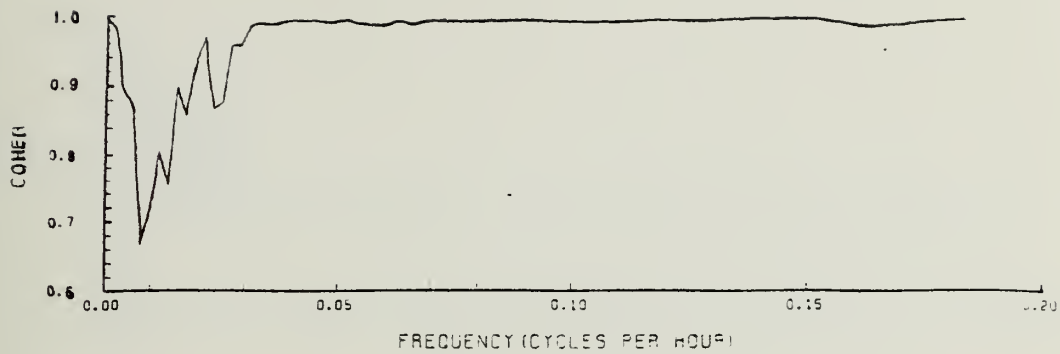


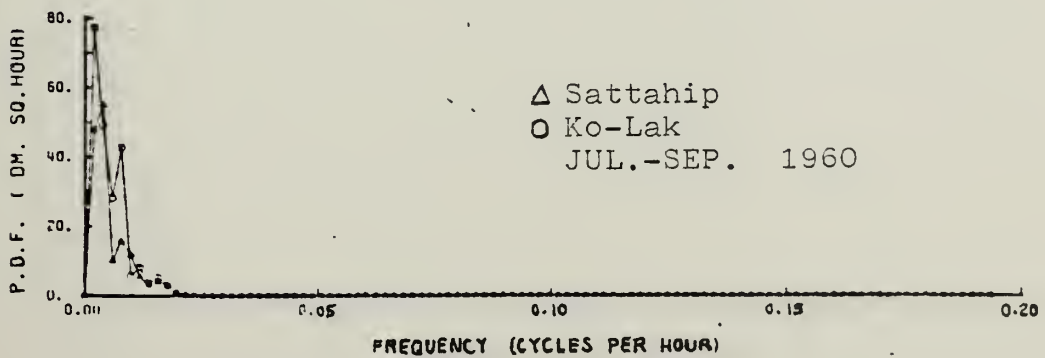
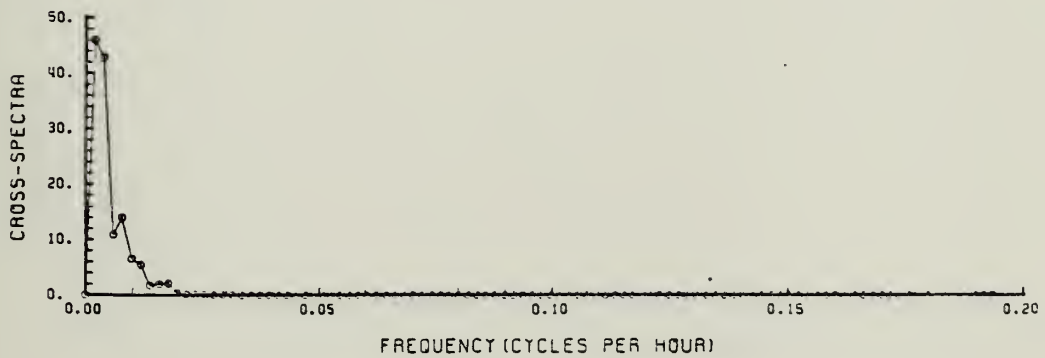
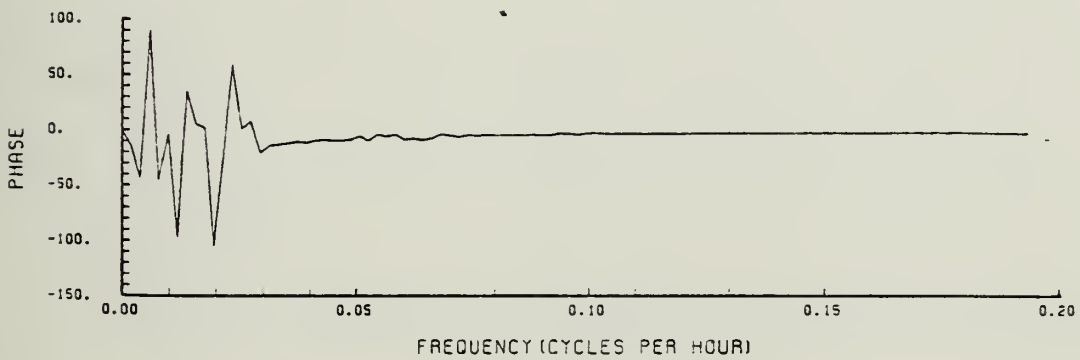
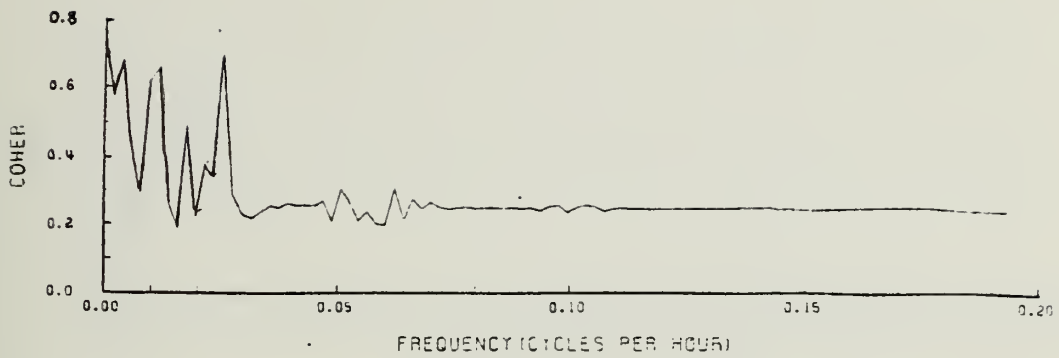
APPENDIX D

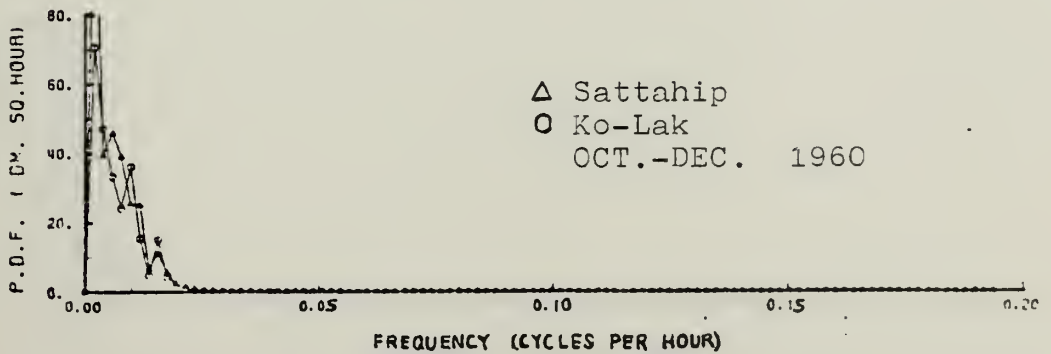
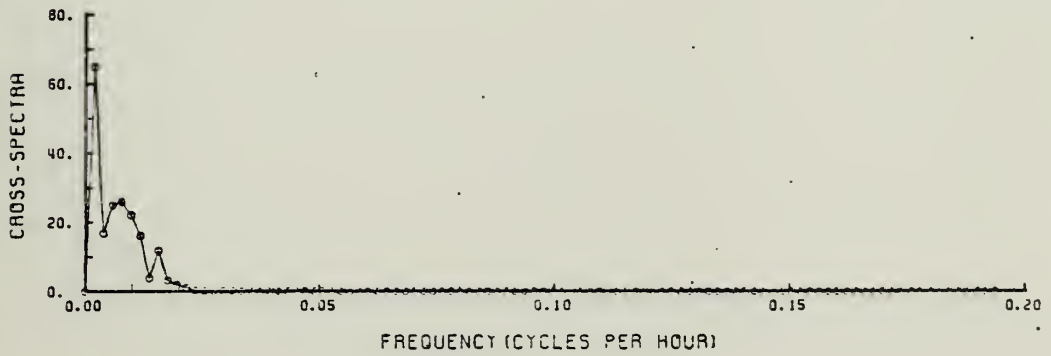
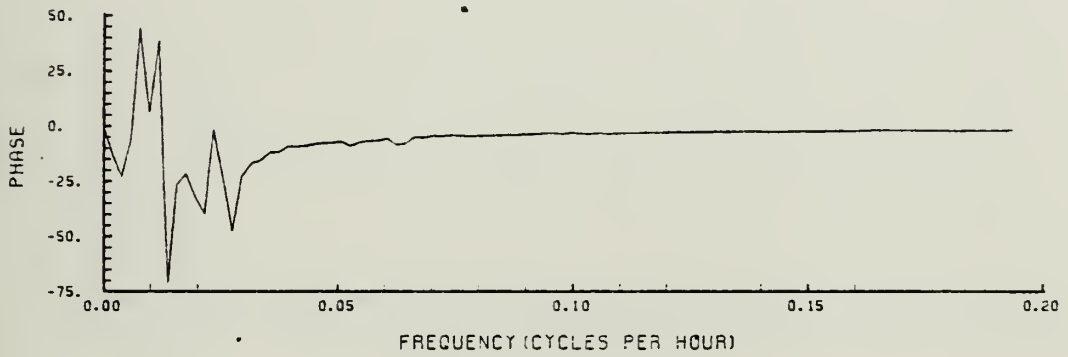
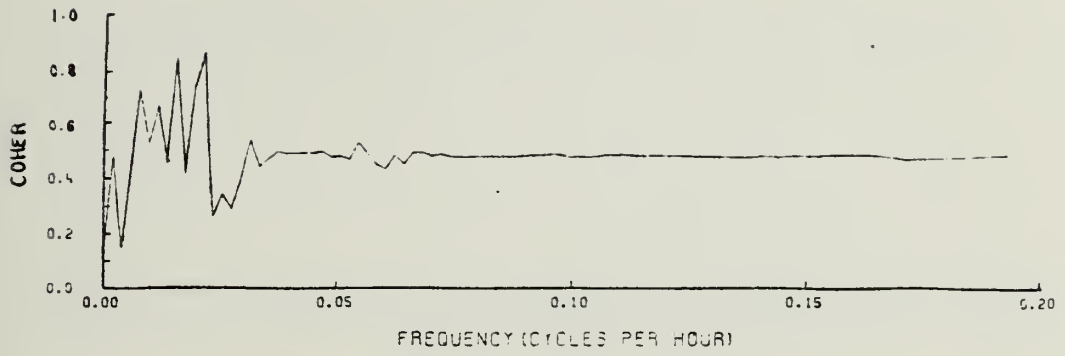
SPECTRA, CROSS-SPECTRA, COHERENCE, AND PHASE OF LOW-PASS FILTERED SEA LEVEL

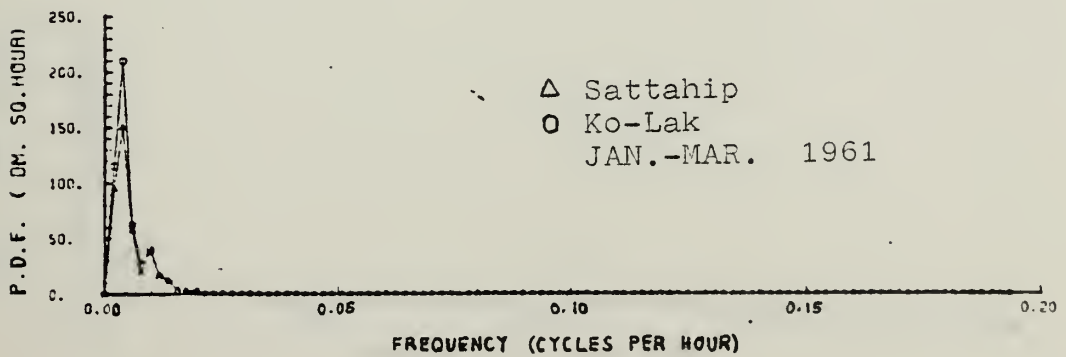
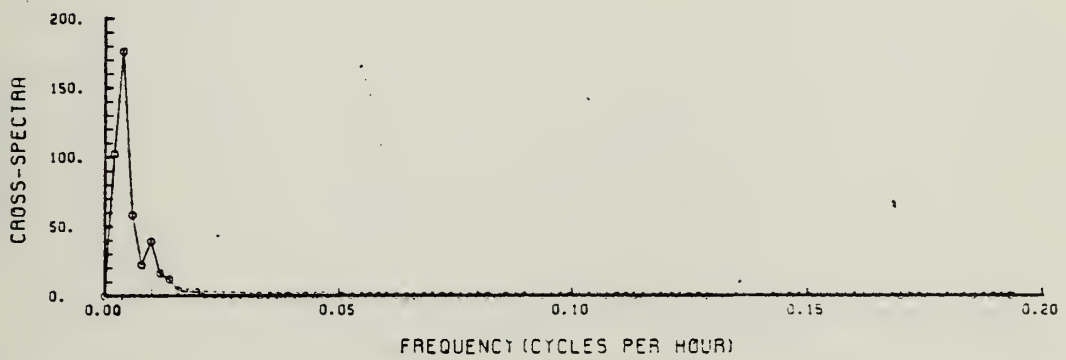
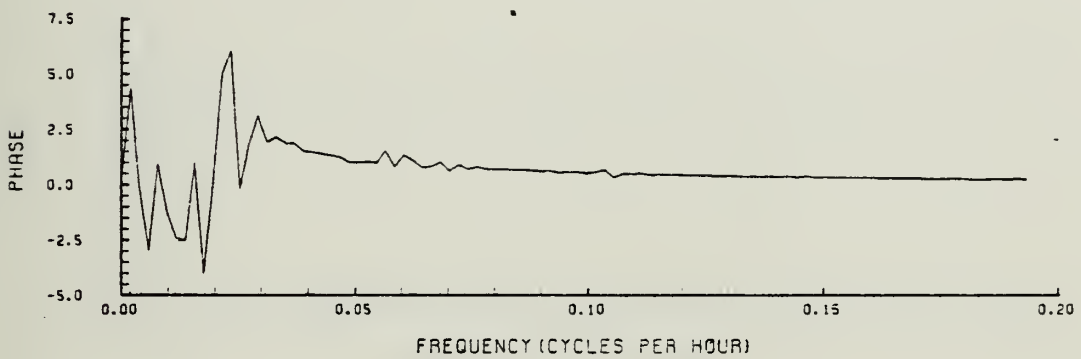
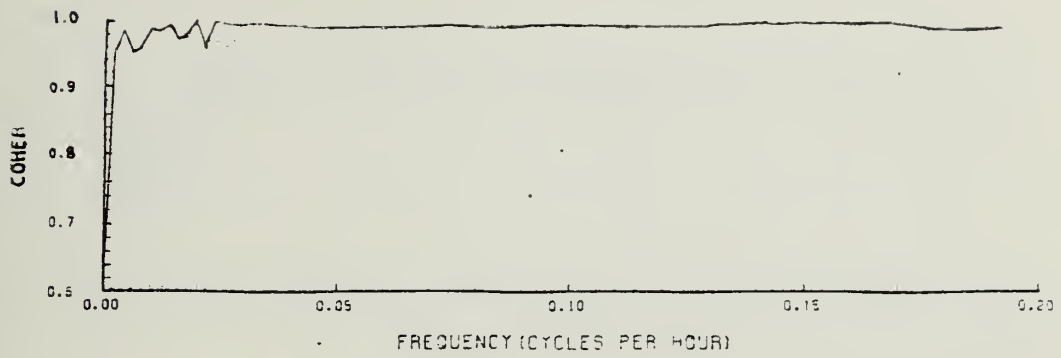
The following graphs for Sattahip and Ko-Lak show (from the top):
(1) phase, (2) coherence, (3) cross-spectra, and (4) spectra for
three-month periods (8 degrees of freedom).

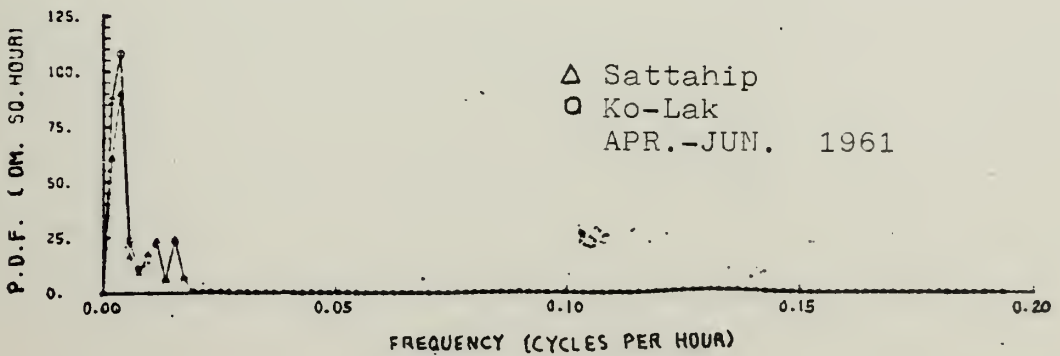
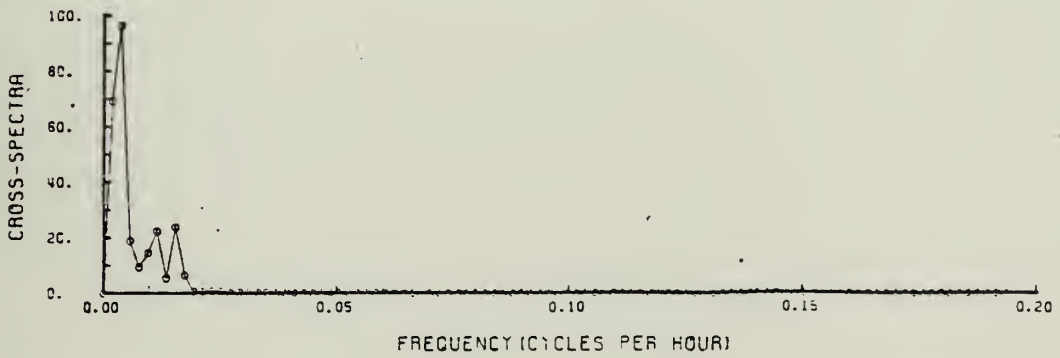
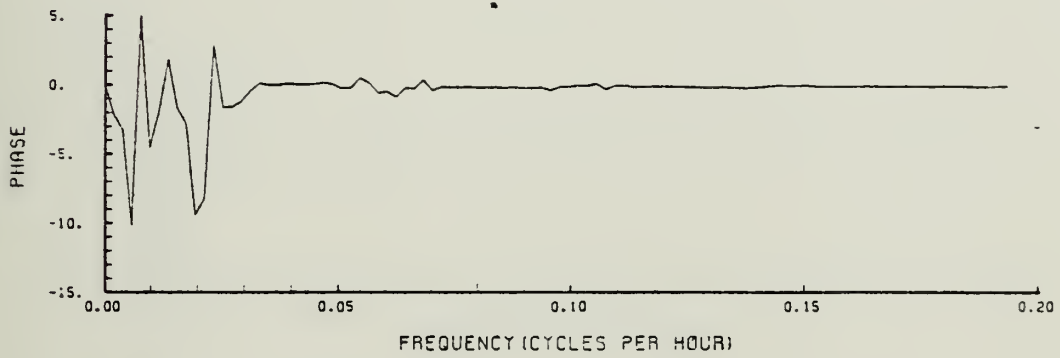
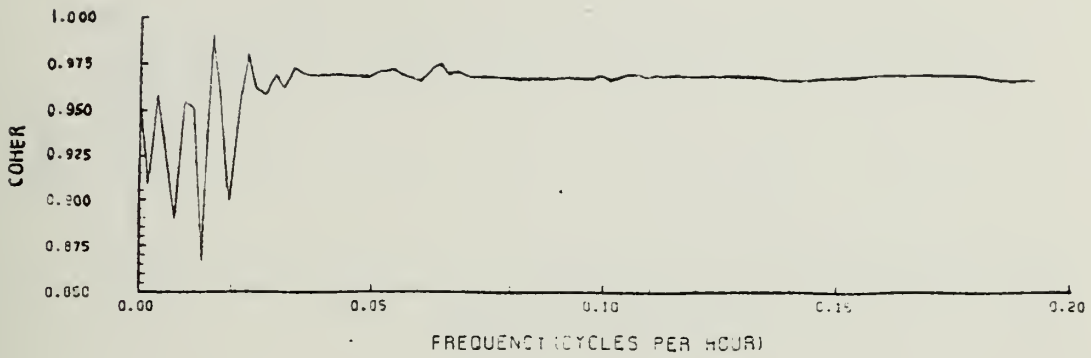


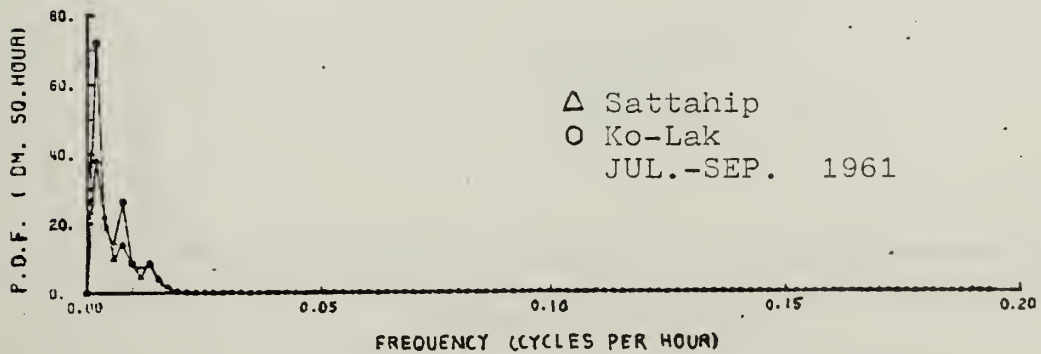
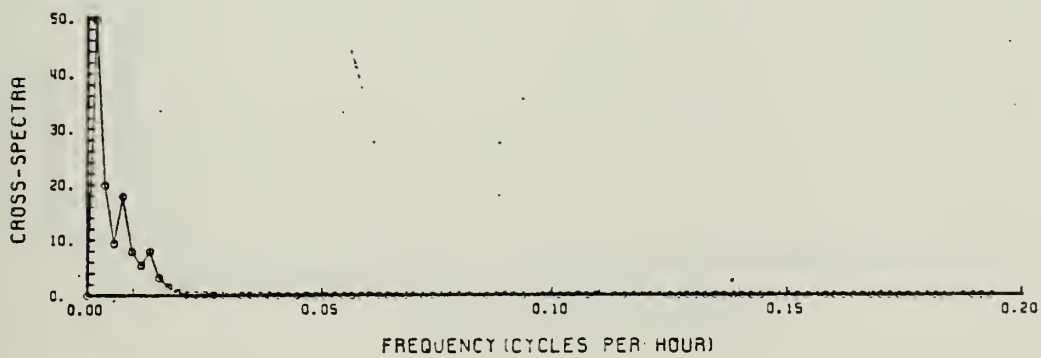
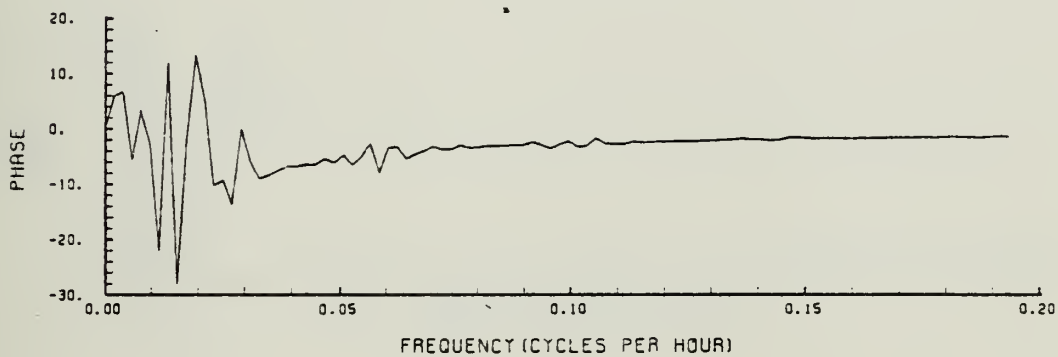
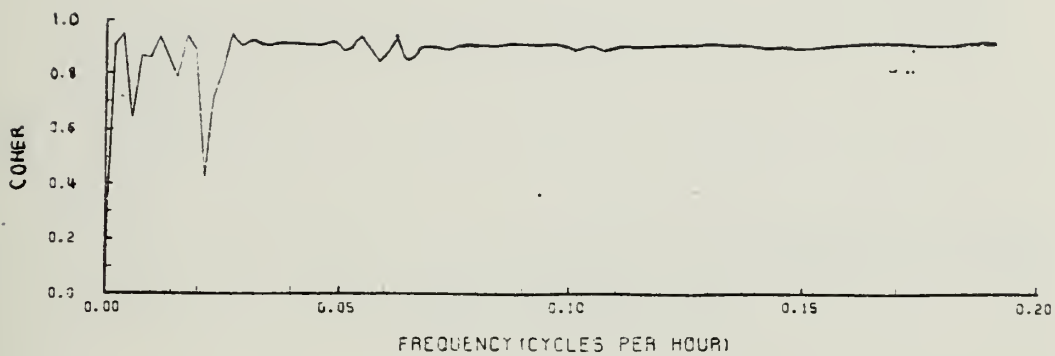


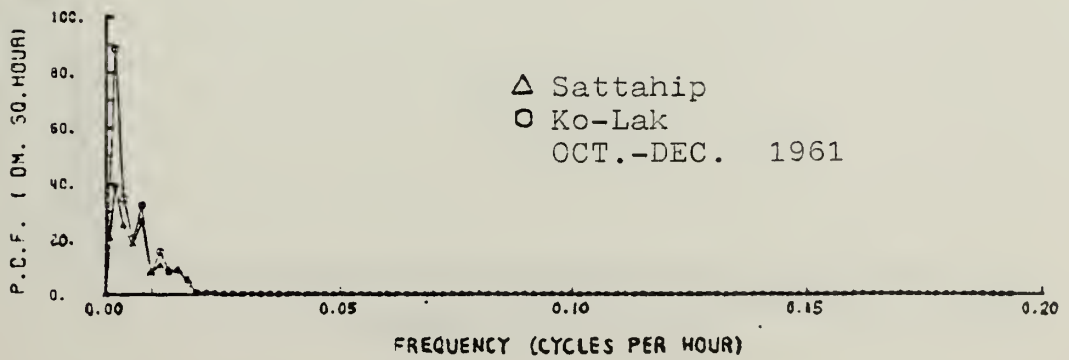
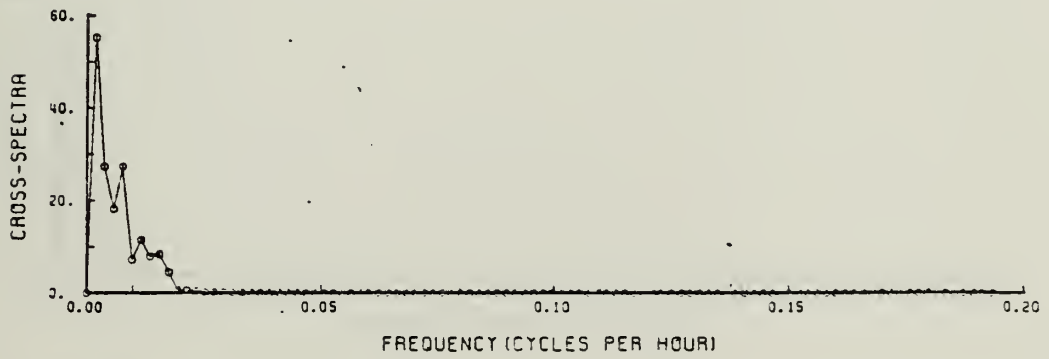
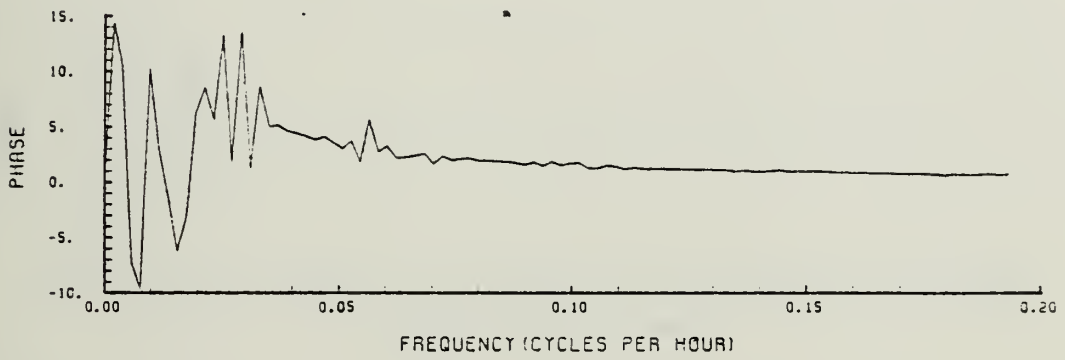
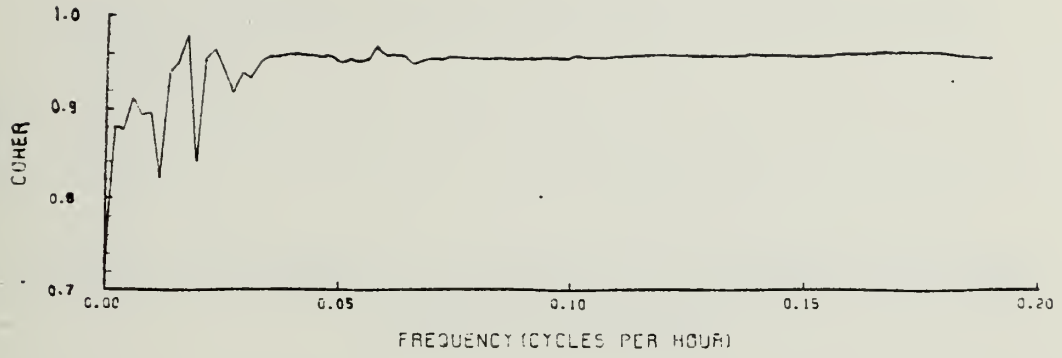


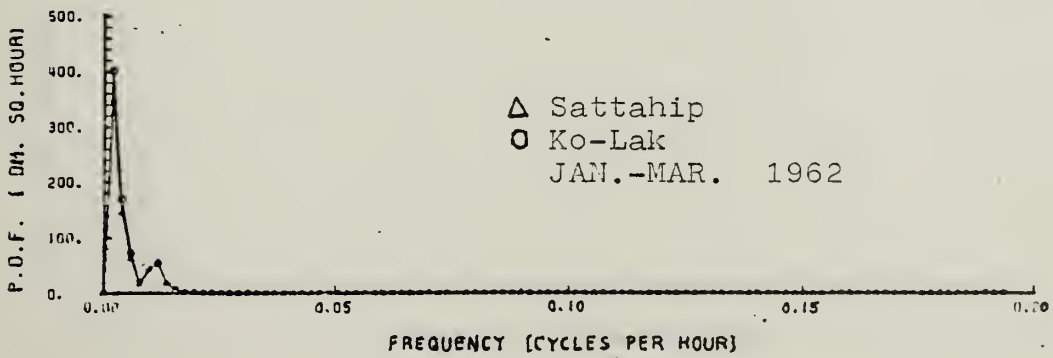
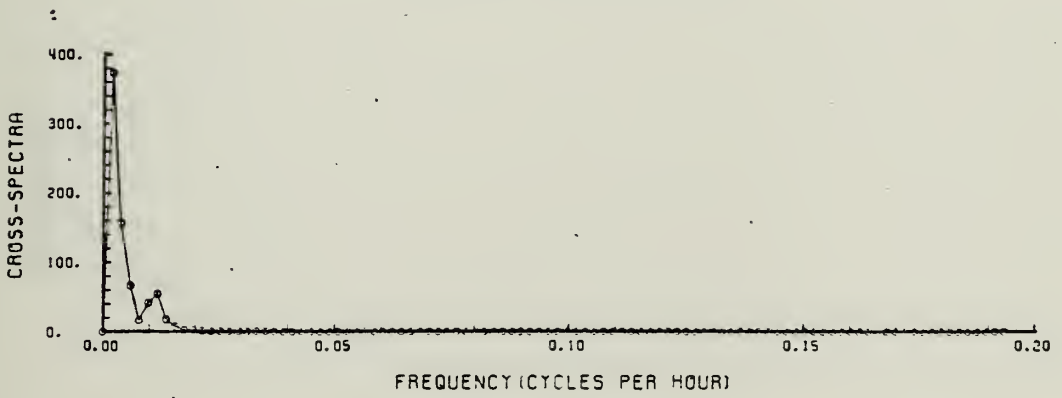
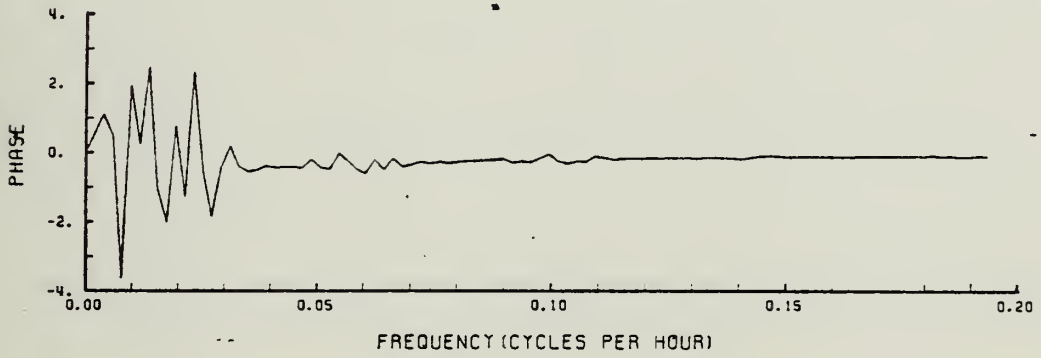
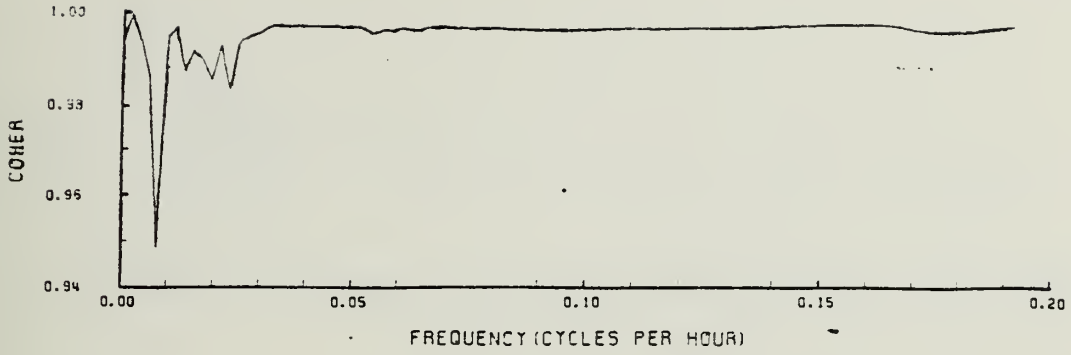


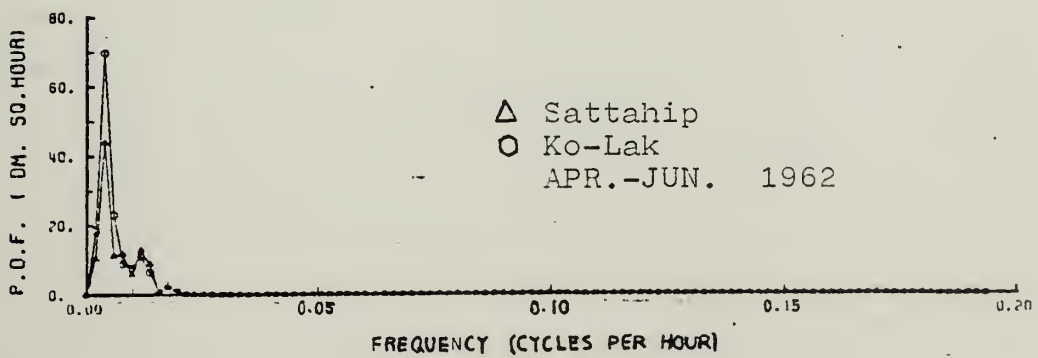
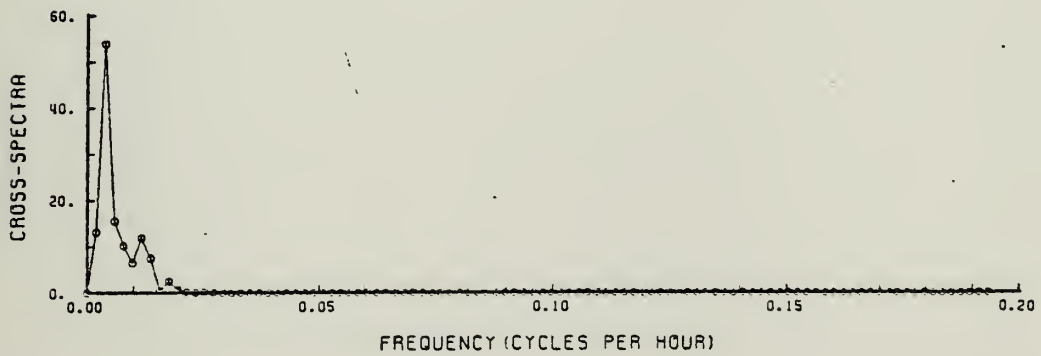
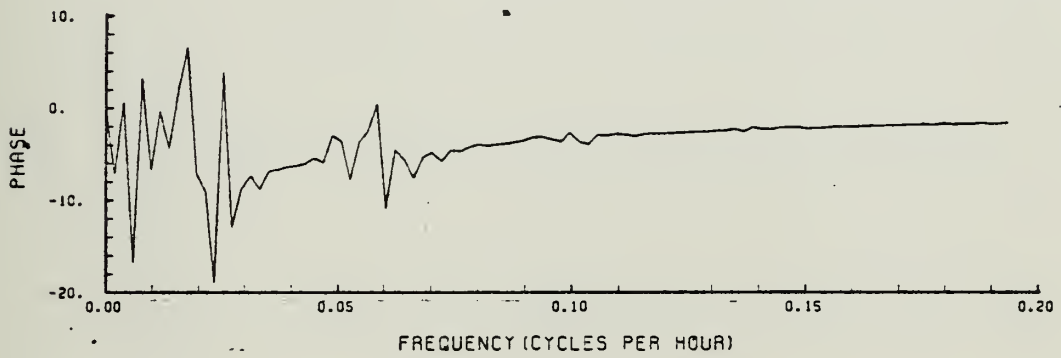
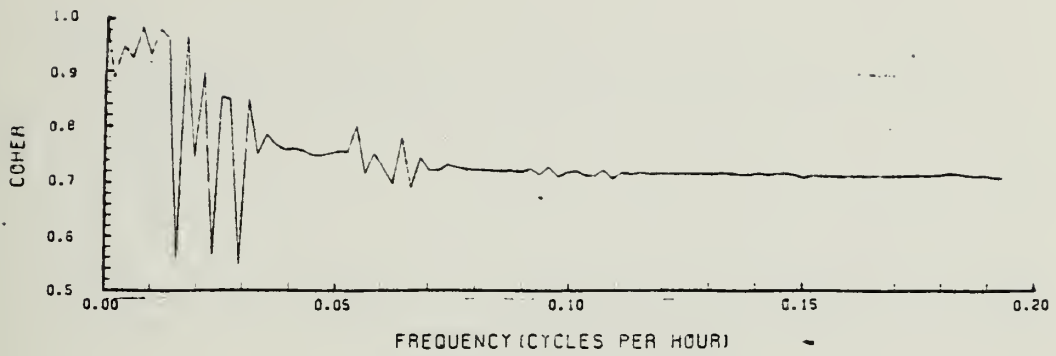


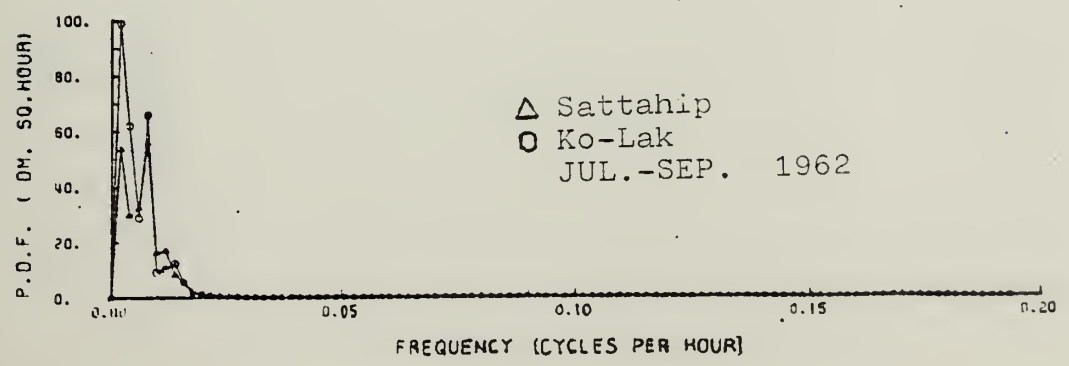
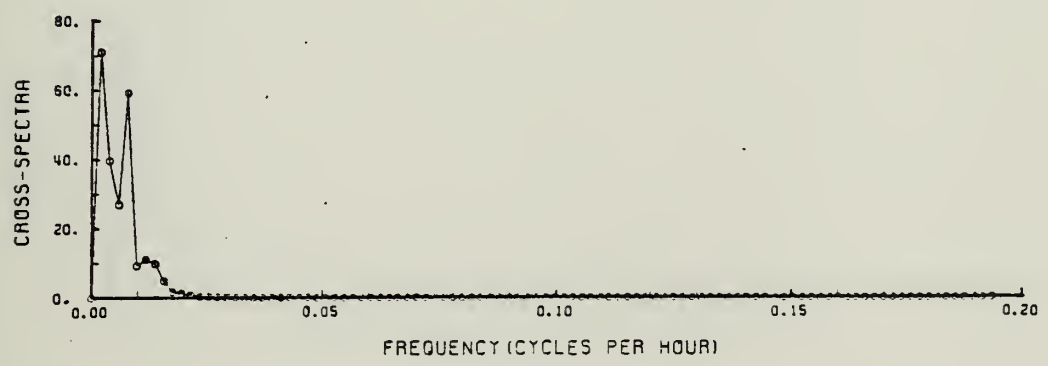
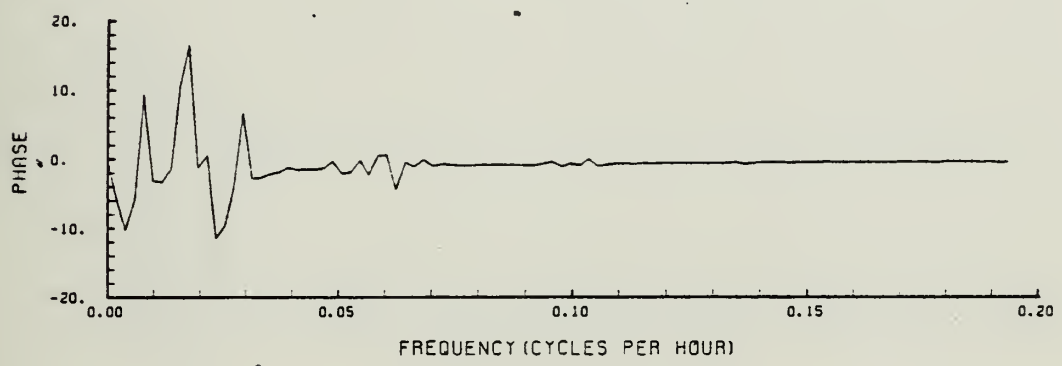
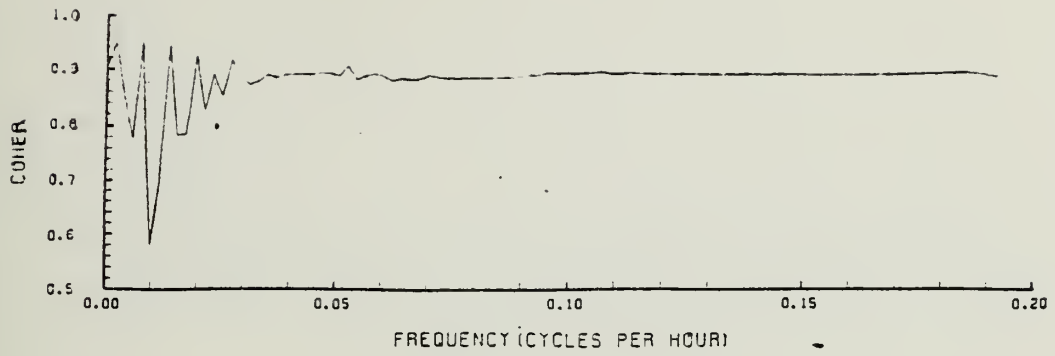


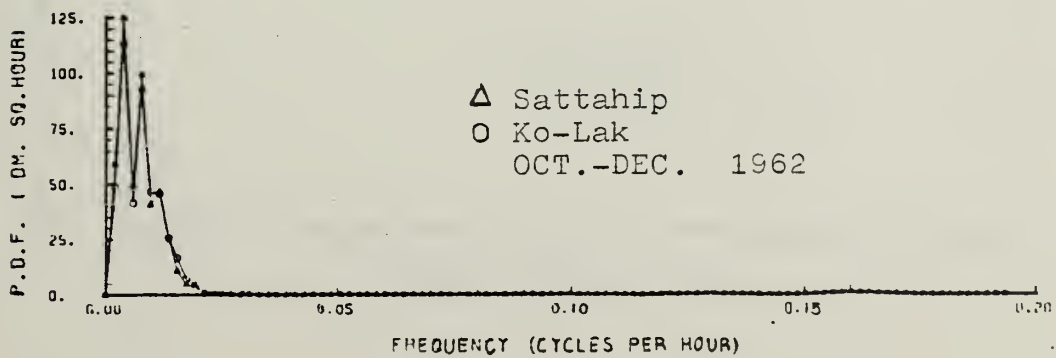
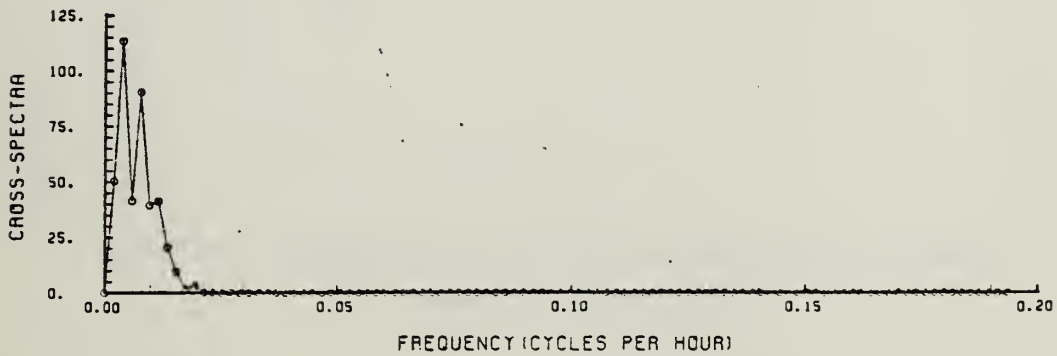
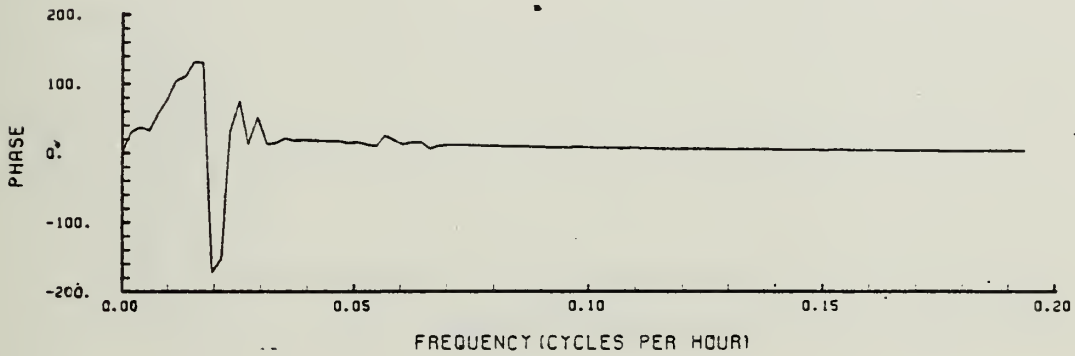
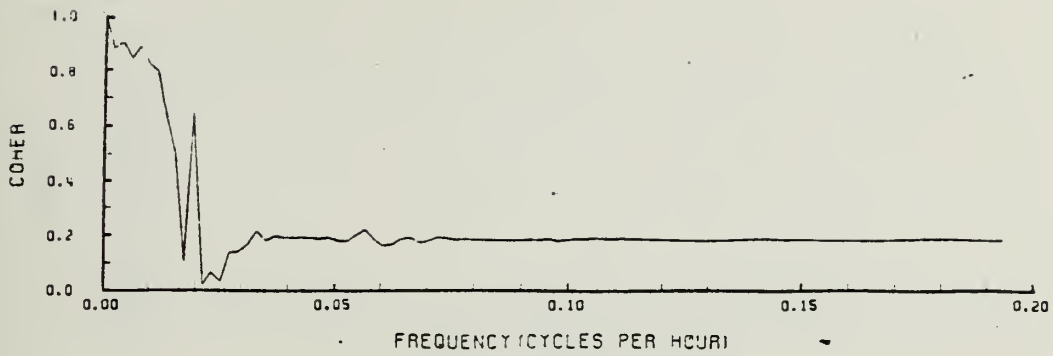


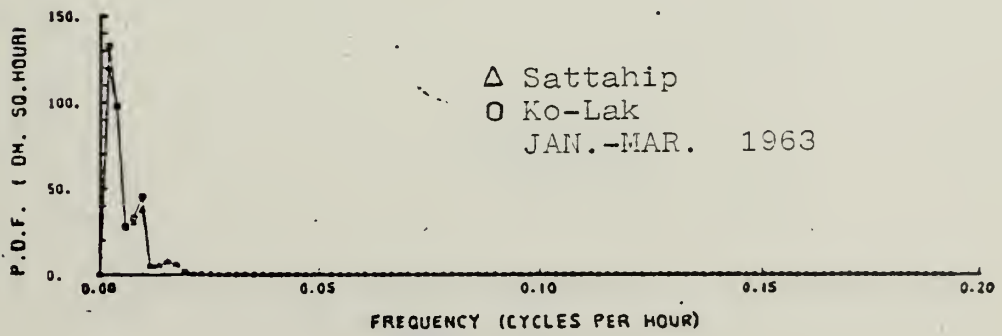
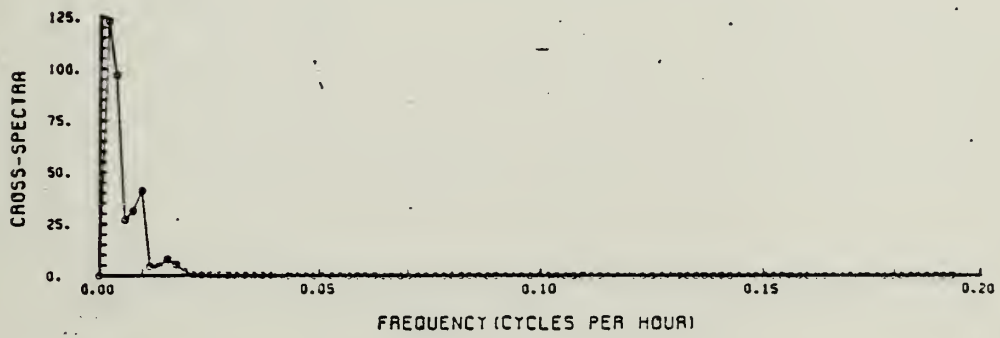
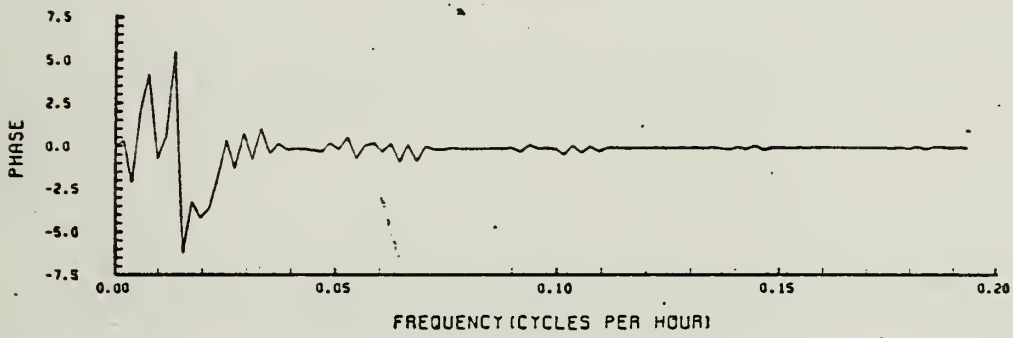
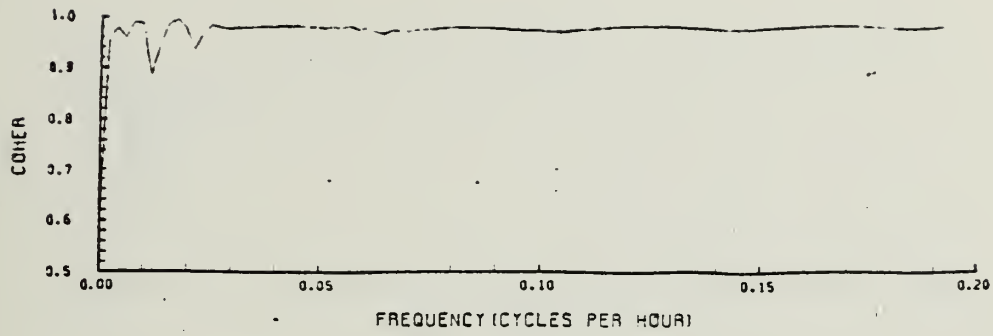


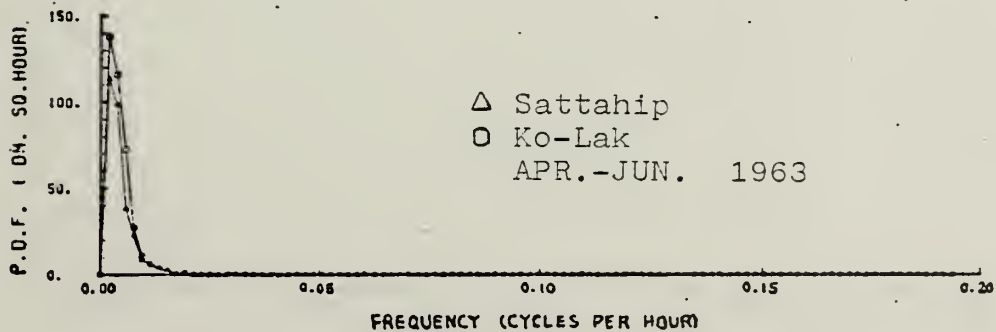
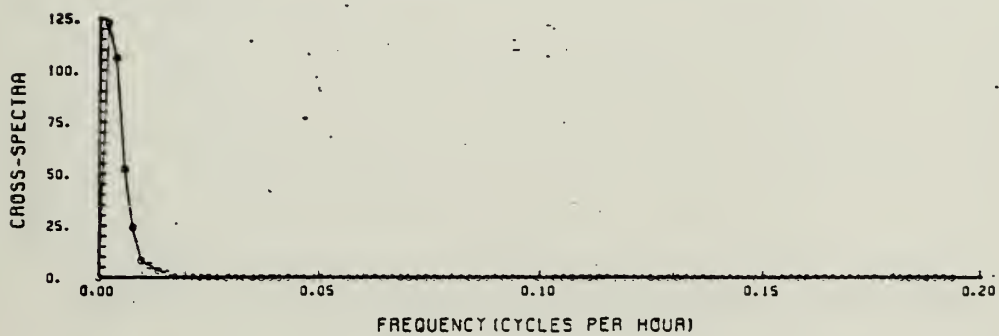
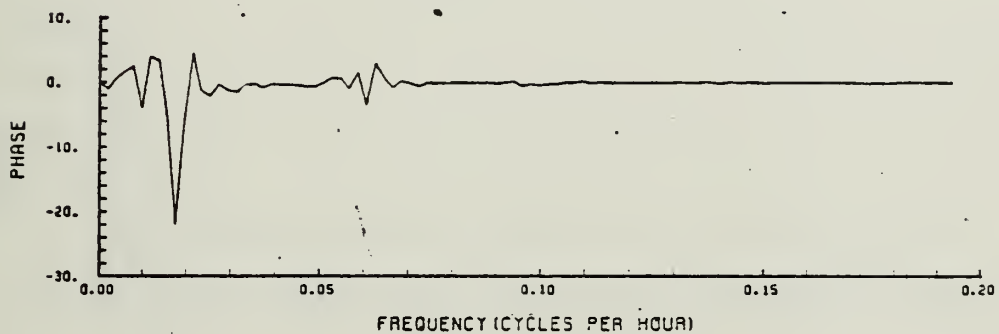
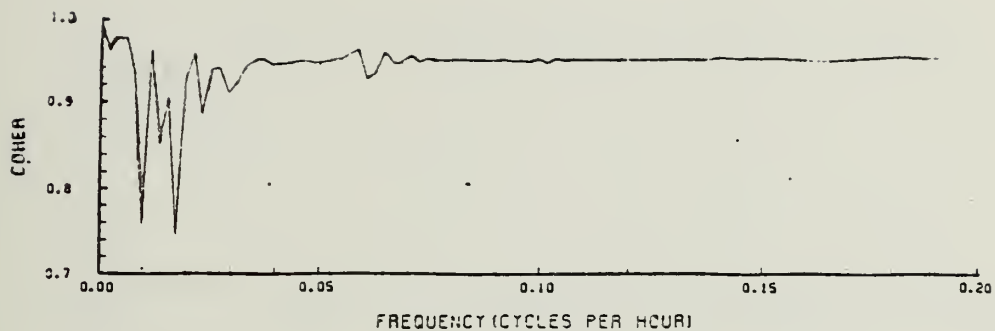


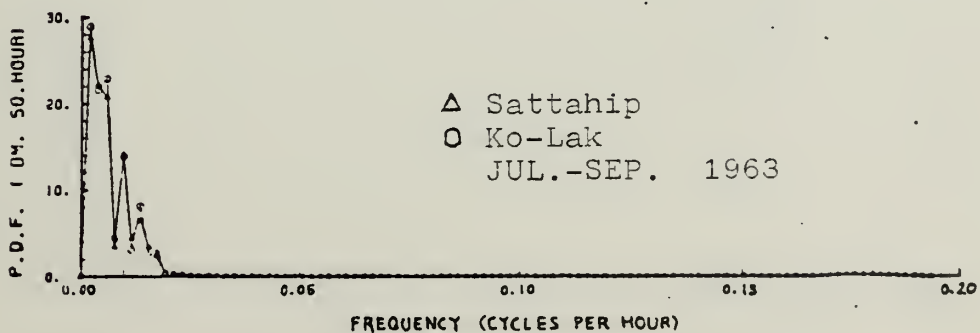
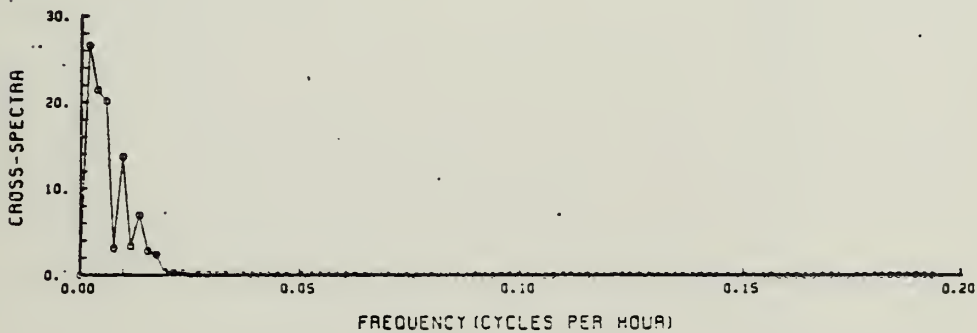
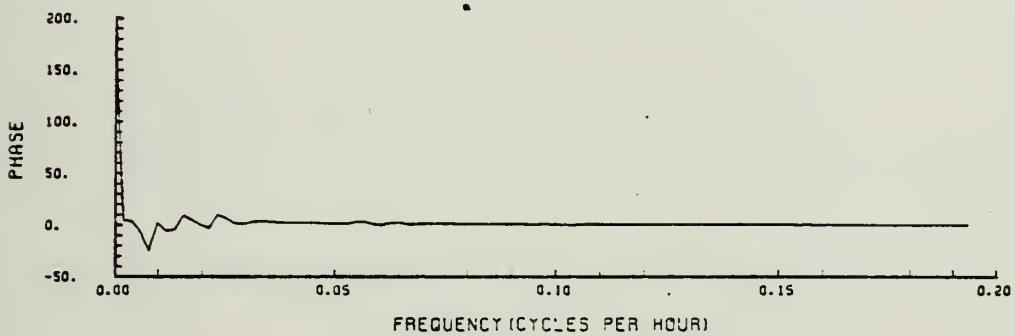
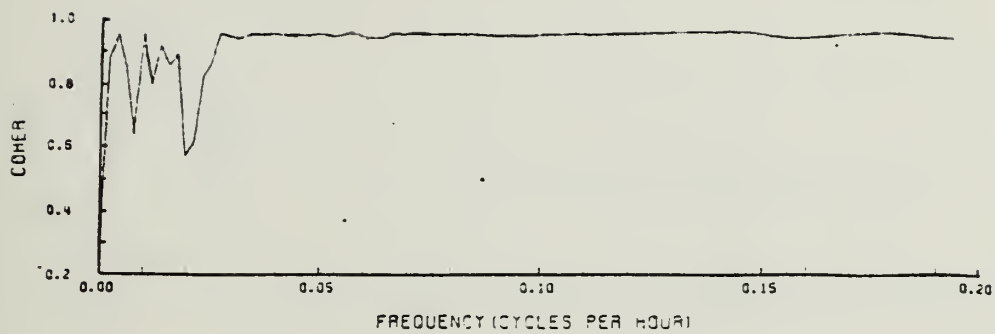


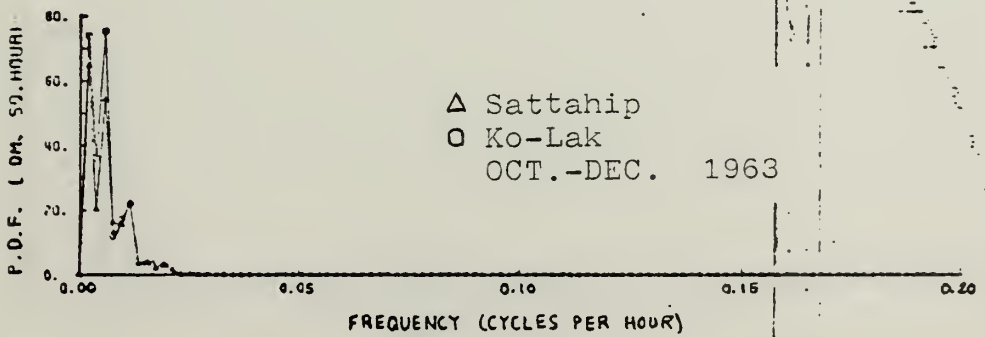
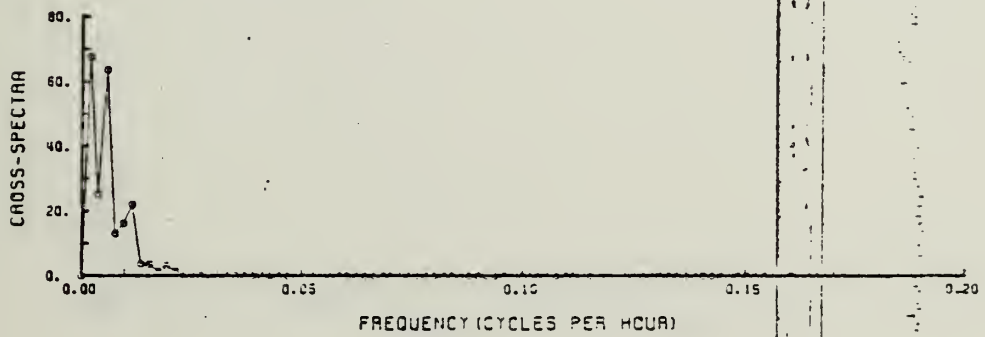
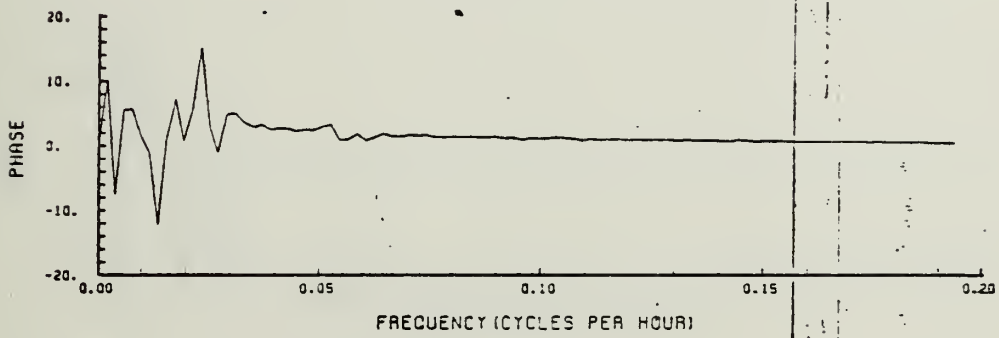
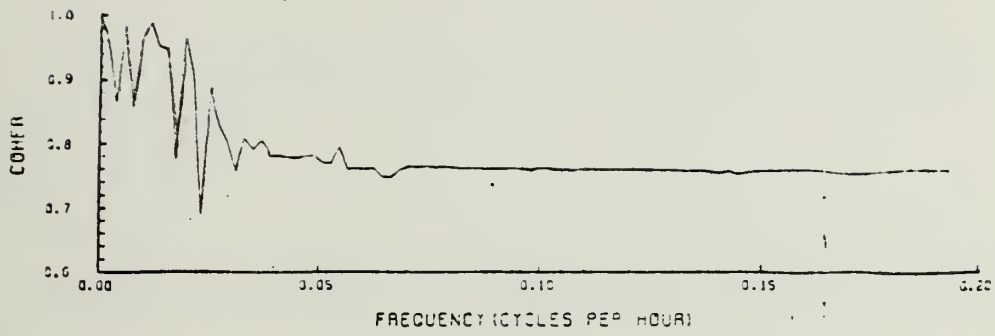


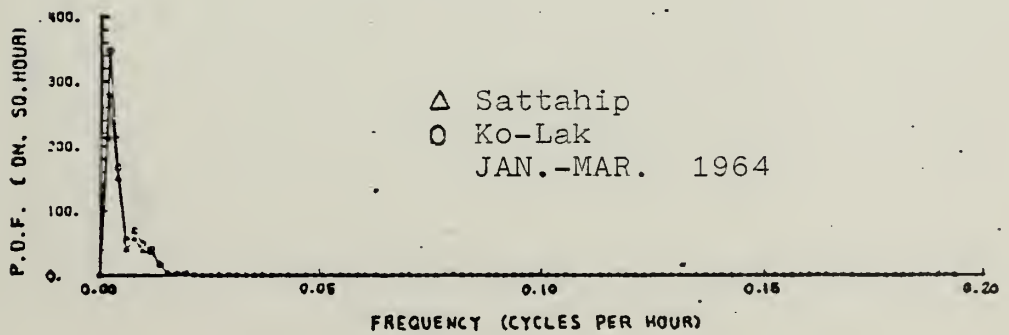
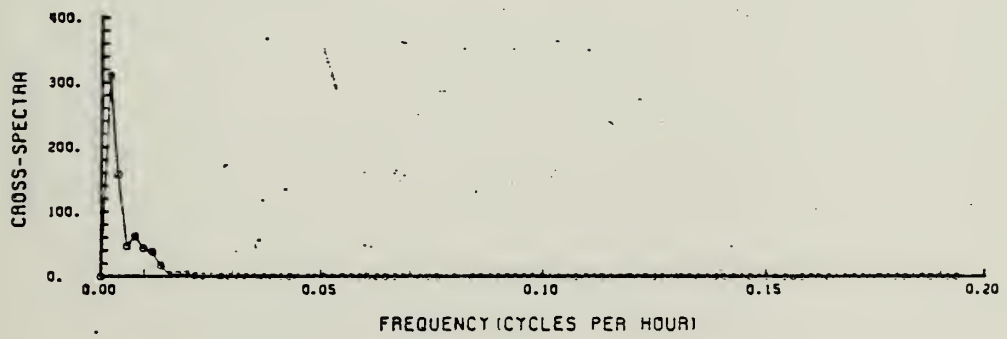
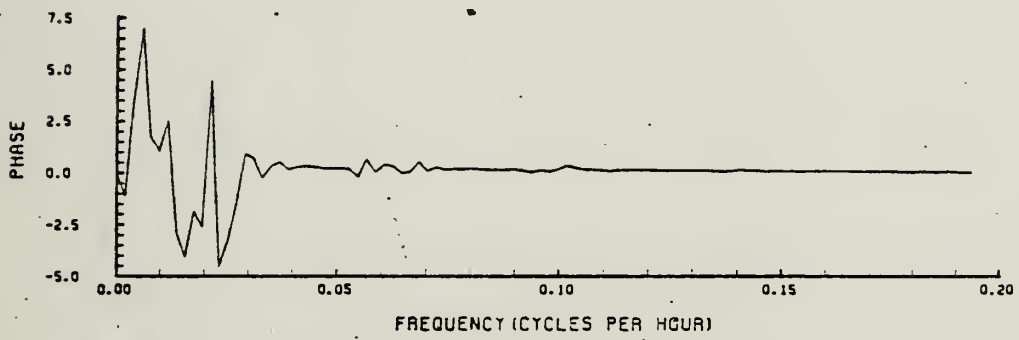
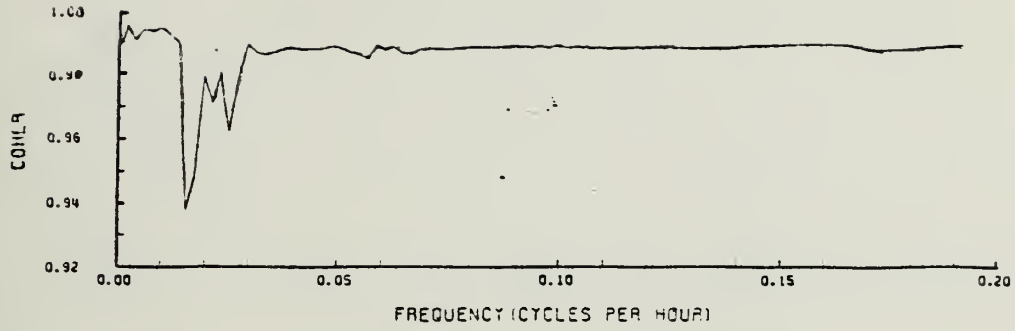


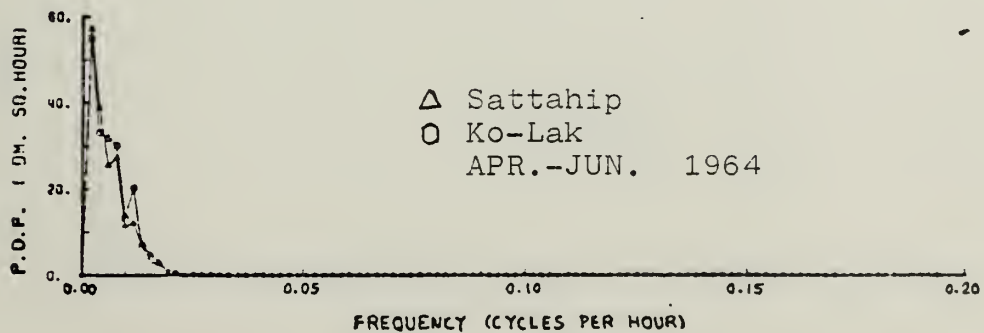
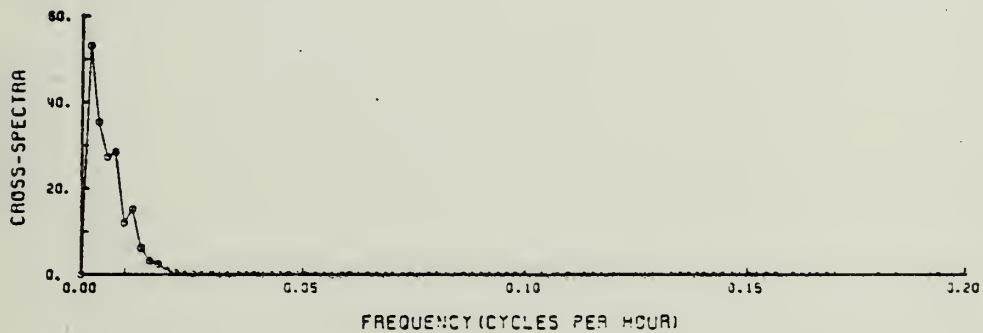
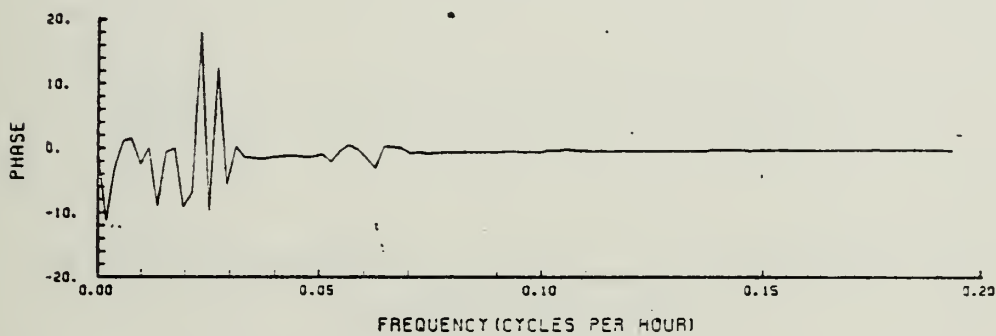
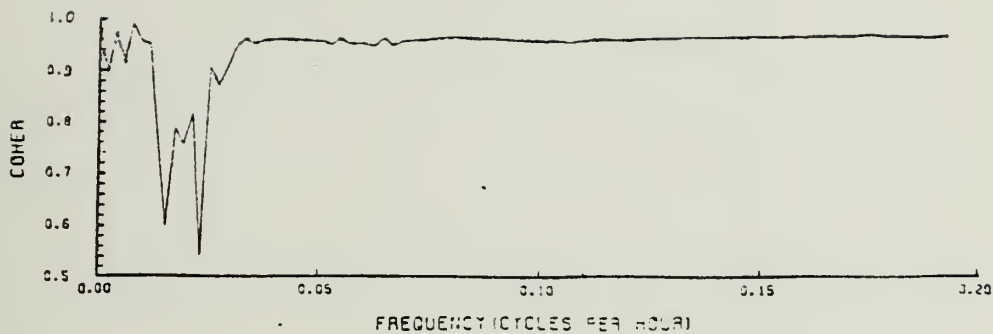


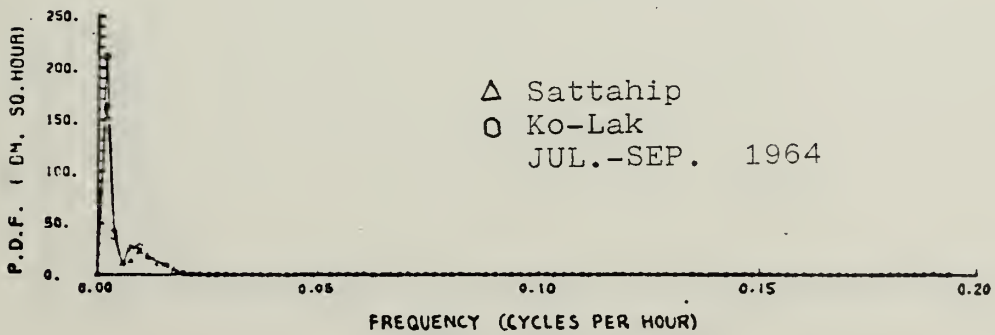
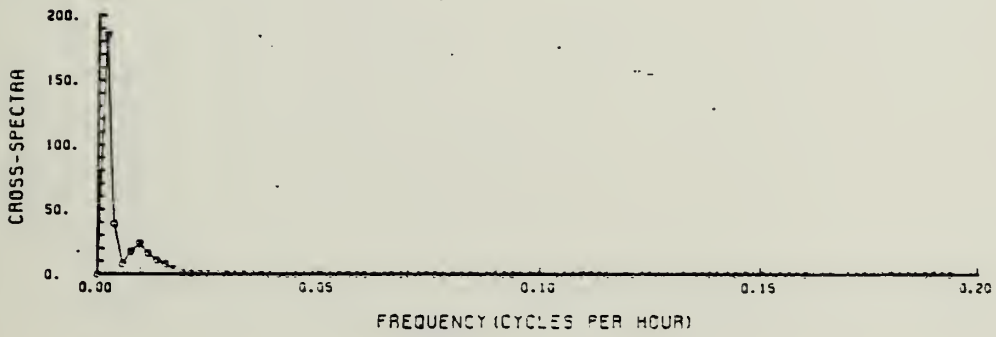
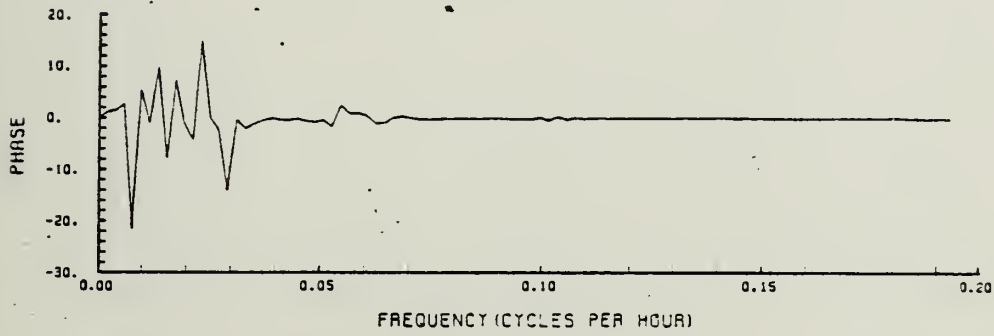
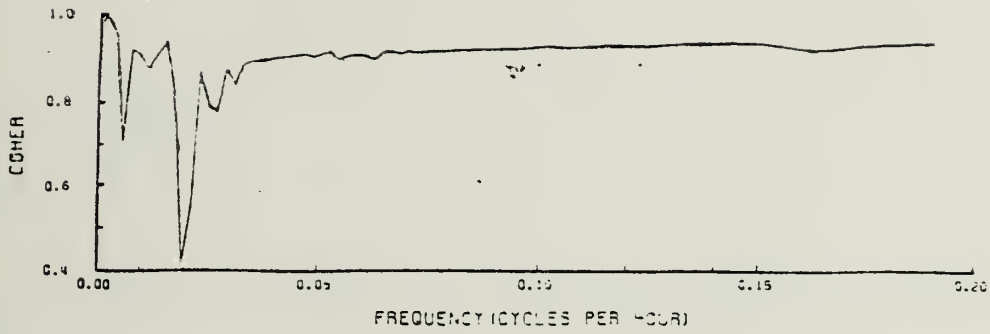


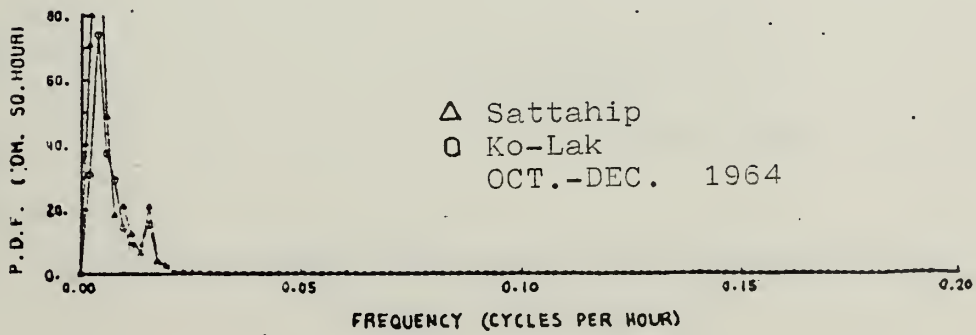
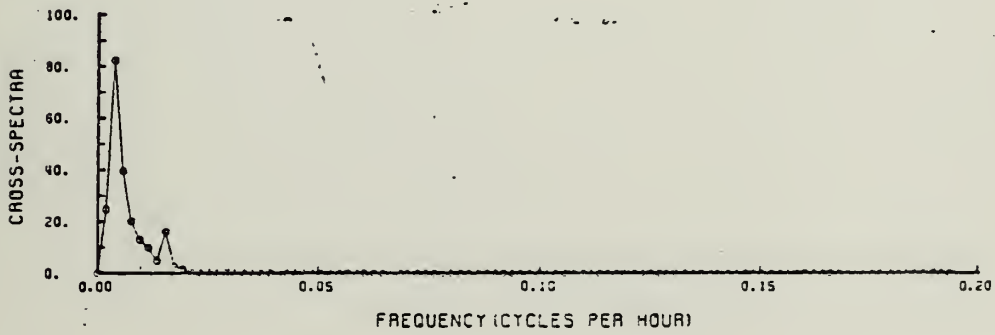
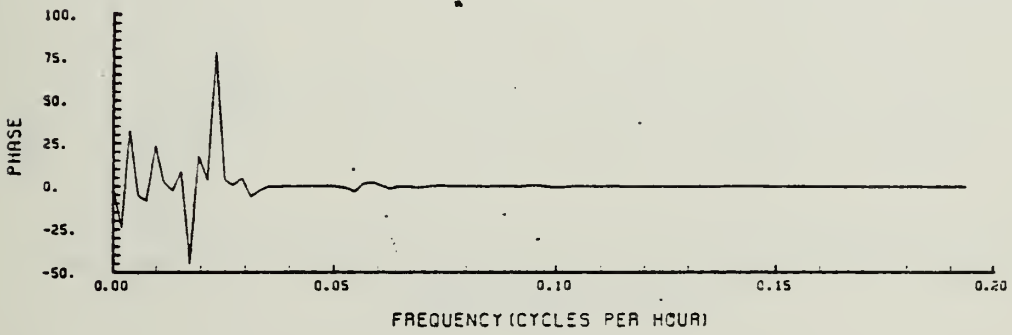
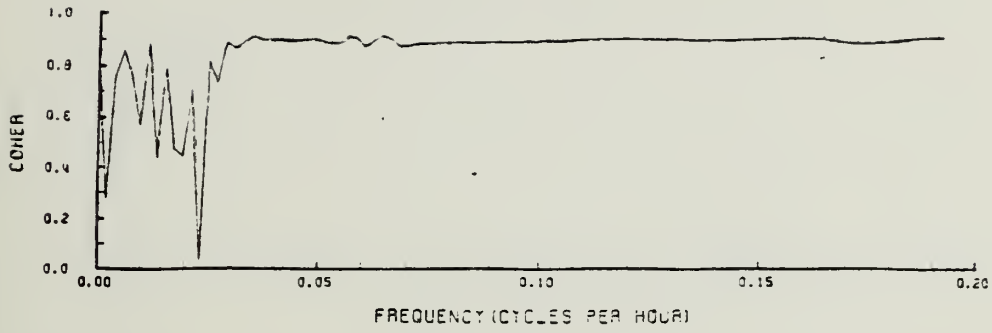


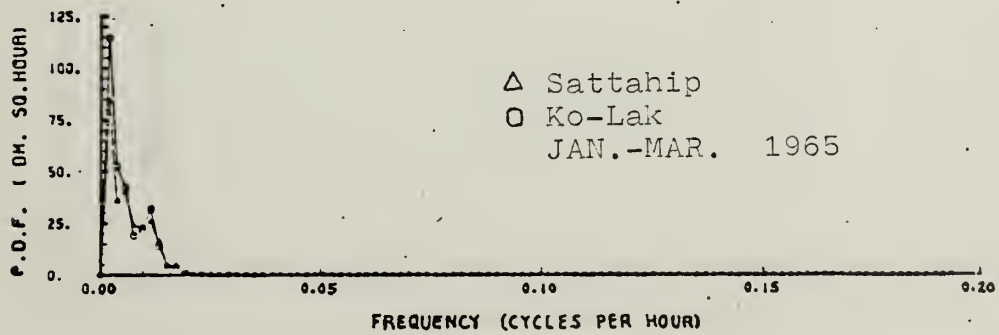
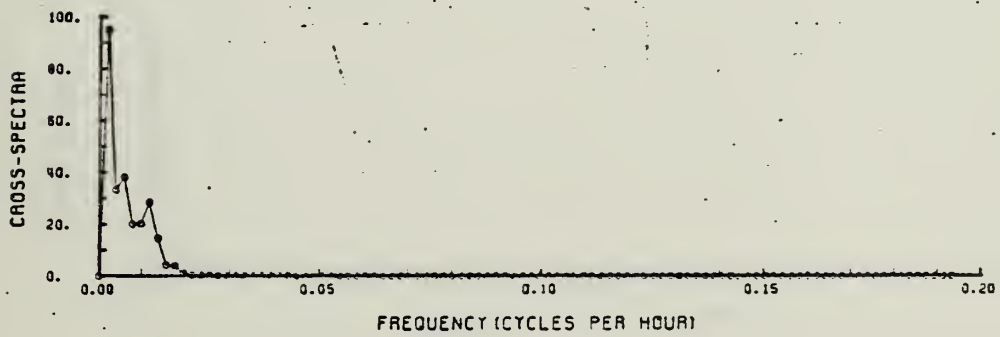
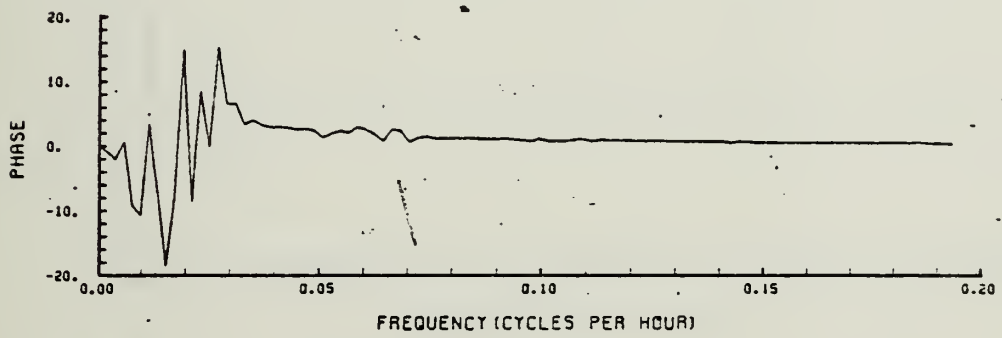
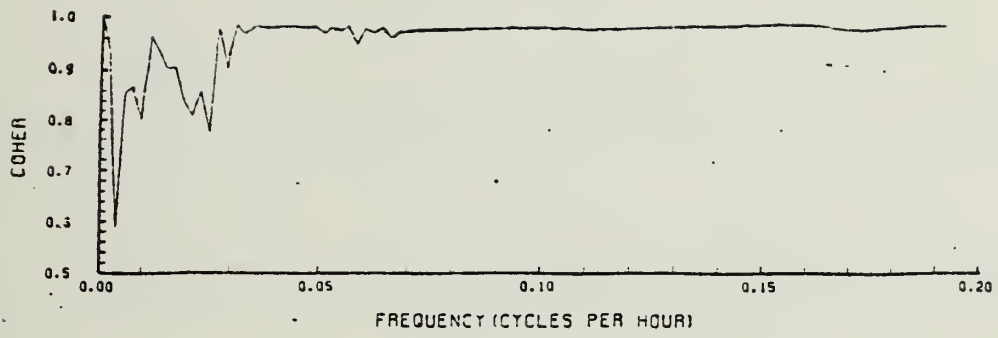


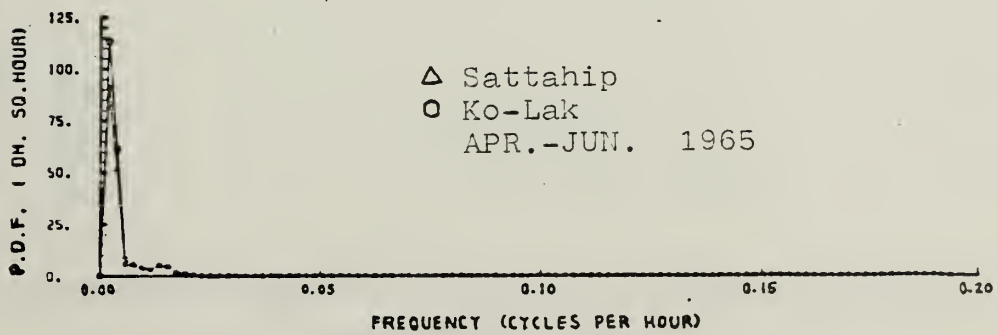
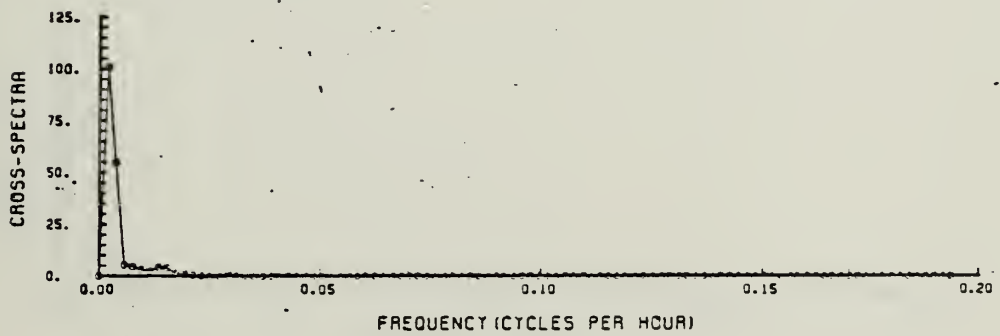
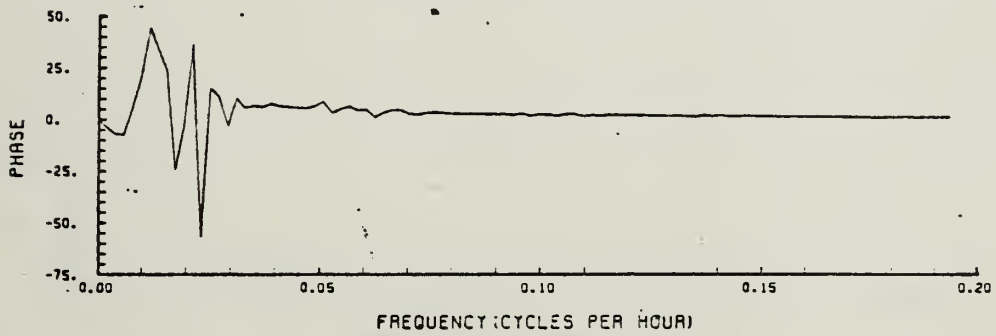
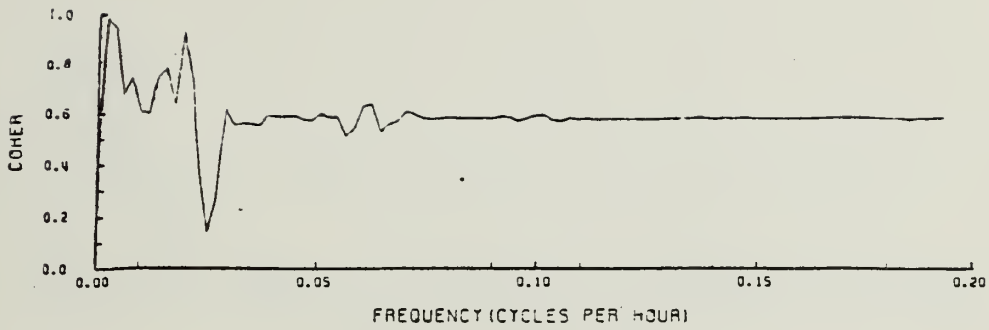


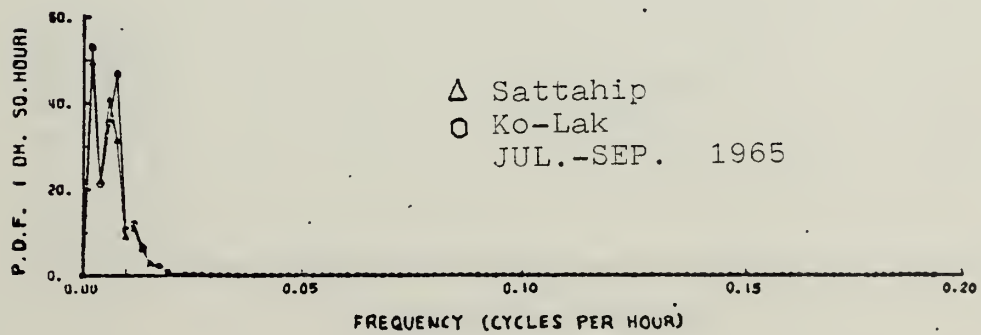
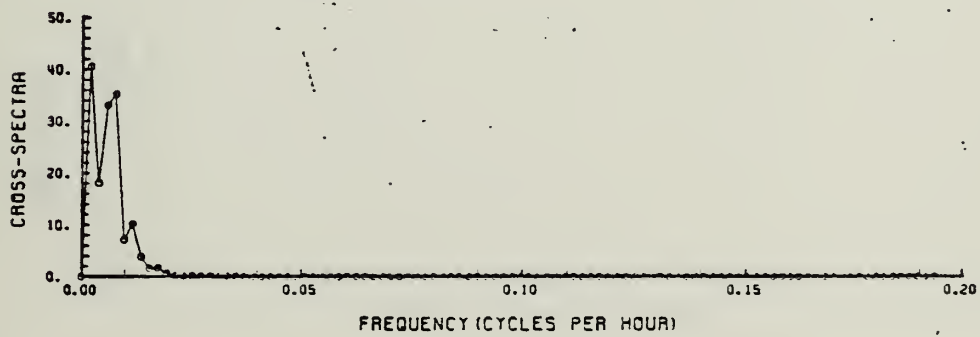
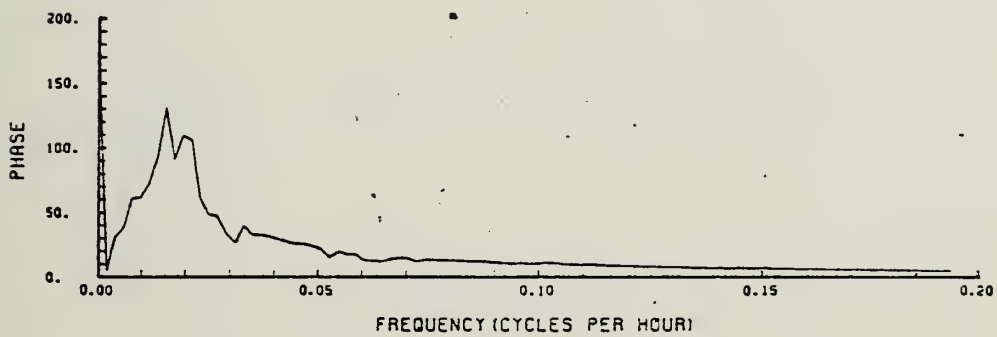
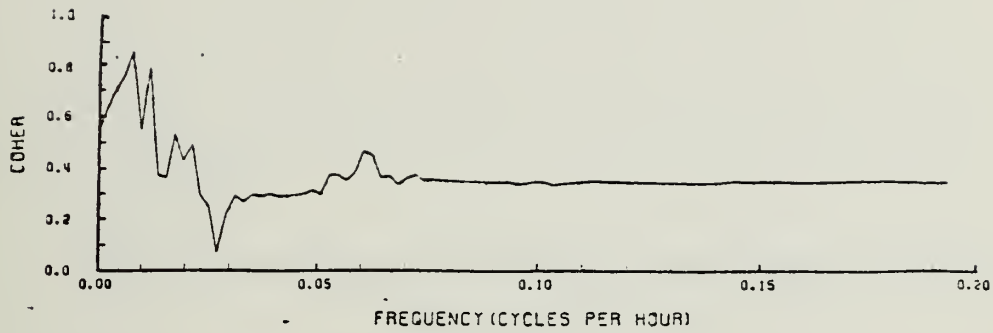


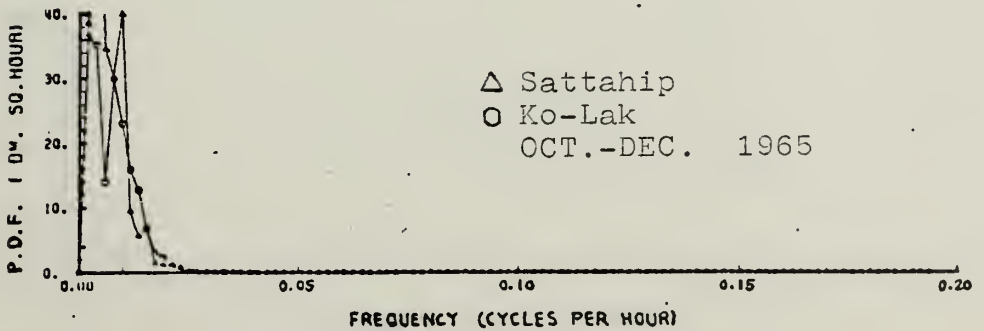
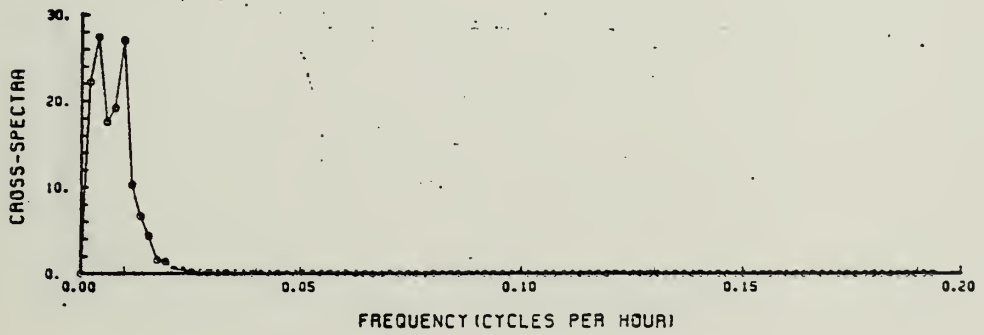
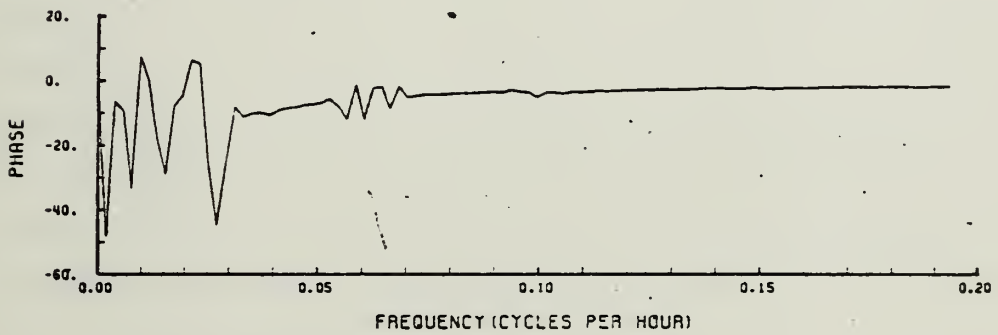
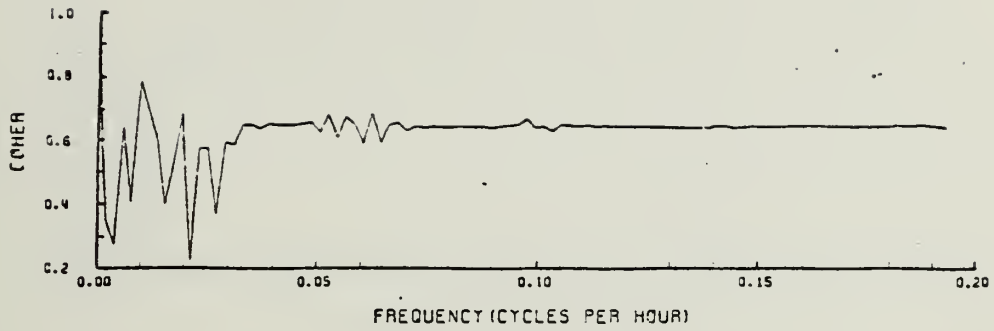


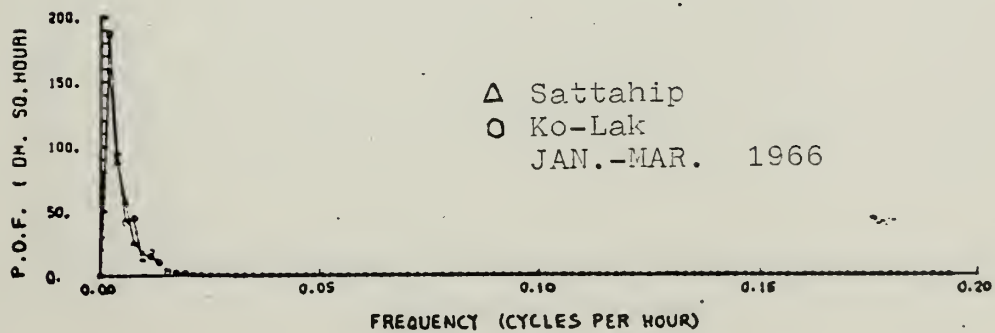
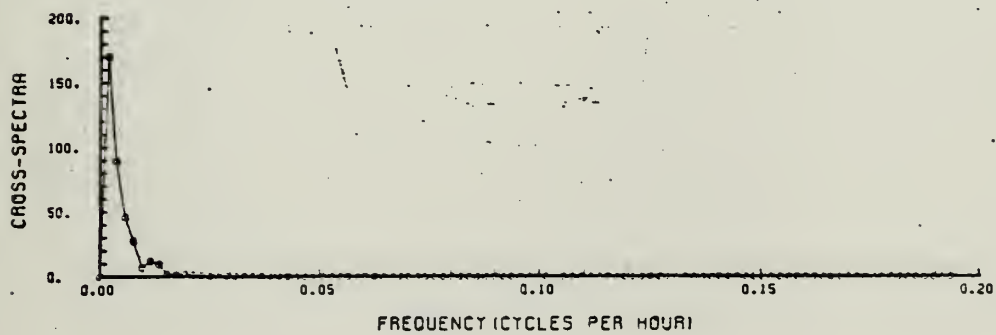
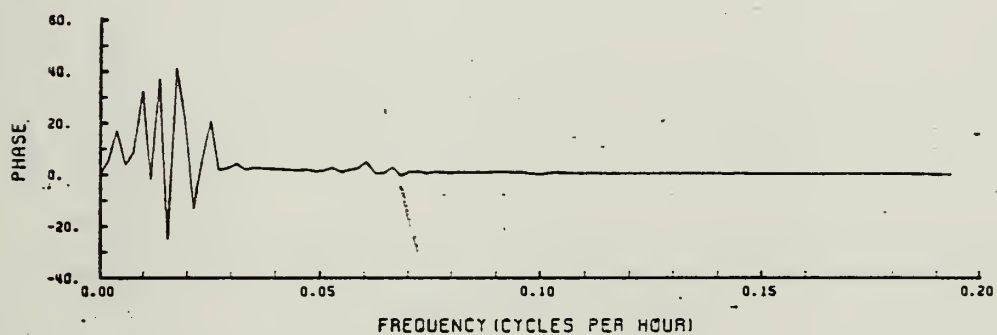
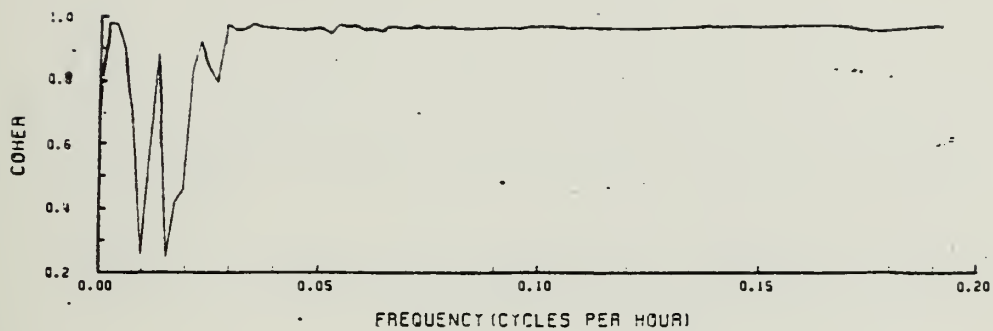


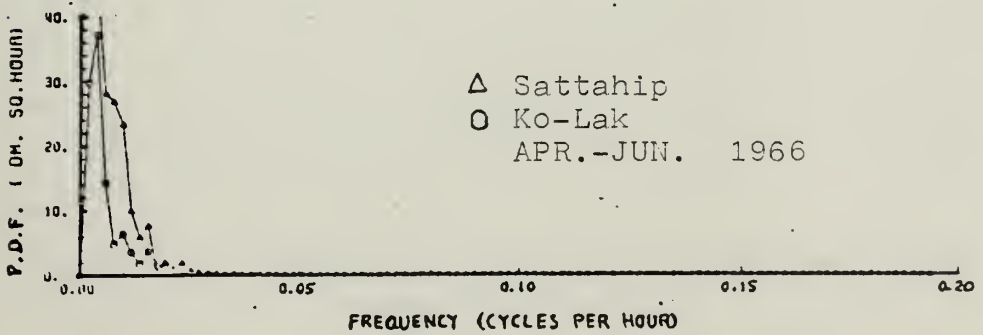
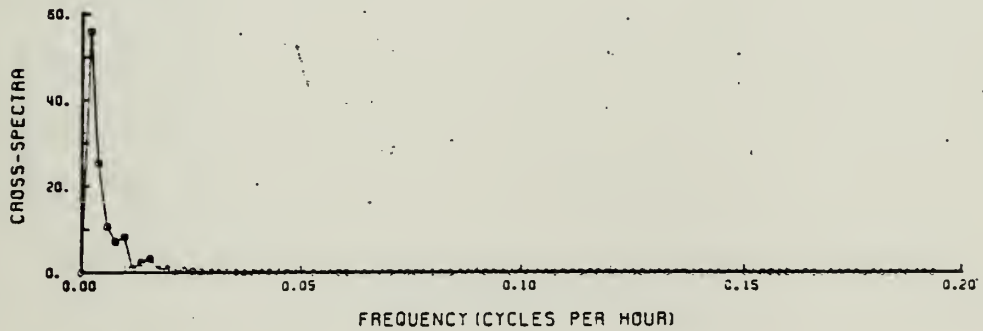
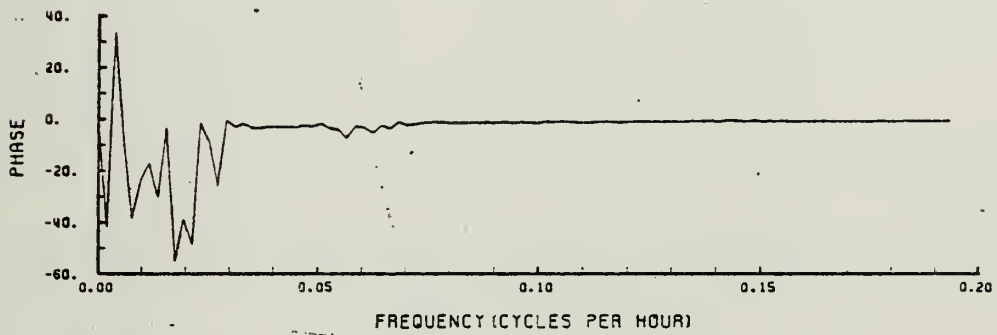
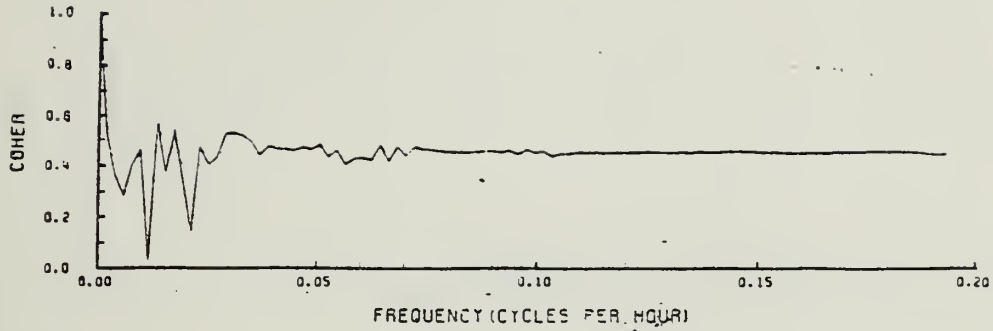


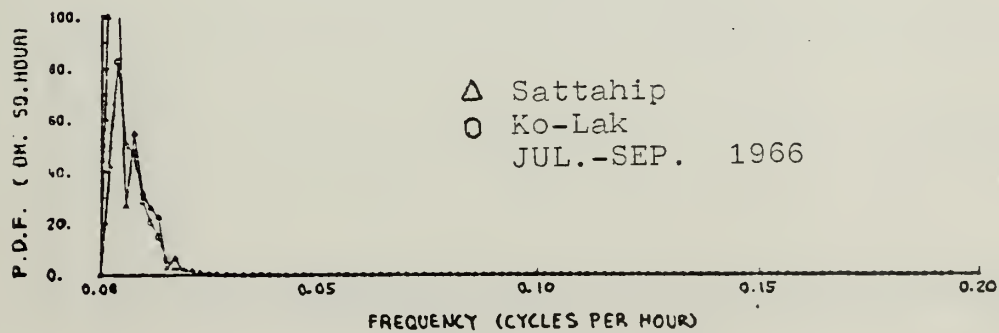
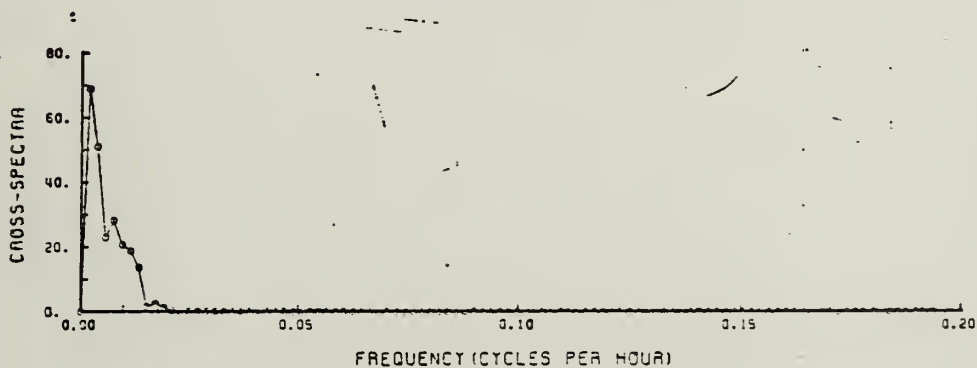
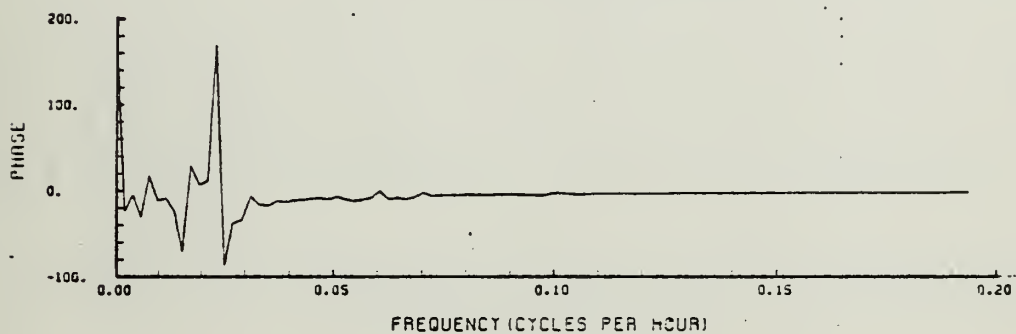
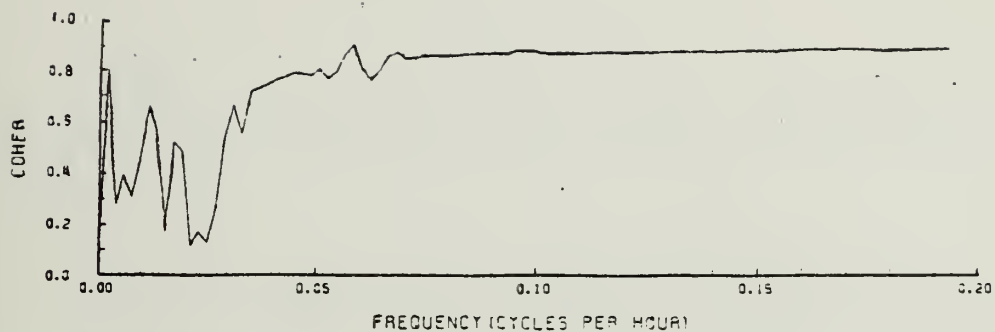


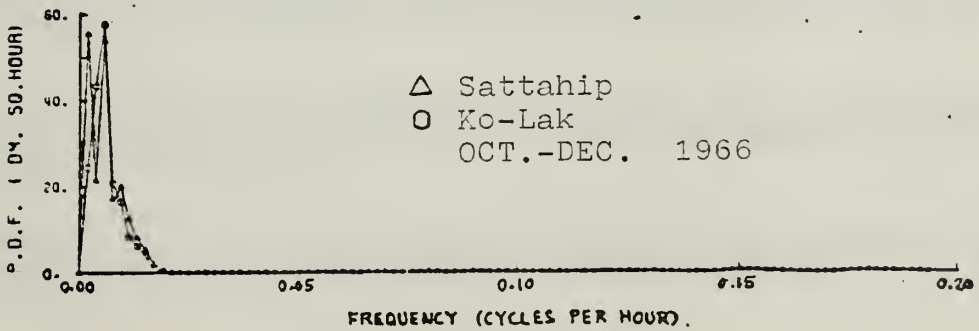
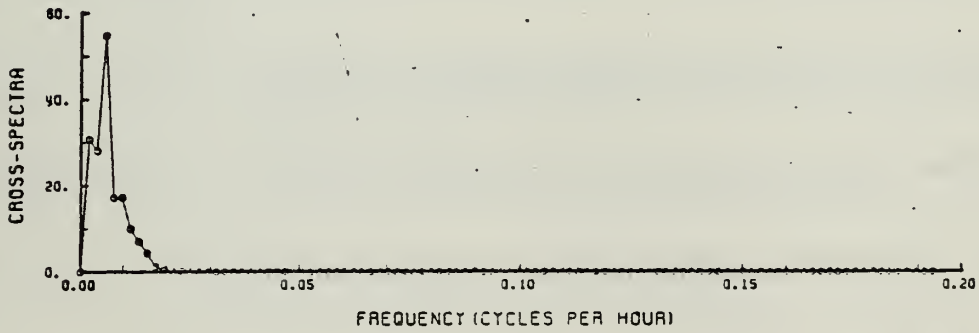
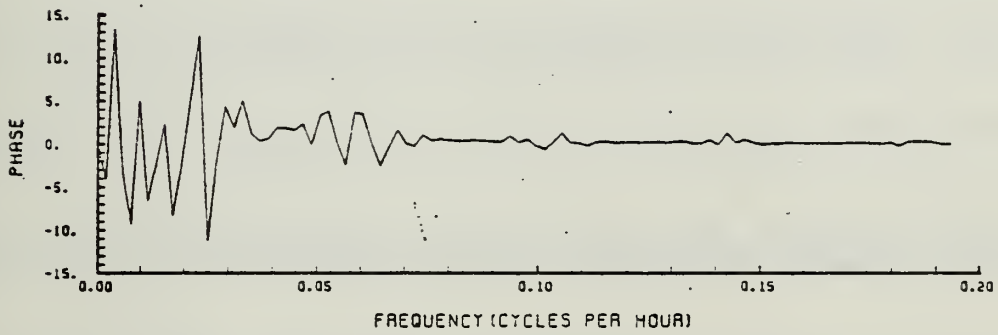
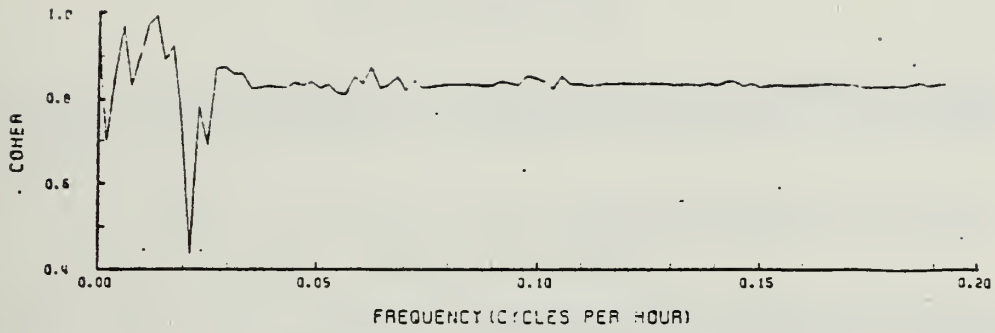












LIST OF REFERENCES

Chelton, D. B., Jr., 1980, Low Frequency Sea Level Variability Along the West Coast of North America, University of California, San Diego, Ph.D. Thesis.

Doodson, A. T., and H. D. Warburg, 1941, Admiralty Manual of Tides, The Hydrographic Department, Admiralty, London.

FNOC., Data Report, 1969, Gulf of Tokin and Gulf of Siam Tide Prediction, U.S. Fleet Numerical Weather Central, Monterey, California, U.S.A.

Godin, G., 1966, Daily Mean Sea Level and Short Period Seiches, International Hydrographic Review, Vol. XLIII, No. 2.

Groves, W. G., 1957, Day to Day Variation of Sea Level, Meteorological Monographs, Vol. 2, No.10.

Hamon, B. V., 1962, The Spectrums of Mean Sea Level at Sydney, Coff's Harbour, and Lord Howe Island, Journal of Geophysical Research, Vol.67, No.13.

IMSL., 1980, FTFREQ, International Mathematical and Statistical Libraries, Texas, Vol. 2, Chapter F.

Miller, R. A., 1957, The Effect of Steady Wind on Sea Level at Atlantic City, Meteorological Monographs, Vol.2, No.10.

Newland, D. E., 1975, Random Vibration and Spectral Analysis, Longman, London and New York.

Petterson, S., 1940, Weather Analysis and Forecasting, McGraw-Hill, New York.

Roden, G. I., 1966, Low-Frequency Sea Level Oscillations Along the Pacific Coast of North America, Journal of Geophysical Research, Vol.71, No.20.

Roden, G. I., 1960, On the Nonseasonal Variations in Sea Level along the West Coast of North America, Journal of Geophysical Research, Vol.69, No.9.

Schureman, P., 1941, Manual of Harmonic Analysis and Prediction of Tides, U.S. Coast and Geodetic Survey, Special publication No.98.

INITIAL DISTRIBUTION LIST

	No. Copies
1. Defense Technical Information Center Cameron Station Alexandria, VA 22314	2
2. Library, Code 0142 Naval Postgraduate School Monterey, CA 93940	2
3. Chairman Code 68 Mr Department of Oceanography Naval Postgraduate School Monterey, CA 93940	1
4. Chairman Code 63 Ha Department of Meteorology Naval Postgraduate School Monterey, CA 93940	1
5. J. B. Wickham Code 68 Wk Department of Oceanography Naval Postgraduate School Monterey, CA 93940	2
6. W. C. Thompson Code 68 Th Department of Oceanography Naval Postgraduate School Monterey, CA 93940	1
7. LTJG. Vichai Punpuk Hydrographic Department Royal Thai Navy Bangkok 6 THAILAND	4
8. Personnel Department Royal Thai Navy Bangkok 6 THAILAND	1

- | | | |
|-----|--|---|
| 9. | Library
Hydrographic Department
Royal Thai Navy
Bangkok 6, THAILAND | 2 |
| 10. | Commander
Naval Oceanography Command
NSTL Station
Bay St. Louis, MS 39522 | 1 |
| 11. | Commanding Officer
Fleet Numerical Oceanography Center
Monterey, CA 93940 | 1 |
| 12. | Office of Naval Research (Code 480)
Naval Ocean Research and Development
Activity
NSTL Station
Bay St. Louis, MS 39522 | 1 |
| 13. | Scientific Liaison Office
Office of Naval Research
Scripps Institution of Oceanography
La Jolla, CA 92037 | 1 |
| 14. | Commander
Oceanographic System Pacific
Box 1390
Pear Harbor, HI 96860 | 1 |
| 15. | Chief, Marine Surveys and Maps (C3)
National Oceanic and Atmospheric
Administration
Rockville, MD 20852 | 1 |
| 16. | Commanding Officer
Naval Environmental Prediction
Research Facility
Monterey, CA 93940. | 1 |

Thesis
P9477 Punpuk
c.1 Sea level variations
in Gulf of Thailand.

193808

20 NOV 83

279461

ons

Thesis
P9477 Punpuk
c.1 Sea level variations
in Gulf of Thailand.

193808

thesP9477

Sea level variations in Gulf of Thailand



3 2768 001 93057 1

DUDLEY KNOX LIBRARY